The NuMI Facility
Technical Design Report

Revision 1.0
October, 1998

Fermilab

Operated by

Universities Research Association

for the

U. S. Department of Energy

Table of Contents

1.0 Executive Summary

2.0 Neutrino Beam Requirements and Conceptual Design

3.0 Technical Components

4.0 Radiation Safety

5.0 Civil Construction

6.0 Cost & Schedule

7.0 Project Management Summary

Appendix A Beam Sheet

Appendix B Glossary

Preface to Revision 1.0

This document, Revision 1.0 of the NuMI Facility Technical Design Report, is intended to establish the technical scope of the NuMI Facility at Fermilab, which is a subproject of the NuMI Project. This document, in combination with the MINOS Detectors Technical Design Report and the MINOS Far Detector Laboratory Technical Design Report, will provide a significant part of the supporting documentation for the Baseline Review of the NuMI Project, scheduled for November 1998. Even after the Baseline Review, this document will not be frozen. As the NuMI Project evolves, this document will be periodically updated to reflect changes and new developments in the NuMI Facility Subproject. The reader is advised to use the most recent version.

Several important changes have been incorporated into this revision. Most notably, the beam is changed from a three-horn wide band beam design to a two-horn tunable energy design. This is a major change to the beam design.

Authors

Fermi National Accelerator Laboratory

K. Anderson, B. Bernstein, D. Boehnlein, K. Bourkland, S. Childress, N. Grossman, J. Hylen, C. James, G. Koizumi, C. Laughton, P. Lucas, J. G. Morfín, S. O'Day, R. Plunkett, D. Pushka, R. Rameika, W. Smart, A. Wehmann, D. Wolff

State Research Center of Russia, Institute for High Energy Physics

A. Abramov, N. Galyaev, V. Garkusha, V. Ferapontov, I. Kurochkin, F. Novoskoltsev, A. Ryabov, V. Zapolsky, V. Zarucheisky

Argonne National Laboratory

M. Goodman

1.0 Executive Summary

Table of Contents

1.0 EXECUTIVE SUMMARY 1-1

1.1 INTRODUCTION 1-2
1.2 HISTORICAL DEVELOPMENT OF NUMI 1-3
1.3 THE TECHNICAL DESIGN REPORT 1-4
1.4 TECHNICAL COMPONENTS 1-4
1.4.1 Primary Beam Systems 1-5
1.4.2 Neutrino Beam Components 1-6
1.4.3 Power Supply Systems 1-6
1.4.4 Hadron Decay and Absorber Regions 1-7
1.4.5 Neutrino Beam Monitoring 1-7
1.4.6 Alignment Systems 1-7
1.4.7 Water, Vacuum and Gas Systems 1-8
1.4.8 Systems Integration 1-8
1.5 RADIATION SAFETY 1-9
1.6 CIVIL CONSTRUCTION 1-9
1.7 COST AND SCHEDULE 1-10
1.8 PROJECT MANAGEMENT SUMMARY 1-10

Table of Tables

Table 1-1 Civil construction of the NuMI Project at Fermilab. ____ 1-11

Table of Figures

Figure 1-1 Layout of the NuMI Facility (See Insert). ____ 1-12
Figure 1-2 Aerial view of the Fermilab site and the proposed NuMI beamline. ____ 1-13
Figure 1-3 Trajectory of the neutrino beam between Fermilab and Soudan, Minnesota. ____ 1-14

1.1 Introduction

The NuMI Facility Project will produce an intense beam of neutrinos to enable a new generation of experiments whose primary scientific goal is to definitively detect and study neutrino oscillations. The beam will be of sufficient intensity and energy so that experiments capable of identifying muon neutrino (ν_μ) to tau neutrino (ν_τ) oscillations, as well as other possibilities, are feasible. A beam of protons from Fermilab's Main Injector will be used to produce the neutrino beam. Interactions of the proton beam in a production target will produce mesons, which decay to muons and neutrinos during their flight through a decay tunnel. A hadron absorber downstream of the decay region will remove the remaining protons and mesons from the beam. The muons will be absorbed by an intervening rock shield while the neutrinos continue through it to the near experimental hall and beyond to the far detector in Soudan, Minnesota. The experimental halls will contain massive detectors specially designed to observe the relatively few neutrinos that will interact in them.

The purpose of this document is to define the technical scope of the NuMI Facility Project, which includes civil construction at the Fermilab site and the technical components required to produce the neutrino beam. This is illustrated in Figure 1-1 (see insert). Each major element of the Work Breakdown Structure (WBS) for the NuMI Facility is discussed in its own chapter, which defines the technical scope of that subtask. Other aspects of the overall NuMI Project, including a discussion of the physics, the neutrino detectors and modifications to the Soudan Underground Laboratory for the MINOS experiment are given elsewhere.[1,2]

An aerial photograph of the Fermilab site with the beamline superimposed is shown in Figure 1-2. The trajectory of the neutrino beam between Fermilab and Soudan is shown in Figure 1-3.

---

[1] The MINOS Collaboration, *The MINOS Detectors Technical Design Report,* October, 1998

[2] University of Minnesota, CNA Consulting Engineers, Erickson-Ellison Associates, Inc., Miller-Dunwiddie, Inc., *MINOS Far Detector Laboratory Technical Design Report (Including Basis of Estimate & WBS) for Cavern Construction, Cavern Outfitting & Detector Outfitting*, NuMI-L-263, August, 1998

1.2 Historical Development of NuMI

From the earliest days of planning for the Fermilab Main Injector, it was clear that the new machine would be able to provide high intensity and high duty cycle extracted beams, which could be used for fixed target experiments. With this in mind, working groups conducted design feasibility studies for both kaon and neutrino experiments. In June 1991 a report[3] describing both conventional neutrino physics and neutrino oscillation experiments was released. The motivation and design proposals for both long baseline and short baseline experiments were discussed. For the long baseline experiment three far sites were considered: the Morton Salt mine in Cleveland, Ohio, home of the IMB proton decay experiment; the Soudan Laboratory in Soudan Minnesota, home of the Soudan 2 proton decay experiment; and Hawaii, proposed home of the DUMAND neutrino detector.

However, because the funding profile and schedule for the Main Injector were uncertain at that time, neither detailed designs nor firm decisions regarding the neutrino oscillation experiments were made for the next two years. During that time the experimental motivation for accelerator based neutrino oscillation experiments continued to grow and experiment proposals[4,5] matured. Fermilab management and the Physics Advisory Committee began to consider these experiments seriously in the summer of 1993. In the fall of that year the Neutrino Oscillation Working Group was re-formed and in November a *Project Definition Report* [6] completed describing a facility to produce a neutrino beam directed from Fermilab to Soudan.

By June 1997 the requirements of the facility were well enough understood to produce a *Conceptual Design Report.*[7] Over the next six months the cost and schedule of the facility design were re-evaluated in the context of different mining techniques. The option of raising the elevation was considered but discounted, primarily due to the potential interference of the target hall enclosure with the 8 GeV transfer line into the Main Injector. The option of constructing the target hall even deeper than presented in the June '97 CDR was studied and found to have major advantages. Several other changes to the layout of the underground enclosures were also incorporated into the current design. The motivation

---

[3] Conceptual Design Report: Main Injector Neutrino Program, Version 1.1, June 1991

[4] P-803

[5] P-822

[6] Project Definition Report, Rev.0, E&P Project No. 6-7-1, November 93

[7] Conceptual Design Report, Rev.0, June 97

for these changes came from both programmatic and financial constraints. These included the addition of muon monitoring pits, reduction to a single experimental hall, reduction of the length of the decay pipe, and reduction of the distance between the end of the decay tunnel and the experimental hall.

In June 1998 the Super-Kamiokande collaboration reported compelling evidence for neutrino oscillations from their studies of atmospheric neutrinos.[8] Their results indicate that the optimum neutrino energy for a beam produced at Fermilab may be lower than that of the preliminary design. As a consequence it was decided that the flexibility to tune the energy of the neutrino beam would be a requirement incorporated into the baseline design. This is described in detail in Chapters 2 and 3.

1.3 The Technical Design Report

This Technical Design Report defines the scope of the NuMI Facility Project. It includes the civil construction at Fermilab and technical components of the beamline, which are included in the Total Estimated Cost (TEC) of the NuMI Project. The other elements of the NuMI Project, the MINOS detectors and the expansion of the Soudan mine, are not included in this TEC.

Chapter 2 contains an overview of the beam requirements and the design of the facility. A brief discussion of the specific experimental measurements that will be made to search for neutrino oscillations is also presented along with a discussion of how the proposed NuMI beam meets the needs of the MINOS experiment. The NuMI/MINOS facility will measure neutrino interactions in both a near detector located on the Fermilab site and in a far detector at the Soudan mine. Differences in the neutrino beam between those two locations must be understood.

1.4 Technical Components

Chapter 3 describes in detail each of the technical subsystems that will be built to construct the NuMI beam. Where appropriate, plans for commissioning and performance monitoring have also been included, as have plans for prototyping and testing of the technical components.

---

[8] www.phys.washington.edu/~superk/sk_release.html, June 1998

The neutrino beams have the following objectives:

- Potentially cover the energy range 1 to 20 GeV. This is accomplished by a hadron focusing system that can be optimized to 1-3 GeV, 3-8 GeV or 8-20 GeV in neutrino energy.
- Predict the neutrino energy spectrum in the MINOS far detector to 2 or 3%, if neutrino oscillations are absent, given a measurement of the spectrum at the MINOS near detector.
- Keep electron neutrino and muon anti-neutrino event background <1% of muon neutrino event rate.
- Center the neutrino beam at the detectors and to keep the effect of mis-steering to less than 2% anywhere in the neutrino spectrum.
- Accommodate 1 millisecond spill to keep event overlap in near detector to less than 1%.
- Long term reliability, stability and reparability such that the facility is usable for a minimum of 10 years while assuring personnel safety and allowing for future modifications and upgrades.

The major technical components that are required for the NuMI beam are:

- the primary beam system
- the neutrino beam devices
- the power supply systems
- the hadron decay and absorber regions
- neutrino beam monitoring
- alignment systems
- water, vacuum and gas systems
- controls, cables, interlocks and systems integration.

1.4.1 Primary Beam Systems

The primary beam system begins with the extraction of the 120 GeV protons from the Main Injector and their transport to the NuMI target. The proton beam at the target will be aimed precisely toward the MINOS detector at Soudan. The primary beam system must deliver of order 4×10^{13} protons per pulse to the target. Containment and control of losses is achieved in part through the use of baffles and shielding. These baffles protect against

possible losses in the long tunnel upstream of the pretarget hall and damage to the horns, from mis-steering of intense primary protons.

1.4.2 Neutrino Beam Components

A flexible beam optics system, which can be tuned to different neutrino energy bands, has been designed. The target for the NuMI beam is designed to maximize the neutrino yield while surviving for at least one year of operation. The present target design calls for either water-cooled graphite or beryllium fins. Pion production from the targets has been calculated. Energy deposition, heating and stress studies have been done. A target prototype module will be placed in a test beam in the next year.

Magnetic horns are used to focus the secondaries from the target. They work by producing an azimuthal magnetic field between concentric inner and outer conductors. This field focuses charged particles of the correct sign and some energy range, and defocuses the particles of the opposite sign. The horns are water-cooled and have their operating magnetic fields known to 1%. A prototype of horn 1, the upstream horn and the one undergoing the greatest stress, will be tested for 50 weeks to demonstrate horn lifetime objectives (except for radiation damage effects). The target and horns at the target station will be mounted on universal modules that are lowered into the steel shielding channel. The design is based on that of the Fermi antiproton target station.

1.4.3 Power Supply Systems

The power supply system consists of power supplies for the beamline elements, cables and connections from the power supplies to the 480 VAC power panel, and cables and connections from the power supplies to the devices that they power, including those for MINOS. The major items for this system are the 200 kA power supply system and the parallel strip transmission line for the horns. For this transmission line the challenges are the long-term reliability of the insulation, the bolted connections and joints, and flexibility in the location where horn 2 can be located within the target hall.

Existing power supplies from decommissioned fixed target areas and the Main Ring are used for all but the septa and the horns. These used supplies will require some upgrades and refurbishment. All but the quadrupole and trim magnet supplies will be ramped to reduce power consumption.

1.4.4 Hadron Decay and Absorber Regions

The decay pipe region, beam monitoring instrumentation and hadron absorber are located downstream of the target hall. The decay region provides a space where secondary particles from the target decay to yield muon neutrinos. The amount of material in this area must be minimized to reduce the anti-neutrino contamination of the beam. This requires that the decay pipe be evacuated and limits the amount of material in its windows. This area must be provided with sufficient shielding to protect groundwater in the adjacent rock.

The hadron absorber at the end of the decay pipe must absorb the bulk of the energy of non-interacting protons and nondecaying secondary particles that reach it and transfer that energy for removal by the RadioActive Water (RAW) system. The only energetic particles exiting the absorber are muons and neutrinos, the muons being stopped in the 150 meters of rock immediately downstream.

1.4.5 Neutrino Beam Monitoring

The neutrino beam monitoring systems are used to control beam quality. This is done by measuring the flux and beam profiles of the non-interacting primary protons and secondary hadrons upstream of the beam absorber and the muons downstream of it in the dolomite muon shield. The information from these beam monitors can be combined with the MINOS near detector neutrino event rate and spatial distribution to insure that the neutrino beam is functioning correctly. Studies indicate that segmented wire ionization chambers (SWICs) operating with He gas in ionization mode can withstand the hadron flux at the start of the decay pipe. The muon monitors are located directly following the hadron absorber and in three slots downstream of the start of the dolomite.

1.4.6 Alignment Systems

Alignment of the beam line components is clearly important in order to hit the far detector 730 km away with a neutrino beam. Although the NuMI beam, for most neutrino energies, is a few kilometers wide by the time it reaches Soudan, the requirement of the alignment effort nonetheless is to have the beam center pass within 167 m of the far detector; this requirement is imposed by the physics analysis. The relative positions of Fermilab and Soudan will be determined by simultaneous measurements using the GPS satellites.

1.4.7 Water, Vacuum and Gas Systems

Cooling water at Fermilab is divided into the Industrial Cooling Water (ICW), Low Conductivity Water (LCW) and RAW categories. These water systems are used to remove the heat generated by the operation of electrical devices and the heat deposited by the interaction of components with high energy beams. ICW is just cooling pond water that dissipates its heat into the air. ICW is unfit for use in magnets and power supplies, which require low electrical conductivity. The LCW passing through magnets, power supplies and other components exchanges its heat with the ICW. Some devices operate in high radiation environments, which induce activation within their cooling water. Heat in activated water containing tritium is handled by RAW systems, which transfer the heat to the LCW system, which in turn exchanges it with the ICW. NuMI will be the first Fermilab facility to operate deep underground, so challenges caused by hydrostatic effects will require special attention and care.

Four types of industrial gas are needed in the NuMI beamline: helium, Ar/CO_2, CO_2 and hydrogen. The helium is needed to fill voids inside of the shielding in the vicinity of the target and the horns in lieu of vacuum. Ar/CO_2 and CO_2 are required for the SWICs in the primary and secondary beams. Some of the beam monitoring instrumentation will require a small amount of a mixture of Helium and Hydrogen.

Evacuated pipe will be present in various locations along the NuMI beamline. With the exception of the septa and Lambertsons, the vacuum requirements are modest since beam will pass through a given component only once.

1.4.8 Systems Integration

The role of systems integration is to provide the technical and administrative oversight throughout the NuMI project so that the performance goals will be met. It also includes beamline cables, beamline control systems and radiation safety system (beamline electrical and radiation interlock systems, activated air mitigation, groundwater monitoring). The radiation safety system also must serve to minimize personnel exposure and to ensure satisfaction of regulatory requirements. The successful coordination of all these aspects requires careful attention from the start of the project.

1.5 Radiation Safety

Chapter 4 presents the radiation safety considerations that have gone into the design of the NuMI beamline, with an emphasis on the shielding requirements. Inherent in the design is the fact that radiation protection is of the greatest importance in both primary and secondary beam areas. The purpose of this chapter is to present the various radiation-related matters and to explain the methodology that has guided the designs of the radiation protection systems in the project. It should be noted that at this stage we have attempted to address all of the major issues that have an impact on determining a baseline design. There are, however, a number of topics that continue to be studied. These include radiation protection issues associated with the Main Injector extraction, quantitative evaluation of the level of airborne activation expected in the target hall and a quantitative assessment of potential activation from the production of tritium in the groundwater in the vicinity of the underground facility.

1.6 Civil Construction

A summary of the conventional construction on the Fermilab site, and in particular a discussion of the technical requirements for the facility, is presented in Chapter 5.

The major civil construction components for NuMI are given in Table 1-1. Of the listed items, the carrier pipe and the access shafts are partially in glacial till and partially in bedrock. The remainder of the list is constructed in bedrock, which begins approximately 60 to 70 feet below the surface. Construction conditions that will be encountered are similar to those seen in the Tunnel and Reservoir Plan (TARP) project in the Chicago area and extensive use of that experience has been used in the NuMI civil design.

The requirements for the pretarget tunnel, the target enclosure, the decay tunnel, the absorber enclosure and the muon alcoves are driven by the components that must be housed in them and by their shielding needs. The requirements for the downstream access shaft, MINOS access tunnel and MINOS enclosure are driven by the components of the MINOS near detector and the muon shielding requirements for it. Heating, cooling, ventilation (including radiological, cooling and humidity control), water inflow control, acoustic control, fire safety and life safety are all issues that are addressed in the design.

1.7 Cost and Schedule

A brief summary of the cost and schedule for the NuMI Facility is given in Chapter 6. It includes a cost breakdown by WBS element and a summary schedule of the tasks. This is addressed in detail in the NuMI/MINOS Cost & Schedule Plan.

1.8 Project Management Summary

Chapter 7 presents a summary of the project management systems for the NuMI Facility Project. This includes the management philosophy for the overall NuMI Project, specific roles and responsibilities for managing the project at Fermilab and a summary of project controls. These management systems are described in detail in the NuMI Project Management Plan, which is prepared and maintained by Fermilab, and the NuMI Project Execution Plan, which is prepared and maintained by the DOE Project Manager.

Subtask	Description
Carrier Pipe Tunnel	Pipe to bring protons from the Main Injector to the NuMI primary beam elements deep underground
Pre-Target Tunnel	Tunnel enclosure to house NuMI primary beam elements deep underground
Target Enclosure	Underground hall to house neutrino beam elements (target & horns)
Upstream Service Building	Building on surface to provide access and services to upstream areas
Upstream Access Shaft	Shaft to access target hall, power supply room and connector tunnel
Decay Tunnel	Underground tunnel to allow secondary mesons to decay in flight, producing neutrinos
Absorber Enclosure	Underground enclosure for the hadron absorber
Downstream Service Building	Building on surface to provide access and services to downstream areas
Downstream Access Shaft	Shaft near hadron absorber to access downstream NuMI areas, including the muon alcoves and the experimental hall
MINOS Access Tunnel	Underground corridor, offset from neutrino/muon flight path, from the downstream shaft to the experimental hall housing the MINOS near detector
Muon Alcoves	Three short tunnels transverse to the beamline from the MINOS Access Tunnel into the neutrino/muon beam to house beam monitoring devices
Experimental Hall	Underground hall to house the MINOS near detector

Table 1-1 Civil construction of the NuMI Project at Fermilab.

Figure 1-1 Layout of the NuMI Facility (See Insert).

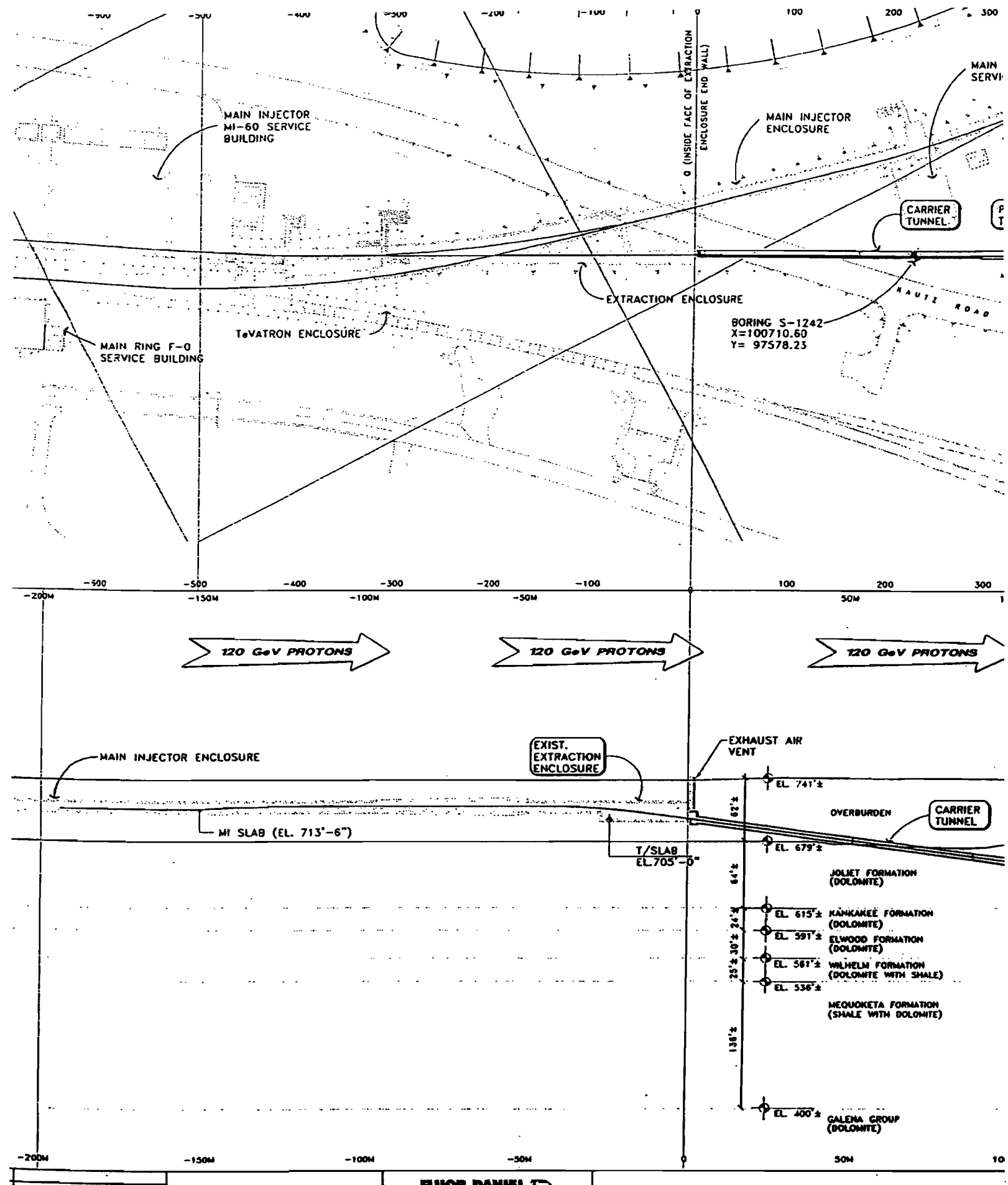

	FLUOR DANIEL / HARZA	
	NAME	DATE
DESIGNED	A. VASONIS	SEPT. 1990
DRAWN	R. JEDZINIAK	SEPT. 1990
CHECKED		
APPROVED		

DESCRIPTIONS
REVISIONS

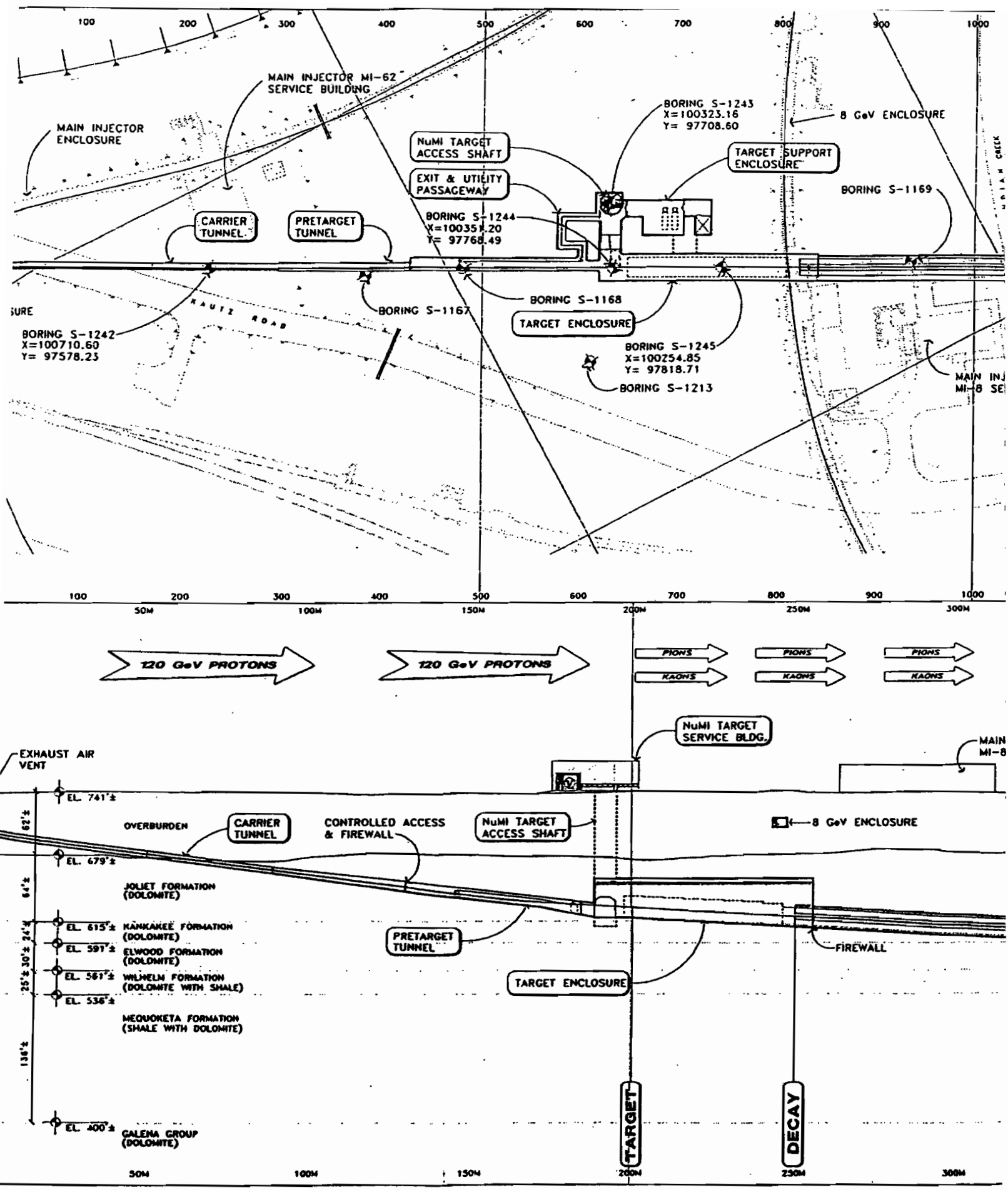
MAIN INJECTOR MI-62 SERVICE BUILDING
MAIN INJECTOR ENCLOSURE
NuMI TARGET ACCESS SHAFT
EXIT & UTILITY PASSAGEWAY
BORING S-1243 X=100323.16 Y= 97708.60
8 GeV ENCLOSURE
TARGET SUPPORT ENCLOSURE
BORING S-1169
CARRIER TUNNEL
PRETARGET TUNNEL
BORING S-1244 X=100351.20 Y= 97768.49
BORING S-1168
BORING S-1167
TARGET ENCLOSURE
BORING S-1242 X=100710.60 Y= 97578.23
BORING S-1245 X=100254.85 Y= 97818.71
BORING S-1213
RAUTZ ROAD
100 200 300 400 500 600 700 800 900 1000
50M 100M 150M 200M 250M 300M

120 GeV PROTONS
120 GeV PROTONS
PIONS
KAONS
PIONS
KAONS
PIONS
KAONS
NuMI TARGET SERVICE BLDG.
EXHAUST AIR VENT
EL. 741'±
OVERBURDEN
CARRIER TUNNEL
CONTROLLED ACCESS & FIREWALL
NuMI TARGET ACCESS SHAFT
8 GeV ENCLOSURE
EL. 679'±
JOLIET FORMATION (DOLOMITE)
EL. 615'±
KANKAKEE FORMATION (DOLOMITE)
EL. 591'±
ELWOOD FORMATION (DOLOMITE)
EL. 561'±
WILHELM FORMATION (DOLOMITE WITH SHALE)
EL. 536'±
MEQUOKETA FORMATION (SHALE WITH DOLOMITE)
EL. 400'±
GALENA GROUP (DOLOMITE)
62'±
64'±
24'±
30'±
25'±
136'±
PRETARGET TUNNEL
TARGET ENCLOSURE
FIREWALL
TARGET
DECAY
50M 100M 150M 200M 250M 300M

Neutri

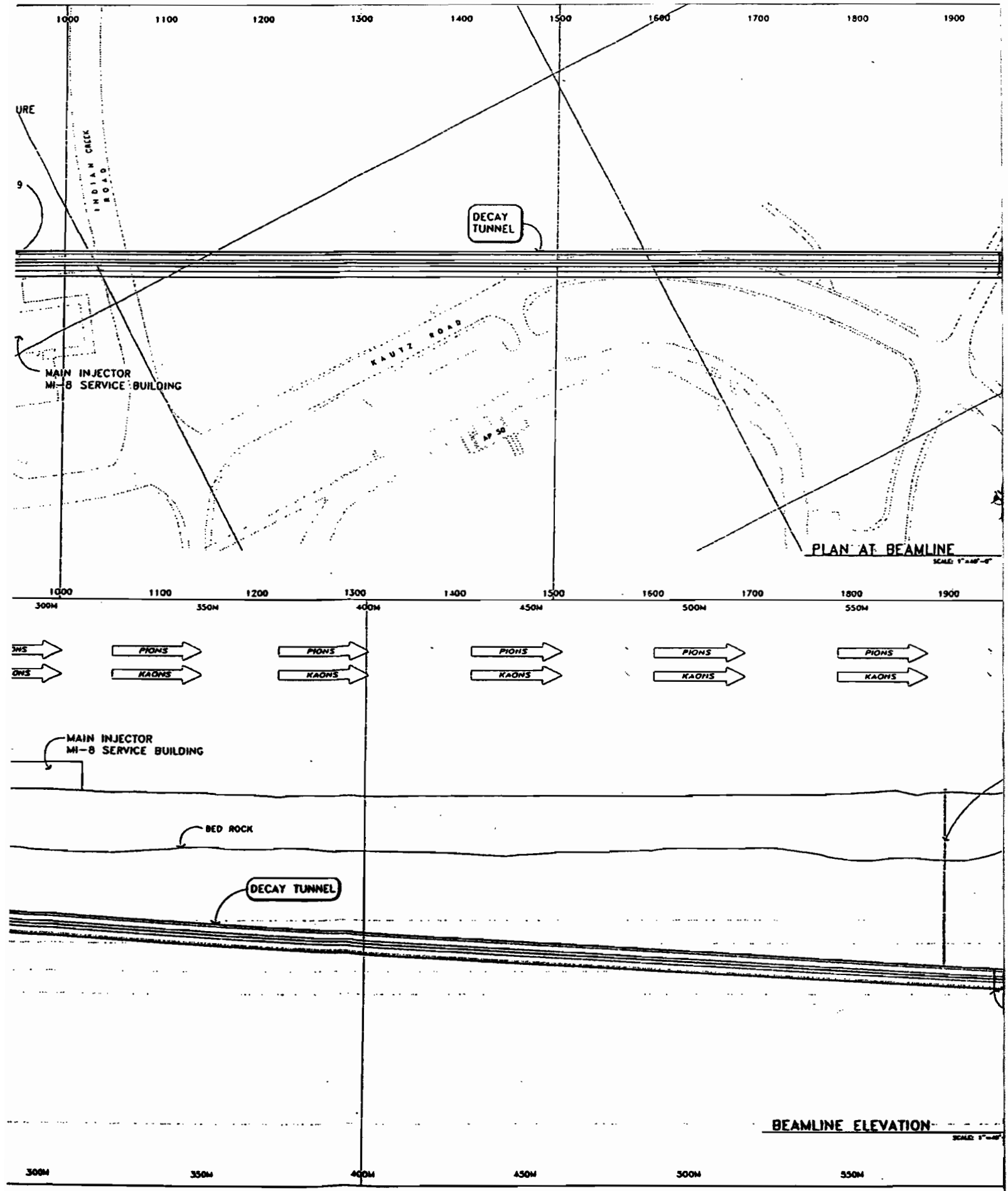

trinos at Main Injector (M

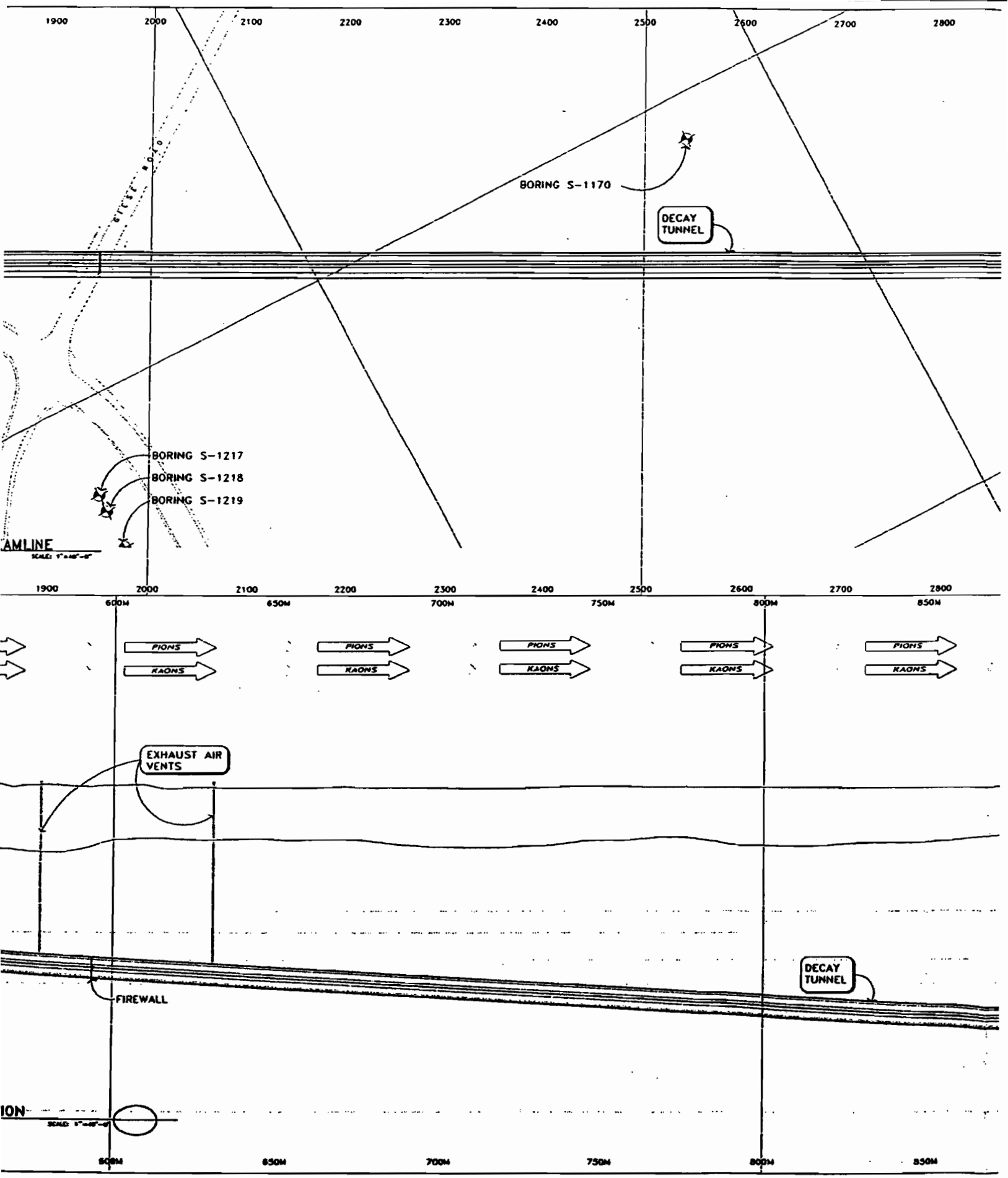

(NuMI) PROJECT

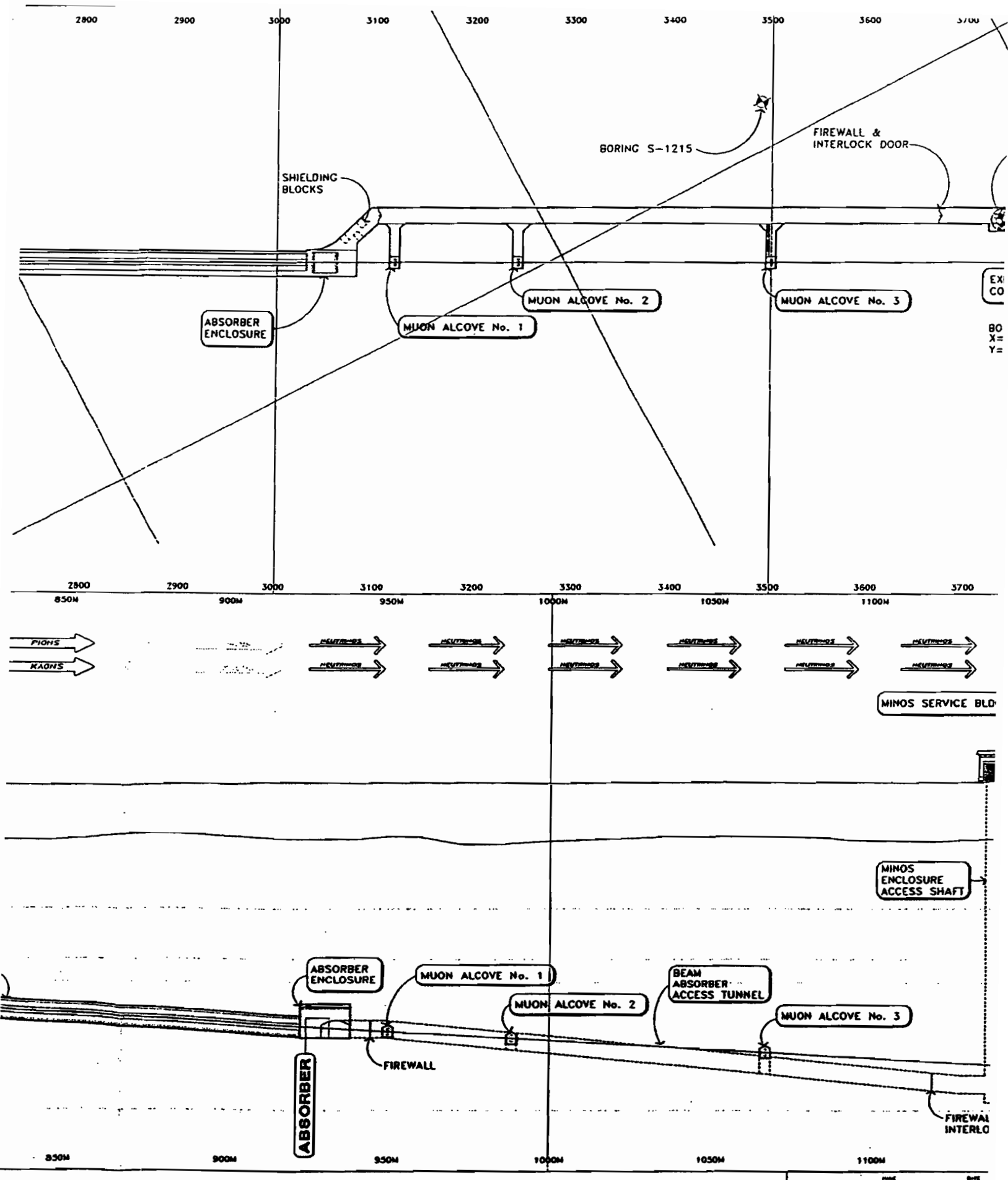
2800
2900
3000
3100
3200
3300
3400
3500
3600
3700
BORING S-1215
FIREWALL &
INTERLOCK DOOR
SHIELDING
BLOCKS
ABSORBER
ENCLOSURE
MUON ALCOVE No. 1
MUON ALCOVE No. 2
MUON ALCOVE No. 3
850M
900M
950M
1000M
1050M
1100M
PIONS
KAONS
NEUTRINOS
MINOS SERVICE BLD
MINOS
ENCLOSURE
ACCESS SHAFT
ABSORBER
ENCLOSURE
MUON ALCOVE No. 1
MUON ALCOVE No. 2
BEAM
ABSORBER
ACCESS TUNNEL
MUON ALCOVE No. 3
FIREWALL
ABSORBER
FIREWAL
INTERLO

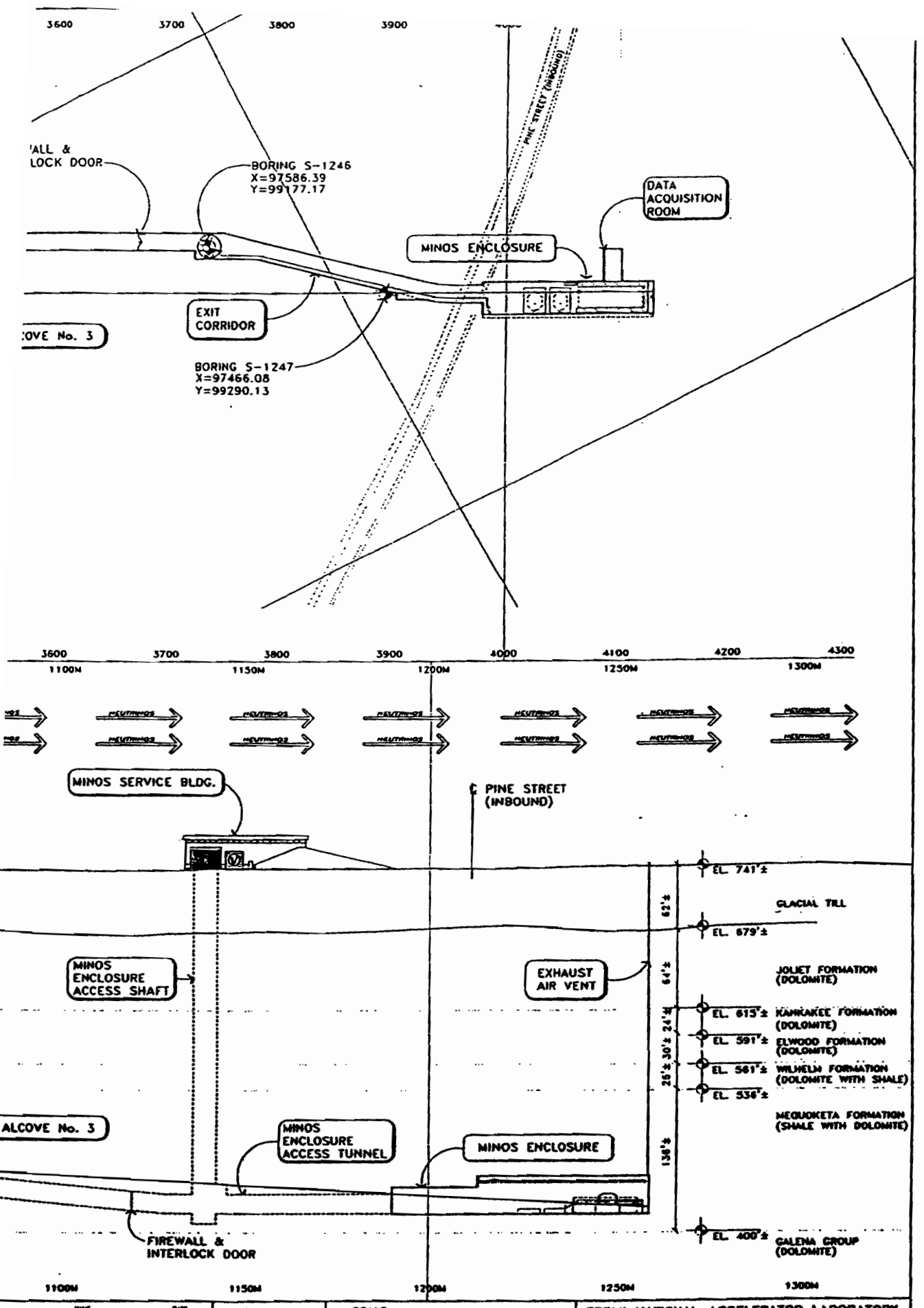

	NAME	DATE

PROJECT NORTH

SCALE:

FERMI NATIONAL ACCELERATOR LABORATORY

UNITED STATES DEPARTMENT OF ENERGY

NuMI PROJECT

NuMI ENCL. OVERALL PLAN & PROFILE

DRAWING NO. 6-7-1 (TITLE-1) C-12 REV.

OCT. 1998

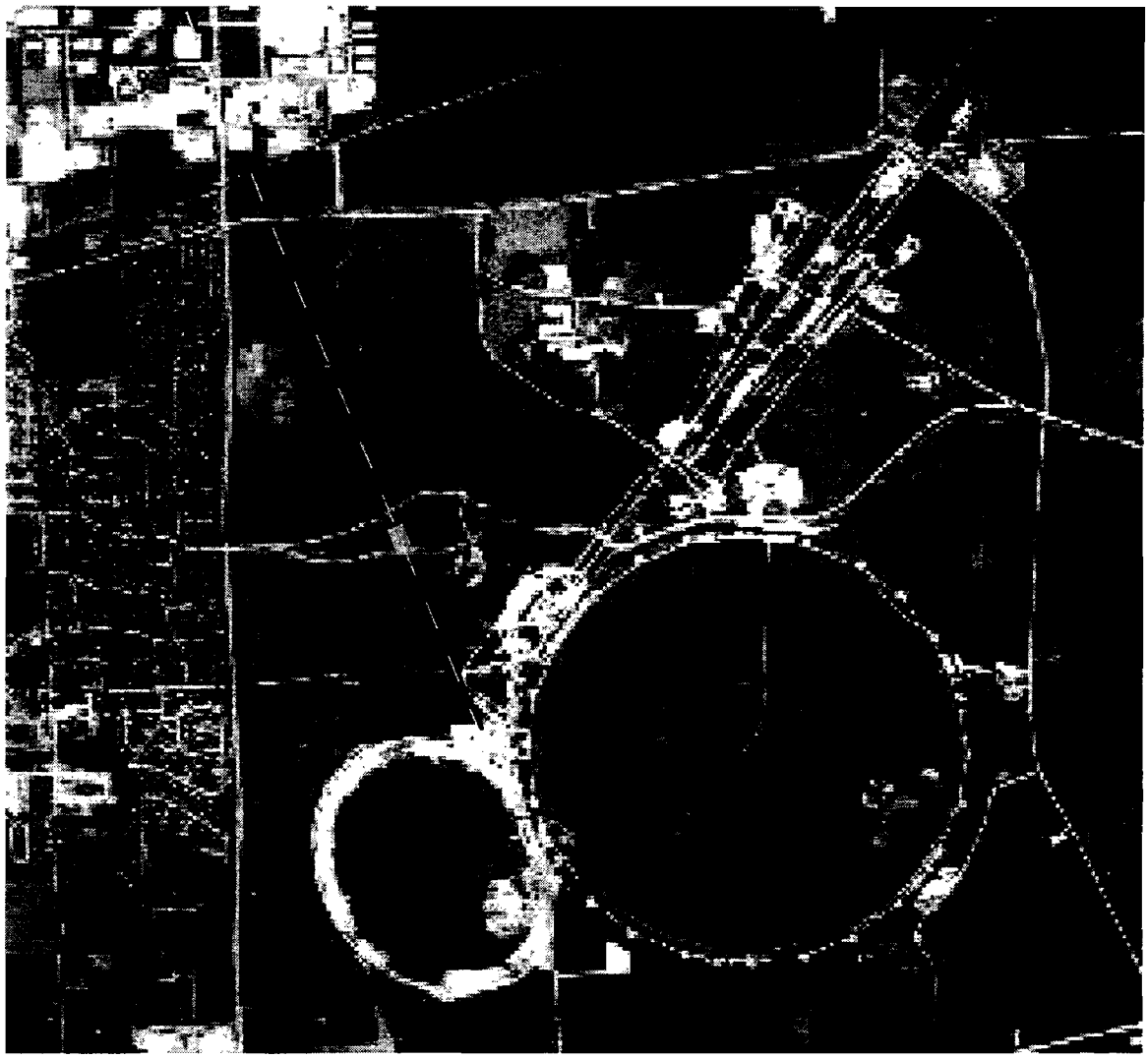

Figure 1-2 Aerial view of the Fermilab site and the proposed NuMI beamline.

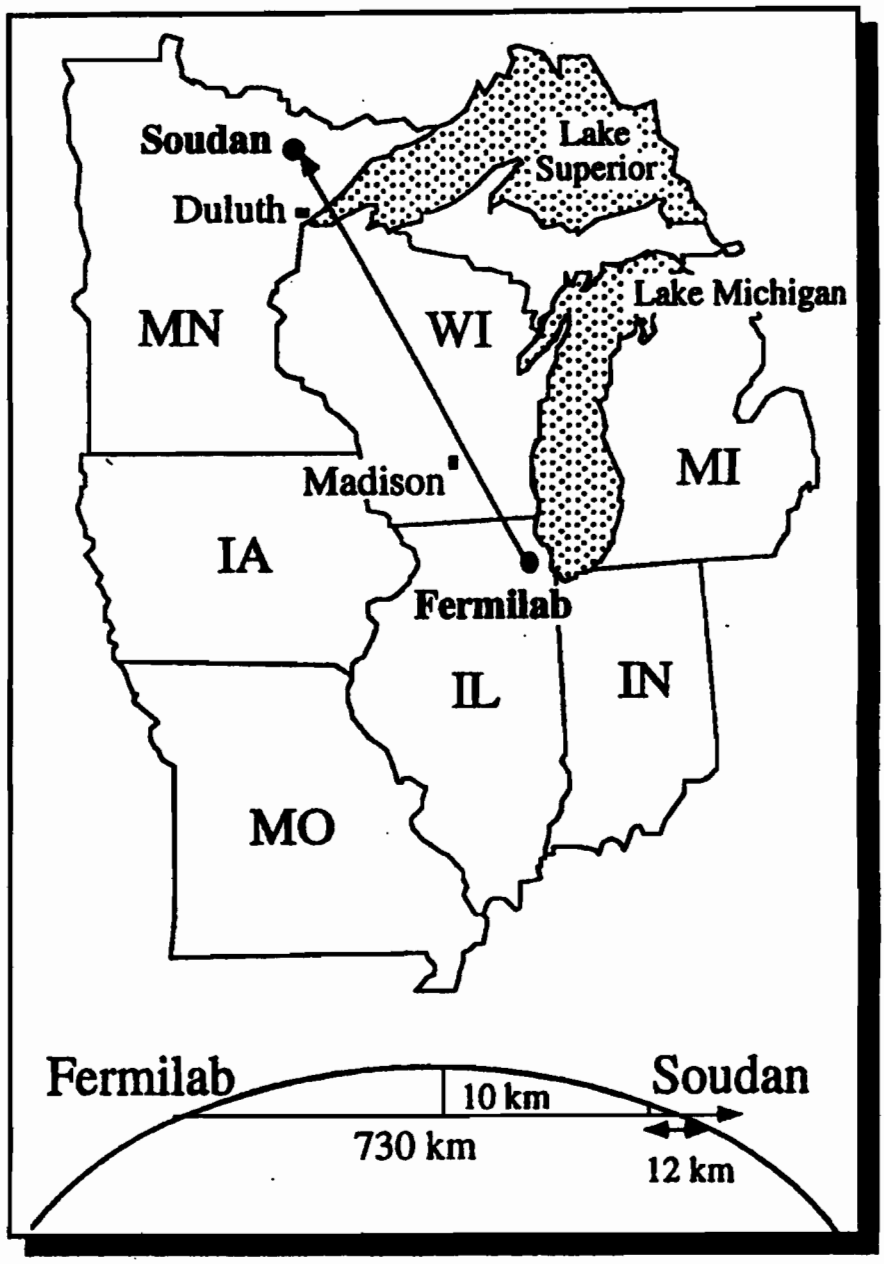

Figure 1-3 Trajectory of the neutrino beam between Fermilab and Soudan, Minnesota.

2.0 Neutrino Beam Requirements and Conceptual Design

Table of Contents

2.0 NEUTRINO BEAM REQUIREMENTS AND CONCEPTUAL DESIGN 2-1

2.1 INTRODUCTION 2-3
2.2 NEUTRINO BEAM FUNDAMENTALS 2-3
2.3 NEUTRINO OSCILLATION EXPERIMENTS 2-4
2.4 NEUTRINO BEAM CONCEPTUAL DESIGN 2-5
2.4.1 Extraction 2-6
2.4.2 Transport of Primary Protons 2-7
2.4.3 Target 2-7
2.4.4 Horn Focusing System 2-8
2.4.5 Decay Pipe 2-9
2.4.6 Hadron Absorber 2-10
2.4.7 Muon Shield 2-10
2.4.8 The "Near" Detector 2-10
2.4.9 The "Far" Detector Event Rate 2-11
2.5 COMPARISON OF NUMI WITH OTHER NEUTRINO FACILITIES 2-11
2.6 NEUTRINO OSCILLATION SIGNATURES IN MINOS 2-11
2.6.1 Neutral Current (NC) to Charged Current (CC) Ratios 2-12
2.6.2 CC Far/Near 2-13
2.6.3 MINOS CC Total Energy Spectrum 2-13
2.6.4 MINOS Electron ID 2-14
2.6.5 MINOS τ ID 2-14
2.6.6 Summary of Systematic Limitations on the Measurements 2-15
2.7 SPECIAL CHALLENGES IN BEAM DESIGN 2-16
2.8 FUTURE NARROW BAND BEAM 2-16

Table of Tables

Table 2-1 Summary of neutrino event rates at Soudan for three tunes of the PH2 wide band beam. ν_τ rates are calculated assuming oscillations with $\sin^2(2\theta) = 1$, while no oscillations are assumed for the other flavors. 2-18

Table 2-2 Comparison of NuMI with other neutrino facilities. 2-18

Table of Figures

Figure 2-1 Schematic drawing of the NuMI neutrino beam-line. 2-19

Figure 2-2 Oscillation probability as a function of energy for values of Δm^2 covering the region appropriate to the atmospheric anomaly. 2-20

Figure 2-3 CC event total energy in the MINOS far detector distorted by oscillations. 2-21

Figure 2-4 The ratio of the of ν_τ charged current interaction cross section to the ν_μ charged current interaction cross section, plotted as a function of neutrino energy. 2-22

Figure 2-5 Comparison of event rates at Soudan in the case of ideal perfect focusing, and rates achieved with three configurations of the PH2 beam design. 2-23

Figure 2-6 Schematic drawing of a long, slim segmented target for optimum meson production and decay of pions. 2-24

Figure 2-7 The energy spectrum of π^+ from a 2 mm radius 2 interaction length carbon 2-25

Figure 2-8 Schematic drawing of PH2 beam focusing configurations in the NuMI target hall. To change the tune to lower energy, the target is moved closer (and finally into) the first horn, and the horns are moved closer together. A physically different target is used for each configuration. 2-26

Figure 2-9 Fraction of π^+s decaying in the 675 m decay pipe as a function of pion energy, and the corresponding approximate neutrino energy for well focused pions. 2-27

Figure 2-10 Comparison of event rates as a function of decay pipe length and radius. 2-28

Figure 2-11 Energy spectra of the various PH2 NuMI beam configurations. Anti-ν_e rates are below the bottom of the plot as are those of ν_τ 2-29

Figure 2-12 Schematic drawing of narrow band beam components. FD1 and FD2 are the same two horns used in the PH2 WBB. As shown, FD1 is moved vertically switching from WBB to NBB. B1, B2, and B3 are dipole bending magnets. 2-30

Figure 2-13 Energy spectrum for various tunes of the narrow band beam. 2-31

2.1 Introduction

This chapter describes how the physics goals of the MINOS experiment impose certain requirements upon the design of the NuMI neutrino beam. Also described are general properties of neutrino beam systems and how these can be tailored to the physics needs. In particular, a quite flexible design has been adopted for NuMI, which allows a versatile future program. For a more detailed description of neutrino oscillation experiments, see the companion document "The MINOS Experiment Technical Design Report".

2.2 Neutrino Beam Fundamentals

Most neutrino beams used in high energy physics are designed to be nearly pure beams of muon type neutrinos, ν_μ. The components to produce such a beam are illustrated in Figure 2-1. High energy protons are fired at a target to produce a high flux of pions (π) and kaons (K), which then decay after some distance into muons and muon neutrinos (i.e. $\pi^+ \rightarrow \mu^+\nu_\mu$). Focusing horns or quadrupole magnets are used to guide a large fraction of the π/K flux along the desired neutrino beam direction. The neutrinos are created along the length of a large diameter decay pipe. The pipe is followed by steel and earth to absorb the undecayed hadrons and the muons. A typical neutrino beamline is hundreds of meters in length from the primary target to the experimental detector, where neutrino interactions can be observed.

The energy spectrum of a neutrino beam created in this manner is calculated from measured π/K production data with simulation of focusing elements and decay kinematics. In general, secondary particles, such as π's from proton-nucleus interactions, are produced with transverse momenta of order 0.3 GeV/c. The longitudinal momenta cover a wide range, with 1 to 50 GeV/c being relevant for NuMI.

Pion decay kinematics leads to the following approximate relationships for the neutrino energy and a quantity proportional to flux

$$E_\nu = \frac{0.427 E_\pi}{(1+\gamma^2\theta^2)}$$

$$Flux = \left(\frac{2\gamma}{1+\gamma^2\theta^2} \right)^2 \frac{A}{4\pi r^2}$$

where γ is the Lorentz boost of the pion, θ is the angle between the pion and neutrino flight directions (not to be confused with the neutrino oscillation θ for which the same symbol is traditionally used), A is the cross-sectional area of the detector, and r is the distance to it. The energy and flux of the neutrinos peak along the pion flight direction, $\theta = 0$.

The typical production angle of a pion is $p_t/p_l \sim 0.3/(m_\pi\gamma) \sim 2/\gamma$; for zero degree targeting this is the same as the angle θ above. Thus one can see from [2] that there is a factor of order 25 to be gained in the flux by focusing the pions towards the detector, the $\theta = 0$ case. This factor, and the desire to keep the radius of the decay pipe reasonably small, are the motivation for a horn focusing system. Note from [1] that for well focused pions and a detector near the axis of the pion beam, the $\theta = 0$ situation. The neutrino's energy is 43% of that of the pion. From [2] the Lorentz boost favors neutrinos from high energy pions, thus high energy neutrinos, in the flux by a factor γ^2. A further implication, since one cannot simultaneously focus pions of all energies, is that one must choose a certain neutrino energy range to emphasize.

The optimization of the focusing system is guided by the desired shape of the energy spectrum of the neutrinos which will result from the π and K decays. For the NuMI beam the shape of this spectrum is chosen to maximize the ability to search for neutrino oscillations in a particular region of parameter space, as is described in the following sections.

2.3 Neutrino Oscillation Experiments

Neutrino oscillation searches can be characterized as either "appearance" or "disappearance" experiments. In an appearance experiment, the flavor composition of the initial neutrino source should be well known, and ideally limited to a single flavor. Then if the experiment is able to detect the interactions of neutrinos of a different flavor, it can be concluded that the original neutrinos have indeed oscillated. Alternatively, an experiment which is capable of distinguishing a single flavor of neutrinos, in particular that of the initial source, can measure the flux of those neutrinos at a distance from the source and determine whether or not the number of neutrinos expected (in the absence of oscillations) has arrived. If the expected number is not observed the conclusion can be drawn that the neutrinos have

"disappeared" or oscillated into a different flavor. There are also a number of "pseudo-appearance" (emergence of a different type of event signature, see Section 2-6) measurements that experiments can make which can provide convincing signatures of neutrino oscillations. Several of these, which will be used in the NuMI/MINOS search, are described later in this chapter.

Beam design goals include achieving the highest possible ν_μ intensity, low backgrounds of other neutrino flavors, well understood spectra so that systematic errors are small, and the selection of a neutrino energy spectrum matched to the oscillation physics. The rest of this section describes how the energy spectrum goals drive the NuMI design.

Given the fixed distance between Fermilab and Soudan, the energy spectrum of oscillations depends only on the parameter Δm^2, with the strength characterized by the parameter θ (neutrino oscillation θ) . Several examples of oscillation probability as a function of energy, chosen to essentially cover the Δm^2 region indicated by the atmospheric neutrino anomaly, are shown in Figure 2-2. At very low energy, oscillations are so rapid that the detector resolution washes out individual wiggles, although one can still look for average signals. With a beam which covers a fairly broad energy spectrum (called a wide band beam), including the highest oscillation energy, one can detect the oscillation shape, as is illustrated in Figure 2-3 for ν_μ charged current interactions. Further, measuring the position and depth of the oscillation signal, such as is seen in that figure, yields precision measurements of Δm^2 and $\sin^2(2\theta)$. Producing neutrinos at even higher energies is not very useful, since the oscillation probability falls off as E^{-2}. It can be shown that to address the atmospheric anomaly MINOS requires neutrinos in the energy range of order 1 to 20 GeV.

In the case of ν_τ appearance experiments, looking for events from the oscillation of $\nu_\mu \rightarrow \nu_\tau$, the threshold for production of a τ lepton also comes into play. Because of the energy turn-on, as shown in Figure 2-4, the region from 5 GeV to 15 GeV remains the interesting one, even at low Δm^2.

2.4 Neutrino Beam Conceptual Design

As is explained in the previous section, a beam energy spectrum that covers from 1 to 20 GeV is desired. However, magnetic-horn beam devices typically deliver maximum focusing over a momentum bite of only about a factor of three. To address this, we have

designed a horn system which can cover the energy region in three steps, using the same horns, although with a different targets and the horns set in different positions; that coverage is shown in Figure 2-5. The resulting event rates for the three configurations are compared in this plot with the idealized case of what one would obtain if one could perfectly focus all pions down the beamline without loss. In each configuration the focusing achieves, at its optimal energy, about half the event rate of the perfect focusing case, which is typical of horn systems.

Parabolic shaped horns were found to be better than conical ones in allowing for such reconfiguration, and two horns are used. Thus the beams are labeled PH2(he), PH2(me) and PH2(le) for the two parabolic horn high energy, medium energy, and low energy configurations.

An additional benefit of the parabolic horn system is that the horns can be reconfigured, with the addition of some dipole magnets and collimators, to produce a beam with a quite limited energy spectrum. Such a so-called narrow band beam can be highly desirable as a tool for detailed studies, once the oscillation parameters are narrowed down. A design of such a beam for NuMI is presented at the end of this chapter.

Finally, the same set of horns could also produce an anti-neutrino beam to study possible CP violation.

The purpose of this section is to give an integrated conceptual overview of the major elements of the baseline wide band beam. Technical and engineering details related to the design, construction, installation and operation of the individual beam components and support systems are presented in Chapter 3.

2.4.1 Extraction

The 120 GeV protons are taken out of the Main Injector accelerator using resonant extraction techniques, with regulation developed specifically for fast beam pulses. An instability is induced in the orbit of the protons using in concert the main quadrupole circuit, one of the correction quadrupole families and the zero harmonic octupoles. At a predetermined point of maximum excursion from the nominal orbit, the unstable protons encounter an electric field that kicks them toward an extraction channel. Three Lambertsons and one C-magnet complete the extraction. In this manner, the entire set of

circulating protons is extracted in roughly 100 turns taking of order 1 millisecond. The machine repetition cycle for this mode of extraction is expected to be 1.9 seconds. To produce the NuMI beam with the intensities required to achieve the MINOS experimental goals will require extraction of at least 2.5×10^{13} protons per pulse. It is expected that a routine operating intensity to NuMI of 4×10^{13} protons per pulse can be achieved by 2003.

2.4.2 Transport of Primary Protons

The extracted protons are focused and bent strongly downward by a string of quadrupoles and bending magnets so that they enter the pre-target hall located 150 feet downstream of the NuMI Stub, a specially constructed appendage to the MI enclosure. (For conventional construction reasons the pre-target and target halls are located in the dolomite rock formation, requiring that the initial trajectory be bent down more than is actually required to aim the neutrino beam to Soudan. See Section 5.1.4.) Another set of bend magnets brings the protons to the correct pitch (-58 mrad) for a zero targeting angle (maximum intensity) beam directed toward the experiment. The size and angular dispersion of the proton beam is controlled by a final set of quadrupoles and is matched to the diameter of the production target. The TRANSPORT "beam sheet" used to specify the primary beam described in Section 3.1 is given in Appendix A.

2.4.3 Target

The extracted protons interact with nuclei in the target, producing pions and kaons with a broad spectrum in both longitudinal and transverse momentum. The design of the NuMI target and focusing system has been done as a unit to maximize the ν_μ charged current event rate at the MINOS far detector.

The target should be sufficiently long to interact most of the primary protons from the Main Injector, but small enough so that *secondary* interactions of the π's and K's are minimized and energy absorption is low. This is achieved with a target that is long and thin, allowing secondary particles to escape through the sides, as illustrated in Figure 2-6. The depth of field of the horn focusing system sets a limit on the length of the target, but is fairly large (of order one meter).

The optimal choice of target radius is driven by two opposing trends: the *desired* flux of pions and kaons out of the target decreases with increasing radius due to particle re-absorption, but *undesirable* target stress from the heat load of the high intensity proton beam also decreases with increasing target and beam spot radius. With several 10^{13} protons striking the target every 2 seconds, the target becomes highly radioactive soon after beam start-up. Replacement of a failed target is then an arduous and time-consuming process. The design of the target is therefore a compromise between obtaining maximum yield and ensuring integrity against mechanical failure due to shock and heat build-up.

The nominal design used in simulation studies is of a segmented graphite target of two interaction lengths for the PH2(he) and PH2(me) configurations. For the PH2(le) configuration a somewhat shorter beryllium target is assumed.

For reference, the energy spectrum of π^+ from a 2 mm radius, 2 interaction length carbon target, from a Monte Carlo simulation, is shown in Figure 2-7.

2.4.4 Horn Focusing System

The target is followed by two focusing horns (see Section 3.2 for a detailed description), which produce toroidal magnetic fields and act as lenses to bend the secondary particles (of one sign) back to the primary proton direction. Of course the neutrinos from the decays of the π's and K's do not all follow the same path, but from the formulas in Section 2.2 it can be seen that they are strongly directed along it. Thus the optimum design has all secondary particles directed toward the detector so that the resulting neutrino flux is maximized. However, in reality one can focus some of the pions at all momenta or all of the pions at some momenta, but not all pions at all momenta for all angles from the target.

NuMI has chosen horns with parabolic shaped inner conductors. These produce magnetic fields that act to first order as lenses, where the focal length is proportional to the pion momentum. Thus a selection of a certain target position causes a certain momentum to be focused by the first horn. Pions that were well focused by the first horn pass unaffected through a central aperture in the second horn. Pions that were somewhat over- or under-focused by the first horn drift to larger radius and are focused by the second horn, extending the momentum bite focused by the system.

The pions actually pass through the current carrying inner wall of a horn to reach the focusing magnetic field, and absorption of the pions in the horn walls ranges from 20% to 40% depending on the incidence angle. The design of a horn is a balance between trying to make the inner wall thin (to reduce absorption) and sturdy (since it is subjected to large pulses of electric current – 200 kA in the NuMI design). A water spray is used to keep the aluminum inner conductor below 100 C.

The deployment of the horns and target to achieve the various PH2 beam neutrino event spectra described above are shown in Figure 2-8.

2.4.5 Decay Pipe

The decay pipe provides an evacuated space for the secondary π's and K's to decay. The choice of length is a compromise between the neutrino flux in the detectors and reasonable cost. The neutrino flux is predominantly from the pions with momentum between 2 GeV/c and 60 GeV/c. At the upper end of this range, the mean decay length of a π is several km. The number of high energy neutrinos for the long baseline experiment thus continues to increase significantly with any reasonable decay pipe length. The current baseline design is driven by cost, calling for a decay pipe length of 675 m. Combining the 675 m decay pipe with the 50 m distance from target to start of the decay pipe results in a 725 m long decay region for the beamline. The fraction of pions that decay in the pipe is plotted *vs.* energy in Figure 2-9.

The choice of radius for the decay pipe is made by balancing the loss of secondaries that interact with the walls of the pipe against the cost increases associated with larger radius pipes. In general, for the nominal beam pipe length the gains in neutrino flux are rather dramatic as the radius of the pipe increases to about 1 m with comparatively modest gains over the next meter of increase.

As shown in Figure 2-10, a larger-radius decay pipe would be more optimal for the low energy (PH2me) configuration, while a longer one would be better for the high energy (PH2me) beam. The baseline combination of 1 m radius and 725 m decay length is a reasonable compromise.

It is important to note that in choosing parameters one should not isolate the optimization of beam pipe parameters from the rest of the NuMI Project, which includes the massive

experimental detectors. It is reasonable to compare tradeoffs in cost and event rates when the sizes of both systems, i.e., the beamline and the neutrino detector, are varied.

2.4.6 Hadron Absorber

The experimental detectors are designed to observe the interactions of neutrinos. Other types of particles must be eliminated since their much higher event rates would dominate data acquisition. All hadrons, including those primary protons that did not interact in the target, are stopped by a hadron absorber at the end of the decay pipe. Because the absorber is far downstream of the target, the natural divergence of the proton beam implies a larger spot size at the absorber, and the absorber does not have to handle nearly so high a deposition energy density as the target does. The absorber consists of a water cooled aluminum central core, surrounded by steel.

2.4.7 Muon Shield

The hadron absorber alone is too short to eliminate the muon component of the beam, which interacts only electromagnetically. These muons must be absorbed before reaching the MINOS near detector. Muons can be eliminated by active shielding based on large and expensive magnetic devices or by providing sufficient medium to slow them down via multiple scattering. The NuMI beamline is located in dolomite which is a dense rock, and 240 meters of dolomite between the end of the hadron absorber and the near detector is sufficient to stop all muons coming from the decay pipe.

2.4.8 The "Near" Detector

The MINOS near detector is used to measure the spectrum of neutrinos produced by the NuMI beamline, at a distance small compared to that normally assumed for oscillations. This produces a beam calibration.

The facility layout provides for 50 meters of empty space just upstream of the detector. The purpose of this space is to reduce the number of muons, produced from neutrino interactions occurring in the dolomite shield, which hit the detector. This space is also the detector assembly area and passageway from the downstream shaft, and hence is available at minimal cost.

2.4.9 The "Far" Detector Event Rate

The different configurations of the baseline NuMI PH2 wide band beam, in the absence of neutrino oscillations, will produce spectra of charged current interactions in the far detector as shown in Figure 2-11. A summary of the event rates from ν_μ, as well as other flavor "background" neutrinos, is given in Table 2-1. The current plan is to begin operations with the PH2(me) configuration, although future results from e.g. the K2K experiment could prompt the choice of one of the other configurations for initial running.

2.5 Comparison of NuMI with other Neutrino Facilities

Table 2-2 shows a list of parameters relevant to comparing facilities for accelerator based neutrino oscillation searches under construction at KEK, namely K2K[1] (aimed toward the Super-K detector) and proposed at CERN, namely NGS[2] (aimed toward the Gran Sasso Laboratory).

KEK will provide beam well before NuMI, and the experiment will produce exciting data. However the event rate is significantly lower than that for NuMI, and the neutrinos are all below τ production threshold.

The CERN NGS beam (which is yet to be approved) would turn on sometime after NuMI. The higher CERN energy gives about 4.5 times as many τ appearance events per proton on target, but the higher NuMI repetition rate more than compensates. For lower Δm^2 disappearance searches, NuMI will have an even larger advantage.

2.6 Neutrino Oscillation Signatures in MINOS

This section presents a discussion of various experimental tests that are used to look for neutrino oscillations. They are presented here due to the constraints which systematic errors in them place on the beam design.

Experiments using the NuMI facility will search for neutrino oscillations by measuring neutrino interactions in both the near detector on the Fermilab site and the far detector at

---

[1] Yuichi Oyama, K2K neutrino oscillation experiment at KEK-PS, talk at the YITP workshop on flavor physics, Kyoto, January 1998, hep-ex/9803 14v2

[2] G. Acquistapace, et.al., The CERN Neutrino Beam to Gran Sasso (NGS), CERN 98-02, INFN/AE-98/05, May 1998

Soudan. We will discuss the following measurements, which have been studied by the MINOS collaboration:

(1) a comparison of the neutral current to charged current event ratios (NC/CC) in the near and far detectors
(2) a comparison of the rate of events containing a muon in the near and far detectors (CC Far/CC Near)
(3) a difference in the energy spectra of charged current events in the two detectors
(4) an excess of events with electrons in the far detector
(5) detection of taus in the far detector

2.6.1 Neutral Current (NC) to Charged Current (CC) Ratios

The most robust test of neutrino oscillations in the MINOS experiment is the measurement of the double ratio of short events (which are mostly neutral current events) to long events (which are mainly muon neutrino charged current events) in the far detector to that in the near detector. The fact that the muons are penetrating particles while hadrons and electrons are not, leads to this easily distinguishable difference in topology.

To explain this test in a simple manner, we first consider a beam consisting solely of muon neutrinos and a perfect detector. The ratio of short to long is then the NC/CC ratio in both the near and far detectors. If ν_μ then oscillates to ν_e or ν_τ between the near and far detectors, the short to long ratio changes in the far detector because ν_e interactions never produce muons and ν_τ charged current events produce muons only 18% of the time.

In reality detectors are not perfect, and some muon events end up in the short category, and some neutral current events end up in the long category. If the beam spectra were identical at the near and far detectors, then these cross-efficiencies would cancel exactly in the ratio of far to near event rates. Similarly, the beam is not a perfect point source, and there are some differences in the near and far beam spectra. If the NC/CC ratio and detector efficiencies were exactly flat with energy, then the differences in beam spectra would cancel out exactly in the double ratio. (In fact over the region of MINOS sensitivity, NC/CC cross section ratios are nearly flat, and in the baseline wide band beam the detector efficiency effects are manageable).

The result is that systematic errors enter into the double ratio of short/long events only in a convoluted second order fashion. The ability to Monte Carlo these differences at even a modest level pushes the systematic error well below the statistical error. Thus this test is rate limited, so higher event rate (i.e. efficiency of the focusing system, number of protons extracted, etc.) is a high priority, but detailed understanding of the spectrum is not.

2.6.2 CC Far/Near

The rate of charged current interactions is essentially a measure of the number of muon neutrinos in the beam without a simultaneous normalization to the number of neutral current events. Compared with the double ratio presented above it trades the dominant statistical error of the small neutral current sample for the statistical power of the three times larger charged current data set. Because it is looking at the integral of the energy spectrum, the CC rate is not so sensitive to the spectrum as the total energy spectrum test discussed in the next section, but does depend more on a reliable simulation of the beam than does the NC/CC double ratio test.

2.6.3 MINOS CC Total Energy Spectrum

Although the (NC/CC)(Far/Near) test is more sensitive to small amounts of oscillation, a fit to the ν_μ CC total energy spectrum has the advantage that it actually measures the values of Δm^2 and $\sin^2 2\theta$. It has the appeal that one may be able to see the oscillation structure directly in the spectrum, as was shown in Figure 2-3 for Δm^2 of 10^{-2} eV^2. This is the test that is most sensitive to the spectrum and a thorough understanding of the spectrum is required before it can be used. The measured near-detector spectrum is used to predict that in the far detector, yielding a comparison which is both statistically powerful and directly sensitive to the oscillation parameters. However, errors in the prediction can induce or mask a signal. Differences in the near and projected far beam spectra come about because the decay region is not a point source as seen by the near detector, and such differences allow for systematic errors if the beam is not well understood.

In order to make estimates we have divided the data into analysis bins and determined the statistical error in each. When design questions, especially alignment, have arisen we have required that the error from the design choice be less than or equal to the statistical error. The typical statistical error in this test in a two year run is 2% and therefore we demand that no uncertainty in the design contributes more than a 2% error in any bin in the prediction of

the far spectrum. This is the most challenging aspect of the NuMI beam design. Measurements that can help to give confidence in the predicted spectrum include:

- measuring the initial spectrum in the near detector,
- measuring the radial distribution of the neutrino beam in the near detector, which gives some added information and cross checks on the nature of the source,
- making precise measurements of the NuMI beam element positions and focusing strengths, in combination with the results of a separate hadron production experiment using the NuMI target to actually measure the π and K fluxes produced by 120 GeV protons, which fluxes can be used in Monte Carlo calculations of the neutrino beam. Such an experiment has been proposed to the Fermilab PAC[3], in collaboration with groups interested in other physics aspects of such data.

The requirements on alignment and magnetic field tolerances to allow 2% precision are not overly difficult to meet (e.g., 20 mils for alignment tolerances) and therefore the goal of 2% is both sensible and achievable.

2.6.4 MINOS Electron ID

Both the $\nu_\mu \rightarrow \nu_e$ and $\nu_\mu \rightarrow \nu_\tau$ oscillation channels give electrons in the detector, and in both cases the inherent ν_e content of the beam is then a background. The NuMI beam naturally has a fairly low ν_e content; ν_e CC interactions happen at < 1% of the rate of ν_μ CC interactions (see Figure 2-11 and Table 2-1). Little can be done to reduce the ν_e's without a consequent substantial reduction in the ν_μ rate. Statistical fluctuations in the beam ν_e events limit experimental sensitivity to $\nu_\mu \rightarrow \nu_e$ oscillations to around 2×10^{-3} in $\sin^2 2\theta$.

2.6.5 MINOS τ ID

For the PH2(he) and PH2(me) WBB configurations, a large fraction of the neutrino spectrum is of high enough energy that ν_τ's from oscillations can produce τ's in the detector, if the neutrino mass difference Δm^2 is large enough. Aside from energy optimization, looking for τ's has little additional impact on our wide band beam design. There is, however, a strong connection between τ identification and our narrow band beam design, because a prime goal was a beam which contained practically no low energy

[3] Proposal to measure particle production in the Meson area using Main Injector primary and secondary beams, P.D. Barnes Jr. et al, FNAL P907.

neutrinos. This requirement arises from the fact that the $\tau \rightarrow \mu$ decays could be identified by a measurement of the total visible energy in the event which would be lower than the nominal beam energy, due to missing energy carried off by the two neutrinos in the decay. An alternative, and more direct way, to detect τ leptons is by direct observation of "decay kinks" in a large emulsion detector at Soudan. This possibility is under active consideration, and does not require a narrow band beam.

2.6.6 Summary of Systematic Limitations on the Measurements

If Δm^2 is in the 10^{-3} eV^2 range, then the far/near ratio of charged current events can be a significantly more sensitive test than the NC/CC double ratio one. The requirements on knowledge of the beam spectrum are not so severe as for the CC total energy spectrum test, which can be used to make actual measurements of the oscillation parameters.

The large size of the MINOS detector and the high intensity of the NuMI beam will provide a high statistics event sample. In the PH2(he) beam neutrino energy range from 8 to 24 GeV there will be of order 1000 charged current events per 1 GeV bin in the far detector for a two year run. The detector energy resolution, about 1.3 GeV for E_ν = 8 GeV and 2.6 GeV for E_ν = 24 GeV, thus sets a natural scale of a few GeV for detecting shape changes in the spectrum. The statistical accuracy on a measurement of the energy spectrum looking for few GeV "wiggles" is of order 2%. For any structures that are of order of the detector resolution, a systematic error of order 2% would match the natural statistical accuracy of the data sample. This is also the range where detector calibration will probably set a systematic limit to the measurements.

Real neutrino oscillations have a definite pattern, and when the energy spectrum is fit with a set of oscillation parameters, most residual systematic wiggles would not look like oscillations. However, having extraneous wiggles would make it hard to convince oneself that the actual small oscillation induced signals were real. Hence we set the goal that the beam systematic effects not produce an uncertainty in the prediction of the spectrum at Soudan by more than 2% over a few GeV region in the appropriate energy range for each beam configuration.

Currently, the biggest uncertainty in the prediction of the ν energy spectrum is the hadronic production of pions by protons hitting the target. Neither the longitudinal nor the transverse momentum distribution of the pions is known accurately. We can use the spectrum in the near detector to "pin down" the longitudinal distribution, assuming some transverse one.

The uncertainty in the transverse distribution then propagates as a systematic error, which ends up as a 5% to 6% error on the prediction of the far neutrino spectrum.

It is desirable to improve this spectrum uncertainty by a factor of three or more, so that it is comparable to or less than beam alignment uncertainties, detector calibration effects and statistical power. A measurement of the transverse and longitudinal momentum spectrum of pion production from the NuMI target at the 1% to 2% level would allow an absolute prediction of the neutrino spectrum in the near detector, which would serve as a powerful cross-check of the prediction of the spectrum in the far detector. A less stringent measurement, of order 5% in the pion momentum spectrum, would constrain the far/near neutrino ratios to the desired 2%. As mentioned previously, the proposal for such an experiment has been submitted to the FNAL PAC.

2.7 Special Challenges in Beam Design

The NuMI beam will be produced from the proton beam of the Fermilab Main Injector accelerator, which is capable of delivering intensity of up to several 10^{13} protons every 1.9 seconds. This intensity impacts beam design in many technical areas such as component cooling and radiation protection. Due to the fact that much of the beamline will be located in an aquifer underlying the site, radiological protection of the groundwater presents a greater challenge than in any beamline previously built at Fermilab; for details see Section 4.3.4 The design of the NuMI facility includes extensive shielding of the beamline elements as well as monitoring wells that will be used to monitor the groundwater during the operation of the facility. If monitoring of the groundwater indicated levels of radioactivity approaching regulatory limits, some control, restriction or modification of NuMI operations would be implemented.

2.8 Future Narrow Band Beam

An narrow band beam (NBB) design differs from the WBB in that it yields a narrower energy spectrum, which may be advantageous in studying oscillations once they have been confirmed in NuMI. We have a WBB design that facilitates future conversion to an NBB. An NBB should provide for better systematics and, when tuned for an optimized energy, a stronger oscillation signal. A pion beam tuned for 45 GeV will produce a ν_μ flux peaked at 20 GeV with a 15% energy spread. The event rate for a 45 GeV narrow band beam is

estimated to be 470 CC ν_μ and 120 NC events per year per kiloton of detector at Soudan. Since the NBB removes most of the low-energy flux, it gives lower background and consequently has a significant advantage in the searches for ν_μ and ν_τ interactions in the baseline MINOS detector.

Figure 2-12 illustrates the conversion of the PH2 WBB into the PH2 NBB, by a small vertical movement of the first horn (labeled FD1 in the figure) and the addition of bending dipole magnets, steel collimators, and a beam absorber. A detailed conceptual design has been done for the absorber, and how the narrow band beam components will fit within the target hall shielding. The continuous alignment rails, removable top shielding, and overhead crane allow for reasonably easy changeover from the wide band beam. The target hall shielding surrounding the absorber region needs to be modestly thicker than would be necessary for the wide band beam alone. A spectrum of neutrinos produced by this configuration in various tunes is shown in Figure 2-13.

per kton per year (3.7 x 10^{20} POT)	PH2 Low Energy	PH2 Medium Energy	PH2 High Energy
ν_μ CC	458	1439	3207
ν_e CC	5.4	13	18
ν_μ (bar) CC	64	45	34
ν_e (bar) CC	1.3	0.9	0.9
ν_τ CC (for δm^2=0.01 eV^2)	27	135	312
ν_τ CC (for δm^2=0.001 eV^2)	0.5	2.6	4.1

Table 2-1 Summary of neutrino event rates at Soudan for three tunes of the PH2 wide band beam. ν_τ rates are calculated assuming oscillations with $\sin^2(2\theta) = 1$, while no oscillations are assumed for the other flavors.

	NuMI	K2K	CERN to GS
Proton Energy	120 GeV	12 GeV	400 GeV
Protons/pulse	4 x 10^{13}	6 x 10^{12}	2.2 x 10^{13}
Cycle time	1.9 sec	2.2 sec	4 /26.4 sec
# protons per year	3.7 x 10^{20}	5 x 10^{19}	3 x 10^{19}
# CC int/kton/yr	460 - 3200	18	1400
Average E_ν	3 - 16 GeV	1.4 GeV	26.7 GeV
L of baseline	730 km	250 km	730 km
Year turn on	2002	1999	2003

Table 2-2 Comparison of NuMI with other neutrino facilities.

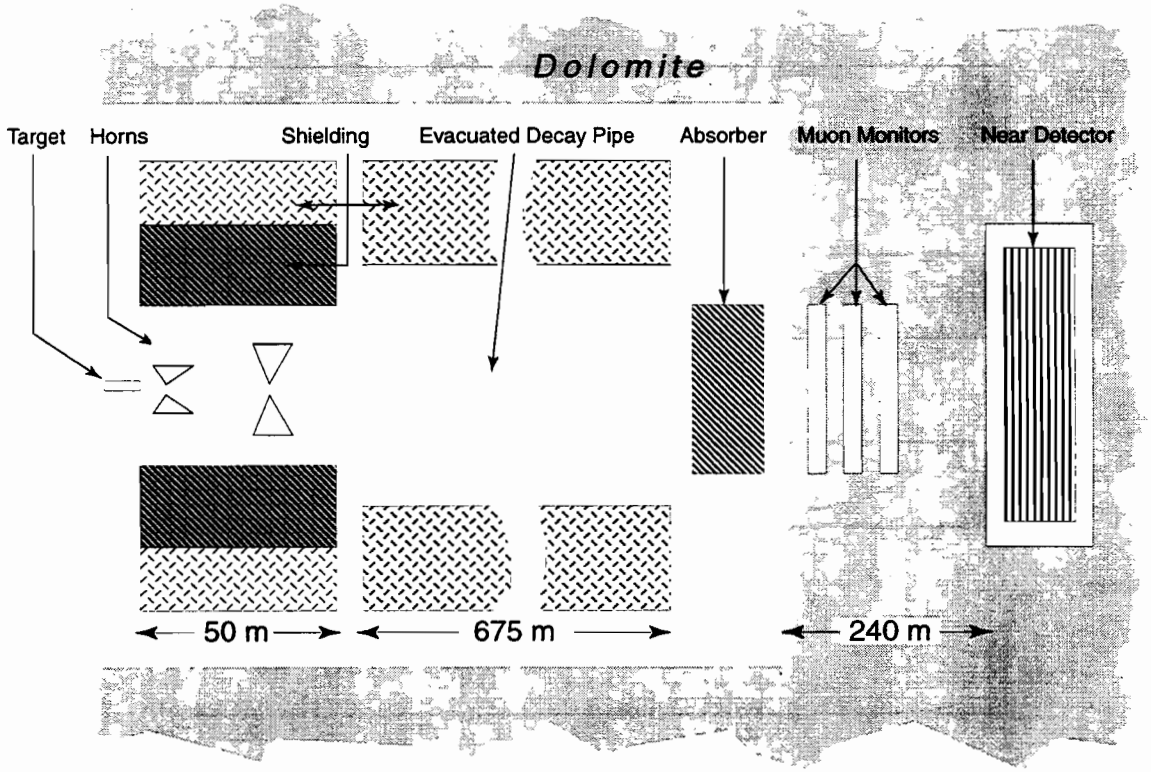

Figure 2-1 Schematic drawing of the NuMI neutrino beam-line.

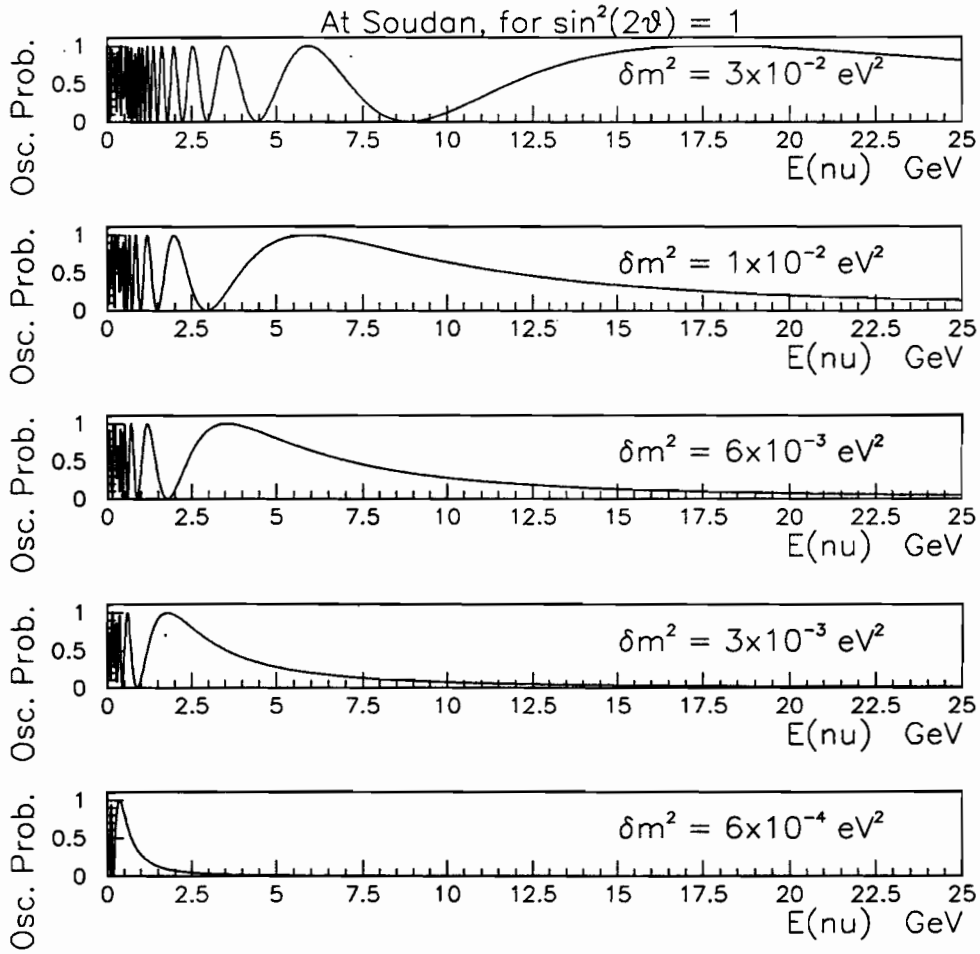

Figure 2-2 Oscillation probability as a function of energy for values of Δm^2 covering the region appropriate to the atmospheric anomaly.

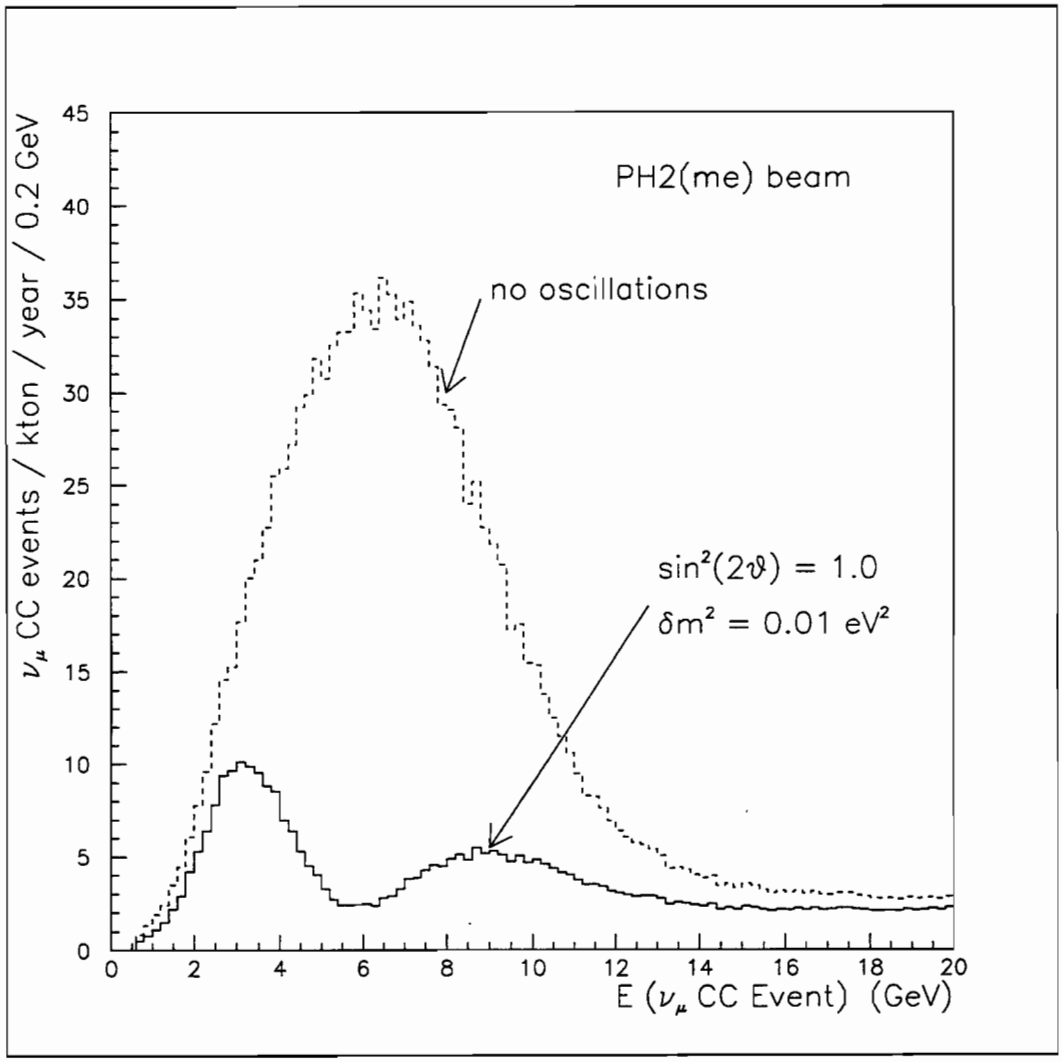

Figure 2-3 CC event total energy in the MINOS far detector distorted by oscillations.

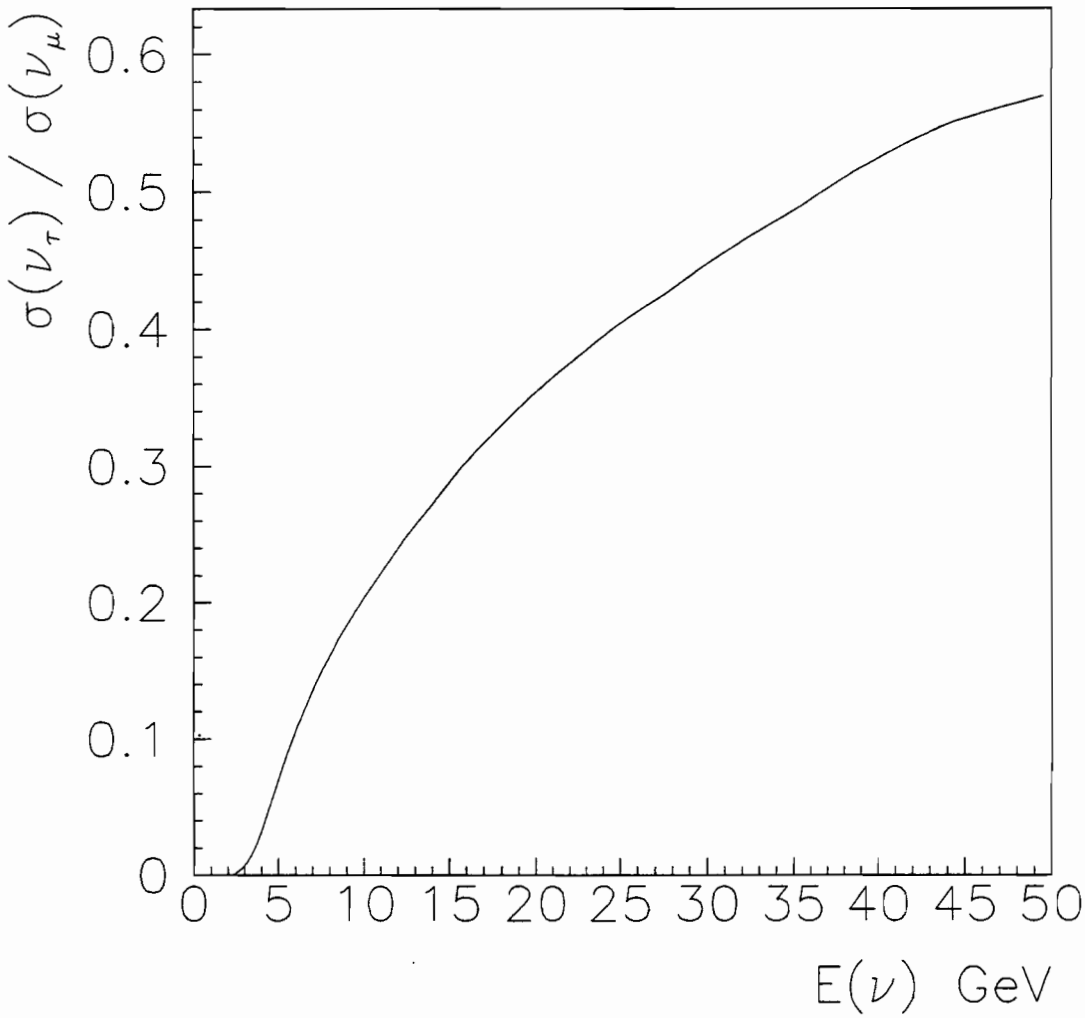

Figure 2-4 The ratio of the of ν_τ charged current interaction cross section to the ν_μ charged current interaction cross section, plotted as a function of neutrino energy.

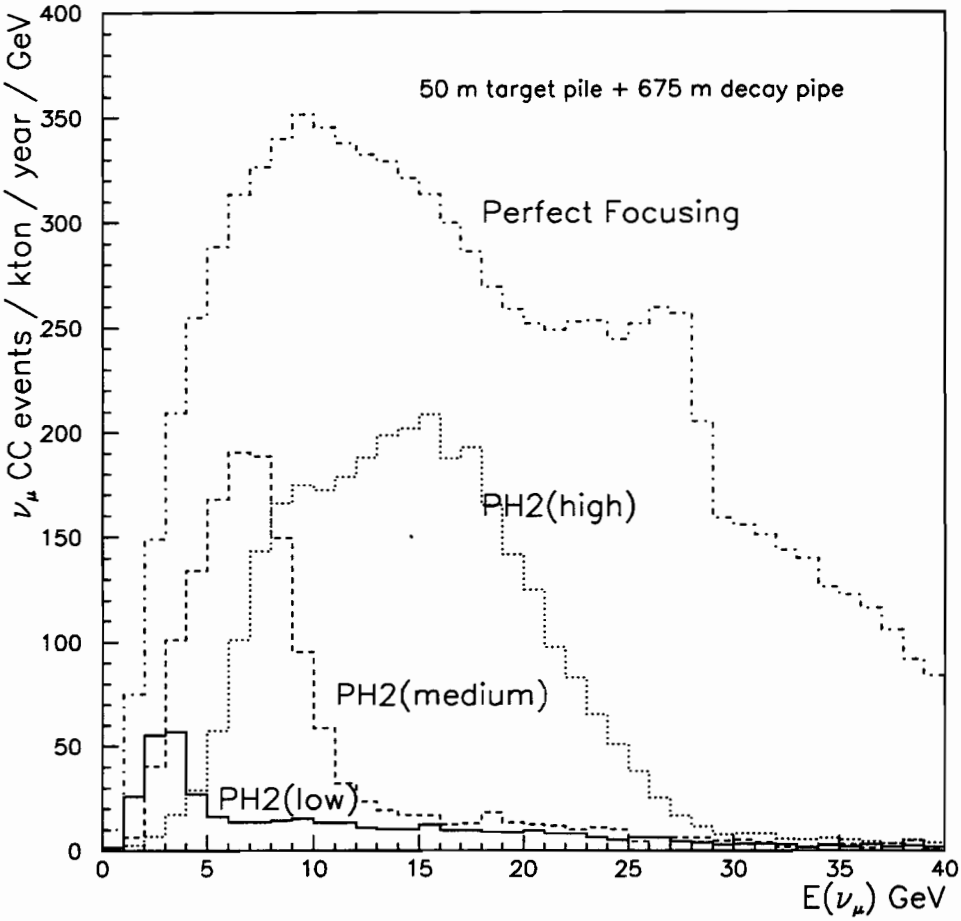

Figure 2-5 Comparison of event rates at Soudan in the case of ideal perfect focusing, and rates achieved with three configurations of the PH2 beam design.

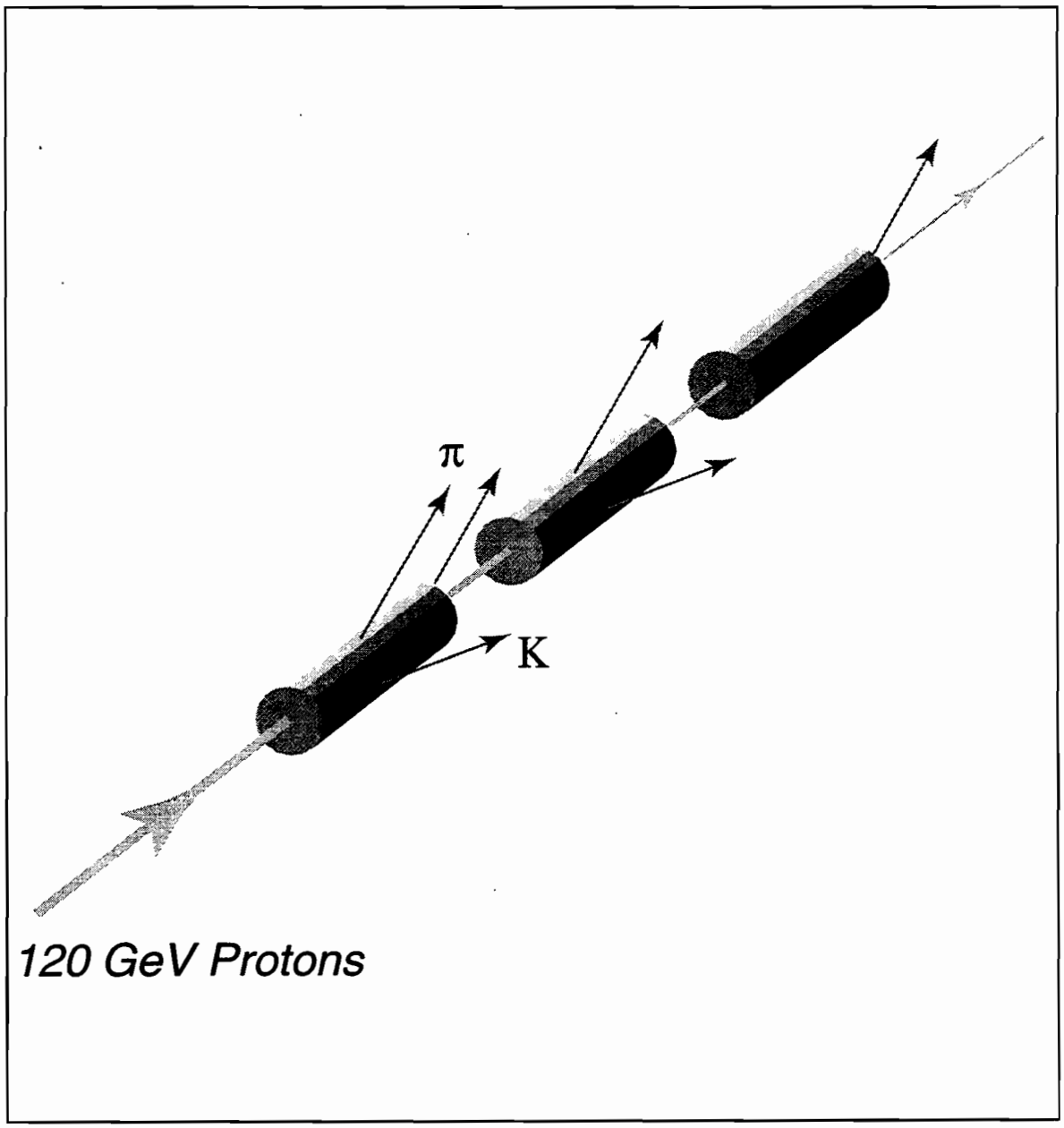

Figure 2-6 Schematic drawing of a long, slim segmented target for optimum meson production and decay of pions.

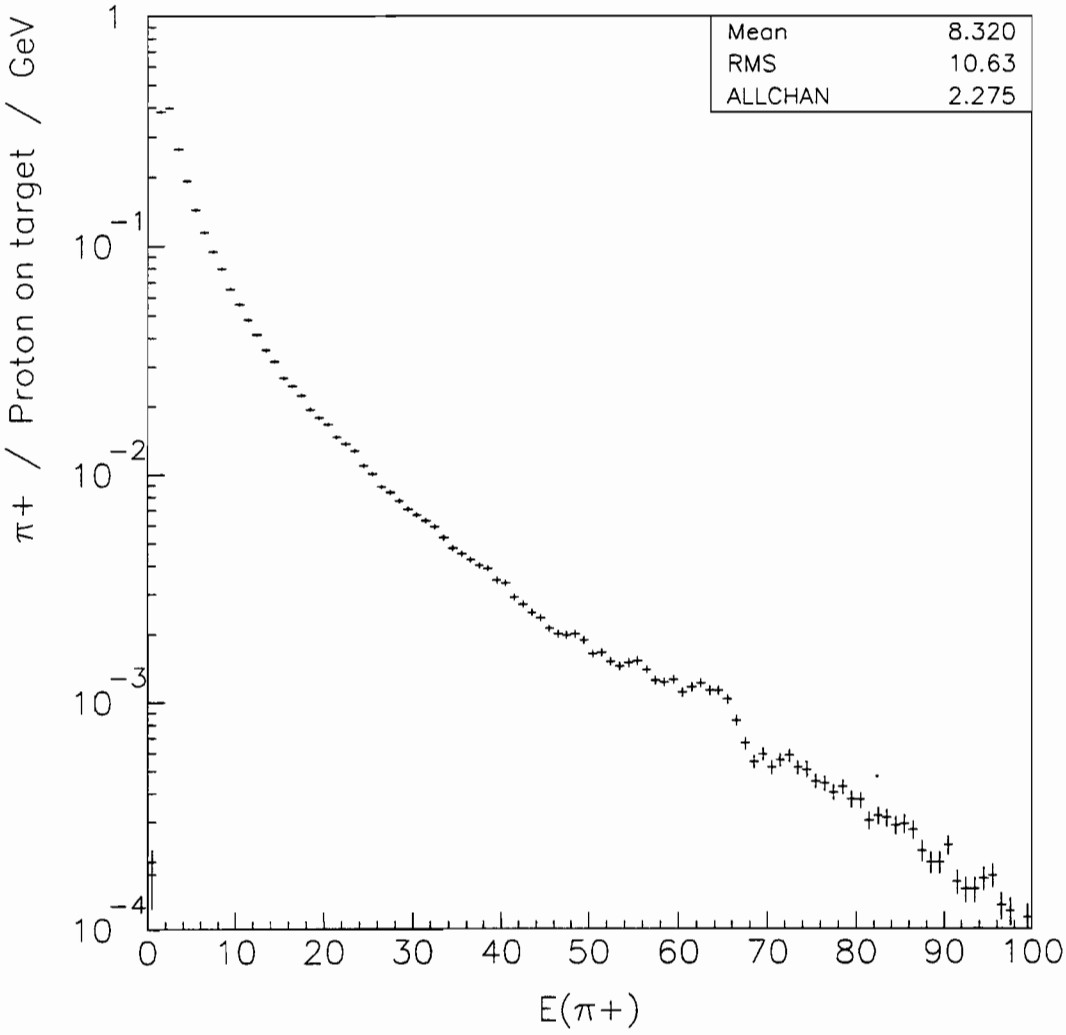

Figure 2-7 The energy spectrum of π^+ from a 2 mm radius 2 interaction length carbon graphite target according to the GEANT/FLUKA Monte Carlo.

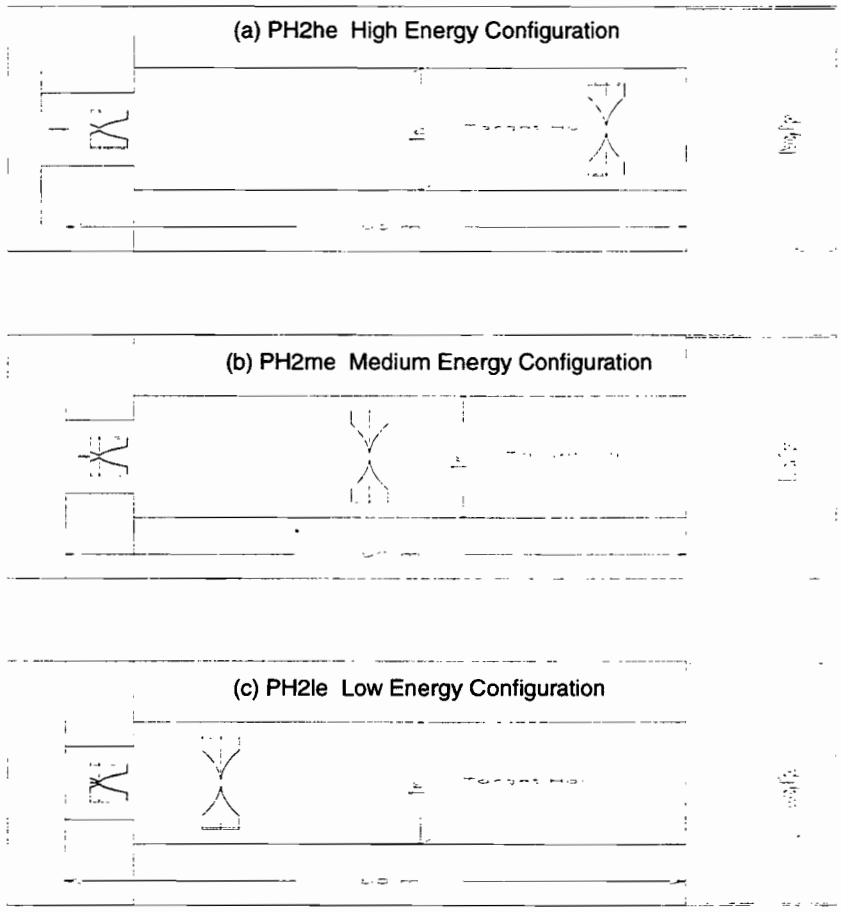

Figure 2-8 Schematic drawing of PH2 beam focusing configurations in the NuMI target hall. To change the tune to lower energy, the target is moved closer (and finally into) the first horn, and the horns are moved closer together. A physically different target is used for each configuration.

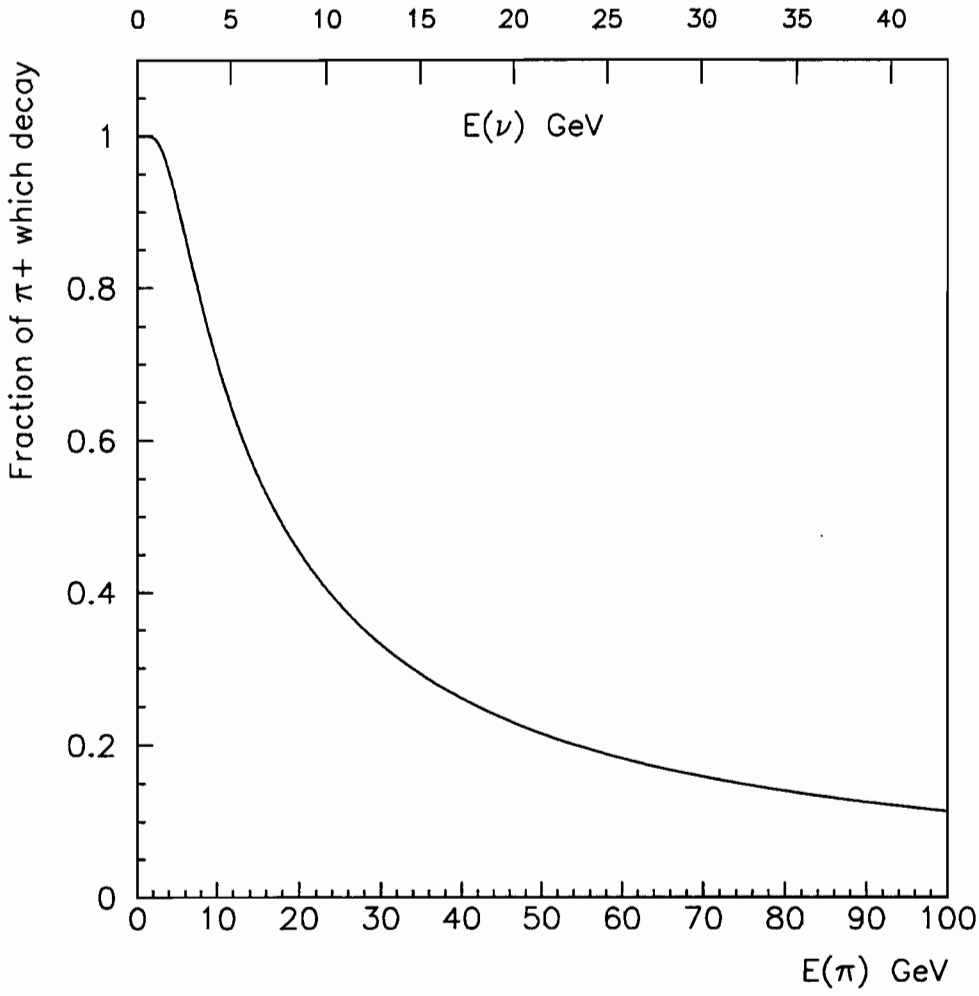

Figure 2-9 Fraction of π^+s decaying in the 675 m decay pipe as a function of pion energy, and the corresponding approximate neutrino energy for well focused pions.

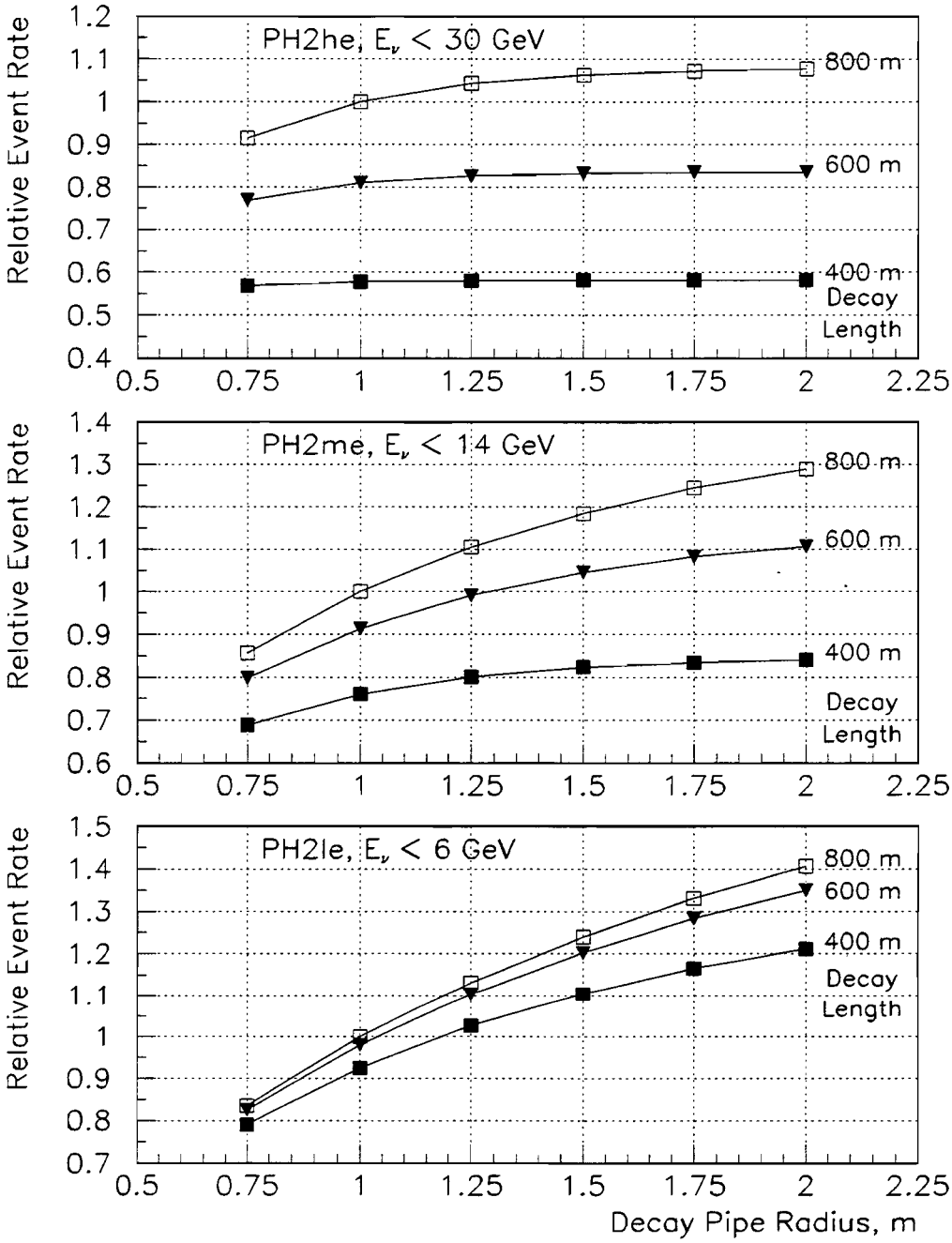

Figure 2-10 Comparison of event rates as a function of decay pipe length and radius.

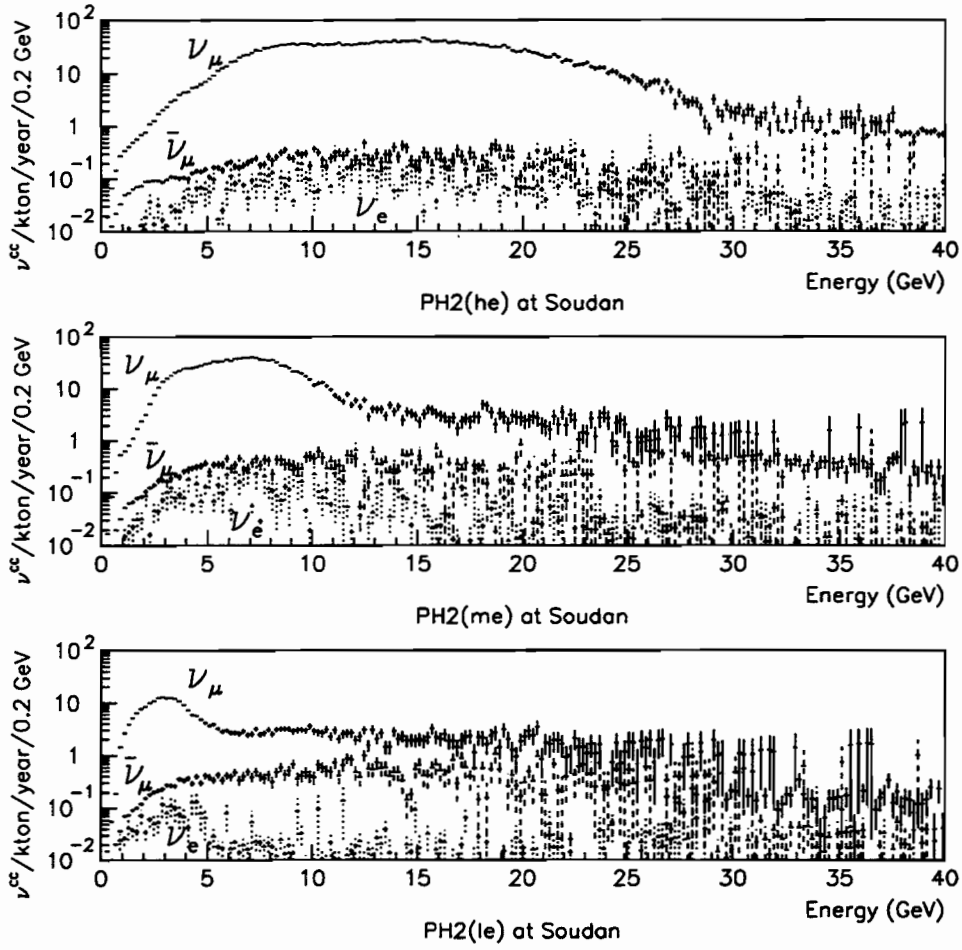

Figure 2-11 Energy spectra of the various PH2 NuMI beam configurations. Anti-ν_e rates are below the bottom of the plot as are those of ν_τ.

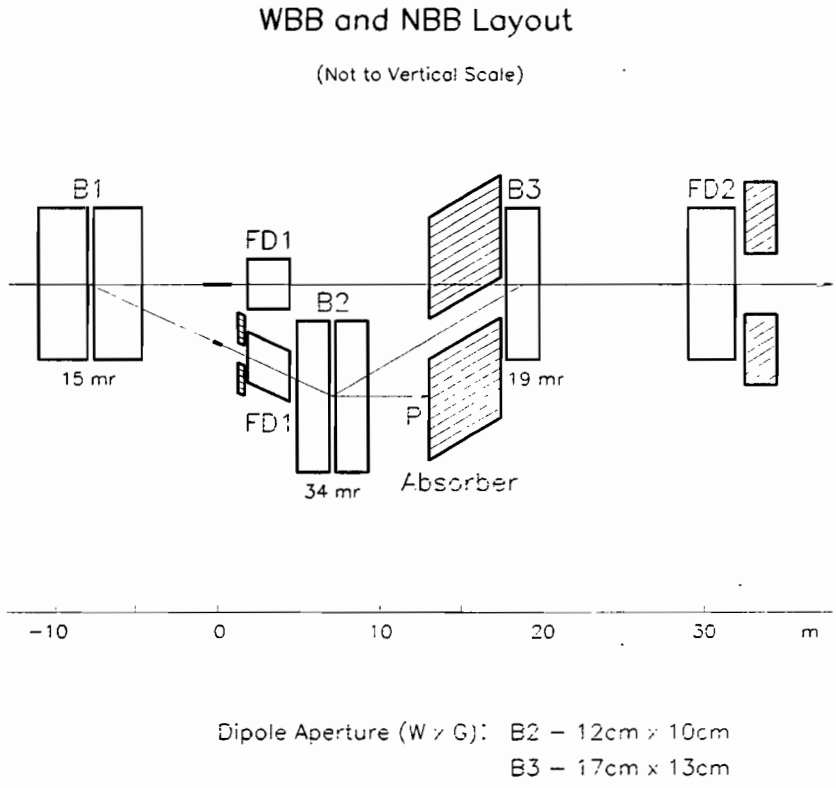

Figure 2-12 Schematic drawing of narrow band beam components. FD1 and FD2 are the same two horns used in the PH2 WBB. As shown, FD1 is moved vertically switching from WBB to NBB. B1, B2, and B3 are dipole bending magnets.

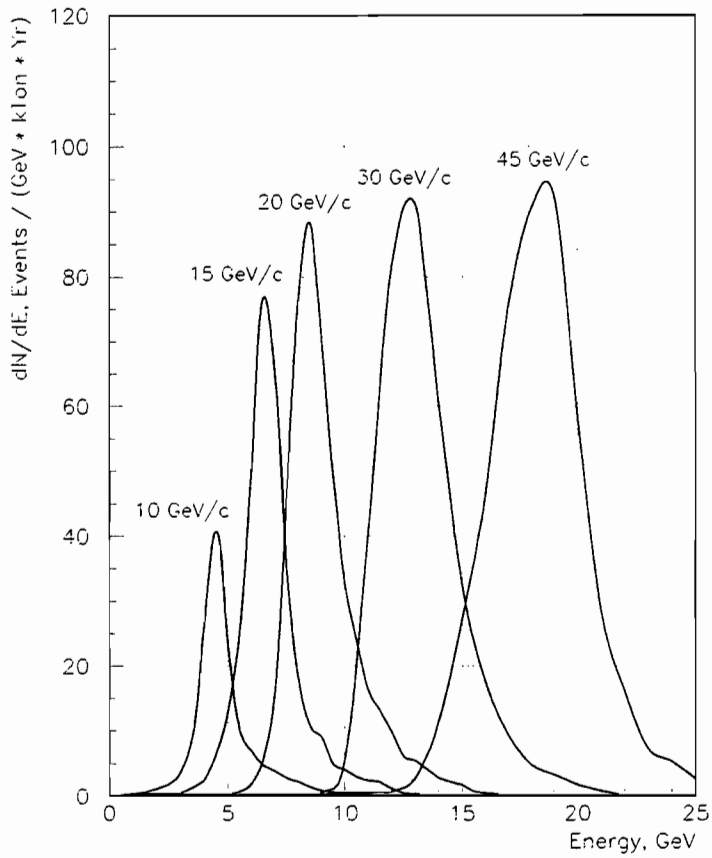

Figure 2-13 Energy spectrum for various tunes of the narrow band beam.

This Page Intentionally Left Blank

3.0 Technical Components (WBS 1.1)

In the following sections of this document we present a description of each of the WBS Level 3 subsystems of the Technical Components. These include:

1.1.1 Primary Beam Systems
1.1.2 Neutrino Beam Devices
1.1.3 Power Supply Systems
1.1.4 Hadron Decay and Absorber Regions
1.1.5 Neutrino Beam Monitoring
1.1.6 Alignment Systems
1.1.7 Water, Vacuum and Gas Systems
1.1.8 Systems Integration

These sections are intended to guide the engineering designs and development of the systems. Each section is a relatively "stand-alone" document that is maintained by the Level 3 manager for that subsystem. In each section we have attempted to present the material in a consistent and logical manner and structured to follow the major phases of the project construction, namely design, construction, installation and pre-commissioning. It should be noted that since the project design is a continuing process, not all systems are developed to the same level of detail. An example of this is the difference in design work on the neutrino beam devices *versus* the elements of the System Integration. Since the neutrino beam devices, in particular the targets and horn, are critical components of the neutrino beam and require significant R&D and prototyping work, these efforts have begun early and are progressing. In contrast, the conventional mechanical and electrical systems (water, vacuum, gas, controls and interlocks) are all standard designs which have been done at Fermilab for many years, and therefore will not be designed in detail until later in the project.

As stated in Chapter 1, this *Technical Design Report* is a living document, in which updates will be made to following sub-sections as the design of each system evolves and matures.

This page intentionally left blank.

3.1 Primary Beam (WBS 1.1.1)

Table of Contents

3.1 PRIMARY BEAM (WBS 1.1.1) 3.1-1

3.1.1 Primary Beam System Objectives *3.1-3*

3.1.2 Technical Requirements and Constraints *3.1-3*

3.1.2.1 Beam Size 3.1-3

3.1.2.2 Energy Deposition in the Target 3.1-4

3.1.2.3 Beam Angle 3.1-4

3.1.2.4 Beam Divergence 3.1-4

3.1.2.5 Loss Limits 3.1-4

3.1.2.6 Spill Length 3.1-5

3.1.2.7 Operating Constraints 3.1-5

3.1.3 Design Assumptions *3.1-5*

3.1.4 System Description *3.1-5*

3.1.4.1 Electrostatic septa 3.1-6

3.1.4.2 Magnets 3.1-6

3.1.4.3 Primary Beamline Instrumentation 3.1-7

3.1.4.4 Baffles and Shielding 3.1-8

3.1.4.5 Magnet stands 3.1-10

3.1.5 Design Procedures and Validation *3.1-10*

3.1.6 Construction Plan *3.1-10*

3.1.6.1 Recycled equipment 3.1-10

3.1.6.2 New equipment 3.1-11

3.1.7 Installation Plan and Issues *3.1-11*

3.1.7.1 Main Injector Extraction Region 3.1-11

3.1.7.2 NuMI Pretarget Region 3.1-11

3.1.8 Commissioning Plan *3.1-11*

3.1.9 Performance Monitoring Procedures *3.1-12*

Table of Tables

Table 3-1-1 Origins of Equipment for the Primary Beam System. A check has been made that all used magnets are indeed available. 3.1-13

Table of Figures

Figure 3-1-1 Schematic elevation view of the NuMI primary beam in a) Main Injector enclosure, b) NuMI stub, c) pretarget hall. Note that the scale varies between these diagrams and that long drift spaces between sections of the beamline are not shown. The beam direction is from right to left. 3.1-14

Figure 3-1-2 Beam sizes from tracking for the primary proton beamline. These are shown in comparison with the horizontal and vertical apertures through which the beam must pass. The upstream baffle assembly is being redesigned on the basis of this figure. 3.1-15

Figure 3-1-3 Loss locations for fast protons resulting from scatters in septa wires. The total is less than 100% as some such protons are not lost but circulate with the MI beam. 3.1-16

3.1.1 Primary Beam System Objectives

The primary beam system for the NuMI facility encompasses the extraction and transport of 120 GeV primary protons from the Main Injector to the NuMI target. Instrumentation of this beamline is also included. As the targeting is at zero degrees, the proton beam at the target must be aimed precisely at the MINOS far detector. Minimizing beam losses and insuring long term reliability and stability have guided the design.

The chief objectives of the primary beam system are as follows:

- Extraction of 120 GeV primary protons from the Main Injector;
- Transport of the 120 GeV primary beam through the NuMI extraction stub to the target located in the NuMI target hall;
- Delivery of 4×10^{13} protons (with possible upgrade to 6×10^{13}) to the target at a rate of one pulse every 1.9 seconds;
- Regularly keeping losses, other than those from septa scattering, to less than 10^{-3} of the primary beam intensity along the length of the beam transport system;
- Containment of losses to locations where their radiological effects, on both hardware components and the environment, are minimal and controlled.

3.1.2 Technical Requirements and Constraints

The technical requirements for the primary beam are closely coupled with those for the neutrino beam and the target. Both of these latter have been subjects of considerable study and are still being optimized. Several specific requirements follow.

3.1.2.1 Beam Size

The beam must fit within the target. This requirement couples together the beam spot size on target, the precision and stability at the target location and to some extent the divergence (beam must stay within the target over the entire target length). The extent to which some beam tails actually are allowed to miss the target results from a series of compromises. As to the beam size one must balance the magnitude of these tails with the amount of target heating caused by the beam core (see Section 3.2.3). As to the target size itself, there is an optimization between making it larger to contain the tails and making it smaller to minimize reabsorption of produced pions.

The present preferred solution, for the medium energy case, is a target of extent 4 mm in the horizontal and somewhat greater in the vertical as it is supported by full width target material from below. The horizontal beam profile on target is a slightly asymmetric Gaussian with FWHM of 2 mm. The corresponding beam divergence is 150 μrad and corresponds to ± 0.07 mm beam size increase at each end of a .96 m target, assuming optimal focus at target center. This leaves ± 0.5 - 1.0 mm error margin for precision and stability. With the instrumentation specified this result should be easily achievable. The vertical beam profile is Gaussian with FWHM 2.2 mm.

3.1.2.2 Energy Deposition in the Target

The beam must not melt the target. This sets a limit on how tightly it can be focused, the limit being of order 1 mm RMS in radius. Target heating issues are described in Section 3.2.3.

3.1.2.3 Beam Angle

The neutrino beam must stay centered at Soudan to the extent that the central 75 m 'spot' hits the detector there. This sets a requirement that the neutrino beam point to Soudan within 50 μrad. Monte Carlo simulations have shown that the corresponding requirement on the primary proton beam is that it point to Soudan only to within 0.6 mrad, although the entire error budget would be consumed if it were this poor. There are other requirements for beam angle on target; namely that uninteracted protons fit within the inner radii of the horns and that they hit the central core of the hadron absorber, 675 m distant. None of these requirements is thought particularly difficult to satisfy.

3.1.2.4 Beam Divergence

The divergence of the beam after the target cannot be so great that a significant amount strikes the material of the horns or misses that of the absorber. Additionally there is the requirement on divergence within the target mentioned above. For the anticipated Main Injector beam emittance there appear to be no difficulties in satisfying these criteria.

3.1.2.5 Loss Limits

Loss limits at several points along the beamline need to be very carefully established; these are related to groundwater protection, residual activation, air activation and equipment

damage. There is an unavoidable ~1% loss on the extraction septa, however the resulting scattered particles are lost primarily before leaving the Main Injector enclosure.

3.1.2.6 Spill Length

Spill length via resonant extraction cannot exceed 1 ms, driven by limitations on high current pulsing of the horns.

3.1.2.7 Operating Constraints

Operation must be compatible with that of the Tevatron Collider and with antiproton production. It appears that for any running simultaneous with fixed target extraction to Switchyard a scheme of alternating cycles would need to be devised. The beam delivered to NuMI would be less than anticipated in this circumstance.

3.1.3 Design Assumptions

As to extraction from the Main Injector, it is assumed that experience will have been gained with beam to Switchyard previous to NuMI commissioning, and that any lessons learned will be incorporated into NuMI design.

In designing the primary beam system the circulating emittance in the Main Injector has been assumed to be 30π mm-mr (95%, normalized) in both planes with original intensity of 4×10^{13} protons per pulse. The assumed extracted beam has been obtained by tracking studies in the ring itself.

The upstream beam components must be physically accommodated within the MI enclosure and the NuMI stub (a MI enclosure appendage constructed for this purpose), where civil construction has been completed. However the length of the tunnel from the stub to the pretarget hall and the space occupied in that hall may be, and indeed have been, varied as part of the design.

3.1.4 System Description

Elevation schematics of the primary beam in the MI enclosure, NuMI stub and pretarget hall are shown in Figure 3-1-1. In addition to the elements shown, the beamline also contains two electrostatic septa which are situated upstream in the MI enclosure. Appendix A contains the layout coordinates of the major system components.

The following subsections describe the elements of the primary beamline.

3.1.4.1 Electrostatic septa

Two MI standard septa (BD drawing # ME-337509) are situated in the MI-60 RF straight section 270° of betatron phase upstream of quadrupole Q608. These devices can provide up to 400 μr of transverse kick to protons at 120 GeV, a sufficient amount to move them across the septa of the extraction Lambertsons. Prior to NuMI construction extraction from the Main Injector at MI52 will have been demonstrated and may have been operated on a full-time basis for some period of time. This region uses identical septa to those planned for MI60, so that the benefits of a certain amount of experience will obtain for construction of the NuMI devices. However it is not likely that there will be experience with these septa at the beam intensities required for NuMI. There are questions pertaining to radiation damage and the effects of radiation-induced heating of the septa wires which have been addressed using the standard radiation program MARS.

3.1.4.2 Magnets

The primary beam contains a standard complement of magnetic elements. These include:

MI Lambertsons

There are three Lambertsons, as described in Technical Division Main Assy No 5520-MD-331492 Rev. F, and one C-magnet, 5520-ME-318648 Rev. D. The beam kicked by the septa is separated 12 mm in the horizontal plane from the closed orbit at the face of the first Lambertson. This separation is sufficient to place the beam into the extraction channel, which passes through the Lambertsons and C-magnet in turn.

Bending Magnet Strings

There are three strings of bending magnets, which serve in concert to place the proton beam on the NuMI target and direct it precisely toward the MINOS far detector in Soudan. All magnets in these strings will be recycled from previous projects. Those of the first and third strings are of the EPB type while those of the second are Main Ring B2s. The properties of these magnets are detailed in Fermilab TM-632. The magnets of the first string are installed in the MI enclosure in a rolled configuration, such as to establish the proper horizontal bearing to Soudan and flatten the upward vertical trajectory induced during extraction. The second string is placed in the NuMI stub and provides the downward vertical bending required for the beam to enter the pretarget hall. The third resides in that hall and establishes the appropriate pitch to Soudan.

Quadrupoles

There are 10 quadrupoles specified, all of type 3Q120 (EPB) detailed in TM-632. The purpose of the more upstream of these is to maintain beam size during transport so that all apertures are respected. The four final elements are used to set the size and divergence at the target. Figure 3-1-2 shows the beamline optics, the beam sizes being obtained from tracking extracted rays through the entire line. Also shown are the restricting apertures. It is seen that there is a difficulty with the aperture of the carrier pipe protection baffle (see below); the baffle design is being altered to remedy the problem.

Trims

The trim specification is for magnets recycled from the Main Ring. Each of four trim stations will contain two horizontal devices and a single vertical one.

3.1.4.3 Primary Beamline Instrumentation

Six types of instrumentation are thus far planned for this primary beamline.

Beam Position Monitors (BPMs)

Seven horizontal/vertical pairs are specified, with at least two, those closest to the target, having a demonstrated 50 micron accuracy. These BPMs are all of types that have been used in the past.

Loss monitors

Due to the high intensity transported by this line, monitoring of associated losses is of greater than usual importance. Loss monitors, currently specified as being 20 in number, will be used to alert operators to unexpected or unusual losses, and will have the ability to abort the Main Injector beam.

Segmented Wire Ionization Chambers (SWICs)

Four of these well known devices are specified as being recycled from decommissioned beamlines and installed in the NuMI primary beam. They provide profiles in horizontal and vertical planes on a raster of pitch of 1mm. However they function by placing a small amount of material in the beam and will probably be found unacceptable for high intensity running, their utilization being limited to tune-up.

Secondary Electron Emission Detectors (SEEDs)

These provide similar information to that of SWICs; however the basis for their operation is the measurement of secondary emission charge from material in the beam, rather than the effects of ionization. SEEDs have been shown to provide more reliable profile information in intense beams than do SWICs, the difference being the absence of space charge effects[1]. It is envisioned that the two final profile monitors before the target will be SEEDs, the more upstream ones SWICs.

RF Intensity Detector

This device provides an intensity signal at a high bandwidth. Its output serves as input to the extraction regulation system QXR/Bucker in a manner similar to that which has been used for Tevatron fixed-target experiments, both for fast spill neutrinos and for slow spill.

Toroids

Two of these will provide intensity readings near the upstream and downstream ends of the beamline. If the second were to read significantly less than the first this would serve as indication of beam loss, separate from any loss monitor signals.

3.1.4.4 Baffles and Shielding

Most of the components of the primary beam system reside in the Main Injector enclosure or the NuMI stub. Both regions are covered by an extensive earth shield and berm built as part of the MI civil construction. The berm over the stub, in particular, was constructed solely for protection from the NuMI beam but not as part of the current project. This earth shielding is explicitly discussed in Chapter 4. Natural earth and rock shielding over the pretarget hall is sufficient for personnel protection.

In the beam enclosures there are locations where it is necessary to shield against possible damage from mis-steering of the very intense primary proton beam. For this purpose baffles are being designed. There are two locations of particular concern.

- The long tunnel between the downstream end of the stub and the upstream end of the pretarget hall. Loss of significant beam in this region would be particularly serious for groundwater protection, as there is virtually no shielding between beam and soil. Design is in progress for one or more baffles to be installed in the stub to protect the

[1] R. Drucker *et al*, Proceedings of DIPAC 97, Frascati 1997

pipe in this region from being struck by beam. (Striking of the pipe by protons leads to absorption by the rock of neutrons.)

- The neutrino line focusing horns. These must be protected from irradiation by primary protons that miss the production target. The particular concern is heating of the horns, which such beam could induce. A design is in progress for a two-baffle system located just upstream of the target.

It is an essential feature of the resonant extraction process that a certain fraction, of order 1%, of the circulating protons strike the wires of the electrostatic septa. For those scatters which are elastic or quasi-elastic from nuclei or nucleons there can result high momentum forward protons, which are close to the extraction orbit and can enter the extraction channel. Due to the intensity of the NuMI beam, these protons can result in a relatively potent radiation source term. Detailed studies of this process have been conducted and a summary of the results is shown in Figure 3-1-3. It is seen that the majority of such protons are lost in the 300' MI region between septa and Lambertsons, but that a small fraction, of order 1%, accompany the extracted beam into the pretarget hall.

As is noted above, one method used to prevent irradiation, particularly of equipment but also of the aquifer, is the triggering of the MI abort by abnormally large signals from loss monitors. This method has proven capable of aborting abnormal Tevatron beam within a few turns, and a comparable time scale for operation is anticipated for the Main Injector. For comparison the NuMI spill length corresponds to 100 turns. Thus much of the intensity of errant pulses can be safely disposed of. Sufficient monitors have been specified that losses anywhere along the primary beam will trigger this process.

Most of the NuMI enclosures will not be accessible during beam-on conditions, and thus need not be protected against prompt radiation. However it is desired that the horn power supplies, located in their own enclosure at target hall depth and to the west behind 20' of rock, indeed be accessible. The rock protects this area from neutrons but not from potential high energy muons from some upstream source. A preliminary simulation of muon production indicates that at its present location this enclosure is adequately shielded. It should be noted that the shielding in other locations that were considered for the enclosure is not adequate according to the same model.

There is an additional shielding matter related to the locations traversed by the primary beam, though not related to the primary beam itself. This is the shielding of the NuMI enclosures from possible losses in the Main Injector, in some manner not related to NuMI operation. No design yet exists for this shielding, but some preliminary work has gone into its requirements. These include the facts that the shielding must be adequate for beam

energy of 150 GeV, the MI maximum, and that it must be far enough upstream to protect the carrier pipe region during excavation.

3.1.4.5 Magnet stands

New stands will be constructed for all primary beam magnets. In the MI enclosure the magnets must be arranged between the Main Injector ring below and the Recycler ring above. In addition the dipoles in this region are rolled at a series of varying angles, requiring unique stands. In both the stub and pretarget hall the beam will be pitched in the vertical plane, so that stand design will have to account for varying distances of magnets above floor level. In some cases it may be decided to hang magnets from the ceiling.

3.1.5 Design Procedures and Validation

A number of standard software packages have been integral to the design of this beamline. These include accelerator modeling programs that have been used to study the extraction process and create the beamline phase space input. TRANSPORT has been used for design of focusing, and placement and alignment of magnets. MAD has been used for particle tracking, TURTLE for aperture checks and loss calculations. CASIM, CASIMU and MARS have predicted the effects of beam losses.

All of the above are standard and reliable codes used extensively at Fermilab and elsewhere. The instrumentation and radiation monitoring procedures that are proposed will allow the design to be tested from the beginning of the commissioning phase. Causes for any off-nominal observations will be sought in reference to the software model.

3.1.6 Construction Plan

The beamline design has involved the use of as many recycled components as possible. This approach has the dual advantages of affordability and well understood equipment for both the installation and commissioning/operations phases. New construction will be undertaken only in cases where appropriate recycled parts do not exist. A summary of the origins of the various pieces of equipment in the line is given in Table 3-1-1.

3.1.6.1 Recycled equipment

All primary beamline magnets will be recycled, either from decommissioned lines or from the Main Ring. Some instrumentation will be recycled as well – at least SWICs and parts of BPMs. All recycled hardware will be thoroughly tested and refurbished before being installed in NuMI. The schedule allocates manpower to perform such testing and the budget presumes that some parts will require replacement.

3.1.6.2 New equipment

The majority of new equipment consists of extraction items that are traversed by Main Injector beam and thus must comply with MI standards – namely electrostatic septa, Lambertsons and the extraction C-Magnet. The majority of the instrumentation components and all of the magnet stands, as noted above, will also be constructed new.

3.1.7 Installation Plan and Issues

3.1.7.1 Main Injector Extraction Region

All installation work in the Main Injector enclosure and the NuMI stub will have to be carefully planned and staged so that it can take place during scheduled MI shutdowns. If the NuMI requirements were the only ones to be considered a three-month shutdown beginning 1 June, 2002 would be scheduled. However, as the Main Injector will likely be providing beam for the collider program at this time, both the starting date and the duration will be subject to negotiation. Since considerable beam will have been accelerated in the MI enclosure prior to NuMI commissioning, all staff involved with installation there and in the stub will require radiation safety training; such training will not be required for construction or installation of NuMI equipment in other locations. As noted above, the NuMI extraction line will be situated with the MI ring below and the Recycler above – the work will have to be carefully engineered to avoid damaging or misaligning these machines.

3.1.7.2 NuMI Pretarget Region

The work in this region will not be tied to the MI schedule and will take place in a non-radiation area. However it will have to mesh with the construction of the enclosure and be compatible with installation of the adjacent target shielding pile.

3.1.8 Commissioning Plan

The commissioning plan involves starting with very low beam intensity – order of a few $\times$ 10^{11} protons per pulse – and testing the extent of proper beam transport and the reliability of instrumentation. As confidence in the instrumentation grows, the latter will be used as designed to tune the transport of beam eventually over the entire length of the line. Next, intensity will be slowly raised toward the design level, or at least toward as high a level as is reasonable at the time. The ability to abort or inhibit beam when high losses or other abnormalities are observed will be tested for integrity.

It should be noted that, as with other recent Fermilab projects, the control system will be fully functional before commissioning. Thus all usual features such as datalogging, alarms and "knobbing" of power supply currents will be available.

Remarks are in order concerning the operation of the Main Injector at low intensity. It will often be the case in practice that MI cycles will contain beam intended both for antiproton production and for NuMI. It will quite likely be the case that NuMI low intensity running will need to be simultaneous, on the same MI cycles, with some high intensity beam. To accomplish this it will be necessary to have separate intensities in the Booster for the beam intended for the separate locations. A more modest approach might involve alternating MI cycles between the users, so that the separate intensities are not in the MI on the same cycle. However rapid variation of Booster intensity as required in either scenario has never been done operationally.

3.1.9 Performance Monitoring Procedures

The ACNET control system contains a number of features to monitor the performance of operating subsystems. These include alarms for off-nominal readings, beam abort and subsequent inhibit when readings such as high losses seem to justify them, datalogging on each accelerator cycle of power supply and beam parameters and logging of all settings made. The extraction regulation system maintains circular buffers of important beam intensity values.

It is intended that once stable operating conditions are achieved the AUTOTUNE program will be utilized to hold beam positions constant over long periods, typically days. This program is a mature product that has been used in Tevatron fixed target operations, controlling three beamlines for a period of months.

EQUIPMENT TYPE	NUMBER OF PIECES	ORIGIN	STATUS OF NEW DEVICES
Magnets and septa			
Electrostatic septa	2	new	Others of the same design exist
Lambertsons	3	new	Others of the same design exist, parts are on hand
C-magnet	1	new	Already constructed, in inventory
Dipoles	19	used	
Quadrupoles	10	used	
Trims	12	used	
Instrumentation			
RF monitor	1	used	
BPMs	14	new/used	Either existing or copies of existing
Toroids	2	new	Commercially available
Loss monitors	~20	Used, if available	Either existing or copies of existing
SWICs	4	used	
SEEDs	2	new	Similar devices exist
Equipment stands	70-80	new	Design required

Table 3-1-1 Origins of Equipment for the Primary Beam System. A check has been made that all used magnets are indeed available.

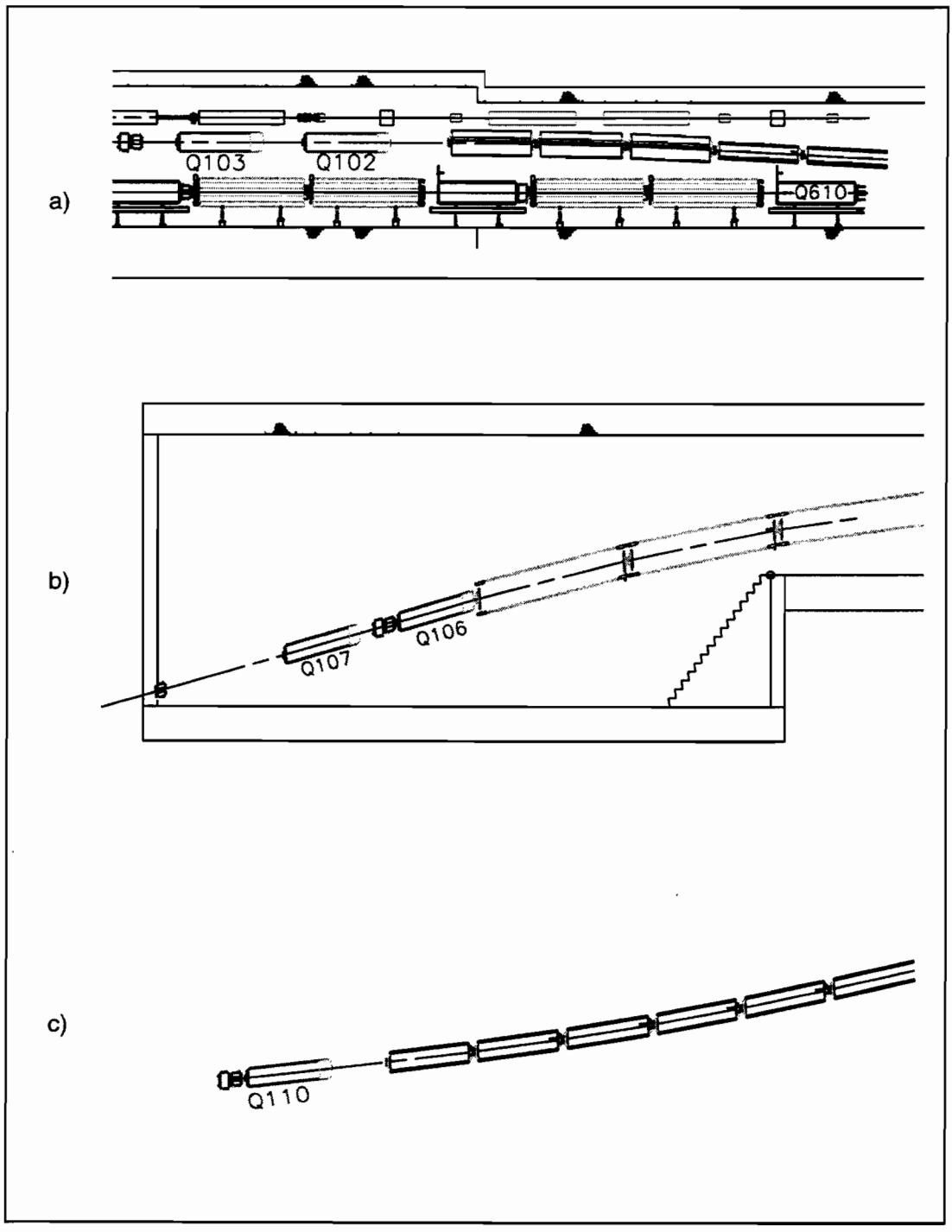

Figure 3-1-1 Schematic elevation view of the NuMI primary beam in a) Main Injector enclosure, b) NuMI stub, c) pretarget hall. Note that the scale varies between these diagrams and that long drift spaces between sections of the beamline are not shown. The beam direction is from right to left.

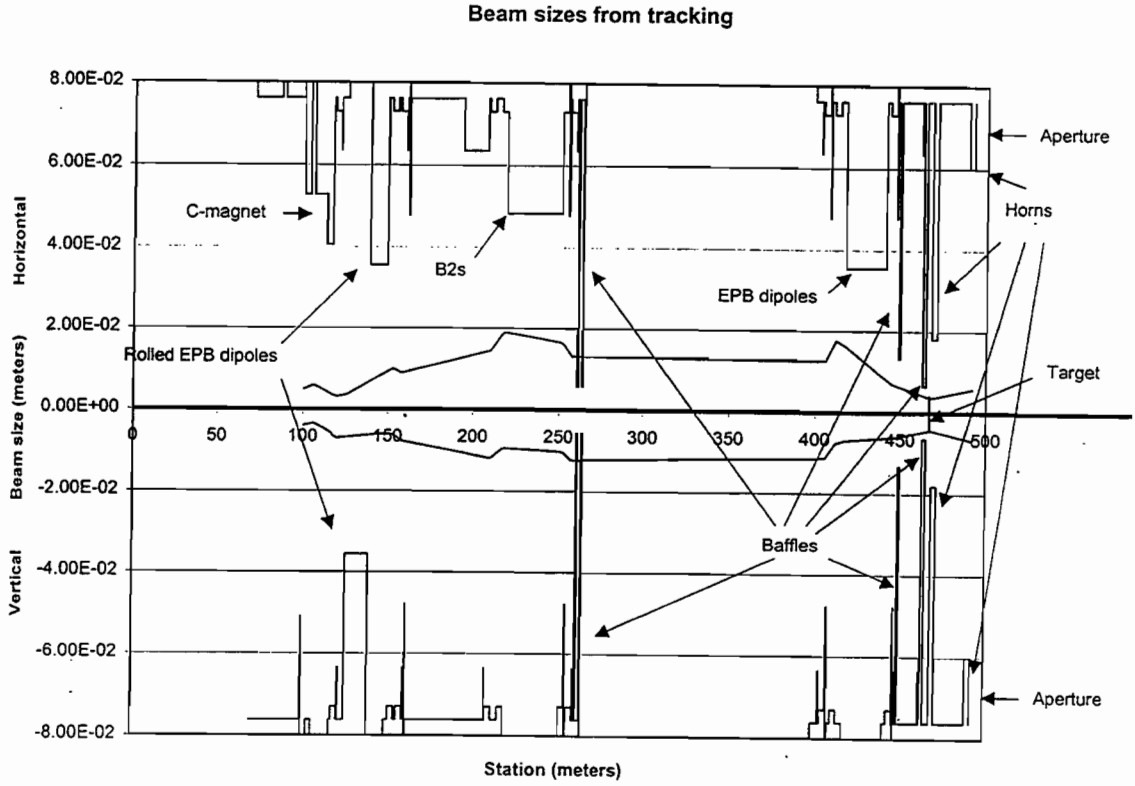

Figure 3-1-2 Beam sizes from tracking for the primary proton beamline. These are shown in comparison with the horizontal and vertical apertures through which the beam must pass. The upstream baffle assembly is being redesigned on the basis of this figure.

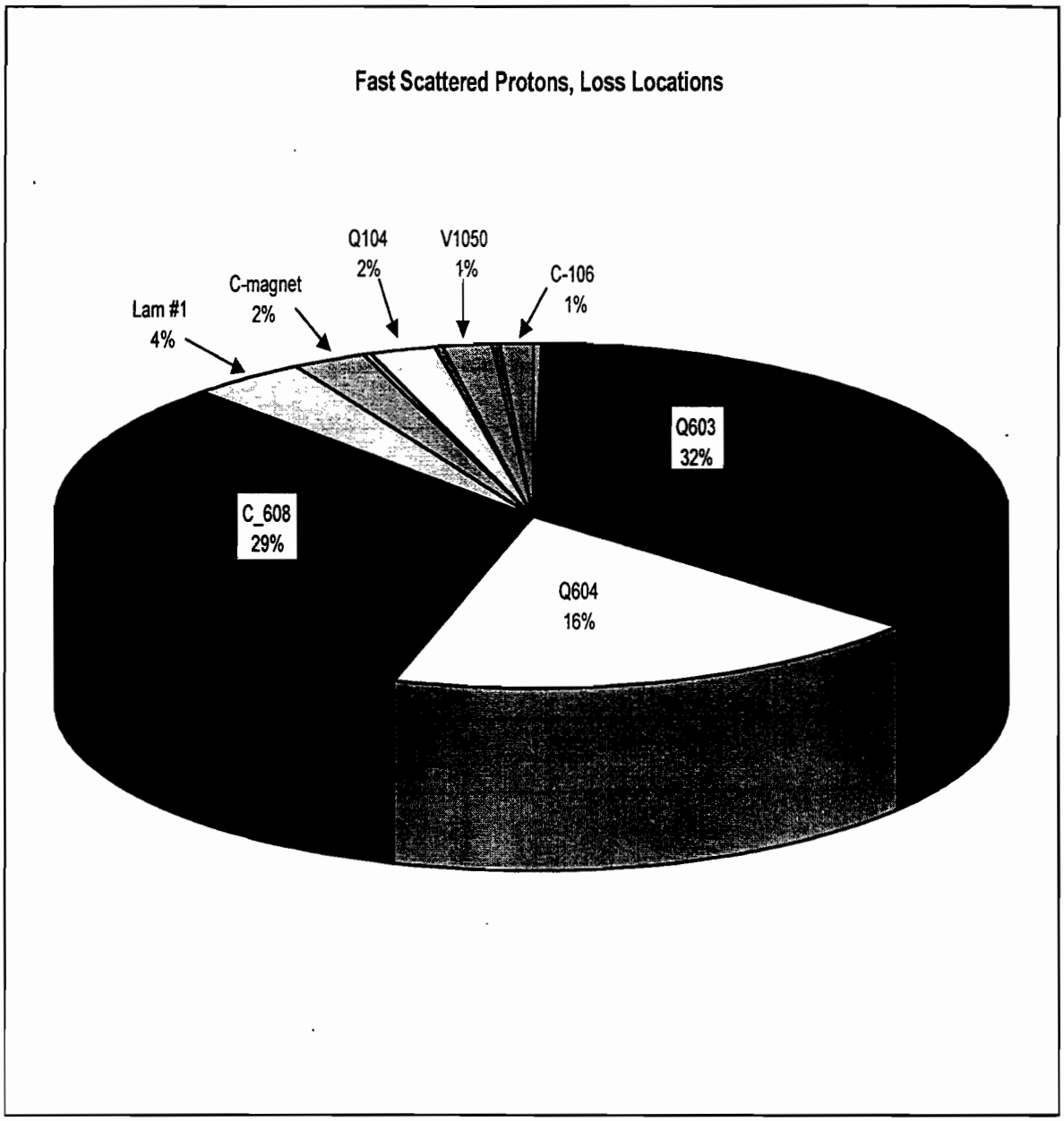

Figure 3-1-3 Loss locations for fast protons resulting from scatters in septa wires. The total is less than 100% as some such protons are not lost but circulate with the MI beam.

3.2 Neutrino Beam Devices (WBS 1.1.2)

Table of Contents

3.2 NEUTRINO BEAM DEVICES (WBS 1.1.2) 3.2-1

3.2.1 Introduction *3.2-4*

3.2.2 Neutrino Beam System Objectives *3.2-4*

3.2.3 The Target *3.2-7*

3.2.3.1 Target Technical Requirements and Design Assumptions 3.2-7

3.2.3.2 Target Design and Description 3.2-8

3.2.3.3 Target Design Validation 3.2-10

3.2.3.4 Target Prototype and Test Program 3.2-11

3.2.3.5 Prototype and Operational Target Construction 3.2-12

3.2.4 Magnetic Focusing Horns *3.2-13*

3.2.4.1 Horn Objectives and Technical Requirements 3.2-13

3.2.4.2 Horn System Description 3.2-14

3.2.4.3 Horn Design and Development Program 3.2-15

3.2.4.4 Horn Fatigue Analysis 3.2-16

3.2.4.5 Horn Modal Analysis 3.2-19

3.2.4.6 Horn Conductor Fabrication 3.2-20

3.2.4.7 Horn Spray Cooling System 3.2-20

3.2.4.8 Testing of Prototype and Operational Horns 3.2-21

3.2.4.9 Horn Design Validation 3.2-22

3.2.5 Target Station Shielding *3.2-22*

3.2.5.1 Design Assumptions 3.2-23

3.2.5.2 Target Station Shielding Description 3.2-24

3.2.5.3 Design Validation 3.2-24

3.2.6 Target Station Beam Pipe *3.2-25*

3.2.6.1 Technical Requirements and Design Assumptions 3.2-25

3.2.6.2 Description 3.2-25

3.2.7 Installation Plan and Issues *3.2-26*

3.2.7.1 Target and Horn Installation 3.2-26

3.2.7.2 Target Station Shielding and Beam Pipe Installation 3.2-26

3.2.8 Commissioning Plan *3.2-27*

Table of Tables

Table 3-2-1 Comparison of the neutrino event yield for various target configurations. ____ *3.2-28*

Table 3-2-2 Scaling of the target tests to the NuMI baseline target configurations. ____ *3.2-29*

Table 3-2-3 Properties of NuMI Horns. ____ *3.2-30*

Table 3-2-4 Shape of the inner conductor for each horn. For each horn, Z=0 is defined as the upstream end of the Inner Conductor (IC). R_{in} and R_{out} are the inner and outer surfaces of the specified conductor. OC refers to the Outer Conductor, which is a cylindrical can. ____ *3.2-31*

Table 3-2-5 Location of target hall components for the various beam configurations. The medium energy PH2 (me) configuration is the current baseline for initial running. ____ *3.2-32*

Table of Figures

Figure 3-2-1 NuMI target module end view. A 4 mm wide graphite or beryllium fin is held between water cooled plates, and sealed in an inert gas filled tube. 3.2-33
Figure 3-2-2 NuMI target module side view. Graphite or beryllium fins have slots cut to form 'teeth', and are clamped between water-cooled plates. Each tooth is 12.5 mm long. There are 8 fins, each with 10 teeth. 3.2-34
Figure 3-2-3 The relative neutrino event rate at Soudan as a function of the proton beam spot size RMS. These are results of a HALO Monte Carlo calculation, using a cylindrical target whose radius was always taken as 2.25 times the beam spot RMS. 3.2-35
Figure 3-2-4 The maximum equivalent stress from quasi-static temperature calculations in a graphite cylinder as a function of proton beam spot size. The dashed line indicates the yield limit. The design calls for a 1 mm RMS beam spot. 3.2-36
Figure 3-2-5 The horizontal and vertical beam profile at the target, from the TRANSPORT Monte Carlo through the extraction and beam line optics, with a gaussian shape fit for comparison. The shapes are characteristic of what will be delivered to NuMI, but the sizes will be tuned depending on the choice of target material. 3.2-37
Figure 3-2-6 Optimization of target density and length. For a given radius of the target R_n the triangles and scale on the right show the density of the target that produces the largest pion yield, while the other points and the scale on the left show the pion yields as a function of that length and density. 3.2-38
Figure 3-2-7 The stress at selected points in the target as a function of the tooth-length, indicating a preference for many short teeth as opposed to a long segment. 3.2-39
Figure 3-2-8 The maximum temperature in the target as a function of time. 3.2-40
Figure 3-2-9 Prototype target segment to be used in a beam test. 3.2-41
Figure 3-2-10 A GEANT Monte Carlo event, showing focusing of a pion by the two horn system. The pion is over-focused by the first horn, and is brought parallel to the beam line by the second horn. Note the difference of a factor of 100 in the vertical and horizontal scales. 3.2-42
Figure 3-2-11 First focusing horn. Dimensions shown are in inches. 3.2-43
Figure 3-2-12 Second focusing horn. Dimensions shown are in inches. 3.2-44
Figure 3-2-13 Cutaway drawing of the first horn. The strip-line connections and the water drain are also shown. 3.2-45
Figure 3-2-14 Horn temperature profile just before and after the pulse. 3.2-46
Figure 3-2-15 Horn conductor displacement just after the pulse (a) in the neck region, and (b) at the upstream end. DMX indicates the maximum displacement in cm. The displacement is much exaggerated in the figure to make it visible. 3.2-47
Figure 3-2-16 Von Mises stress in the horn conductor just after the pulse at steady state (a) in the neck region, and (b) at the upstream end. 3.2-48
Figure 3-2-17 A cross section of the target pile, which is a thick shield to absorb radiation produced when the primary beam hits the target. The second horn is shown hanging from its alignment module, which rests on alignment rails at the top of the channel. 3.2-49
Figure 3-2-18 The target pile in place in the target hall. The horn locations for the Low Energy, Medium Energy, and High Energy Beam configurations are shown, as well as locations for working on and storing horns. 3.2-50

3.2.1 Introduction

The neutrino beam devices use the primary proton beam coming from the Main Injector to produce a beam of neutrinos. This is done in a three-step process. Protons strike a target to produce short lived hadrons, the hadrons are focused towards the neutrino experimental areas, and as the hadrons travel through a long pipe a fraction of them decay to neutrinos. The hadrons are focused by devices called horns, which produce intense magnetic fields. At the end of the pipe the remaining hadrons are absorbed in a beam stop. Neutrinos, which are weakly interacting particles, continue through the hadron absorber and the earth to the experimental areas. To minimize the number of hadrons that are absorbed by air, pipes filled with helium are placed between the horns, and the air in the long decay pipe is evacuated.

In this section, we concentrate on the individual elements that are involved in transforming the proton beam into a neutrino beam; the conceptual design of the neutrino beam has been more extensively described in Chapter 2. The NuMI horns and target will be required to operate at nearly 4 times the repetition rate of the horn system currently in operation in the CERN West Area Neutrino Facility[1], (which pulses for two extractions each 14.4 second cycle), and with around 20 times the delivered number of protons on target per year. This presents challenges in the areas of target stress and cooling, horn stress and cooling, radiation damage to components, and more limited access for repair because of higher residual radiation levels. A set of prototypes and tests are planned to validate our designs with respect to these concerns, and are described later in this section.
The integrated shielding and support system for the neutrino beam devices are included in this WBS element, and hence in this section.

3.2.2 Neutrino Beam System Objectives

The primary objectives of the neutrino beam system are:

1. Produce a wide band muon neutrino beam at the MINOS Far Detector with as many muon neutrinos as possible. The neutrino energy spectrum which is optimal for measuring neutrino oscillations in the MINOS detector depends on the Δm^2 of the neutrinos; lower energy neutrino beams are in general more effective for lower Δm^2. Since the value of Δm^2 is not known at this time, a flexible optics system which can be tuned to different energy bands is desired. Given current limits on Δm^2, neutrinos with energies much above

[1] NEUTRINOS FROM THE CERN SPS, V. Palladino, Warsaw 1996, ICHEP '96, vol. 2, 1723-1726.

20 GeV are known not to be useful, as the oscillation probability will be small. On the other end, event flavor identification by tagging of the muon in the MINOS detector falls off below one GeV, and will limit the usefulness of lower energy neutrinos. The neutrino focusing system described covers this energy region in three tunes, which respectively emphasize approximately the 1 to 3 GeV region, the 3 to 8 GeV region, and the 8 to 20 GeV region. Given the long NuMI decay pipe, it is practical to achieve 10^{-9} neutrinos/m^2/Proton-on-target at Soudan for the medium and high-energy configurations. Pion production rates and decay kinematics limit the low energy configuration to about 0.4 10^{-9} neutrinos/m^2/Proton-on-target at Soudan.

2. Facilitate prediction of the spectrum in the MINOS Far Detector to 2 or 3%, given a measurement in the MINOS Near Detector and absent neutrino oscillations. At this level, the beam systematics would be comparable to the statistical precision of the experiment and MINOS detector calibration effects. This further leads to tolerances on alignment of beam elements that, while exacting, have been achieved in other FNAL fixed target experiments. This goal also leads to requirements on the knowledge of hadron production spectra, and magnetic fields in the horns as a function of time during the spill which must be correlated with beam intensity during the spill.

3. Keep electron neutrino and muon anti-neutrino event backgrounds small, < 1% of the muon neutrino event rate.

4. Center the neutrino beam so that the neutrino event rate in the MINOS detector is maximized and the effect of mis-steering is less than 2% anywhere in the neutrino spectrum. (For scale, a 2% change in the spectrum occurs at about a 75 m offset from the center of the beam at Soudan for a high energy beam, and at about a 167 m offset for a medium energy beam).

5. Accommodate a primary beam intensity of 4×10^{13} protons every 1.9 seconds, in order to match the production capability of the Main Injector.

6. Accommodate a spill length of 1 millisecond, which avoids pile-up of neutrino events in the near detector. With 1 millisecond extraction, somewhat less than 1% of events in the near detector overlap with the current electronics design, which is quite comfortable. Single turn extraction from the Main Injector would result in a spill length of only 8 microseconds, which is much too short. Although having a shorter spill would make cooling the NuMI horns less challenging, the Main Injector resonant extraction system will not run faster than 1 millisecond without hardware upgrades. 1 millisecond extraction implies that the half-sine-wave current pulse to the magnetic horns have a baseline of order

5 milliseconds long, which keeps the difference in horn magnetic field between the center and ends of the extraction to 5%.

7. Assure long-term reliability, stability, and reparability. The facility needs to be usable for a minimum of 10 years, although it is probable that the target and horn configuration would be modified during that time. The target and the first horn, which are the components under the most stress, are designed to operate for at least of order 1 year, so that down-time for replacement is not excessive. The problem with assuring longer lifetime is not from normal fatigue, but from radiation damage, which we are not able to estimate very well at this time. On the other hand, overly conservative target and horn designs lead to significant reductions in the neutrino production rate.

8. Assure personnel safety from possible mechanical, electrical, ODH and radiological hazards associated with this system.

Secondary objectives considered during the conceptual design phase of the project include:

- Assuming we start with the Medium Energy Beam, accommodate future conversion to a Low Energy or High Energy Beam. This refers to a beam where the neutrino spectrum peaks at a lower or higher neutrino energy; the proton beam power would remain the same. (Note this and other goals in this sub-section impact mainly the target hall shielding and target pile channel access designs).
- Accommodate future conversion from the baseline muon neutrino beam to a muon anti-neutrino beam. This can be done by reversing the direction of the current in the horns, thus focusing negatively charged pions instead of positively charged pions. In order to reduce the muon neutrino contamination, one might also install a small angle beam stop or plug after the first horn, similar to that for the Low Energy Beam.
- Accommodate future conversion to a Narrow Band Beam. We foresee using the same pair of horns; it would be necessary to add some dipole magnets and a beam stop with a collimating hole in the target hall.
- Accommodate future Main Injector increases in proton intensity, up to 6×10^{13} protons per pulse, from the baseline 4×10^{13} protons per pulse. This makes sense to do up front for items like installed cooling capacity. For the target, where higher capacity means giving up some neutrino production efficiency, one would install a new target when required by increased Main Injector intensity.

3.2.3 The Target

In designing the target for the NuMI beam, the following objectives must be met:

1. Maximize the neutrino yield. This is accomplished mainly by maximizing secondary pion production and minimizing pion re-absorption through optimal choice of target material and geometry, but also depends on the focusing system depth of field.
2. Provide reliability for at least ten million pulses, corresponding to one year of running.
3. Ensure the ability to check that the beam is properly centered on target, and that the target is centered in the overall beam-line.
4. Permit replacement of the target module when the target fails.

In the target design, a trade-off is made between stress in the target and particle production. Given the higher intensity of the Main Injector proton beam compared to the intensity for previous neutrino beams, and the consideration of newer graphite and beryllium alloy materials, a prototype and testing program is necessary.

3.2.3.1 Target Technical Requirements and Design Assumptions

The technical requirements placed on the target design include:

1. sufficient length to absorb the majority of the proton beam, while staying within the depth of field of the primary proton beam and the horn focusing system;
2. sufficient cross-sectional area to intercept most of the proton beam;
3. sufficient cross-sectional area to allow for the expected level of beam position variation;
4. minimal cross-sectional area (plus gaps between segments) to maximize pion production by minimizing secondary particle re-absorption;
5. selection of a material and geometry which can withstand the stress due to differential heating during the beam spill (graphite and beryllium are the most suitable choices);
6. sufficient steady state cooling to keep the target from being destroyed;
7. survival in the case of mis-steered beam (beam hitting the edge of the target can cause larger stress than beam in the middle of the target; also the target segment supports must be located where mis-steered beam cannot reach them);
8. an inert atmosphere surrounding target (in the case of graphite);
9. an electrically insulated target, if the target is to be monitored with a charge-readout (Budal) monitoring system.

In the target design, we have assumed that the desired neutrino beam is a Medium Energy to High Energy Wide Band Beam, thus emphasizing the production of high-energy pions at small production angles. (The Medium Energy and High Energy targets differ only in the

gap space between target segments). The target for the Low Energy Beam has not been engineered yet, although a reasonable target configuration has been used in the neutrino beam Monte Carlo simulation. The target is designed for a primary beam intensity of 4×10^{13} protons over a 1 millisecond spill every 1.9 seconds. The stress limitations then imply that the primary beam spot radius be at least of order 1 mm RMS, and the optimization of the flux implies that it be no larger than this. The requirement on the proton beam depth of field implies less than a 0.4 milliradian proton beam divergence. We have also assumed that the primary beam position instability is at worst 0.25 mm. (Recent fixed target experiments have done better than this). In order to check the position alignment, the target will be mounted with sufficient remote movement capability to scan it through the beam.

In addition, we will provide for remote installation and removal, so as to minimize radiation dose to workers. We will hermetically seal the target module to prevent spread of radioactive contamination in case the target is destroyed. The target box will hang from its own shielding module, separate from horn 1, for the Medium and High Energy configurations, and is replaceable independent of horn 1.

3.2.3.2 Target Design and Description

The current design is a 3 mm to 6 mm wide, 1.0 to 1.6 m long water-cooled graphite or beryllium fin, as illustrated in Figure 3-2-1 and Figure 3-2-2. The proton beam travels through the tip of the target; the fin extending to the cooling channel provides for support and conduction cooling of the active target volume. The aluminum clamping plates holding the fin are at a large enough distance from the beam centerline to be protected from mis-steered beam by the horn baffle protection system. Approximately 90% of the protons striking the target interact while passing through the two interaction lengths of target material; these interactions produce the pions that will decay to produce the neutrino beam.

The target and horn focusing system are designed as a unit to maximize the muon-neutrino charged current event rate at the MINOS far detector. Since the system of horns has a large depth of field, the maximum event rate is achieved through use of a long target with a small cross-sectional area. The optimal choice of target "radius" is driven by two opposing trends: the flux of pions and kaons out of the target decreases with increasing target "radius" due to particle re-absorption, but undesirable target stress from the heat load of the high intensity proton beam also decreases with increasing target and beam spot radius. (The beam spot size is tunable in both the horizontal and vertical directions via upstream

quadrupole magnets). **Figure 3-2-3** indicates the neutrino event rate dependence, and Figure 3-2-4 shows the quasi-static temperature stress in a graphite cylinder as a function of beam spot size. The proton beam spot size should be of order 1 mm RMS for the target to have a reasonable safety factor with respect to the stress limit. With an axially symmetric gaussian beam profile, secondary production is maximum when the target radius is about 2.3 times the beam spot RMS, which would imply a target radius of order 2 mm. (A larger ratio of target to beam spot implies more re-absorption, while a smaller ratio leads to more of the gaussian tail missing the target entirely). Both our target and beam are not exactly axially symmetric.

Although helium gas jet cooling is not out of the question, conduction cooling of the target segments with water cooling of the base is felt to be more conservative. (One concern is that at the very high helium velocities required, the graphite might erode). Conduction cooling leads to the "fin" design, where both cooling path and support are provided by a solid slab of the target material, but short exit paths for particles are provided out the other three sides. In this case, a thinner target with an elliptical beam spot provides higher neutrino production rate than a symmetrical beam spot. The resonant extraction scheme also sculpts the shape of the beam spot, which produces some asymmetry in the horizontal direction, while leaving the beam close to gaussian in shape in the vertical direction, as shown in Figure **3-2-5.** The effects of target misalignment (0.25 mm), beam divergence (0.32 mm), and beam wandering (0.25 mm) are reasonably small compared to even a 2 mm radius target. The fin design is also operationally more flexible than the rod design; for instance if higher beam intensity became available, one could spread the beam further down the fin (to keep the stress under control) thus making use of the extra intensity.

Figure **3-2-6** illustrates the studies carried out to optimize target density and length. The yields are maximal at a desired average density that is lower than the density of graphite. This density is achieved via gaps between target segments. Table 3-2-1 lists relative yields for various target configurations and shows the progression from rod to fin targets, and then to non-symmetric beam shape. The material properties and the allowable beam spot size are significantly different for the graphite and beryllium designs, but the yields are still competitive.

Figure **3-2-7** illustrates the dependence of the stress at selected points in the target as a function of the segment-length, indicating a preference for many short target pieces as opposed to a few long ones. Short sub-segments are produced by cutting slots part way

through the target fin, forming "teeth" in the slab. This sub-segmenting is fairly easy in the fin design, but would be hard in a rod design.

Figure **3-2-8** shows the maximum temperature in the target as a function of time. The target reaches equilibrium after only a few pulses. The graphite is hot enough that an inert atmosphere is required. The target will thus be contained in a box, which is helium filled or evacuated, with thin beryllium windows at the beam entrance and exit regions. (Thin windows are less stressed than chunk targets by the same beam intensity, and should not have a problem surviving at NuMI intensities).

One technique for monitoring whether the beam is properly hitting the target involves instrumenting the target itself. One electrically insulates the target, and simply measures the charge knocked out of the target by the beam. The electrical insulation of the target fin will be provided by a 40 micron thick anodization layer on the aluminum cooling plates. The rest of the monitor consists of a wire from the target segment to carry the charge outside of the shielding, where a preamplifier and bias supply is located. (The ability to bias the segments up to +100 V is envisioned). With our intense beam, and a reasonable RC, the signal is expected to be very robust, in the range of a volt per segment. While it is not certain that this technique will work in our target environment (e.g. what is the effect of ionized helium surrounding the target, and will radiation damage the anodization layer), it is a simple way to separately monitor each target segment, which is very difficult to do otherwise.

3.2.3.3 Target Design Validation

A 2 meter long, 3 mm diameter segmented beryllium rod target has been in use at CERN for neutrino production for some years. Thus the general concept of a long thin target, with gaps for lowering the effective density, has been well tested. We will however run with higher proton intensity and a different spill structure, and careful calculations and tests are needed to assure reasonable target operation.

The effect on pion production of variations of target geometry has been calculated using the NUADA and MARS computer codes. Initial designs used CASIM to model energy deposition, and heating and stresses were calculated analytically. Later design studies used MARS for energy deposition, and HEAT2D and STRESS3D from the HAST simulation

package to study heating and stresses[2]. Further design studies will be done with the ANSYS package for heating and stress. Thus far, only quasi-static stress calculations have been done. From work done at CERN[3], the indications are that thermal shock effects are not important for our spill length of 1 ms, but we plan to do dynamic stress calculations to confirm this. Finally, target prototype modules will be placed in a test beam. The test beam will be a factor of a few less intense than the NuMI design beam, so it is planned to run with the spot size and target thickness reduced to produce an equivalent stress, as shown in Table 3-2-2.

The test beam run will also provide a test of the Budal monitor concept.

3.2.3.4 Target Prototype and Test Program

It must be demonstrated that the NuMI target design can survive the thermal stress and shock wave impulse generated by the beam. The full target design will follow the test of a prototype water-cooled target segment. The IHEP neutrino beam group has designed prototype carbon and beryllium target modules for NuMI[4]. Target segments based on this design are being constructed for a beam test, which is scheduled to take place December 1998 through January 1999. The test will use Main Injector beam at the Anti-Proton target hall AP0. One segment of the target is shown in Figure **3-2-9**. The target is water-cooled and the cooling will be supplied by an existing closed loop cooling system at AP0. The target assembly will be hermetically sealed. The target box will be mounted on an existing module at AP0. The water lines, electrical leads, and target box will be remotely removable consistent with ALARA.

High intensity testing of the target segments is officially part of the Fermilab schedule. The test will last for approximately one month. The goal is to have a proton beam consisting of 1.E13 protons per pulse with a 2-3 second duty cycle and a spot size of 0.4mm. (If the Main Injector does not reach that intensity so early in its commissioning, we will compensate by reducing the beam spot size.) The target will be located in the AP0 target

---

[2] Pre-engineering Design for the Technical Components of the NuMI Beams, A. Abramov *et al.*, Institute for High Energy Physics, 1997, and Preliminary Design Work on NBB Absorber and Target Prototype, A. Abramov *et al.*, Institute for High Energy Physics, 1998.

[3] Thermo-Mechanical Calculation and Optimisation of a Thin Cylindrical Target, appplied to Neutrino Beam Production toward Gran Sasso, Serge Peraire (CERN), 1998 Joint Meeting of the American Physical Society and the American Association of Physics Teachers.

[4] REPORT: Preliminary Design Work on NBB Absorber and Target Prototype, A. Abramov *et al.*, Institute for High Energy Physics, 1998.

vault for the test. The intensity will be achieved by loading the Main Injector with six booster batches each of which contains 1.7E12 protons. Full turn extraction will be done at MI52 using the multi-mode kicker. The extracted beam will pass through the F0 lambertson (de-energized for this application) to reach the AP1 beamline and finally the AP0 target vault.

Since the intensity specified for the test is a factor of 2 larger than that required for Run II antiproton production, a revision to the shielding assessment for AP0 and the AP1 beamline is necessary. For their protection, the antiproton production target SEM, target, lithium lens and single turn pulsed dipole will reside on blocks out of the beam. Calculations will be done to verify that the AP0 beam dump can withstand the heat deposition of the test beam.

The spot size of the 120 GeV proton beam on the antiproton target can be as small as 0.15 mm RMS. The spot sizes required for the test will be easily achievable by re-tuning quadrupoles in AP1 at low intensity with the target secondary emission monitor in the beam. If the intensity goal is not met, then the spot size will be reduced to achieve an increased energy deposition density. The energy deposition density is critical to achieving a stress distribution in the target which is similar to that which will be experienced under NuMI operating conditions. A vertical dipole (M:VT108) and a horizontal dipole (M:HT107) have variable 25 Ampere power supplies which enable the experimenter to tune beam position from an ACNET (accelerator control) console. Checking of the proper positioning of the beam on the target will be provided by a beam scan through three positioning spikes near the target which are instrumented with thermocouples, and a Budal monitor and temperature probe attached to the target itself.

When the module is lifted out of the AP0 beam channel, the target segments can be examined for damage through a quartz window in the side of the target module.

The results of the prototype target test and subsequent thermal and structural calculations will determine the design of the operational target.

3.2.3.5 Prototype and Operational Target Construction

The target construction plan is to have the graphite or beryllium target fins obtained pre-machined from a vendor. The other target module components will be constructed and assembled by the Institute for High Energy Physics, Protvino, Russia, then shipped to

Fermilab. The target fin locations will be mapped to fiducial marks on the end-plates of the target module.

3.2.4 Magnetic Focusing Horns

3.2.4.1 Horn Objectives and Technical Requirements

The baseline focusing system is designed to produce a Wide Band Beam, with the flexibility to cover the neutrino energy region between about 1 GeV and 20 GeV. Any one configuration of the target and horns provides optimal focusing over only about a factor of three in neutrino energy. The design allows for redeployment of the second horn and the installation of a separate target for each of three configurations, which together then cover the desired region. For the High Energy and Medium Energy configurations, the neutrino energies are above tau lepton production threshold. The primary objectives of the magnetic horn focussing system are to collect the pion phase space that will yield the highest possible ν flux; and point the ν beam precisely at Soudan. The center of the beam should be within about 75 meters of the detector at Soudan.

We want to provide at least ten-million pulse reliability during ν beam production, corresponding to one year of running. We also want to maintain geometrical shape/magnetic field quality over the horn lifetime. It is desirable to know the field integrals for particles passing through the horns to 1%.

We must design ALARA friendly connections. Connections to the horn must be either outside the radiation shielding, or else makable/breakable via remote handling. Other goals are to produce a modular design, choose materials whose activation levels reduce quickly after beam off, and provide high reliability for motion control motors and position read-back monitors.

The technical requirements include providing a 1 ms flat-top 200 kA current pulse to each horn, where current variation is less than +/-5%. This is currently provided by a 5 ms baseline damped half-sine wave pulse. The magnetic field characteristics must approach that used in the beam Monte Carlo design models. Significant deviations (of order 1% in the field integrals seen by particles) should be mapped during prototype testing. Current should be monitored to 0.4%.

Neutrino beam alignment requirements lead to 0.5 mm total alignment tolerance for each horn.

Water spray cooling is required for the horn inner conductor, which must be corrosion and radiation resistant. Radiation hard insulators must be exclusively used.

The horn inner radius should be large enough that a baffle system on the primary beam can prevent mis-steered primary beam from directly hitting the horn. The horn would be destroyed if even a few pulses of the primary beam hit it directly.

3.2.4.2 Horn System Description

The horn focusing system is discussed in some detail in *Conceptual Design for the Technical Components of the Neutrino Beam for the Main Injector (NuMI)*[5]. Briefly, the horn system works as follows. The pions emerging from the target have a typical momentum component transverse to the primary beam direction of 300 MeV/c. A much more intense neutrino beam can be produced at Soudan if those pions are focused more parallel to the beam centerline. This is accomplished with a series of "horns". A current runs down the center conductor of the horn, then back through the outer conductor, thus forming a loop that produces an azimuthal magnetic field in the volume between the inner and outer conductor of the horn. Positively charged pions that enter the horn volume are focused toward the beam center, negatively charged pions are defocused. The required integral field strengths, of order 1 Tesla meter, are achieved by using 200 kA of current over lengths of order two meters. Figure **3-2-10** illustrates the working of the NuMI two-horn focusing system. In the Monte Carlo event shown, a positive pion enters the first horn through the sloping inner conductor, is initially overfocused, and is focused parallel to the decay pipe by the second horn.

Horn parameters are listed in Table 3-2-3, with more detailed shapes for the conductors described in **Table 3-2-4**. The locations of the components in the target hall for the various beam configurations are given in **Table 3-2-5**.

Horns 1 and 2 are shown in Figure **3-2-11** and Figure 3-2-12 respectively. The general horn design was optimized to maximize the event rate in the MINOS detector, over a wide neutrino energy range. The innermost radius of the first horn was chosen comparable to other horn systems that have been built and operated, and to have a reasonable clearance to protect it from mis-steered primary beam. The inner conductors of the horns are made as thin as possible to reduce the beam loss due to pion interactions in the aluminum. The

electrical current is pulsed for as short a time as possible, while still covering the beam spill, but the inner conductor still requires water spray cooling. Figure 3-2-13 is a cutaway drawing of the first horn, showing strip-line connections and the water drain.

The horns will be mounted on alignment fixtures, as shown in **Figure 3-2-17,** which are close copies of fixtures called Universal Modules that are currently being used in the anti-proton production target hall at Fermilab.

The horn electrical connection to the stripline leading to the power supply is not yet designed. There are several issues involved that will have to be addressed, such as allowing for horn alignment motion, and keeping the radiation dose to humans low during connection and disconnection of radioactivated horns. The stripline is discussed in Section 3.3.

3.2.4.3 Horn Design and Development Program

The horn system is sufficiently complex that experience will have to be gained in a testing program in order to satisfy the primary objective of 10 million pulse reliability. This goal is equivalent to one year of NuMI running and is a compromise between high neutrino flux and structural robustness.

The principal technical concerns that make a development and testing program necessary are:

- structural integrity of the horns
- erosion/corrosion on the water spray cooled Al 6061 T-651 inner conductor
- mechanical durability of the radiation hard insulators used
- achievement of .5 mm total alignment tolerance for each horn
- electrical current control/monitoring tolerance of 1%
- high heat removal rate needed for the horn inner conductor

The structural integrity issue is the most critical for horn 1. Horn 1 will be prototyped before the operational horns are built because it contains the point of highest stress. The stress is the highest in horn 1 because its overall size is the smallest while its current density and Joule heating are the highest. Repetitive thermal and magnetic stresses will

[5] J. Hylen *et al.*, FERMILAB-TM-2018, September 1997.

weaken the horn inner conductor over many pulses until the fatigue limit is reached. The design goal is to minimize the maximum cyclic stress in the prototype. The design and fabrication of horns for use in NuMI operation will follow tests of the prototype horn 1.

3.2.4.4 Horn Fatigue Analysis

A description of the analysis work in progress follows for the horn 1 prototype. This horn is the most challenging of NuMI target station horns because of its small cross sectional area at the neck that results in high electrical resistance and formidable Joule heating. This heating produces thermal stresses. After examining stresses at mid-pulse (with magnetic forces present) and again just after the pulse, it has been concluded that stresses are highest just after the pulse at steady state.

The fatigue analysis to be described is based on the von Mises stress in the system. The tensor that describes the stress in an infinitesimal element of a solid structure may be separated into hydrostatic and deviatoric contributions. The hydrostatic portion is simply the average stress present on all element faces. The deviatoric stresses are responsible for changing the shape of the element and creating material fatigue. The von Mises criterion states that the yielding of an isotropic material begins when the effective stress reaches a limiting value. An element oriented such that shear stresses are equal to zero has stresses normal to each face called principal stresses (σ_1, σ_2 and σ_3). These are used to define the effective stress: $\sigma_e=(1/2^{1/2})((\sigma_1-\sigma_2)^2+(\sigma_2-\sigma_3)^2+(\sigma_3-\sigma_1)^2)^{1/2}$.

For cyclic loading, the limiting value to compare the effective stress with is the fatigue strength. A Goodman diagram plots the fatigue strength as functions of cycles to failure, minimum cyclic stress and maximum cyclic stress. The most likely point of failure in our design turns out to be the most upstream part of the horn. The calculated minimum and maximum stresses at this location are used to determine the mean and alternating stresses. The fatigue strength limit for a lifetime of 10^7 cycles at the effective mean stress will be used to calculate the safety factor. A safety factor N will be quoted which is the limiting fatigue strength divided by the effective alternating stress.

A detailed finite element structural analysis of horn 1 has been done using ANSYS[6]. The prototype horn inner conductor is 3.16 m long. The inner radius at the neck is 0.9 cm and the most upstream portion of the cone has an inner radius of 3.54 cm. The thickness of the

[6] ANSYS 5.0(1992), Swanson Analysis Systems, Inc., Houston, PA.

conductor wall grows from 2 mm to 4.5 mm as one moves downstream from the target to the neck. Just downstream of the target is a doughnut-shaped transition piece that increases in thickness with radius as one moves from inner to outer conductor. The outer conductor is cylindrical in shape and approximately 1 cm in thickness. Four sprayers will be mounted symmetrically about the azimuth to cool the surface of the inner conductor evenly through convective water spray heat transfer.

The thermal and magnetic pressure loads were applied to an ANSYS PLANE42 structural model. Joule heat loads were calculated by a C language program which uses electrical pulse characteristics given, the material properties of Al 6061 and geometry to calculate deposited heat load in the horn inner conductor. The equation for the electrical current pulse used to generate heat for the thermal load is $I=325{,}000\ e^{-211t} \sin(626t)$ amps, which gives a half-cycle baseline of 0.005 s. The time between cycles is 1.9 s. The aluminum 6061 material properties (including temperature and electrical ac effects for ρ_e) used were $\rho_e = 5.8 \times 10^{-8}\ \Omega$-m, $\rho_m = 2700$ kg/m^3 and $k_{Al} = 200$ W/m-C.

The water spray convective heat transfer coefficient will have to be measured as part of the prototype program since it is not well known. The value used in the model is $h_{spray} = 1700$ W/m^2-C with $T_{spray} = 15$ degrees C. With this heat transfer coefficient, the inner conductor maximum temperature is just under 100 degrees C. This is significant since at the boiling point of water, the heat transfer becomes film boiling type. The corrosion associated with this type of heat transfer is significant. Estimations from an industry standards table and from a convective calculation for a heated cylinder in turbulent water flow[7] indicate that a higher value of the heat transfer coefficient should be achievable. Film boiling can be avoided if this is the case.

The given parameters are used in the following equations for steady state temperature and per pulse heating:

$$T_{steady\ State} = (\int I^2 dt)(\rho_e dx/A)/(t_{cycle} h_{spray} 2\pi r dx)$$

$$T_{pulse}(x) = (\int I^2 dt)(\rho_e dx/A)/(c\ \rho_m A\ dx)$$

[7] "Thermal Design and Optimization", A. Bejan, G. Tsatsaronis, M. Moran, John Wiley & Sons, P.186, 1996.

Target shower radiation heat loads were calculated by the CASIM program for a simplified baseline geometry. The radiation heat load is small and accounts for a uniform temperature rise of 1.5 degrees C in the inner conductor.

Magnetic forces were calculated by a C language program using an analytic formulation of the **J x B** Lorentz force given by:

$$\mathbf{F}=\int \mathbf{J} \times \mathbf{B}\, dV \text{ and } d\mathbf{p}= \mathbf{J} \times \mathbf{B}\, dr = J_o^2 \mu_o \pi (r^2 - r_i^2)/2\pi r$$

Steady state temperature and temperature gradients were cross-checked using an ANSYS THERMAL 55 2-D axisymmetric model. The initial temperature distribution was iteratively increased until the initial temperature distribution was returned at the completion of the cooling cycle.

The maximum temperature in the horn is 97° C at the neck of the inner conductor. The temperature profile of the inner conductor just before and after the pulse is shown in Figure 3-2-14. The average total power generated and deposited in the horn inner conductor from all sources was found to be 17.5kW.

The structural analysis shows that the maximum von Mises stress occurs in the most upstream part of the horn just after the electrical pulse. The temperature rise in the inner conductor causes the inner conductor to elongate with respect to the outer conductor. This is shown in Figure 3-2-15. The upstream inner to outer conductor transition piece is doughnut-shaped, and is shown in half-symmetry cross section in Figure 3-2-15(a). The total elongation is 1.3 mm. This causes significant bending stresses at steady state in the upstream section of the horn. The neck region also experiences significant displacement and deformation as shown in Figure 3-2-15(b). The deformation and stress in the neck has been reduced by allowing the outer conductor to thermally strain. The temperature in the outer conductor is assumed to be a constant 25 degrees C in the model as compared to the cooling water temperature, which is 15 degrees C.

The maximum von Mises stress distributions for the downstream end and the neck are shown in Figure 3-2-16(a) and Figure 3-2-16(b) respectively. To do the fatigue analysis, it is necessary to know the maximum von Mises stress (which occurs just after the pulse) and the minimum (which is just before). The most downstream point is taken to be the most likely point of failure and it cycles from 2950 N/cm^2 to 5175 N/cm^2. The mean and alternating stresses are then 4100 and 1115 N/cm^2 respectively. The fatigue limit for this

stress ratio which will give a lifetime of 10^7 pulses in a structure made of Al 6061 T6 aluminum at 100 degrees C is 5400 N/cm^2 from Department of Defense Aerospace literature[8]. This analysis thus predicts that a safety factor of 4.8 is present according to the von Mises criterion with our safety factor definition (fatigue limit divided by alternating stress).

The cyclic cooling of the horn has been considered as well and will not result in significant stresses in horn 1. An analytic plane strain calculation based on a temperature difference of 4° C from inner to outer radius at the neck says that the maximum stress is 400 N/cm^2 under steady state conditions at the outer surface[9]. Under plane strain conditions, the maximum principal stress is circumferential. The 4 degree C temperature gradient across the 4.5 mm thickness may be regarded as small and relatively unimportant compared with the upstream end bending stress.

A prototype for testing has been designed based on this analysis, but more analysis and bench testing of the prototype will be done before the first operational horn is built. Horn 2 can be more robust and will require less scrutiny since the beam physics constraints are less structurally restrictive. Analysis on operational designs for horns 1 and 2 will include a coupled field structural-thermal analysis. A complete vibrational analysis will be done as well.

3.2.4.5 Horn Modal Analysis

A modal analysis has been done to determine the modes that are present in Horn 1. The power supply provides a 100 Hz azimuthally symmetric current pulse every two seconds. The modal analysis shows that the lowest azimuthally symmetric mode is 385 Hz. Thus, the power supply should not be able to excite this mode. The lowest longitudinal mode is at 50 Hz, and there is a small probability that electrical noise or water system mechanical vibration could excite this mode. To combat these sources, two radial spider supports will be introduced into the design. These supports will raise the lowest modes to a few hundred hertz. This will lessen the impact of low frequency mode drivers.

[8] "Aerospace Structural Materials Handbook", Metals and Ceramics Information Center, Code 3206, p.13-15 (1990).
[9] "Advanced Mechanics of Materials", R. Cook and W. Young, Prentice Hall, p.116 (1985).

3.2.4.6 Horn Conductor Fabrication

Horn conductors and end flanges will be constructed of aluminum 6061-T651. The neck pieces and end flanges will be made from billet stock material using computer numerically controlled (CNC) machining. The larger radius inner conductor pieces will be formed by a process known as spinning, where an aluminum sheet is worked to conform to the shape of a wooden mandrel. These pieces will be welded together using CNC tungsten inert gas (TIG) welding. The project calls for .02" total alignment tolerance on horn 1. This is apportioned as .01" survey tolerance and .01" fabrication tolerance. The machining and welding methods mentioned should ensure the satisfaction of the fabrication tolerance. The survey tolerance is addressed in section 3-6.

3.2.4.7 Horn Spray Cooling System

The outer conductor will contain four equally spaced line slots parallel to the horn axis about its azimuth. Line nozzle water sprayers will be installed in these slots to spray cool the inner conductor during operation.

Since water spray cooling will be used on the inner conductor (whose wall thickness varies from .08" to .12"), erosion and corrosion are significant considerations. To resist water corrosion and possibly electrical breakdown, the horn surface will be coated. The coatings under consideration are:

- hard anodizing which has the added benefit of providing electrical insulation (Note: IHEP information from CERN suggests 175V/mil dielectric strength; IHEP has tested 0.1mm anodized coating to 4 kV before breakdown)
- alodine -passivated chromate conversion coating, electrically conductive
- dicronite/tribonite(WS_2) - wear hard surface
- irridite/Chromate - Zn components are undesirable from mixed waste considerations
- electroless Ni - conductive
- tin – conductive

Corrosive effects are minimized in slightly alkaline water (corrosive effects on Al are greatest in acidic solutions). Corrosive effects are also minimized by selection of appropriate water system materials (e.g., copper tubing used in a system to deliver water to aluminum is undesirable as dissolved Cu ions in water lead to deposition corrosion due to the formation of galvanic cells).

In order to keep the inner conductor reasonably below 100 °C, the spray nozzle system must be such that the effective heat transfer coefficient at the inner conductor surface is at least 1700 W/m^2-C. A mass flow rate much above 30 gallon/minute is problematic. The spray droplet velocity must not be so high as to erode the coated aluminum surface. The volume fraction of water to air near the inner conductor, in the path of the beam, must be kept low to minimize absorption of pions, since absorption reduces neutrino production. The nozzle will be designed so that more cooling is present in the neck region of the horn. Care will be taken to avoid a design that can easily plug. Nozzle design and heat transfer coefficient measurements on a test system will be done before nozzle installation on the prototype horn outer conductor. A closed loop water system for spray/evaporation cooling of the inner conductor must be built before testing can begin.

3.2.4.8 Testing of Prototype and Operational Horns

A horn 1 prototype test of 50 weeks duration is desirable since it is long enough to demonstrate that the primary horn lifetime objective has been met (barring radiation degradation of the material parameters). The prototype testing will done at the AP0 Target Station building. The prototype horn will be connected to a lithium lens 3:1 step up current transformer and test power supply which exist. The power supply is capable of providing an average heat load similar to that which will be present on horn 1 during NuMI operation. The differences between prototype testing and operation are that the pulse length will be 1 ms in testing versus 5 ms in NuMI operation while the time between pulses will be 67 ms in testing (7 to 8 pulses are needed) and 1.9 seconds in operation. A dummy load has been constructed and placed in the circuit to verify whether the supply and transformer can withstand this horn testing. Initial measurements with the load are encouraging.

The following measurements will be done during testing:

- inner conductor warping as a function of pulse number
- convective water spray heat transfer coefficient
- vibration spectral density
- magnetic field map (including fringe field)
- alignment drift
- expansion of horn during pulse

Operational horn testing will be done at the Tagged Photon Lab (TPL) at Fermilab. Testing of operational horn 1 will commence once the operational horn power supply is complete and installed at TPL. Structural FEA will begin on horn 2 once horn 1 is in the drawing phase. It is expected that work on horn 2 will proceed in parallel and lag horn 1 by about a

half year. A closed loop water spray system will need to be constructed for the test program. A controls and interlocks system will need to be constructed as well before the horn tests begin. Since both horns are powered by the same supply and since the electrical parameters are tuned for this mode of operation, a dummy load will be used in place of not yet completed horn 2 during the initial testing of operational horn 1. When horn 2 is added to the horn 1 test in progress, the dummy load will be removed. After the horn 1 test is completed, a dummy load will be added to the circuit to complete the testing of horn 2.

3.2.4.9 Horn Design Validation

Horn heating and stress are being calculated analytically and also using the ANSYS, POISSON and EXCEL programs for both a prototype horn section and the operational horns. Small-scale anti-corrosion tests are planned. Small piece welding tests will be done, and then a prototype horn section will be constructed and tested (see section 4.1) for mechanical properties, and for efficacy of the cooling system. X-ray inspection of the welds is planned. An operational horn will be constructed, where the design has been iterated based on the results from the prototype, and will undergo long-term tests before installation in the target hall.

The relative rates of muon-neutrino production for different beam optics designs have been studied with the NUADA and HALO computer codes. The systematics of the focusing systems and the amount of other-flavor neutrino backgrounds have been studied with the Monte Carlos PBEAM and GNUMI. (Discussion of the ranges of validity and use of these models can be found in *Conceptual Design for the Technical Components of the Neutrino Beam for the Main Injector (NuMI)*). There is some variation in the results of different programs, due largely to differing assumptions about hadronic production in the target, but these differences do not have much affect on the system design, only on the final rate of neutrino production.

3.2.5 Target Station Shielding

The objectives for the target station shielding are as follows:

- Provide adequate target station shielding to prevent groundwater radioactivation during normal and accidental beam loss scenarios.
- Provide a stable platform on which to accurately locate neutrino beam line devices and deliver electrical power, component cooling, and hold required instrumentation.

- Provide for device inspection and facilitate device removal/replacement while observing personnel ALARA exposure limits.

The shielding will allow beam line device position adjustment capability to properly align components and allow beam line tuning. It provides part of the shielding that allows beam-on access to the power supply room.

The shielding has a flexible, modular design to accommodate beam line reconfiguration and placement of future beam line components (e.g., Narrow Band Beam focusing components and absorber). In building the shielding, we will recycle available shielding on site to the extent practical, and provide for disassembly and decommissioning.

Specific requirements of the shielding are:

- The support system must maintain static horn and target alignment within 0.5 mm of nominal true position, to meet neutrino beam alignment requirements.
- The horn mechanical attachment structure must be sufficient to restrain mechanical transient vibrations resulting from electrical pulses to less than 0.5 mm.
- Positioning modules, electrical stripline routing, and water cooling systems must allow for a minimum of 6 mm range of motion, to allow for target scans through the beam.
- Support connections and hardware must be well out of the central beam region to avoid secondary particle interactions.
- The horn and target support systems must allow operational flexibility including relative ease in beam line removal and reinstallation, inspection, and repairs.
- Materials used in the target station should be of sufficient radiation resistance to maintain functionality (e.g., module positional read backs and electrical insulation are of special concern).
- Stray magnetic fields from the target station iron that are of order 10 gauss could affect beam optics. It is desirable to avoid magnetizing the slabs, so they should not be lifted with magnetic fixtures. The residual fields must be measured after installation.

3.2.5.1 Design Assumptions

Target station shielding thickness is determined from simulations using the MARS computer code, which accurately predicts the fraction of radiation that penetrates the shielding.

Heating calculations and residual radiation rates assume an incident proton beam on target of $4x10^{13}$ protons per pulse with a 1.9 second repetition rate.

Existing design of the AP0 Universal Module will be used to support and provide adjustment capability to NuMI horns and target; some mild redesign may be necessary to accommodate NuMI specific requirements.

3.2.5.2 Target Station Shielding Description

Figure **3-2-17** shows a cross section of the target pile, which is a thick shield to absorb radiation produced when the primary beam hits the target. Figure **3-2-18** shows a side view of the target pile in place in the target hall. The target shield pile consists of the following:

- The base and sides will be constructed of continuous cast steel.
- Steel T-block assemblies will provide removable shielding at the top of the channel except where modules are located.
- FNAL standard size concrete shielding blocks will be stacked outside the steel channel.
- Inside the U channel will be chase sides of flat steel of total rough dimensions 10 in. thick x 159'4" length x 114 in. tall; residing on top of these chase walls will be an adjustable rail system consisting of adjustable vee-block assemblies fixturing 4 in. diameter ground rails. The neutrino beam target and horn modules will precision align to these rails to facilitate accurate placement and survey. The misalignment budget for the target and first horn is 0.5 mm, so survey of the rail system to 0.25 mm of true position is desired.

3.2.5.3 Design Validation

ANSYS and IDEAS modeling and finite element analysis will be used to generate designs to adequately support the horns during pulsed operation. Engineering reviews will be conducted to insure robust target and horn support designs and operational functionality. ES&H reviews will be conducted during the design phase to insure efficient designs that allow radioactive device removal/replacement while minimizing the risk of personnel radiation exposure. Pulse testing of a prototype horn will provide feedback relating to effectiveness of horn support mechanisms.

3.2.6 Target Station Beam Pipe

By installing beampipes between the horn locations, we accomplish two things. One is to minimize airborne activation, in accordance with ALARA. The other purpose is to minimize interaction lengths of material in the secondary beam path, and thus to maximize the neutrino production. In additional, the pipe should be removable to accommodate future modifications to the beam optics. The pipe could either be evacuated or filled with helium. Although the evacuated pipe would present a somewhat smaller amount of material to the beam (of order 0.8% of an interaction length), the helium solution is currently preferred because it is significantly cheaper and allows more flexibility in the design since it does not have to be built to withstand significant pressure differentials.

3.2.6.1 Technical Requirements and Design Assumptions

Windows in the central 30 cm radius of the beam will be of the minimal thickness necessary to withstand the modest pressure differential induced when purging from air to helium, and are expected to be either aluminum or titanium. The pipe will be helium filled to reduce interaction lengths of material. Sufficiently low concentrations of air in the carrier pipe can be achieved by purging with helium, so that a large pressure differential and thus windows strong enough to hold a vacuum are not necessary.

3.2.6.2 Description

Two sections of helium-filled pipe will be installed to reduce the interaction of beam particles with air. Conventional "helium bags" used in many other beams would not survive in our radiation environment, so Aluminum is chosen as the material for the helium container. The pipes must be reconfigured along with the horns when changing the beam energy. For the Medium Energy Beam one pipe will be located inside the target pile between horns 1 and 2 (length approximately 17.5 m); a second pipe will be located between horn 2 the beginning of the decay pipe (length approximately 18.5 m).

The first pipe displaces 2.34% of an interaction length of air with 0.26% of an interaction length of aluminum for the end windows and 0.45% of an interaction length of helium fill. The second pipe replaces 2.48% of an interaction length of air with 0.73% of an interaction length of aluminum and helium.

The final design of the pipe is dependent on further study of the size required to prevent radioactivation of air that can escape the target hall. In the current design, the 20 ft. pipe of 3 ft. diameter could be fabricated using rolled and seam welded 3003 aluminum sheet stock

sections 84 in. x 113 in. x 0.190 in thick and joined by circumferentially welding individual rolled sections (84 in. length sub-assemblies) together to construct the appropriate length. The 100' pipe would have 3 interface flanges to join 25' sections (in lieu of a continuous 100 ft. length which would make beamline reconfigurations, disassembly, and decommissioning more difficult). The total quantity of 4 windows could be constructed of 0.020" thick 3003 Aluminum. The longer pipe would be located in the shielding chase by resting on rollerized vee-blocks to allow for pipe rotation during flange interface bolt tightening/loosening. Small gas lines will run from the pipes to outside the shielding, to allow helium filling and monitoring after installation. Calculations of air activation and ventilation are required in order to validate the current design. Engineering review will check the adequacy of the window thickness and protection from overpressurization.

3.2.7 Installation Plan and Issues

3.2.7.1 Target and Horn Installation

The target module and horn modules will be mounted on the universal modules, while the universal modules are in the alcove of the target hall. The water, gas, and electrical connections through the universal module will be made and tested. Fiducials on the target and horns will be surveyed relative to fiducials on the universal modules, and checked as the alignment motor drives are stepped. The universal modules with target and horns attached will be lowered into the shielding channel, and the alignment fiducials will be checked again, to assure that alignment can be transferred from the alcove stand to the final placement. Water, gas and electrical connections will be completed. Cooling water flow will be checked. Target box will be purged of air and filled with inert gas and leak tested. Horns will be tested for electrical shorts. Horns will be pulsed, gradually increasing current to design current, while monitoring temperatures.

3.2.7.2 Target Station Shielding and Beam Pipe Installation

Continuous cast salvage steel will be rigged into place, forming the shielding channel. Standard size concrete shielding blocks will be rigged in to complete the side shielding. The alignment rails will be installed at the top of the continuous cast salvage steel, and adjusted until the surveyors indicate they are properly aligned. Target and horn installation will be followed by the carrier beam pipe installation. The carrier pipe will be filled with helium and leak-checked. Then the top T-blocks will be installed.

3.2.8 Commissioning Plan

With the target out of the beam path, beam will be directed down the decay pipe, and beam/decay pipe alignment will be checked by measuring the beam position at the end of the decay pipe with a SWIC. Target/beam alignment will be checked by moving the target across the beam, and measuring the response in several locations, including the muon monitors, the SWIC at the end of the decay pipe, and the hadron monitoring installed in the target hall. Beam current will start low, and as it is increased the temperature of the target will be monitored to assure that the cooling is working as designed.

Secondaries from low intensity beam on target will be focused by the horn system, and the response measured in several monitors, including the muon monitors, the SWIC at the end of the decay pipe, and the hadron monitoring installed in the target hall. Timing of the horn pulsing with respect to the beam spill will be checked and adjusted. Positions of individual horns will be scanned, and the response in the muon monitors will be used to check alignment. If the particle monitors do not show the expected response patterns to pulsing the horn focusing system, the response from pulsing individual horns can be obtained by replacing the connection to the other horns by dummy loads. After some period of pulsing, but before the shielding is rendered too radioactive, an optical re-survey of fiducials on the horn endplates will be done.

Radiation survey of the target hall after initial beam running will identify any places where shielding needs to be improved, such as around penetrations.

Material and configuration	Length and diameter (cm x cm)	Sub-segment length (cm)	Proton beam spot size σ_x x σ_y (cm)	Thermal Stress σ_{eq} (MPa)	WBB relative ν_μ CC event rate
C-cylinder	156 x 0.40	12.5	0.089 x 0.089	30	1.00
C-fin (sym.)	156 x 0.40	2.0	0.089 x 0.089	26	0.95
C-fin (asym.)	156 x 0.32	1.8	0.067 x 0.128	25	0.98
Be-cylinder	171 x 0.63	19.3	0.14 x 0.14	140	0.97
Be-fin (asym)	171 x 0.41	1.3	0.088 x 0.20	152	0.93

Table 3-2-1 Comparison of the neutrino event yield for various target configurations.

	Graphite			Beryllium	
	Baseline	Prototype		Baseline	Prototype
Sub-segment length (mm)	18.4	8.0		12.6	6.0
Thickness (mm)	3.2	1.78		4.1	2.29
Beam Intensity (protons per pulse)	$4x10^{13}$	$0.5x10^{13}$	$1x10^{13}$	$4x10^{13}$	$1x10^{13}$
Beam size σ_x x σ_y (mm x mm)	0.67 x 1.28	0.30 x 0.30	0.40 x 0.40	0.88 x 2.00	0.49 x 0.98
T_{max} at steady state (°C)	508	467	557	220	173
ΔT (°C)	280	394	425	82	90
Maximum equivalent stress (MPa)	25	27	30	152	150

Table 3-2-2 Scaling of the target tests to the NuMI baseline target configurations.

	Horn 1	Horn 2
Overall Length	316.0 cm	354.17 cm
Outer radius	16.19 cm	35.87 cm
Inner Conductor:		
Neck inner radius	0.9 cm	3.0 cm
Neck length	15.31cm	4.17 cm
Upstream parabolic length	60.88 cm	147.91 cm
Downstream parabolic length	223.80 cm	147.91 cm
Thickness neck	0.45 cm	2 mm
Thickness ends	0.2 cm	3 mm
Current	200 kA	200 kA
Current "flat top"	1 ms	1 ms

Table 3-2-3 Properties of NuMI Horns.

Horn 1					
	Upstream Parabola		**Neck**	**Downstream Parabola**	
Region In Z (cm)	0.0 to 35.38	35.38 to 60.89	60.89 to 76.20	76.20 to 93.54	93.54 to 300
R_{in}^{IC} (cm)	$\sqrt{\frac{(70-Z)}{5}} - 0.2$	$\sqrt{\frac{(64.9375-Z)}{5}}$	0.9	$\sqrt{\frac{(Z-73.4425)}{3.4}}$	$\sqrt{\frac{(Z-70)}{3.4}} - 0.2$
R_{out}^{IC} (cm)	$\sqrt{\frac{(70-Z)}{5}}$		1.35	$\sqrt{\frac{(Z-70)}{3.4}}$	
R_{in}^{OC} (cm)	15.33				
R_{out}^{OC} (cm)	16.20				

Horn 2			
	Upstream Parabola	**Neck**	**Downstream Parabola**
Region In Z (cm)	0.0 to 147.915	147.915 to 152.085	152.085 to 300
R_{in}^{IC} (cm)	$0.996\sqrt{\frac{(150-Z)}{0.2}} - 0.187$	3.03	$0.996\sqrt{\frac{(Z-150)}{0.2}} - 0.187$
R_{out}^{IC} (cm)	$\sqrt{\frac{(150-Z)}{0.2}}$	3.23	$\sqrt{\frac{(Z-150)}{0.2}}$
R_{in}^{OC} (cm)	35		
R_{out}^{OC} (cm)	35.87		

Table 3-2-4 Shape of the inner conductor for each horn. For each horn, Z=0 is defined as the upstream end of the Inner Conductor (IC). R_{in} and R_{out} are the inner and outer surfaces of the specified conductor. OC refers to the Outer Conductor, which is a cylindrical can.

	PH2 (le)	PH2 (me)	PH2 (he)	PH2 NBB
Target				
Z (upstream)	0.00 m	-1.00 m	-3.4 m	-3.15 m to –0.90 m
Z (downstream)	0.60 m	-0.04 m	-1.80 m	-2.65 m to –0.40 m
length	0.60 m	0.96 m	1.60 m	0.50 m
radius	2.3 mm	2 mm	2 mm	2 mm
material	Beryllium	Graphite	Graphite	Graphite
Ave. density	1.85 g/cm^3	1.8 g/cm^3	1.2 g/cm^3	1.8 g/cm^3
Horn 1				
Z (upstream)	0 m	0 m	0 m	0 m
Z (downstream)	3 m	3 m	3 m	3 m
Vertical offset	0 m	0 m	0 m	0.15 m
Horn 2				
Z (upstream)	9 m	21 m	40 m	40 m
Z (downstream)	12 m	24 m	43 m	43 m
Vertical offset	0 m	0 m	0 m	0.00 m
Plug Option				
Z (upstream)	3 m			
Z (downstream)	4 m			
radius	15 mm			
material	Beryllium			
Dipole Magnets				
D1: Z (upstream)				3.5 m
D1: Z (downstream)				5.5 m
D2: Z (upstream)				5.9 m
D2: Z (downstream)				7.9 m
D3: Z (upstream)				16.5 m
D3: Z (downstream)				18.5 m
Collimators				
C1: Z (upstream)	-3.0 m	-3.0 m	-5.0 m	-5.0 m
C1: length	1.5 m	1.5 m	1.5 m	1.5 m
C2: Z (upstream)				-2.65 to –0.40 m
C2: length				0.30 m
C3: Z (upstream)				11.7 m
C3: length				4.4 m
C4: Z (upstream)				19.0 m
C4: length				1.0 m

Table 3-2-5 Location of target hall components for the various beam configurations. The medium energy PH2 (me) configuration is the current baseline for initial running.

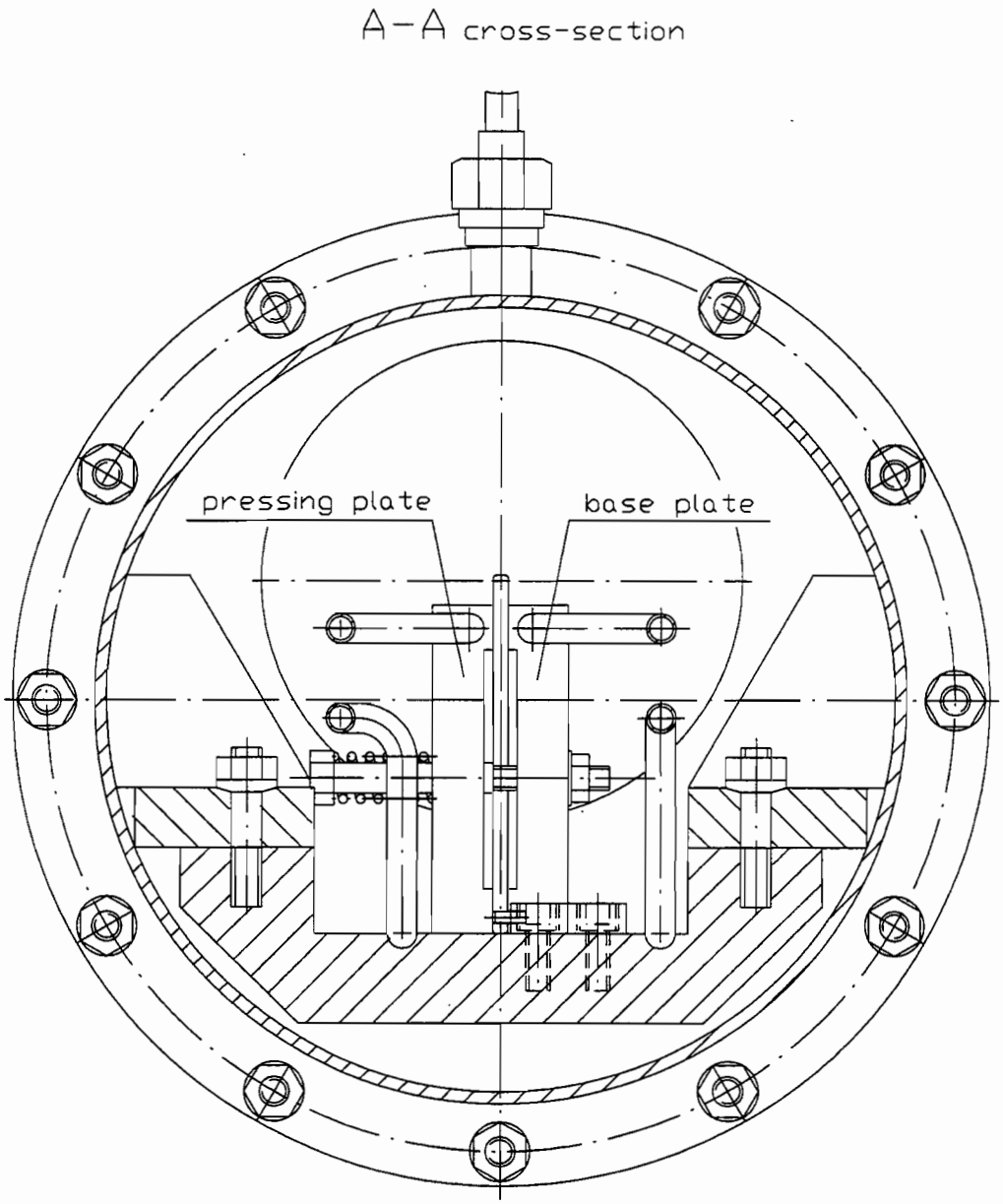

Figure 3-2-1 NuMI target module end view. A 4 mm wide graphite or beryllium fin is held between water cooled plates, and sealed in an inert gas filled tube.

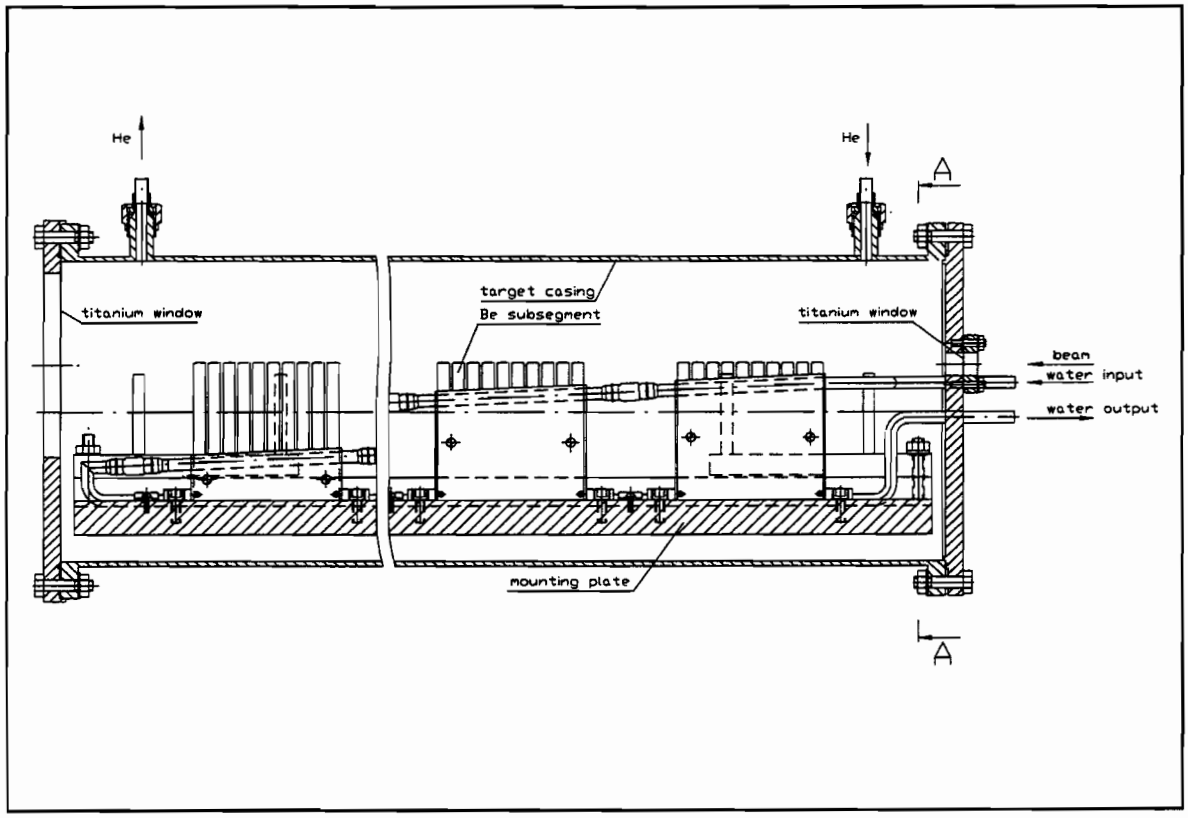

Figure 3-2-2 NuMI target module side view. Graphite or beryllium fins have slots cut to form 'teeth', and are clamped between water-cooled plates. Each tooth is 12.5 mm long. There are 8 fins, each with 10 teeth.

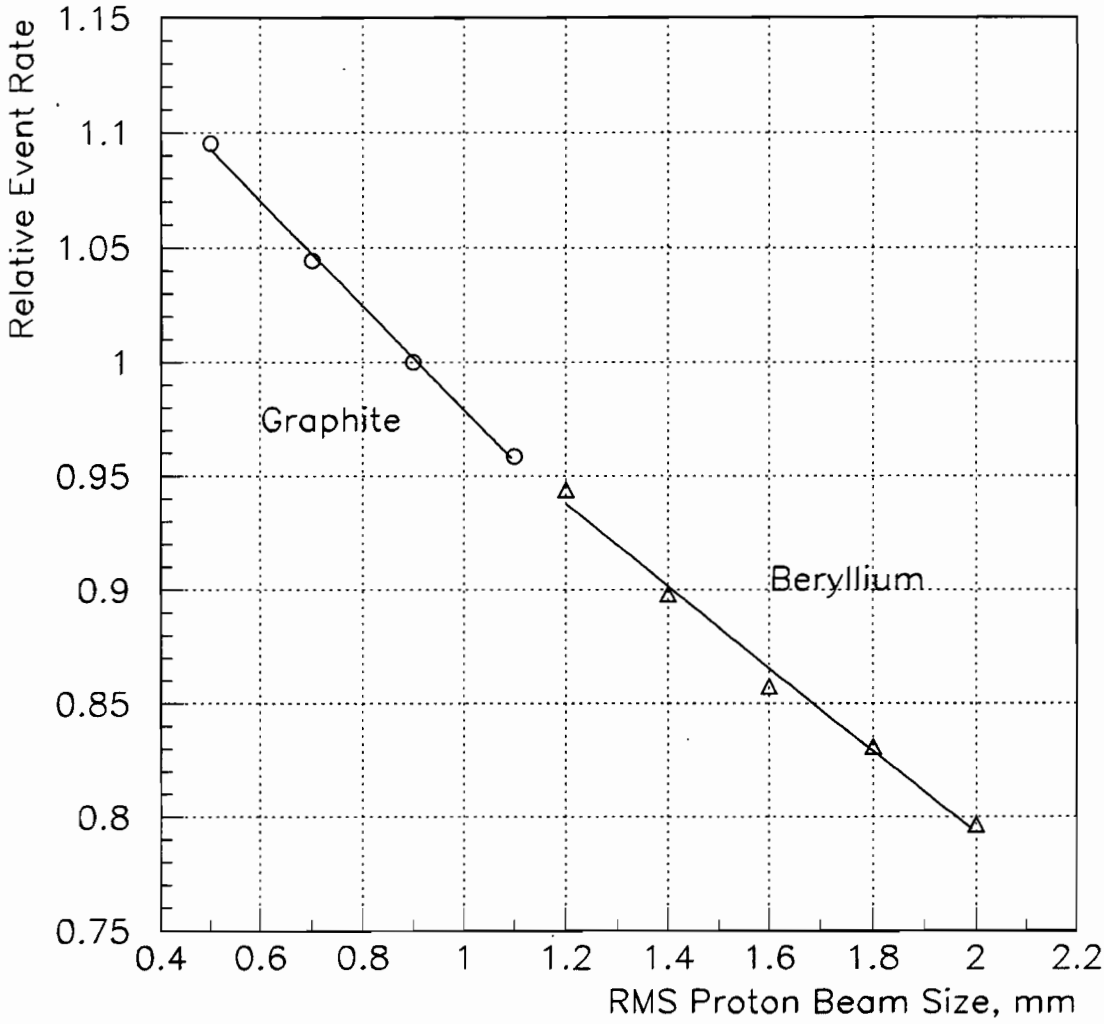

Figure 3-2-3 The relative neutrino event rate at Soudan as a function of the proton beam spot size RMS. These are results of a HALO Monte Carlo calculation, using a cylindrical target whose radius was always taken as 2.25 times the beam spot RMS.

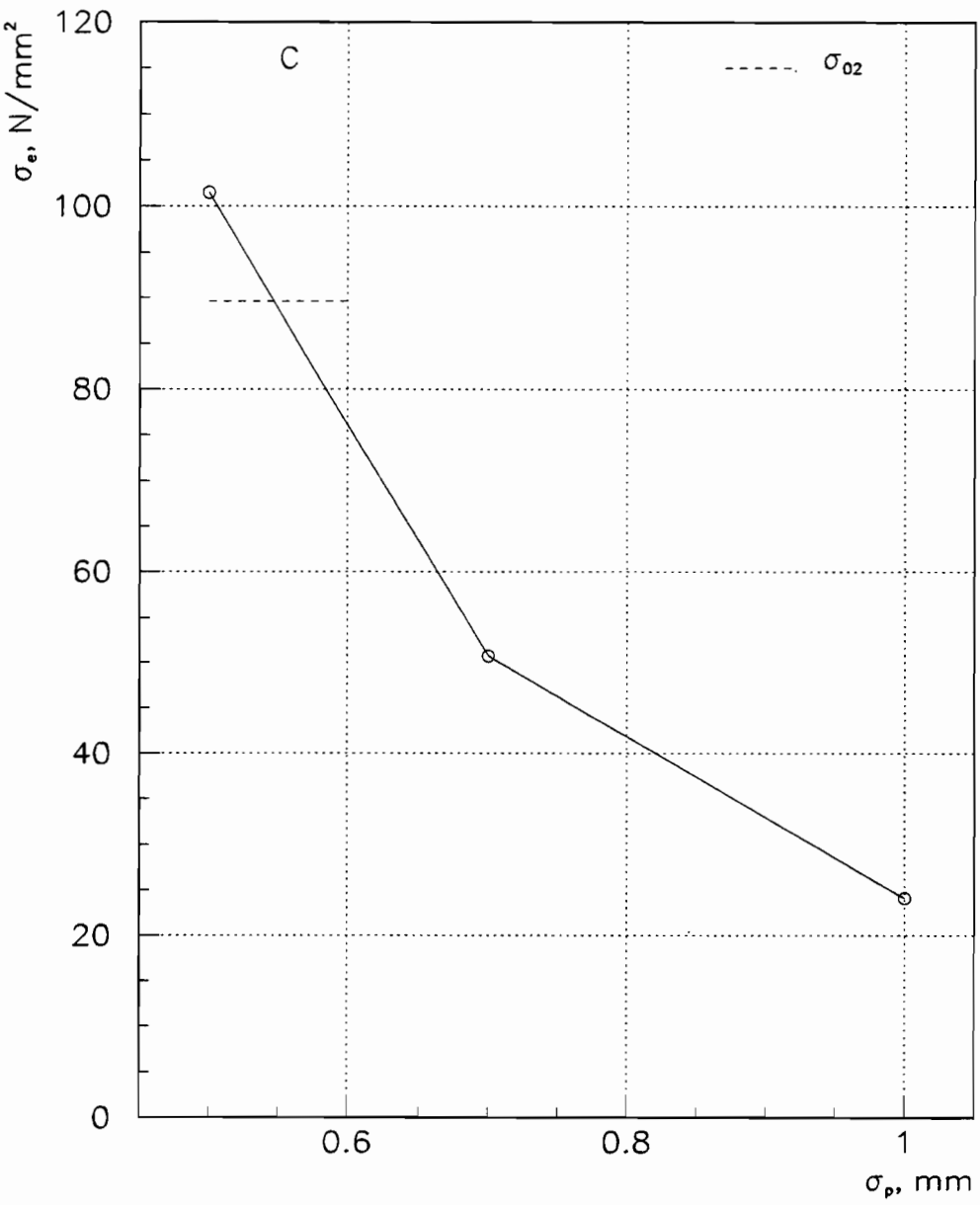

Figure 3-2-4 The maximum equivalent stress from quasi-static temperature calculations in a graphite cylinder as a function of proton beam spot size. The dashed line indicates the yield limit. The design calls for a 1 mm RMS beam spot.

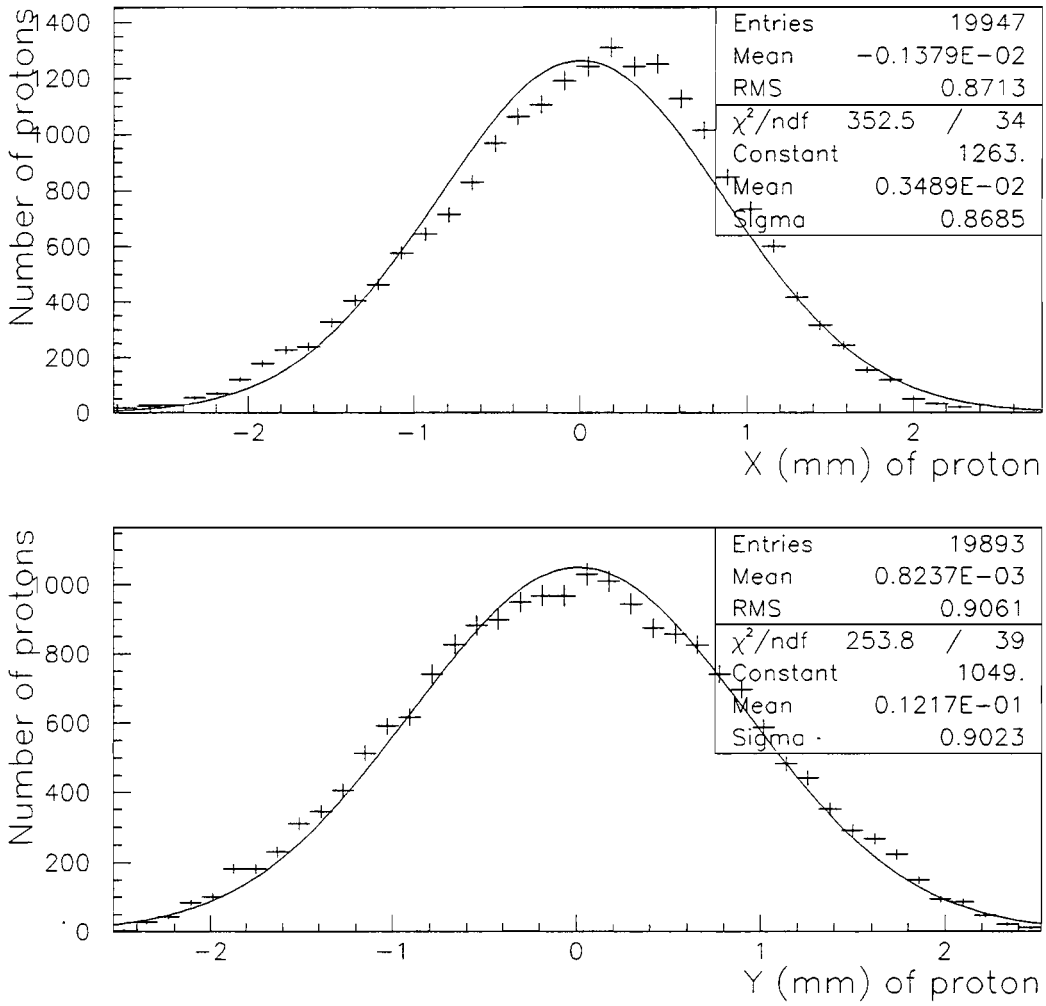

Figure 3-2-5 The horizontal and vertical beam profile at the target, from the TRANSPORT Monte Carlo through the extraction and beam line optics, with a gaussian shape fit for comparison. The shapes are characteristic of what will be delivered to NuMI, but the sizes will be tuned depending on the choice of target material.

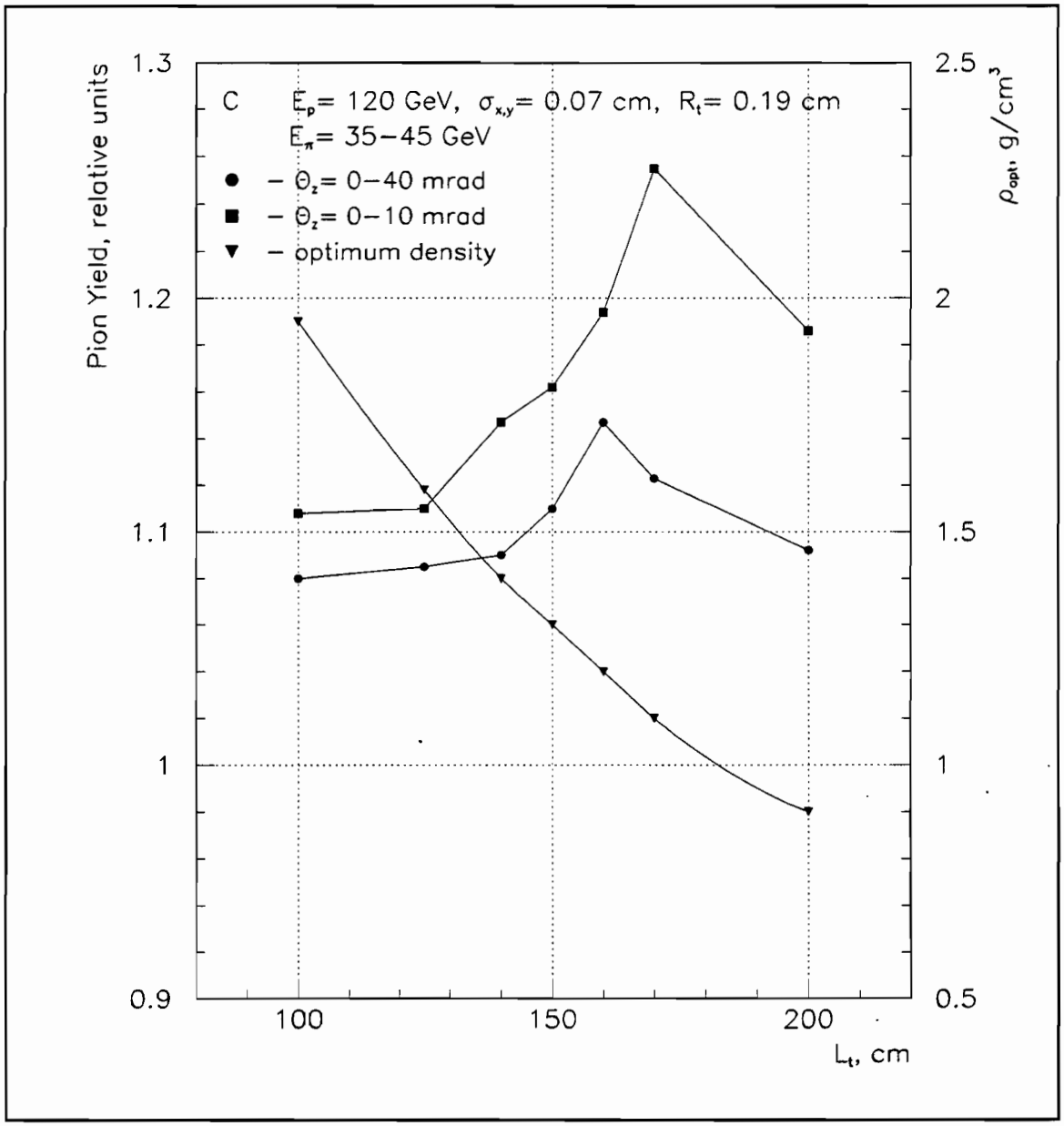

Figure 3-2-6 Optimization of target density and length. For a given radius of the target R_t, the triangles and scale on the right show the density of the target that produces the largest pion yield, while the other points and the scale on the left show the pion yields as a function of that length and density.

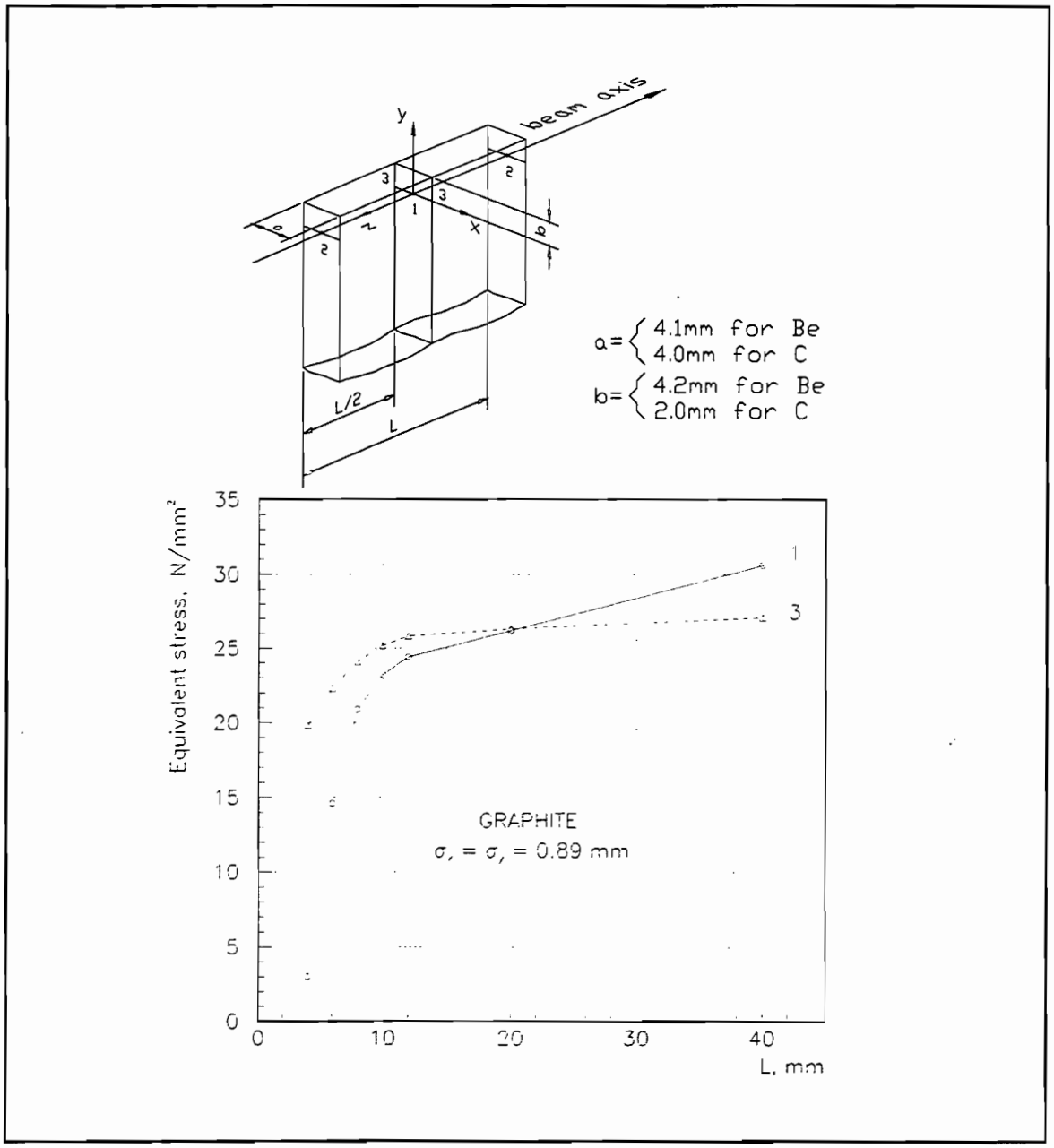

Figure 3-2-7 The stress at selected points in the target as a function of the tooth-length, indicating a preference for many short teeth as opposed to a long segment.

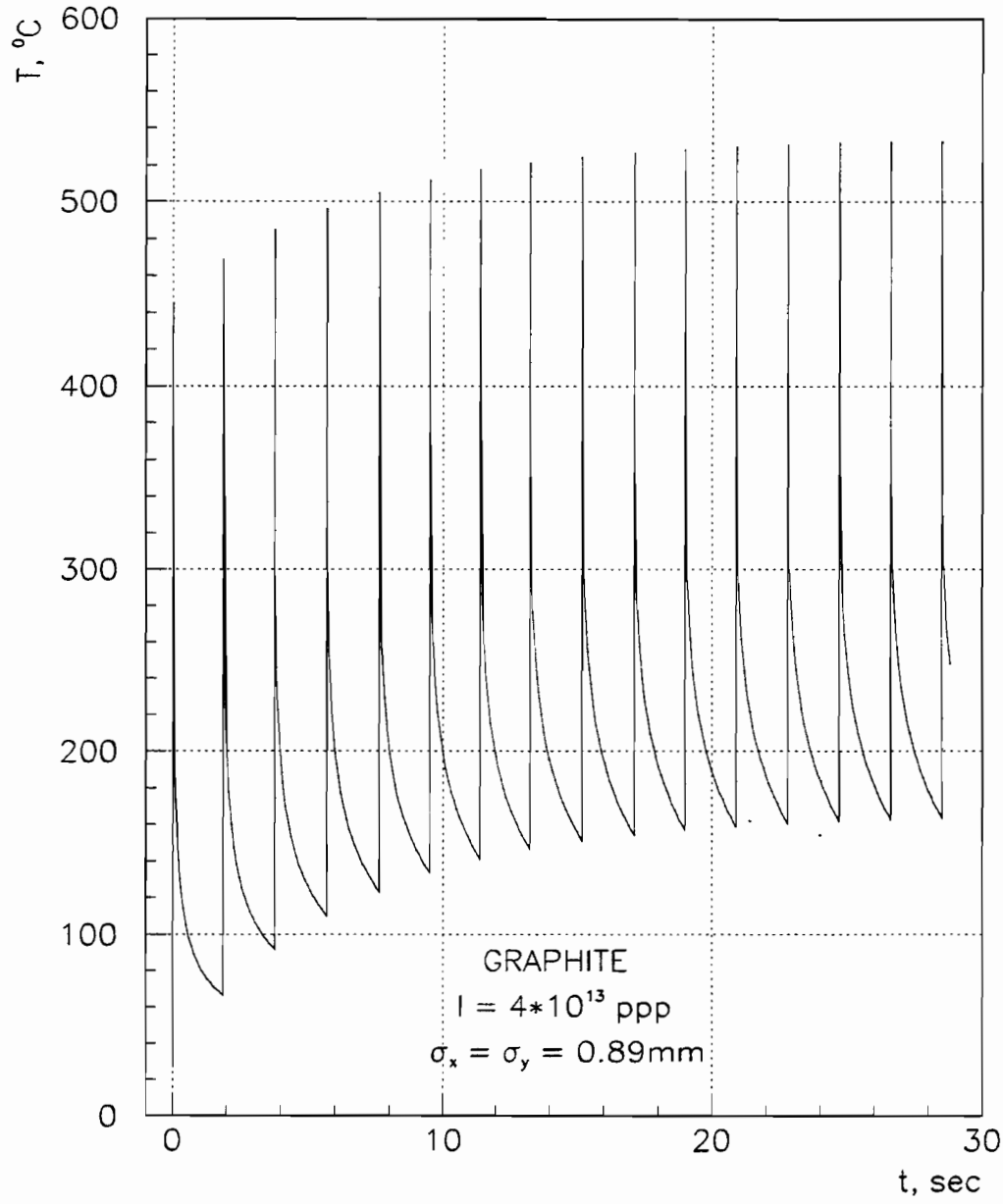

Figure 3-2-8 The maximum temperature in the target as a function of time.

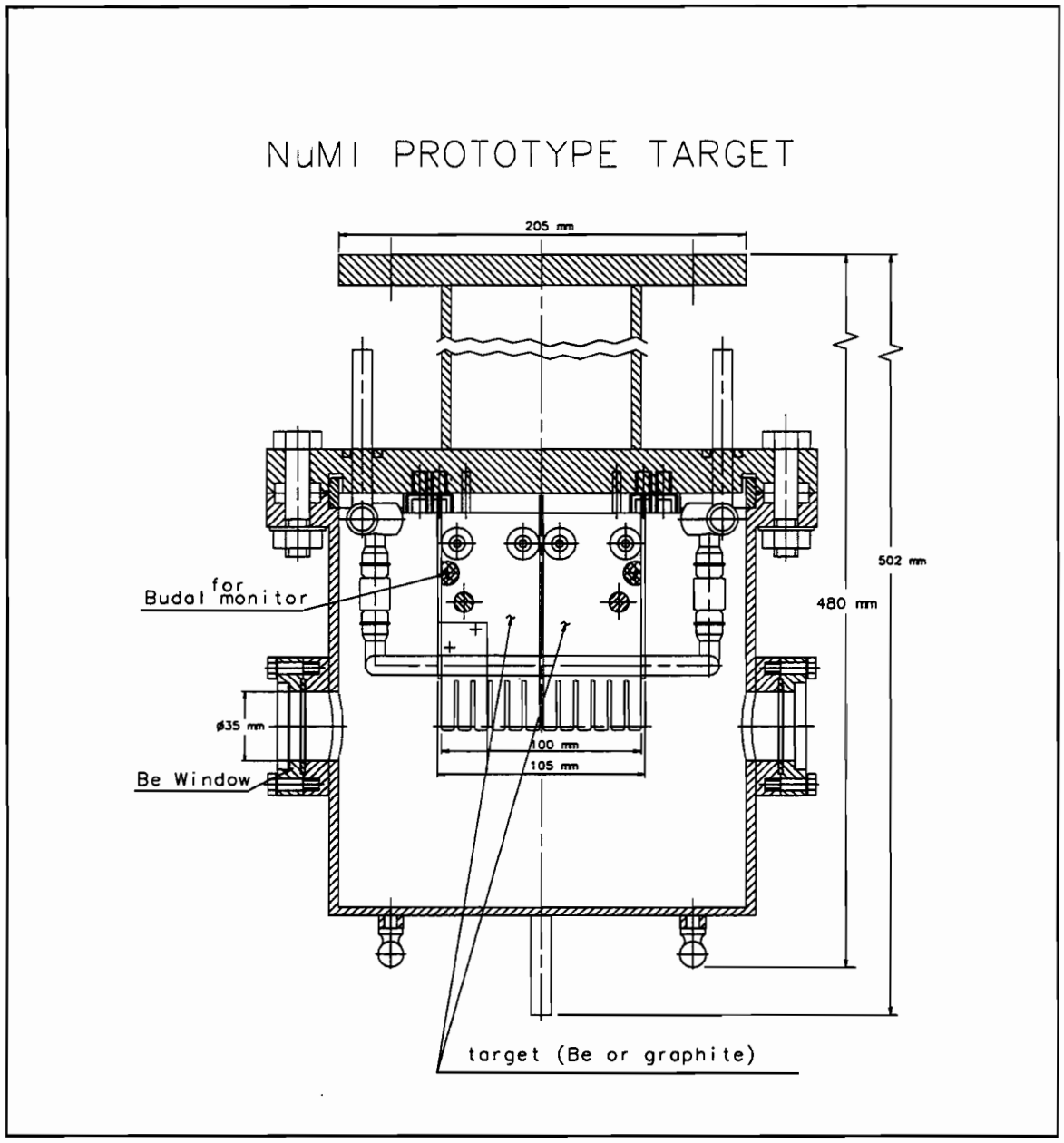

Figure 3-2-9 Prototype target segment to be used in a beam test.

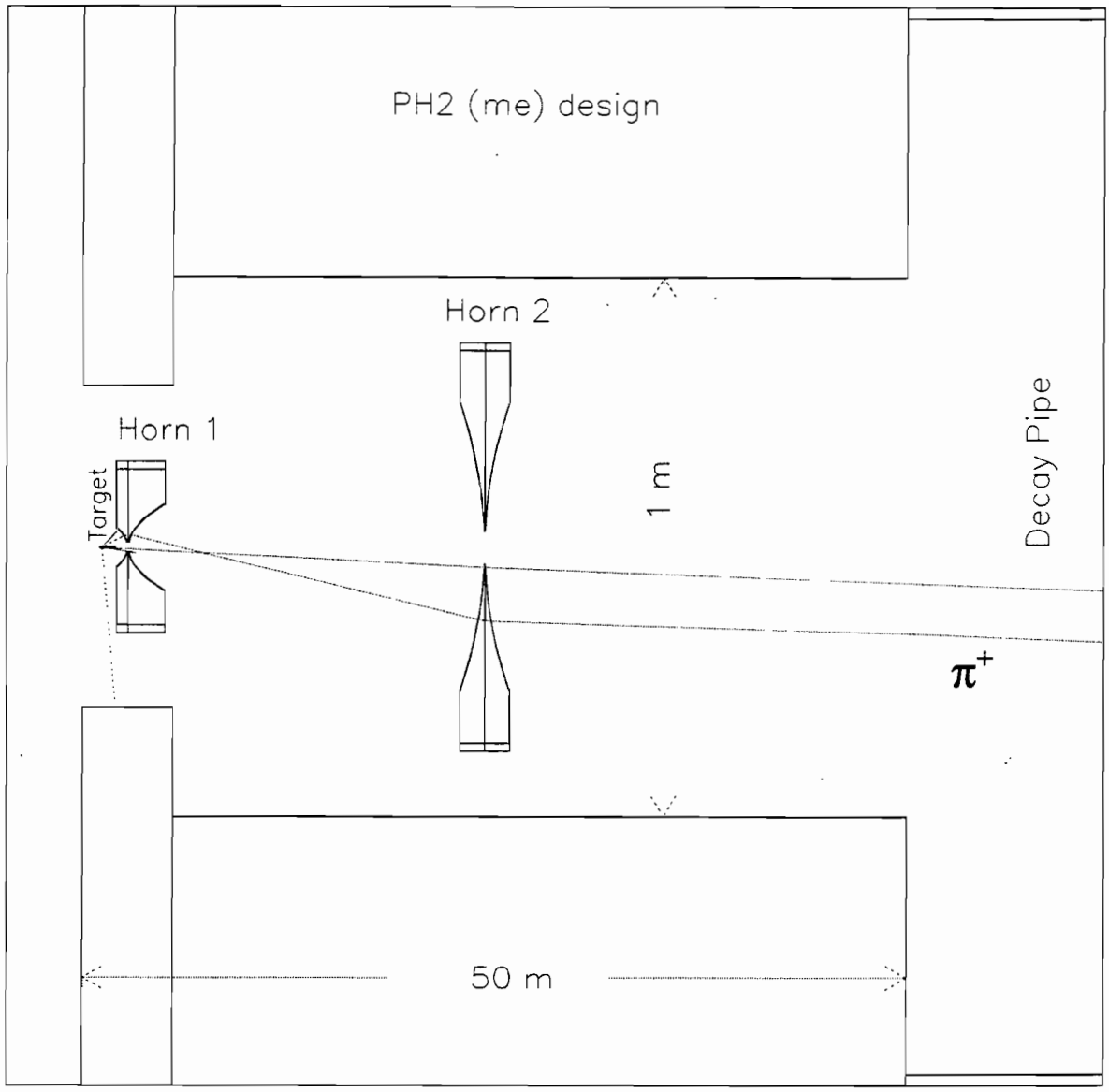

Figure 3-2-10 A GEANT Monte Carlo event, showing focusing of a pion by the two horn system. The pion is over-focused by the first horn, and is brought parallel to the beam line by the second horn. Note the difference of a factor of 100 in the vertical and horizontal scales.

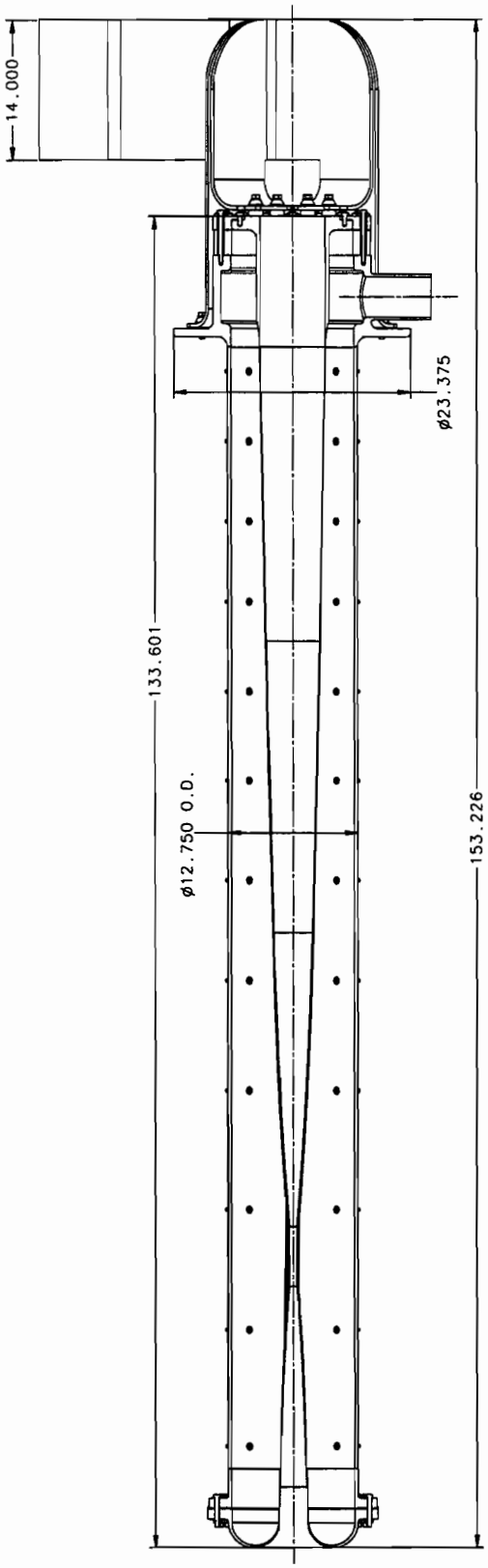

Figure 3-2-11 First focusing horn. Dimensions shown are in inches.

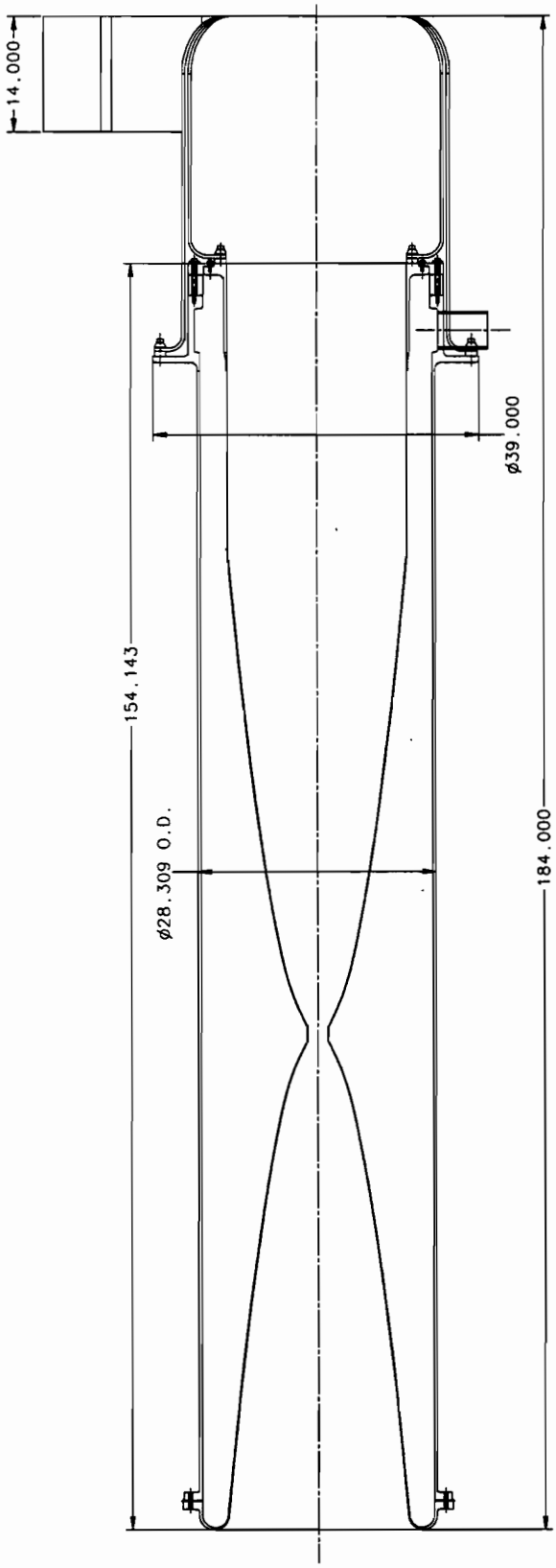

Figure 3-2-12 Second focusing horn. Dimensions shown are in inches.

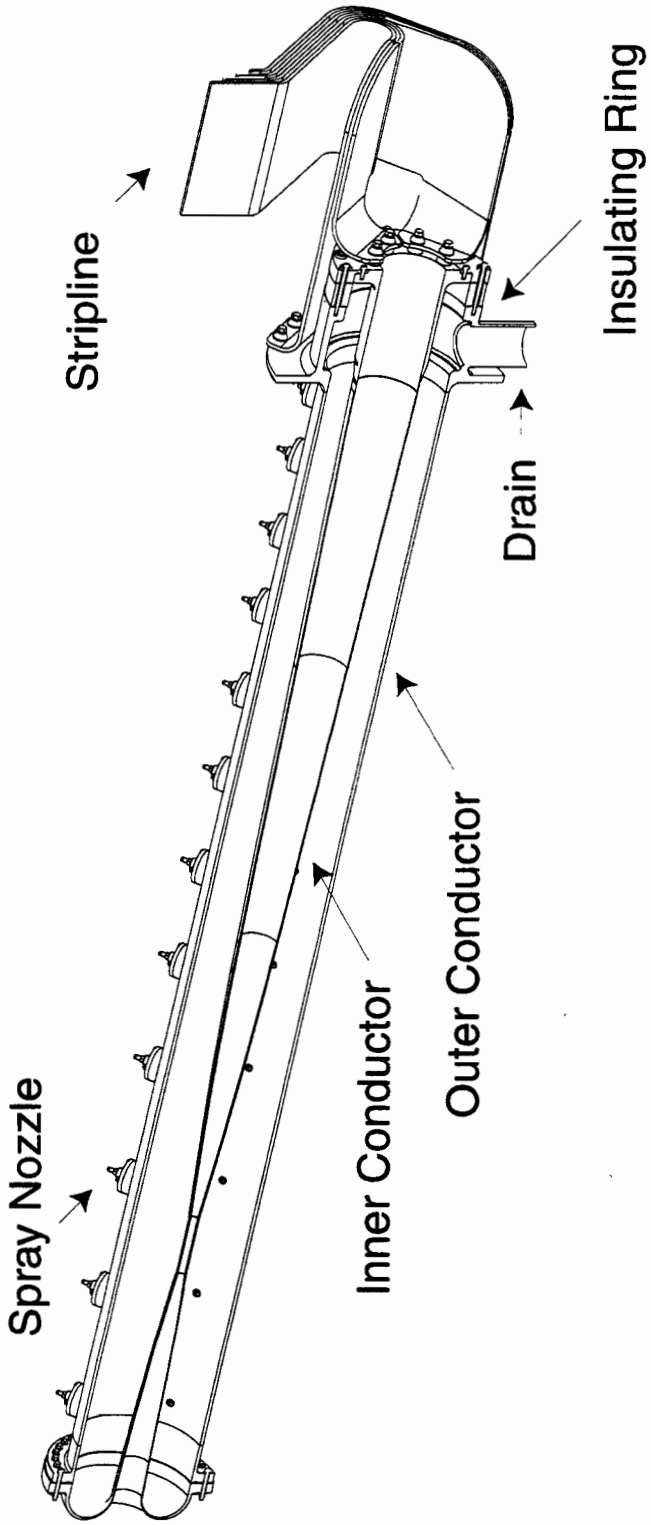

Figure 3-2-13 Cutaway drawing of the first horn. The strip-line connections and the water drain are also shown.

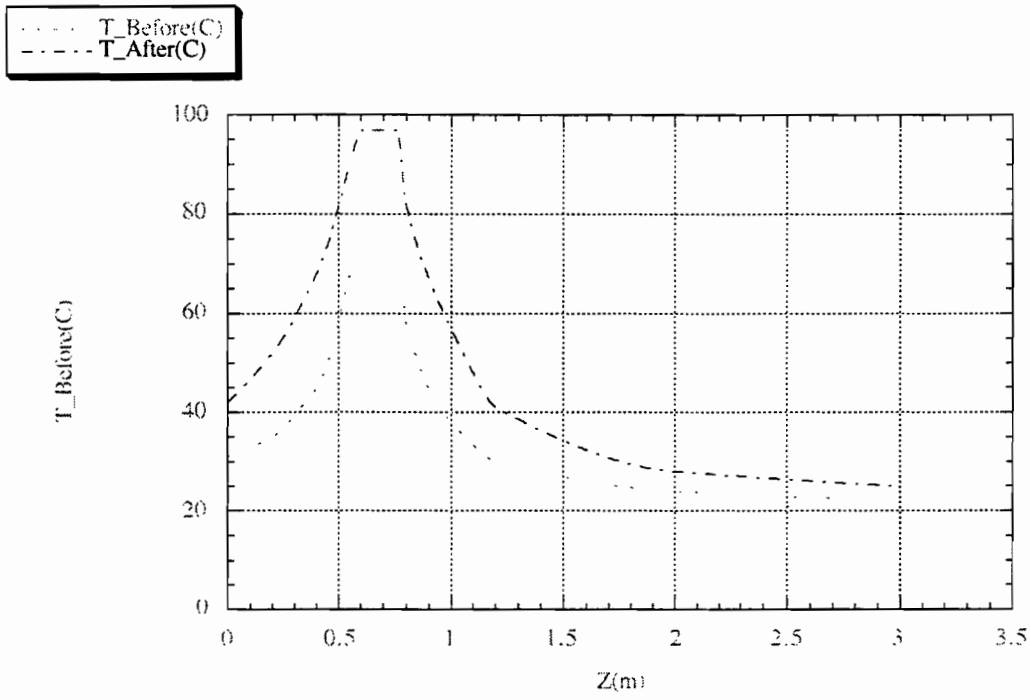

Figure 3-2-14 Horn temperature profile just before and after the pulse.

a)

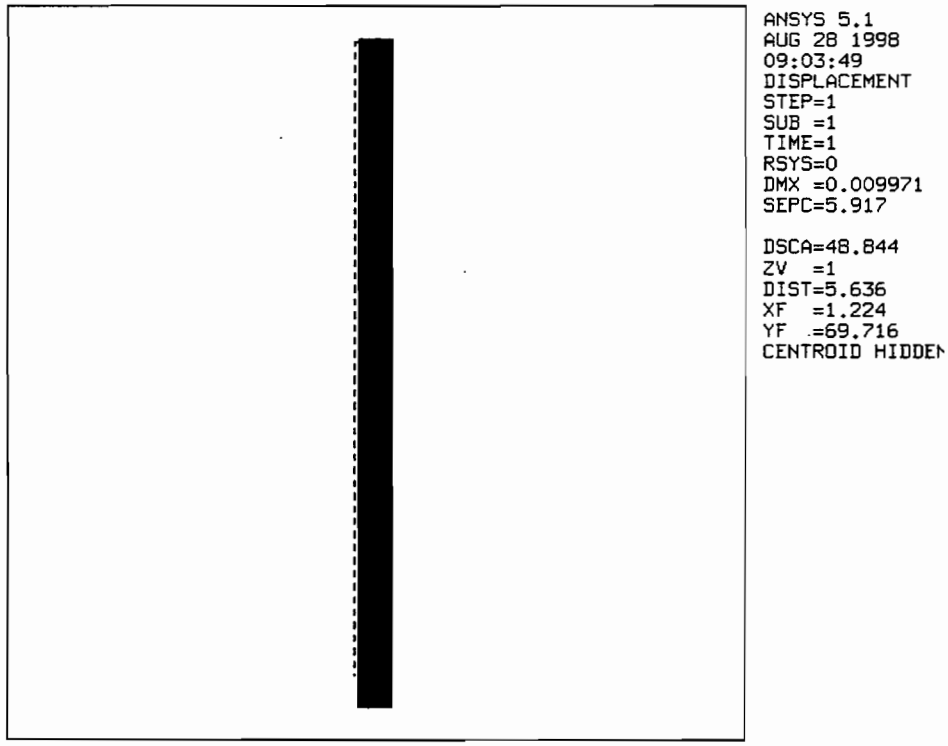

b)

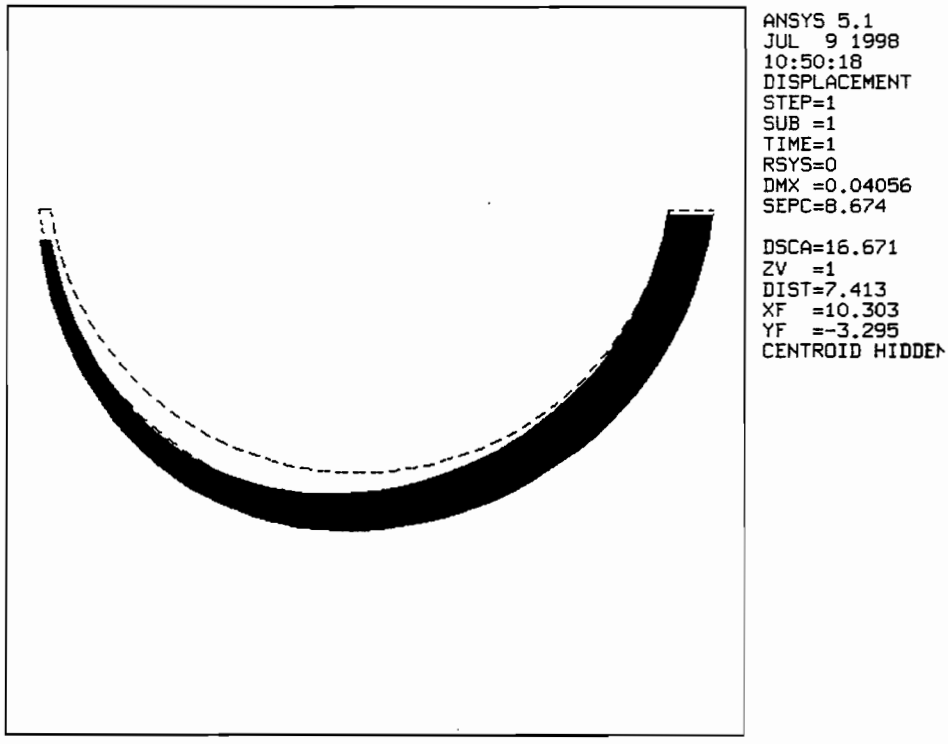

Figure 3-2-15 Horn conductor displacement just after the pulse (a) in the neck region, and (b) at the upstream end. DMX indicates the maximum displacement in cm. The displacement is much exaggerated in the figure to make it visible.

a)

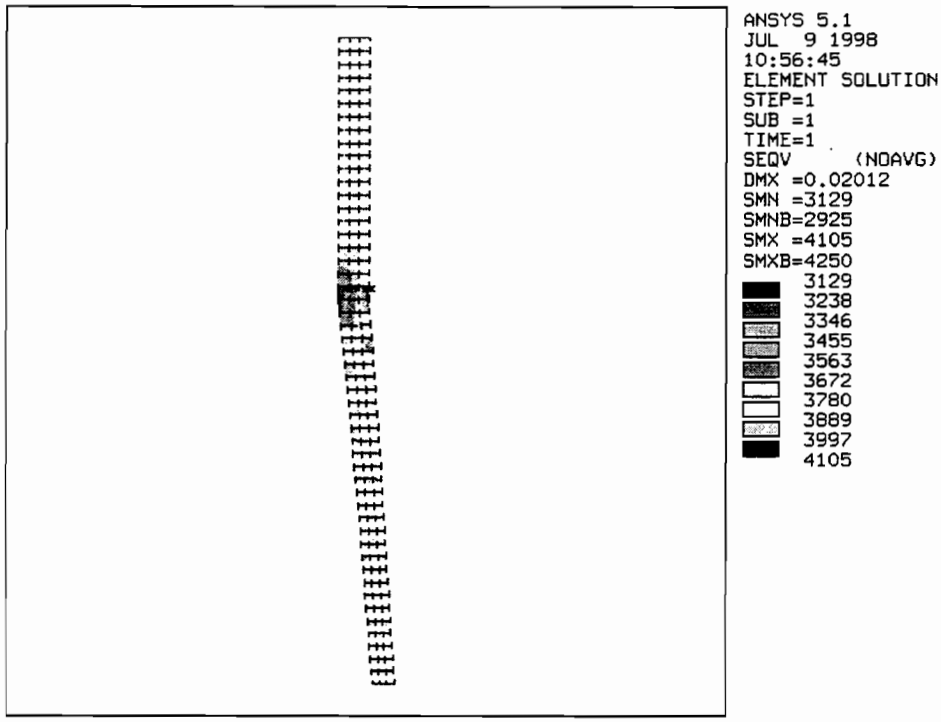

b)

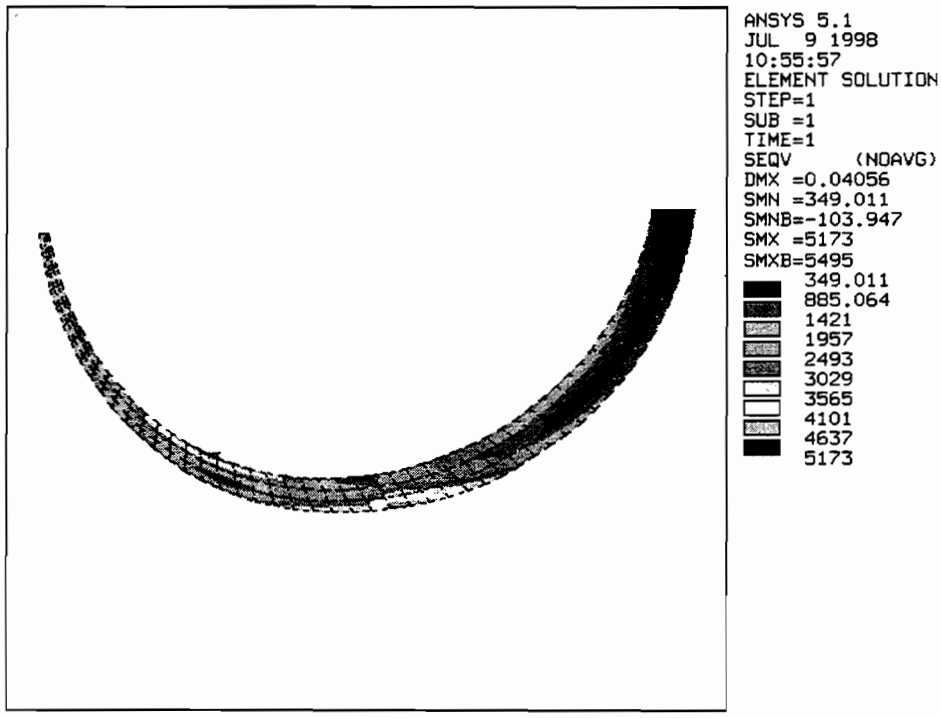

Figure 3-2-16 Von Mises stress in the horn conductor just after the pulse at steady state (a) in the neck region, and (b) at the upstream end.

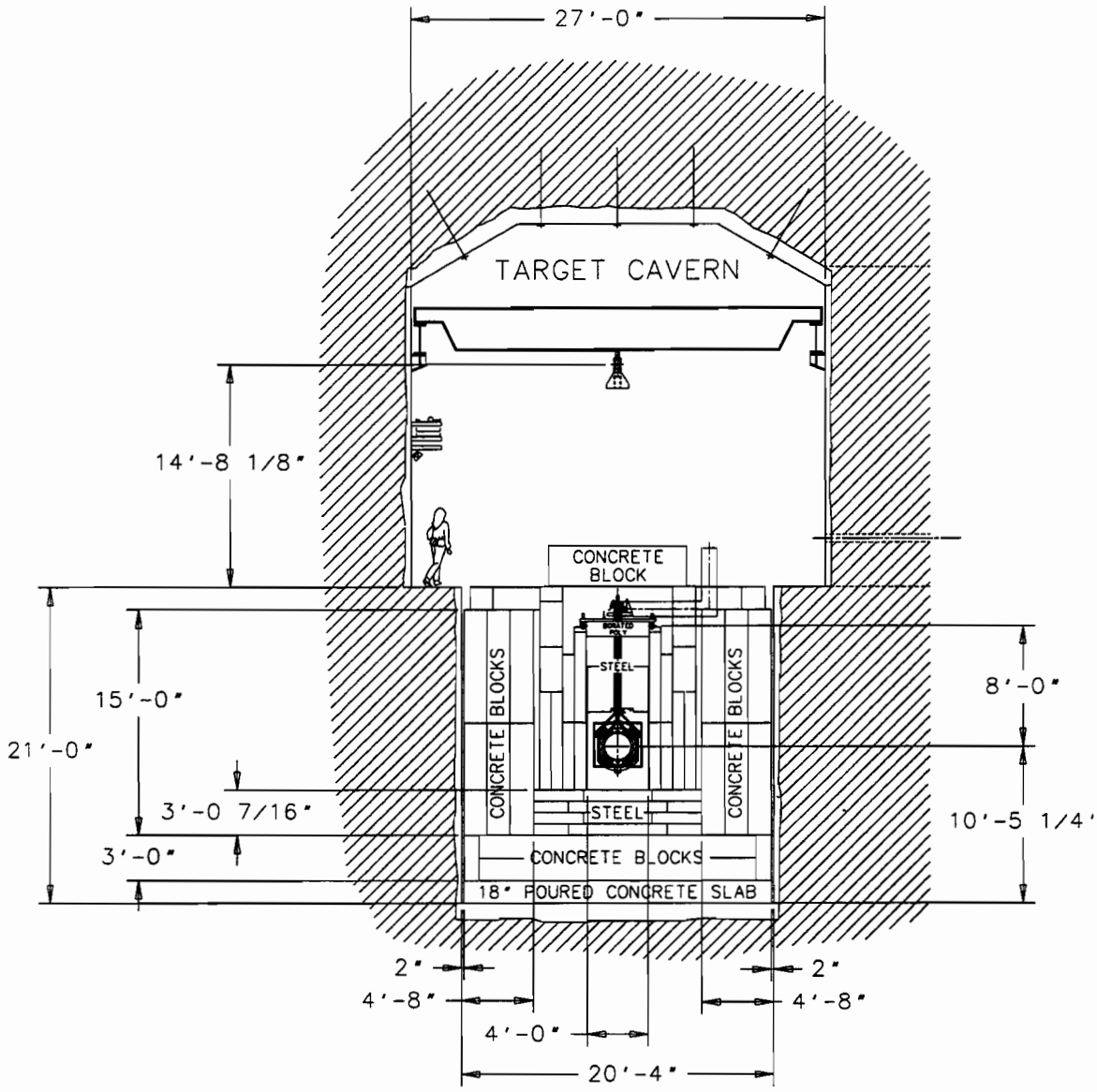

Figure 3-2-17 A cross section of the target pile, which is a thick shield to absorb radiation produced when the primary beam hits the target. The second horn is shown hanging from its alignment module, which rests on alignment rails at the top of the channel.

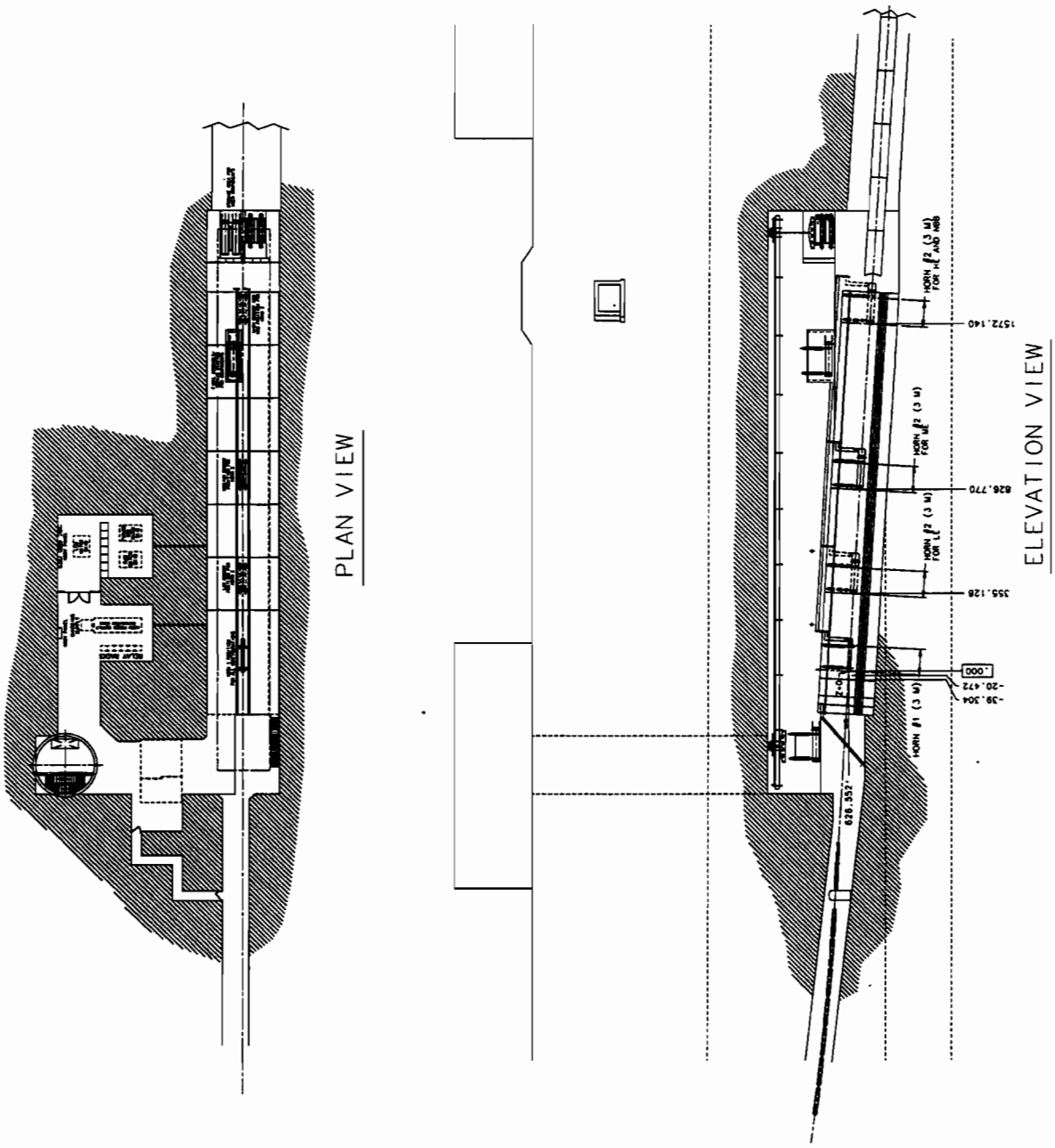

Figure 3-2-18 The target pile in place in the target hall. The horn locations for the Low Energy, Medium Energy, and High Energy Beam configurations are shown, as well as locations for working on and storing horns.

3.3 Power Supply Systems (WBS 1.1.3)

Table of Contents

3.3 POWER SUPPLY SYSTEMS (WBS 1.1.3) 3.3-1

3.3.1 Introduction *3.3-3*

3.3.2 Power Supply System Objectives *3.3-3*

3.3.3 Technical Requirements and Constraints *3.3-4*

3.3.3.1 Septa and Magnet Power Supplies. 3.3-4

3.3.3.2 Horn Power Supply System and Transmission Line. 3.3-4

3.3.4 Design Assumptions *3.3-4*

3.3.5 Septa and Magnet Power Supplies Description *3.3-5*

3.3.6 Horn Power Supply System and Transmission Line Description *3.3-5*

3.3.6.1 Charging System 3.3-6

3.3.6.2 Discharge Switch 3.3-6

3.3.6.3 Capacitor Bank and Enclosure 3.3-7

3.3.6.4 Discharge Resistors and Safety System 3.3-7

3.3.6.5 Current Transducers for Monitoring 3.3-7

3.3.6.6 Water Cooling 3.3-8

3.3.6.7 Transmission Line 3.3-8

3.3.6.8 Horn Power Supply and Transmission Line Testing Program. 3.3-9

3.3.7 Construction Plan *3.3-10*

3.3.7.1 Recycled Equipment. 3.3-11

3.3.7.2 New Equipment. 3.3-11

3.3.8 Installation Plan and Issues *3.3-11*

3.3.8.1 MI Enclosure and NuMI Stub Region. 3.3-11

3.3.8.2 MI60 Service Building, MI62 Service Building and New Construction. 3.3-11

3.3.9 Pre-Commissioning Plan *3.3-12*

3.3.10 Performance Monitoring Plan *3.3-13*

3.3.10.1 Septa and Magnet Power Supplies. 3.3-13

3.3.10.2 Horn Power Supply System and Transmission Line 3.3-13

Table of Tables

Table 3-3-1 Technical Requirements and Design Assumptions for the NuMI Power Supply System (see insert). ____ *3.3-14*
Table 3-3-2 Horn Circuit Estimated Resistance and Inductance. ____ *3.3-14*
Table 3-3-3 Horn Power Supply System Operational Requirements. ____ *3.3-15*
Table 3-3-4 Charging Power Supply (240 kW Transrex) ____ *3.3-15*
Table 3-3-5 Typical SCR Switch Ratings ____ *3.3-15*
Table 3-3-6 Two Horn System Transmission Line. ____ *3.3-16*

Table of Figures

Figure 3-3-1 Target Hall and Power Supply Room Cross Section ____ *3.3-17*
Figure 3-3-2 Electrical Schematic of the NuMI Horn Power Supply System with Energy Recovery ____ *3.3-18*
Figure 3-3-3 Capacitor Bank Structure ____ *3.3-19*
Figure 3-3-4 Conceptual Layout of Capacitor Bank and Transrex ____ *3.3-20*
Figure 3-3-5 Transmission Line Cross-section and Layout ____ *3.3-21*

3.3.1 Introduction

The Power Supply Systems for the NuMI Facility consist of the power supplies for the NuMI beamline elements (described in Sections 3.1 and 3.2), the cables and connections from the power supplies to the 480 VAC power panel, and the cables and connections from the power supplies to the devices that they drive. The MINOS magnet power supply and cables are also included. The prototype horn testing program needs a prototype horn power supply (and its associated transmission line and dummy load), the TSB horn testing program needs a transmission line and dummy load(s) and for precommissioning the horns in the target hall, dummy loads are also needed. These transmission lines, dummy loads and the prototype horn power supply are included in this WBS.

The major items for this system are the power supply system for the two series connected focusing horns and the parallel strip transmission line used to connect this power supply system to the horns. The magnetic focusing horn system and its prototype and testing programs are described in Section 3.2.3. This section will highlight those portions of the horn system and testing program that relate to the horn power supply system. A silicon controlled rectifier (SCR) switch and sample transmission line testing program will also occur in the fall of 1998. Goals of this program are identified throughout this section.

Similar power supply systems and transmission lines have been designed and built at Fermilab. Fermilab has not built a transmission line as large as this, although CERN and KEK have. Thus the technology is not new. The main challenges of the horn power supply system are safety, due to the amount of stored energy, and long term reliability. The main challenges of the transmission line are the long term reliability of the insulation, and the design of the bolted connections and the flexible joints. With the possibility of a humid environment, potential problems with the insulation and corrosion is a concern.

3.3.2 Power Supply System Objectives

The primary objectives of this system are to provide reliable, stable power to beamline elements and to minimize power consumption. The NuMI facility needs to be operational for at least 10 years, and the power supply system will be designed with that in mind. Power supplies (and their cables) must be repairable, specifically the horn power supply and transmission line. They must also accommodate a spill length of at least 1 msec, which is necessary to avoid pile-up of neutrino events in the near detector. This implies that the half-sine-wave current pulse to the magnetic horns have a baseline 5 msec

long. Due to radiation considerations, connections to the horns must be ALARA friendly and materials should be chosen that contain short-lived activation products. Personnel safety must be assured from possible electrical, mechanical and radiological hazards. Provisions need to be made in the transmission line for operating horn 2 at a number of positions along the target hall such that different energy beams can be produced (see Section 2.6).

3.3.3 Technical Requirements and Constraints

3.3.3.1 Septa and Magnet Power Supplies.

Voltage and current requirements for the various beamline elements determine what power supplies and cables will be needed.

Table 3.3-1 (see insert) summarizes these requirements and the chosen power supplies for each of the beamline elements. Specifically all power supplies must be able to deliver a 1 msec flat-top pulse at a repetition rate of 1.9 seconds. For beam tuning and focusing, trim and quadrupole magnets must each have their own power supplies. The three bend circuits use several 500kW supplies in series in order to obtain the desired voltage levels.

3.3.3.2 Horn Power Supply System and Transmission Line.

The horn power supply is based on the two horn zoom lens design. It must deliver 200 kA (average, $\pm$ 2.5%) pulses every 1.9 s. with a pulse to pulse repeatability of 1% and current monitoring to 0.4%. As a safety margin the power supply system will be designed to operate at up to 240kA. This results in a system load current of 7250 Arms operationally (8700 Arms design). The estimated circuit parameters are listed in Table 3.3-2. These calculated load values include effects of DC resistance, skin effect, temperature, transmission line conductor cross section and spacing. Connections to the horns, including the transmission line, must be either outside radiation shielding or else makable/breakable via remote handling.

3.3.4 Design Assumptions

The civil construction for NuMI includes all electrical work up to and including the 480 VAC power panel, breakers and safety switches. A 13.8kV pulsed power substation connected to the MI beamline feeder and a 480 VAC power panel with sufficient spare capacity for NuMI will be installed at the MI62 Service Building as part of the Main

Injector project. Substations, 480 VAC power panels, and associated AC wiring for NuMI power at MI60, the NuMI Upstream Service Building and the NuMI Downstream Service Building are all included in the NuMI civil cost estimate (see Section 5.3).

Specifications for all power supplies are based on the beam transport requirements described in Section 3.1.1 and are shown in Table 3.3-1. The needs for MINOS magnet are estimated to be 1000 Amps at 200 volts, thus a PEI 240kW supply is costed. Sufficient unused power supplies exist at Fermilab to provide all but the horn power supply. An existing PEI 240 kW power supply will be used as the horn capacitor bank charging power supply.

The horn power supply design presented here assumes a well-defined load inductance and resistance and is based on the two horn zoom lens design with connecting transmission line (Table 3.3-2).

3.3.5 Septa and Magnet Power Supplies Description

The NuMI beamline power supply system uses existing power supplies from decommissioned fixed target areas and the Main Ring. The NuMI beamline will have 5 high-current bend circuits: the Lambertson magnet, the "C" magnet and the three bend circuits. There will also be 10 different quadrupole circuits, and 12 different low-current trim magnet circuits. The power supplies obtained from unused areas at the laboratory and will require some upgrades and refurbishment. In order to reduce power consumption all but the quadrupole and trim magnet supplies will be ramped. The 500 kW, 240 kW and 150 kW supplies will all use 500 kcm cable for the DC cable runs as shown in Table 3.3-1.

3.3.6 Horn Power Supply System and Transmission Line Description

The horn power supply system is located in the power supply room, underground, next to the Target Hall (see Figure 3.3-1). This minimizes the length of the transmission line. Having both the charging power supply and capacitor bank in the same location will help in resolving any operational problems. The power supply for the two horn zoom lens system is of the direct coupled design as shown in .

The main components are the charging power supply, the capacitor bank, the silicon controlled rectifier (SCR) switches, the current transducers, and the safety system. The

present system allows for reversing the current by changing the transmission line connections at the power supply. The *NuMI Power Supply Proposal*, revised 9/1/98 is the most complete description of the horn power supply system.

In the horn power supply system, energy is stored in a capacitor bank and switched via a parallel array of SCR switches into the horn load. A parallel strip transmission line is used to connect the power supply to the horns. The circuit is a damped LC discharge circuit that will reach peak current when the SCR switch releases stored energy from the capacitor bank to the horns via the transmission line. Table 3.3-3 lists the operational requirements of the horn power supply system based on the circuit parameters in Table 3.3-2. Figure 3.3-2 shows the cellular structure of the capacitor bank, SCR switches, energy dump resistors and transmission line.

3.3.6.1 Charging System.

Based upon the inductance and resistance values provided for the two horns and the transmission line, the capacitance required for the bank is 0.90 Farads. The capacitor bank will be recharged by one of the standard Fermilab 240 kW power supplies. During operation of the horns the calculated power consumption is 83 kW. The required voltage for operation is 515 volts. Table 3.3-4 shows the parameters of a 240 kW supply. To avoid creating transients on the power line a 1 mH inductance will be inserted between the power supply and the capacitor bank.

3.3.6.2 Discharge Switch.

The discharge of stored energy from the capacitor bank to the horns is performed by an SCR array of 8 parallel devices. The number of SCR's required and their arrangement is being revisited for the (higher current) two horn system. It is thought that the arrangement of 8 parallel devices will be sufficient. It will be investigated in the fall of 1998. A typical SCR rating is shown in Table 3.3-5. For cost estimating purposes, a specific commercial device was chosen resulting in eight devices in parallel for the switch element. The SCR switch design would need to be changed if pulse to pulse reversing of the current is desired. A testing program for the SCR's will investigate the suitability of available SCR's for this application. The high currents and "low" (as compared to standard applications) repetition rates needed for the NuMI horn system requires that the SCR's operate near their

surge ratings, which is not their normal mode of operation. Vendors have stated that this can be done for a period ~10 years.

3.3.6.3 Capacitor Bank and Enclosure.

Figure 3.3-3 and Figure 3.3-4 show the layout of the capacitor array and horn power supply system. The capacitors are connected in parallel, but separated into eight cells. The number of cells is chosen to limit the amount of stored energy for that cell to a value that can be safely contained within an individual capacitor case without rupture in the event of an internal fault.

The capacitor support structure must be able to hold approximately 120 capacitors estimated at 150 pounds each (18000 lb.). It is envisioned that an enclosure nearly the same as that used for the recently completed TESLA Modulators would be well suited for the capacitor bank system. It measures 6.25' high by 17.5' long by 5.75' deep. Cost estimates for the enclosure and internal structure are based upon this recent purchase.

3.3.6.4 Discharge Resistors and Safety System.

A safety system will monitor operating parameters of the power supply and capacitor bank and safely shut it down if out of tolerance conditions are detected. The parameters that will be monitored are personnel entry, over voltage and over current conditions of the charging supply, over voltage and over current conditions of the capacitor bank, ground fault currents, current imbalance in the transmission line, excessive temperatures, and loss of cooling to the power supply, transmission line or horns. When fault conditions are detected, the charging supply will be turned off and the capacitor bank discharged via a redundant arrangement of dump resistors and shorting relays to remove stored energy. The dump resistors shall be rated to absorb the worst case maximum stored energy of the capacitor bank, 288 kJ. If an over voltage of the capacitor bank is detected, triggering of the SCR switch is inhibited, thereby protecting the horns from an excessive current pulse.

3.3.6.5 Current Transducers for Monitoring.

A passive current transformer is the device chosen for monitoring the output current from the horn power supply system. A number of smaller monitors, one associated with each of the parallel SCR's, will be used with their outputs summed together to read total current.

This has the advantage of allowing the monitoring of the performance of each capacitor bank cell/SCR combination. Cost estimates are based upon vendor prices for commercially available components. Using standard current transducers, +/-0.5% current monitoring is possible. The horn current needs to be known to +/-0.4%. Being able to reach +/-0.4% current monitoring with current transducers is possible and is being investigated. The current values that would be monitored are those in each cell, each transmission line pair and the total current.

3.3.6.6 Water Cooling.

The SCR's will require water cooling at a flow rate of ~4 gpm. The capacitors and safety dump resistor will not need to be water-cooled. The present cost and schedule includes water cooling for the SCR's.

3.3.6.7 Transmission Line.

A transmission line consisting of a four layer assembly of two parallel plates will be necessary to connect the output of the power supply system to the horns. Figure 3.3-5 shows the dimensions of the transmission line and the layered configuration. The transmission line will be made of 6101-T61 aluminum, as it is the most cost effective material and is compatible with the aluminum materials being used in constructing the horns. Each pair of aluminum alloy bus conductors will be separated by an insulator. Adjacent pairs are separated by aluminum spacers. Inside the Target Hall beamline shield the insulation will be a 1cm air gap with Alumina ceramic spacers. Outside the shield, Kapton polyimide insulation of 0.5 mm total thickness will be used. The completed assembly will be held in compression by ceramic sleeved through bolts at the spacer locations and compression clamps in the region where Kapton is used (if it is used). This configuration yields an equivalent transmission line width of 1.2 meters in a compact cross section. Table 3.3-6 lists estimated transmission line dimensions and parameters. The calculated parameters will be verified during the SCR and transmission line testing program. Figure 3.3-5 shows the transmission line layout and Figure 3-2-13 (in Section 3.2) is a cutaway drawing of the first horn, showing the transmission line connections to horn one. This connection is complicated by the issues of allowing for horn alignment and minimizing radiation doses to personnel during connection/disconnection. The prototype

horn testing program will investigate these issues further. The inductance and resistance shown in Table 3.3-2 are calculated values.

Power losses in the transmission line, 23.4kW, are roughly equivalent to that of the two horns. Power dissipation in the line is 340 watts per meter of length. The design allows convective air cooling but may require water cooling in the penetration between the power supply room and target hall. Allowances for cooling costs and time have been incorporated in the cost and schedule. The SCR and transmission line sample testing program will provide better information with respect to heating of the transmission line. In addition, the transmission line must have minimal inductance and resistance, allow for thermal expansion and contraction at the horn connections, have insulation tolerant of the high radiation flux, and permit rapid and reliable connection/disconnection at each horn terminal.

There are several mechanical issues associated with the transmission line. It is a 12,000 lb. structure and thus its support is non-trivial. Several joints need to be flexible for horn and transmission line removal. Consideration must be give to minimizing fatigue failure from pulsed magnetic forces. The transmission line must also be protected in some manner from foreign objects and condensation of water that may cause electrical shorts. This complicates air cooling. There are also several other concerns with respect to temperature rise and cooling such as thermal expansion and bi-metallic effects. The transmission line must be made as accessible as possible, especially in the joint regions, and repairable.

3.3.6.8 Horn Power Supply and Transmission Line Testing Program.

Section 3.2 discusses the horn system testing program in more detail. The prototype horn testing program will validate fatigue life of horn conductors, transmission line interconnect reliability, cooling efficiency and corrosion control. This testing will be done at the APO Target Station Building. The prototype horn power supply utilizes an existing Fermilab power supply and transformer. This power supply is capable of providing an average heat load similar to that which will be present on horn 1 during NuMI operation, but the pulse length will be much shorter. A dummy load has been constructed and placed in the circuit to determine the maximum pulse length and the repetition rate that this test power supply system could withstand. The prototype power supply will most likely run in a mode where it produces a burst of seven or eight 0.7 ms pulses 67 ms apart and repeat this every 1.9 seconds. This will supply a heat load similar to the operational system. The limitation on

this prototype horn power supply system is the transformer. The operational power supply pulse will be 5 ms every 1.9 seconds. The completion of the horn power supply and transmission line design will follow these prototype tests in order to incorporate the results if necessary.

A test cell and testing program for the SCR's is being assembled in the Transfer Gallery to investigate the suitability of candidate SCR's from various vendors. In the NuMI horn power supply system, the SCR's will be operating repetitively in surge mode where a large amount of energy is quickly deposited in the fusion. This is not the usual mode for SCR's. This testing program will also investigate temperature rise and the cooling requirements of the SCR's. A 15cm wide by 5.5m long sample piece of transmission line will be built as part of the SCR test fixture in order to measure the AC resistance and inductance of the transmission line. Temperature rise of the transmission line conductor and insulation materials to be used with the transmission line will be investigated in the this testing program also.

Operational horn and power supply system testing at TSB will commence once the operational horn power supply is complete and installed at TSB. Since the two horns are powered by the same supply and since the electrical parameters are tuned for this mode of operation, dummy loads will be used in place of not yet completed horn 2 during the initial testing of operational horn 1. A dummy load will be exchanged with horns as necessary for testing to proceed. Thus the transmission line for this test setup will consist of a short length of operational transmission line with the addition of series connected inductance and resistance simulating the total length of the target hall transmission line and the two horns. The transmission line and dummy load are costed in this WBS. This provides a testing period for the operational horn power supply system. The TSB testing drives the operational horn power supply design, as it requires the horn power supply system to be operational long before it is needed for the NuMI beamline.

3.3.7 Construction Plan

All magnet and septa power supplies will be recycled by refurbishing supplies no longer needed in the accelerator complex. This provides a great cost savings in both materials and labor since the equipment already exists and is well understood.

3.3.7.1 Recycled Equipment.

Recycled power supplies will need to be located, disconnected and re-located to NuMI. They will also need to be re-furbished and perhaps modified to allow invert operation. All recycled hardware will be thoroughly tested before being installed. The schedule allocates manpower and materials for this disconnecting, relocating, refurbishment and testing.

3.3.7.2 New Equipment.

The only power supply to be constructed is the horn system power supply. The horn power supply and transmission line are the major new components for this system and, as such, considerable labor time has been allotted to their construction and testing. As mentioned earlier, an operational test stand will be set up using the production horn power supply and a production horn, in order to test the power supply, a piece of transmission line and dummy loads, mechanical connections, and each horn under actual operating conditions. This will allow the power supply to operate with the equivalent load and achieve the proper pulse width, current, and voltage. The project schedule indicates start dates for construction of these new power supplies and transmission line such that they will be tested and ready for installation at the appropriate time. The need for the operational horn power supply for horn testing drives the horn construction schedule. The transmission line, on the other hand, would be constructed as late as is reasonable to make the installation date. This allows the testing results to be incorporated into the transmission line design and construction.

3.3.8 Installation Plan and Issues

3.3.8.1 MI Enclosure and NuMI Stub Region.

All installation work in the MI enclosure, including the NuMI stub, must be carefully planned to take place during scheduled MI shutdowns. Workers in this area may need specialized training due to the radiation levels in the area or other safety concerns. For the Power Supply Systems, the work in these areas mainly consists of cable installation and termination, and thus these training needs will apply to the cable contractor.

3.3.8.2 MI60 Service Building, MI62 Service Building and New Construction.

Power supplies will be located in the MI60 Service Building, the MI62 Service Building, the Upstream Service Building, the Power Supply Room and the tunnel near the MINOS enclosure. Table 3.3-1 lists the locations of most power supplies. The exceptions are the

horn power supply, which is located underground in the Power Supply Room and the MINOS power supply which is located underground near the MINOS enclosure. The power supplies for the Lambertson, C Magnet, and bend circuits will need to be rigged in place and thus their installation will have to be planned to not interfere with other installations occurring in these areas. Due to the short installation time for each supply, this should not be a problem. The septa, quadruple and trim magnet power supplies are small and can be installed by hand. Most likely the power supplies located in MI60 and MI62 Service buildings will be rigged into the buildings well in advance of their need since those buildings exist and the excess power supplies need to be stored somewhere. Similarly the power supplies in the new construction will most likely be moved into the appropriate service buildings well in advance of their need.

The horn power supply, capacitor bank, and transmission line will be rigged into the Power Supply Room through the upstream shaft. They will be lowered by crane down the shaft. Most likely the capacitor bank (25,000 lbs. and somewhat fragile) will be in several pieces, although the shaft will be large enough to accommodate it in one piece. The horn power supply components will then be transported by pallets to the horn power supply room and reassembled. The transmission line will be in approximately 20' long sections and will be assembled in place in the Target Hall. Transmission line joints will be welded except where connection/disconnection is needed. One piece of the transmission line will run across from the Target Hall to the horn power supply room (see Figure 3.3-1). The second long piece of the transmission line runs along the Target Enclosure to the horns. Disconnects/connects will most likely be located in the horn power supply room, in the Target Hall where the transmission line emerges from the penetration, above the shielding at each horn and inside the shielding at each horn.

Power supply cable installation down the shaft will have to be done carefully to provide stress relief to cables and allow access for repairs. Extra time and costs have been allocated in the schedule for this. During cable installation in the shaft, other installation activities will not be able to use the shaft, except perhaps the stairs. An installation plan will need to be developed due to the large number of items needing sole access to the upstream shaft during installation.

3.3.9 Pre-Commissioning Plan

All power supplies will be tested with AC power once they are refurbished. They will also have an extensive power test after the DC connections are made, before commissioning

beam. These tests will point out any problems with power supply cables, power supplies and power supply monitoring devices and cables. Water for magnet cooling will have to be operational before the power test occurs. The controls system will be fully functional before commissioning, with data-logging, alarms and power supply adjusting available. This will allow further pre-commissioning of the power supplies and cables. The horn power supply will initially be tested at the test facility, as will connections similar to the final transmission line connections. Once rigged into the power supply room and connected to the transmission line, the system will be tested with dummy loads replacing the horns. It will then be connected to the production horns, tested, and monitored.

3.3.10 Performance Monitoring Plan

3.3.10.1 Septa and Magnet Power Supplies.

For the septa and magnet power supplies, the beam dynamics will not be noticeably affected by the predicted line locked ripple, and slow drifts will be corrected by AUTOTUNE, an automatic software feedback system. All power supplies will also be continually monitored by ACNET alarm system (with tolerances set appropriately). An alarm system and logged data will point out required power supply repairs. Access will be available to all power supply locations and sufficient spare power supplies exist.

3.3.10.2 Horn Power Supply System and Transmission Line.

A horn power supply safety system will monitor operating parameters of the horn power supply and safely shut it down if out of tolerance conditions are detected. The parameters that will be monitored are personnel entry, over voltage and over current conditions of the charging supply, over voltage and over current conditions of the capacitor bank, ground fault currents, current balance in the transmission line, excessive temperatures, and loss of cooling to the power supply, transmission line and horns. Critical spare parts will be purchased for the horn power supply system (capacitors, SCR's etc.). The spare parts envisioned necessary for the transmission line are some connectors, bus bar and a flexible linkage.

Table 3.3-1 Technical Requirements and Design Assumptions for the NuMI Power Supply System (see insert).

Component	Inductance (μH)	Resistance (mΩ)	Power @ 200kA, 7400Arms (kW)
Horns:			
Horn #1	0.689	0.316	16.6
Horn #2	0.457	0.112	5.9
Transmission Line:			
Power supply to beamline (17.7m)	0.286	0.084	4.4
Distance between horns (55.6m)	1.223	0.361	19.0
Capacitor bank plus connections (estimated)	1.0	0.050	2.6
Total:	3.655	0.923	48.5

Table 3.3-2 Horn Circuit Estimated Resistance and Inductance.

Ramp Cycle Time: 1.9 seconds

CIRCUIT	MAGNET TYPE	# MAGs	PEAK FLD/GRD kG/(kg/m)	MAG. IND. (henry)	MAG. RES. (ohms)	CABLE TYPE kcmil	CABLE # 1 way	CABLE R/kFt ohms	CABLE L (ft)	CABLE RES. ohms	Total Res. ohms	PEAK CURR. (amps)
MI60 Power Supplies												
Septa	Septa	2				DS314	1		555			0.01
LAMB	Lamb.	3	8.93	0.017	0.013	500	5	0.026	155	0.001612	0.041	1506
CMAG	Cmagnet	1	10	0.002	0.007	500	6	0.026	165	0.00143	0.008	2786
Q1	3Q120	1	72.37	1.5	2.25	1/0	1	0.125	105	0.02625	2.276	35.2
BND1	EPB	7	14.15	0.03	0.0175	500	5	0.026	217	0.0022568	0.125	1449
Q2	3Q120	1	69.93	1.5	2.25	1/0	1	0.125	215	0.05375	2.304	34
Q3	3Q120	1	53.72	1.5	2.25	1/0	1	0.125	231	0.05775	2.308	26.13
MI62 Power Supplies												
Q4	3Q120	1	53.72	1.5	2.25	1/0	1	0.125	607	0.15175	2.402	26.13
Q5	3Q120	1	53.72	1.5	2.25	1/0	1	0.125	584	0.146	2.396	26.13
BND2	B2	5	17.64	0.008	0.00718	500	8	0.026	573	0.0037245	0.040	4589
Q6	3Q120	1	51.62	1.5	2.25	1/0	1	0.125	527	0.13175	2.382	25.1
Q7	3Q120	1	54.35	1.5	2.25	1/0	1	0.125	543	0.13575	2.386	26.4
TPS1	MR Corr.	1	?	0.1	6	10ga	1	1.2	764	1.8336	7.834	12
TPS2	MR Corr.	1	?	0.1	6	10ga	1	1.2	764	1.8336	7.834	12
TPS3	MR Corr.	1	?	0.1	6	10ga	1	1.2	764	1.8336	7.834	12
TPS4	MR Corr.	1	?	0.1	6	10ga	1	1.2	535	1.284	7.284	12
TPS5	MR Corr.	1	?	0.1	6	10ga	1	1.2	535	1.284	7.284	12
TPS6	MR Corr.	1	?	0.1	6	10ga	1	1.2	535	1.284	7.284	12
Upstream Service Building and Horn Power Supplies												
Q8	3Q120	1	82.8	1.5	2.25	1/0	1	0.125	498	0.1245	2.375	40.3
Q9	3Q120	1	97.94	1.5	2.25	1/0	1	0.125	478	0.1195	2.370	47.6
BND3	EPB	7	14.17	0.03	0.0175	500	4	0.026	435	0.005655	0.128	1493
Q10	3Q120	1	34.06	1.5	2.25	1/0	1	0.125	370	0.0925	2.343	16.6
TPS7	MR Corr.	1	?	0.1	6	10ga	1	1.2	487	1.1688	7.169	12
TPS8	MR Corr.	1	?	0.1	6	10ga	1	1.2	487	1.1688	7.169	12
TPS9	MR Corr.	1	?	0.1	6	10ga	1	1.2	487	1.1688	7.169	12
TPS10	MR Corr.	1	?	0.1	6	10ga	1	1.2	360	0.864	6.864	12
TPS11	MR Corr.	1	?	0.1	6	10ga	1	1.2	360	0.864	6.864	12
TPS12	MR Corr.	1	?	0.1	6	10ga	1	1.2	360	0.864	6.864	12
HORN PS	Horn	2		3.655	0.932	500	1	0.026	435	0.02262	0.001	300
MINOS Power Supply, located in the MINOS Hall												
MINOS PS		1	80	0.03	2.25	500	1	0.026	250	0.013	2.263	1000
Assume 1 240kW supply (no passive filter) and space for 2 relay racks.												
Upgrade with Most Addtional Magnets: Narrow Band Beam												
NBB1	EPB	2	14.17	0.03	0.0175	500	4	0.026	400	0.0052	0.040	1500
NBB2	NBR	1	80	0.03	2.25	500	4	0.026	400	0.0052	2.255	1500
NBB3	NBB	1	80	0.03	2.25	500	4	0.026	400	0.0052	2.255	1500

Notes:

1. Assumptions for transrex-type power supplies:
   - Regulation .05%
   - Water Flow 5gpm
   - PS losses 5% of load (80% of which is in water, remainder in air)
   - Line kVA 140% of calc. Load (assumes 860 A for 500kW supply)
   - PS Footprint 48.5" wide, 50" deep, 75" high
2. PEI 20kW power supplies are air-cooled
3. B2END (B2) and E{BEND (EPB) dipoles have been increased 5% from Transport values as safety margin
4. Q1 through Q9 (3Q120) quad gradients have been incread by 20% from Transport values as safety margin
5. Q10 (3Q120) quad gradient has been increased by 100% from Transport values as safety margin
6. The septa for NuMI are located at the upstream end of MI60
7. Beamline elements updated: 1430, 21 May 98
8. The MINOS magnet coils have not been designed and the NBB NBR and NBN magnets are not well known. Estimates were put in the above table as to their resistance and inductance.

JIREMENTS

Min.		PEAK	RMS	PEAK	Power	Power Supply				RMS	Fdr	Peak
Curr.	dI/dT	VOLT.	CURR.	PWR	Supply	TYPE	Volt	Curr.	Losses	PWR	Load	Fdr
(amps)	(A/s)	(volts)	(amps)	(kW)	Location	#, Man./Pwr	(volts)	(amps)	(kW)	(kW)	kVA	kVA
0.01	0	125000	0	1	MI60N	1, Glassman	125000	0.016	0.06	1	2	2
0	1585	142	869	214	MI60N	1, Xrex/500kW	200	2500	8.69	39	243	422
0	2933	29	1608	82	MI60N	1, PEI/150kW	30	5000	2.41	24	68	117
35.2	0	80	35	3	MI60N	1, PEI/20kW	200	200	0.35	3	10	10
0	1525	501	837	726	MI60N	3, Xrex/500kW	600	2500	25.10	112	703	1217
34	0	78	34	3	MI60N	1, PEI/20kW	200	200	0.34	3	10	10
26.13	0	60	26	2	MI60N	1, PEI/20kW	200	100	0.26	2	7	7
						MI60N Power Totals:			37	184	**1040**	1783
26.13	0	63	26	2	MI62	1, PEI/20kW	200	100	0.26	2	7	7
26.13	0	63	26	2	MI62	1, PEI/20kW	200	100	0.26	2	7	7
0	4831	375	2649	1721	MI62	4, Xrex/500kW	400	5000	52.99	331	1484	2570
25.1	0	60	25	2	MI62	1, PEI/20kW	100	200	0.13	2	4	4
26.4	0	63	26	2	MI62	1, PEI/20kW	100	200	0.13	2	4	4
12	0	94	12	1	MI62	MR DipoleTrim	150	12	0.09	1	3	3
12	0	94	12	1	MI62	MR DipoleTrim	150	12	0.09	1	3	3
12	0	94	12	1	MI62	MR DipoleTrim	150	12	0.09	1	3	3
12	0	87	12	1	MI62	MR DipoleTrim	150	12	0.09	1	3	3
12	0	87	12	1	MI62	MR DipoleTrim	150	12	0.09	1	3	3
12	0	87	12	1	MI62	MR DipoleTrim	150	12	0.09	1	3	3
						MI62 Power Totals:			54	345	**1521**	2607
40.3	0	96	40	4	TH SB	1, PEI/20kW	200	100	0.40	4	11	11
47.6	0	113	48	5	TH SB	1, PEI/20kW	200	100	0.48	6	13	13
0	1572	521	862	778	TH SB	3, Xrex/500kW	600	2500	25.86	121	724	1254
16.6	0	39	17	1	TH SB	1, PEI/20kW	200	100	0.17	1	5	5
12	0	86	12	1	TH SB	MR DipoleTrim	150	12	0.09	1	3	3
12	0	86	12	1	TH SB	MR DipoleTrim	150	12	0.09	1	3	3
12	0	86	12	1	TH SB	MR DipoleTrim	150	12	0.09	1	3	3
12	0	82	12	1	TH SB	MR DipoleTrim	150	12	0.09	1	3	3
12	0	82	12	1	TH SB	MR DipoleTrim	150	12	0.09	1	3	3
12	0	82	12	1	TH SB	MR DipoleTrim	150	12	0.09	1	3	3
0	316	700	173	210	TH SB	1, PEI/240kW	800	300	6.93	162	194	336
				Upstream Service Building Power Totals:					34	301	**962**	1635
1000	0	200	1000	200	DS SB	1, Xrex/240kW	400	600	20.00	2283	560	560
				Downstream Service Building Power Totals:					20	2283	**560**	560
0	1579	155	866	233	US SB	1, Xrex/500kW	200	2500	8.66	39	242	420
0	1579	3430	866	5145	US SB	1, Xrex/500kW	200	2500	8.66	1700	242	420
0	1579	3430	866	5145	US SB	1, Xrex/500kW	200	2500	8.66	1700	242	420
		Additional NBB Upstream Service Building Power Totals:							26	3439	**727**	1260
		Upstream Service Building Power Totals (w/NBB):							60	3739	**1690**	2895

Table 5-2

	Operational Requirements	Design Ratings
Capacitor bank voltage	515 V	700 V
Capacitor voltage rating		1000 V
Capacitor bank		0.90 Farads
Peak current	200 kA peak	240 kA (120%)
RMS current	7250 A	8700 A
Pulse	1/2 sine	1/2 sine
Pulse width	5.2 ms	5.2 ms
Repetition rate	1.9 sec.	1.9 sec.
Duty	continuous	continuous
di/dt	198 A/μs	238 A/μs

Table 3.3-3 Horn Power Supply System Operational Requirements.

Maximum output voltage	800 V
Maximum output current	300 A
Current regulation	0.1%
Voltage regulation	0.05%

Table 3.3-4 Charging Power Supply (240 kW Transrex)

Peak forward and reverse blocking voltage	2000 V
Average current	2500 A
RMS current	4820 A
(max. surge rating)I_{tsm}	45,000 A

Table 3.3-5 Typical SCR Switch Ratings

Thickness	0.953 cm (0.375")
Total width	1.22 m (48")
Spacing	1 cm air inside shield block 5, 0.0127 cm outside shield block
Inductance	27.2 nH/meter inside shield block 16.8 nH/meter outside shield block
Resistance	5.6 μΩ/meter

Table 3.3-6 Two Horn System Transmission Line.

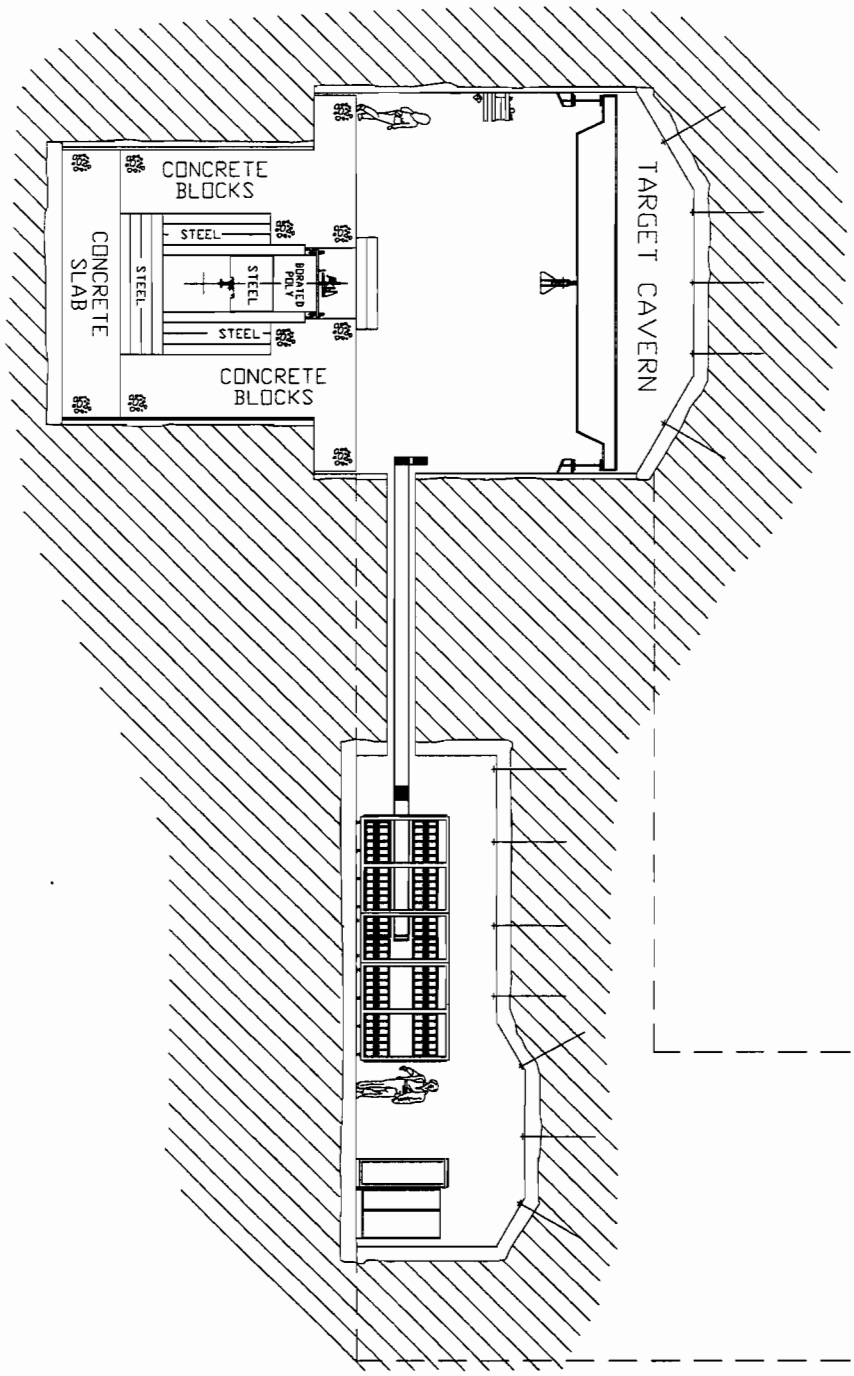

Figure 3.3-1 Target Hall and Power Supply Room Cross Section

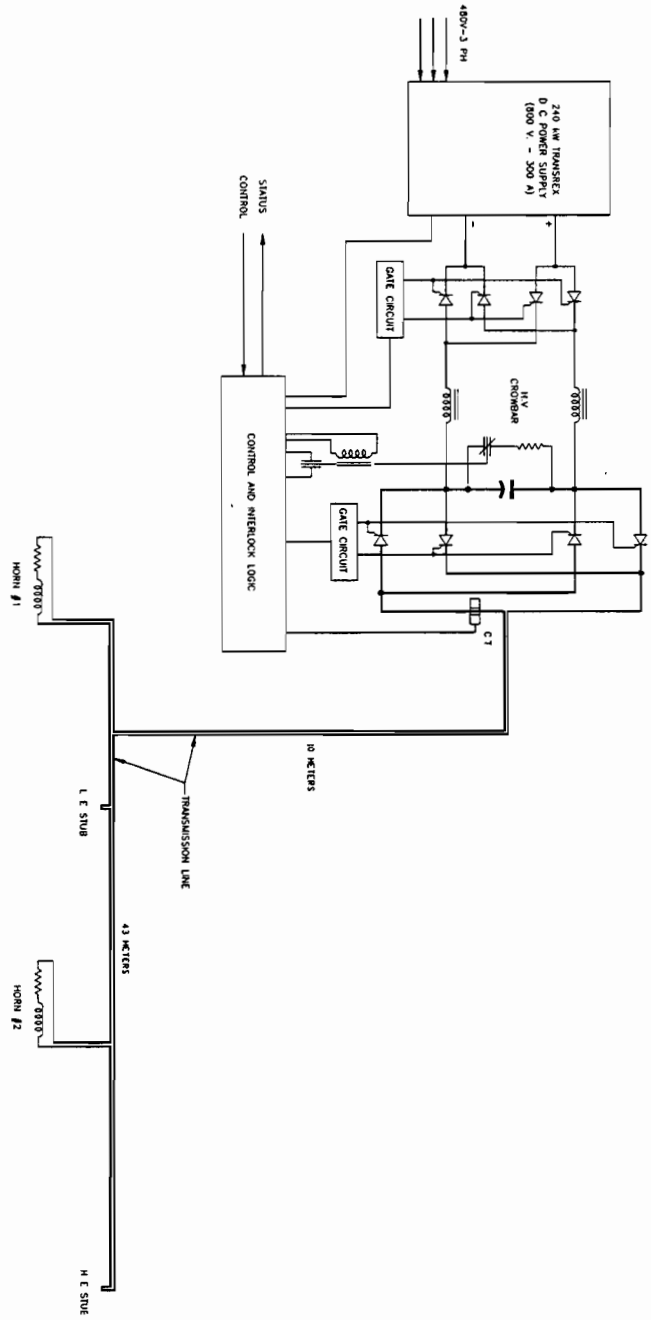

Figure 3.3-2 Electrical Schematic of the NuMI Horn Power Supply Syste m with Energy Recovery

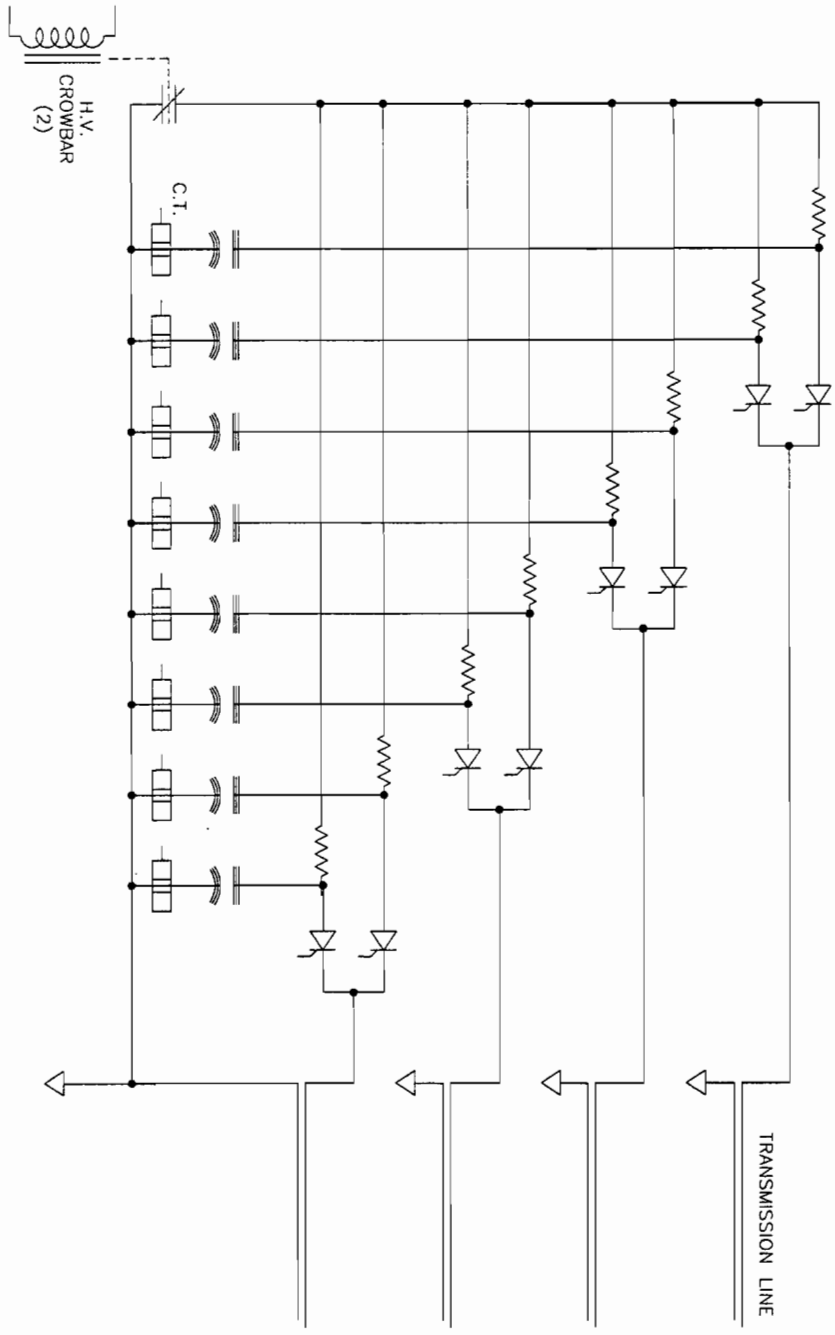

Figure 3.3-3 Capacitor Bank Structure

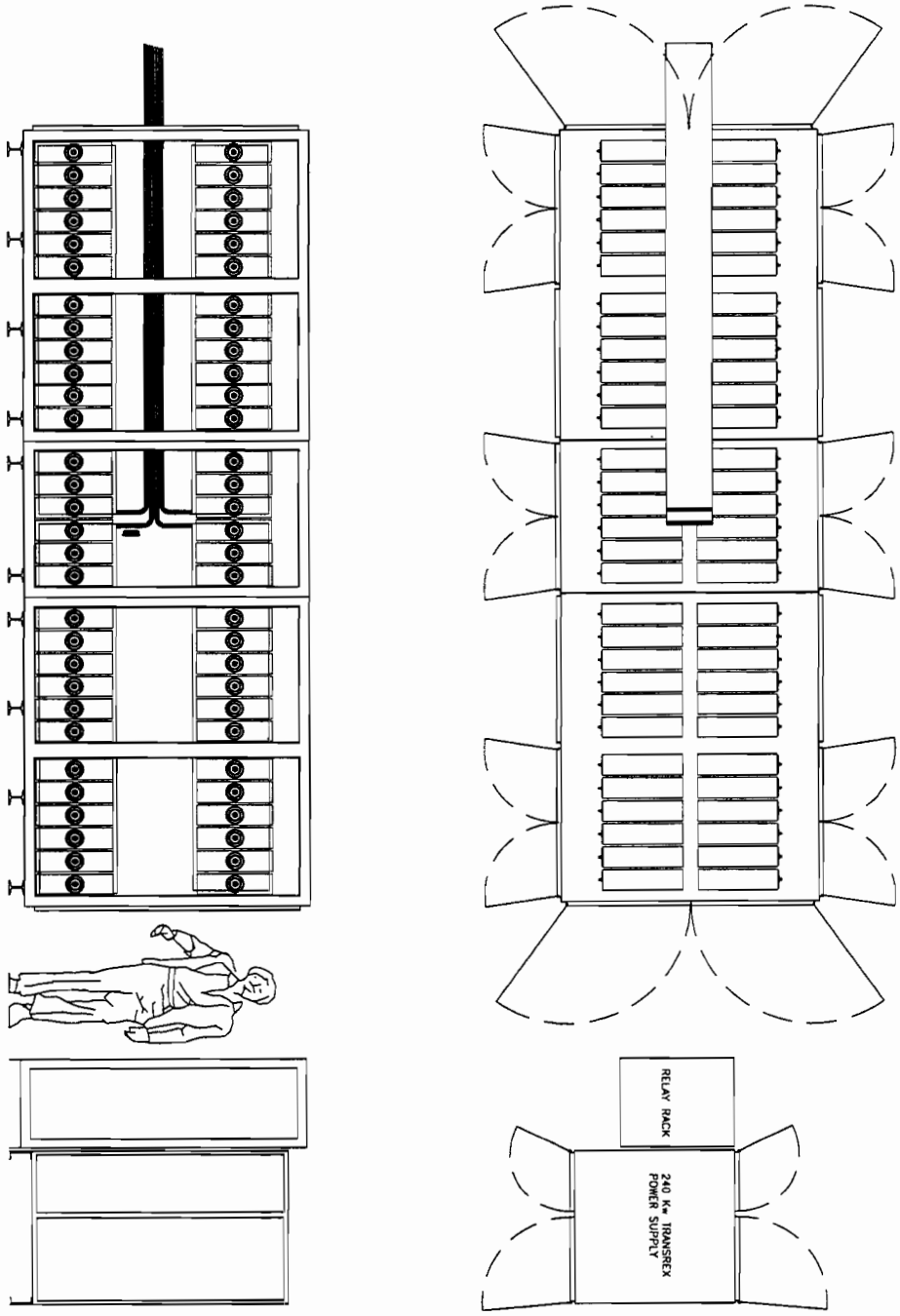

Figure 3.3-4 Conceptual Layout of Capacitor Bank and Transrex

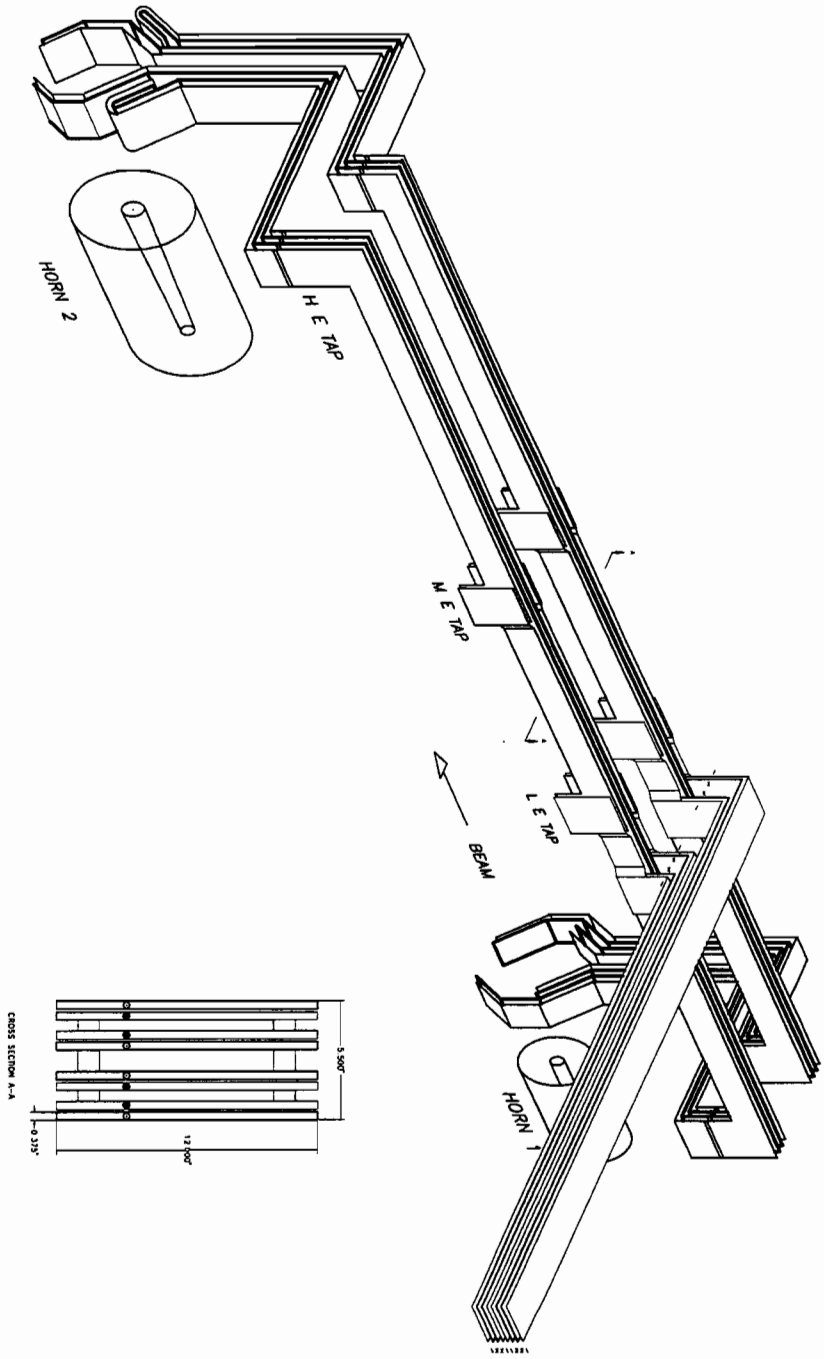

Figure 3.3-5 Transmission Line Cross-section and Layout.

This Page Intentionally Left Blank

3.4 Decay Region and Hadron Absorber (WBS 1.1.4)

Table of Contents

3.4 DECAY REGION AND HADRON ABSORBER (WBS 1.1.4) 3.4-1

3.4.1 Introduction *3.4-2*

3.4.2 Objectives of the Decay Region and Absorber *3.4-2*

3.4.2.1 Shared objectives of the Decay Region and Absorber 3.4-2

3.4.2.2 Decay Region Objectives 3.4-3

3.4.2.3 Hadron Absorber Objectives 3.4-3

3.4.3 Technical Requirements and Constraints *3.4-4*

3.4.4 Design Assumptions *3.4-5*

3.4.5 System Description *3.4-5*

3.4.6 Design Procedures and Validation *3.4-7*

3.4.7 Construction Plan *3.4-8*

3.4.8 Installation Plan and Issues *3.4-8*

3.4.8.1 Decay Region 3.4-8

3.4.8.2 Hadron Absorber 3.4-8

3.4.9 Commissioning Plan *3.4-9*

3.4.9.1 Decay Region and Hadron Absorber 3.4-9

3.4.9.2 Hadron Absorber 3.4-9

3.4.10 Performance Monitoring Plan *3.4-9*

3.4.10.1 Decay Region and Absorber 3.4-9

3.4.10.2 Decay Region 3.4-10

3.4.10.3 Hadron Absorber 3.4-10

Table of Figures

Figure 3-4-1 Hadron absorber, located at the end of the decay pipe. *3.4-11*

Figure 3-4-2 Momentum weighted distribution of hadrons incident on Absorber. *3.4-12*

3.4.1 Introduction

This section concerns the region where hadrons decay to produce neutrinos and other particles, and where non-interacting protons and secondary particles are intercepted by a hadron absorber at the end of the decay volume and give up their energy in a multi-generation cascade of interacting particles. The energy that isn't absorbed in the absorber consists mainly of muons and neutrinos that exit the rear of the absorber and enter the rock behind the absorber. A small fraction of the energy will exit the absorber as neutrons--in virtually all directions.

The other WBS elements active in this region include water and vacuum systems, and alignment. A self-contained, radioactive water (RAW) system will provide the cooling for the inner core of the Hadron Absorber. A vacuum pumping system will evacuate the air from the decay pipe volume, so that positive pions produced and focused upstream of the decay pipe have a long path length free of material in which to decay, to produce muon neutrinos with an aiming point towards Soudan, Minnesota. Alignment needs for the decay pipe and absorber are not as critical as for the proton beam, target, and focusing horns, but are present nonetheless.

There will be some interaction with other WBS elements--namely, those for interlocks, beam monitoring, civil construction, groundwater monitoring, and controls. The decay and hadron absorber region must be inaccessible while beam is enabled. Beam monitoring devices will be placed between the decay pipe and absorber, as well as downstream of the absorber. We anticipate having temperature sensors installed in the hadron absorber; these will be read out via the control system.

3.4.2 Objectives of the Decay Region and Absorber

This section describes the objectives, both shared and separate, of the Decay Region and the Hadron Absorber.

3.4.2.1 Shared objectives of the Decay Region and Absorber

The objectives enumerated in this section are common to both the decay region and the hadron absorber.

- Make provision for monitoring for radionuclides (^{3}H, ^{22}Na) in local groundwater.

- Assure personnel safety from possible mechanical, electrical, ODH[1] and radiological hazards associated with these systems.
- Assure long-term reliability, stability, and reparability. The facility needs to be usable for a minimum of 10 years.
- Minimize the cost and difficulty of decommissioning the equipment and shielding, when the time comes that the NuMI facility is no longer in use and the decision is made to no longer run the sump pumps and the ventilation systems.

3.4.2.2 Decay Region Objectives

- Provide a large, evacuated space in which horn-focused particles from the wide band neutrino beam can decay to produce muon neutrinos.
- Facilitate prediction of the neutrino energy spectrum in the MINOS Far Detector to 2 or 3%, given a measurement in the MINOS Near Detector and absent neutrino oscillations. This leads to tolerances on alignment of the decay pipe along its length.
- Keep electron neutrino and muon anti-neutrino event backgrounds small, < 1% of the muon neutrino event rate. This implies minimizing the amount of material in the decay pipe windows, and determines the limit on the amount of residual air in the decay pipe.
- Have sufficient shielding outside the decay pipe to protect the groundwater in the rock walls of the enclosing tunnel.
- Minimize the residual magnetic field inside the decay pipe.

3.4.2.3 Hadron Absorber Objectives

- Accommodate a primary beam intensity of 4×10^{13} protons every 1.9 seconds in order to match the production capability of the Main Injector.
- Accommodate full Main Injector proton intensity, up to at least 3×10^{13} protons per second, under short-term accidental conditions of missing the primary target.
- Absorb most of the energy of the non-interacted protons and other strongly interacting particles that reach the end of the NuMI decay pipe, and transfer the resultant heat to a water-cooling system.

---

[1] Oxygen Deficiency Hazard

- Maintain the number of neutrons exiting the absorber at a level that doesn't represent a prompt radiation hazard in uncontrolled access areas near the hadron absorber.
- Maintain the number of particles entering the surrounding rock walls at a level that doesn't activate groundwater to levels of concern.
- Minimize the airborne radioactivity created in the region of the hadron absorber

3.4.3 Technical Requirements and Constraints

The decay pipe length of 675 meters provides a sufficient flux of muon neutrinos in the wide energy band mode (of the neutrino beam) for the MINOS experiment (E875) to achieve its initial goals in a two-year run. The decay pipe must aim at the new MINOS cavern at Soudan. Misalignment of the decay pipe along its length should not occlude the 1-meter radius aperture by more than 2%. The vacuum level in the decay pipe should be 1 Torr or lower.

The support system for the decay pipe has to constrain the pipe's transverse position, yet allow for the pipe to flex longitudinally as it is pumped down from atmospheric pressure to better than 1 Torr vacuum level. The decay pipe will also flex longitudinally as it is subjected to differing levels of beam heating[2]. The support system has to fix the pipe at one longitudinal position (e.g. the middle). The support system has to provide space for doing the butt-welding of the pipe sections. It has to allow for alignment of the pipe--according to the initial survey that is done.

The residual magnetic field in a comparable pipe (the KTEV decay pipe) has been measured to be 0.1 - 0.2 gauss. This is less than the value of the earth's magnetic field, which is dismissed as a problem in TM-2018[3]. We conclude that similar levels will be achievable in the NuMI decay pipe--provided that we avoid handling the decay pipe sections by magnetic devices.

The Hadron Absorber has to protect groundwater under normal running conditions over long periods of time (the relevant time scale is measured in years). It has to maintain prompt levels of radiation at acceptable levels in tunnel regions accessible to personnel, for both normal running conditions and abnormal running conditions--such as the proton beam

[2] A Geant beam simulation with the old, 3-horn beam gave the result that 15% of the energy of the beam exits the decay pipe side walls as hadronic energy.

[3] J. Hylen et al., "Conceptual Design for the Technical Components of the Neutrino Beam for the Main Injector (NuMI)", FERMILAB-TM-2018, http://fnalpubs.fnal.gov/archive/1997/tm/TM-2018.html

missing the target (in which case the beam is significantly narrowed in size at the hadron absorber). The absorber core and surrounding iron shielding has to maintain its integrity during both normal and abnormal running conditions.

3.4.4 Design Assumptions

This section describes the set of assumptions that has been applied to the present design of the decay region and hadron absorber. Should any of these assumptions change, the design will be revised accordingly.

No mechanical shutter is necessary to protect either the upstream or downstream windows of the decay pipe. They are of sufficient thickness that a shutter system is not required for personnel protection while accessing the vicinity to work on beam instrumentation.

The crane at the downstream access shaft will be the primary means of bringing steel and concrete blocks from the surface. This crane has a capacity of 15 tons.

The prompt radiation dose calculated at the end of the access labyrinth to the Hadron absorber assumes a beam intensity of 6×10^{13} protons per spill[4]. An interlocked safety door will preclude access into the upstream portion of the tunnel to the absorber cavern during beam on conditions.

3.4.5 System Description

The WBS element (1.1.4) for the decay region and absorber encompasses a subset of the EDIA[5] costs for the decay pipe. The remaining cost items for the decay pipe and its shielding are located in WBS element 1.2 (Civil Construction). WBS element 1.1.4 contains only those EDIA items for the decay pipe that must undergo a formal ES&H review. These are the shell calculations for the decay pipe sections and the designs for the end windows. WBS element 1.2 (Civil Construction) contains the rest of the EDIA items for the decay pipe and its shielding--as well as construction and installation items. Consequently, the system description of the decay pipe and its shielding in this chapter of

[4] The value 6×10^{13} for the intensity is 50% higher than the nominal beam intensity delivered from the Main Injector. It seemed wise to use a higher value than nominal to design the labyrinth attenuation, in order to allow for the possibility that the beam intensity would exceed the nominal value. This value also corresponds to the full Main Injector proton intensity listed in Objective #2 of Section 3.4.1.3, which was talking about short term accidental conditions of missing the primary target. The value listed there was 3×10^{13} protons per second, which translates to 5.7×10^{13} protons per spill (1.9 sec spill). In fact, if the proton beam manages to miss the target under accident conditions, the amount of beam energy reaching the absorber goes up by a factor of 5 or more. This is discussed in more detail in the report.

the report (3.4) is deliberately sketchy. A fuller description can be found in Chapter 5, which describes Civil Construction (drawings of the tunnel and shielding configuration are found there).

The decay pipe will be made up of steel pipe sections that are sized to be delivered by truck and conveniently negotiate the path from surface to Target Hall. The pipe wall thickness will be 2 cm. Welding will be the joining method for the sections of decay pipe. Pipe sections will be 40 feet long or shorter, and will be butt-welded inside and out, in place. KTEV experience is that such welds have no leaks.

The decay pipe will be surrounded in radius by ~5.5 feet of 2000 psi-rated concrete. This concrete constitutes the groundwater shield. The decay pipe tunnel will be sized to provide space for the pipe, its surrounding concrete shield, and a walkway on one side.

At its downstream end the decay pipe will be followed by instrumentation to measure the beam position and profile; following that will be the Hadron Absorber. A front. elevation view of the Hadron Absorber is shown in Figure 3-4-1. The Absorber has a water-cooled aluminum core at the upstream end, which is surrounded transversely by steel and concrete. This is followed by an inner core of steel that is also water cooled--pending a detailed cooling analysis. It too is surrounded transversely by steel and concrete, and is followed downstream by steel and concrete. The bulk of the steel will be pieces of continuous cast salvage steel (like that in the Target Hall). The concrete will be concrete blocks from the Fermilab concrete block inventory.

The heat exchanger, deionizing "bottles", and pumps for the radioactive water (RAW) system cooling the core of the Hadron Absorber will be located in an area at the entrance to the absorber cavern which is protected from severe radiation exposure. The choice of this location also minimizes the volume of RAW water that might be lost in the case of leakage. Vacuum pumps will also be located in this alcove area. There is a significant loss of vacuum pump efficiency as the length of the vacuum pipe between the Decay Region and the vacuum pumps increases. The vacuum pumps must be kept close to the Decay Pipe; at the same time the pumps must be protected from severe radiation exposure.

[5] EDIA--Engineering, Design, Inspection, and Administration.

3.4.6 Design Procedures and Validation

The effect of the decay pipe length and aperture on the number of neutrino events in the MINOS far detector was studied with the program NUADA. The results are shown and discussed in Fermilab TM-1946[6]. The subject is further discussed in Fermilab TM-2018[7].

Shown in Figure 3-4-2 is the energy-weighted x distribution of all hadrons incident on the absorber as determined using Geant, for the PH2-LE beam. The weighting is the expression (hadron momentum)/(120 GeV * number of protons on target for the calculation). The standard deviation (sigma) of a Gaussian fit to the x distribution is 12.25 cm. Twenty percent of the incident beam energy (incident on the primary target) strikes the face of the absorber; it is dissipated in the absorber materials and is transferred as heat to the RAW system. The corresponding distribution for the PH2-ME beam contains 14% of the incident beam energy; it is less well fit by a Gaussian distribution, but has a central peak between -10 cm and 10 cm which has a Gaussian sigma of 8 cm.

The programs CASIM and MARS, together with some of the assumptions and parameters of Fermilab's Concentration Model, have been used to assess the effectiveness of the shielding of the Hadron Absorber for groundwater. The concentration of the radionuclides ^{3}H, ^{22}Na in the groundwater outside the tunnel was calculated from the output of these programs. This subject is discussed in detail in Fermilab TM-2009[8], and is further discussed in Chapter 4 of this report. The programs CASIM/MARS will also be used to calculate energy deposition in the absorber materials in detail.

The dimensions of the shielding used in the design of the Hadron Absorber have been compared to the design of the MI40 Beam Absorber described in TM-1985[9]. This has provided us with some useful checks.

The amount of hadronic energy exiting a 1 meter radius decay volume has been calculated by Geant; this has been cross-checked with CASIM energy deposition calculations.

---

[6] D. Crane et al., "Status Report: Technical Design of Neutrino Beams for the Main Injector (NuMI)", NuMI-B-92, FERMILAB-TM-1946, July 21,1995.

[7] TM-2018, Opt. Cit.

[8] A. Wehmann, W. Smart, S. Menary, J. Hylen, and S. Childress, "Groundwater Protection for the NuMI Project", FERMILAB-TM-2009, NuMI-B-279, August 1997.

[9] C.M. Bhat and A.L. Read, "Ground-Water Activation from the Upcoming Operation of MI40 Beam Absorber", Fermilab-TM-1985, September, 1996

The effectiveness of the labyrinth used to access the Hadron Absorber (coming from the DS access shaft) was studied with the program EXITS2. The methodology is the same as that used elsewhere at Fermilab for shielding assessments. The results will be documented in a technical memorandum.

The shielding plans are being subjected to a formal, internal Fermilab review. There will be an ES&H safety review of the vacuum vessel shell and window design. The PSAD review may serve as another review of the groundwater shielding. It may also review the safety of the decay pipe.

3.4.7 Construction Plan

The construction plan for the decay pipe and its shielding are being developed as part of the conventional construction package (see Chapter 5 of this report).

3.4.8 Installation Plan and Issues

3.4.8.1 Decay Region

The installation plan for the decay pipe and its shielding are being developed as part of the conventional construction (see Chapter 5 of this report). Stray magnetic fields in the decay pipe sections will be measured to the level of a fraction of one gauss during installation.

3.4.8.2 Hadron Absorber

The pieces of the Hadron Absorber will be lowered by crane, individually, down the ~300' DS access shaft. A transporter cart, attached by 700' of cable to an electric winch, will be used to bring the steel plates and concrete blocks up the ~650' long, inclined ramp (10% grade) to the landing adjacent to the Absorber Cavern. Since the landing and Absorber Cavern will be at the same level, a rigger's "pull bar" should be sufficient to take the loaded transporter cart the short distance from the winch attachment point to the Absorber Cavern proper. Riggers will use the 15 ton crane in the Absorber Cavern to unload the transporter cart and assemble the Absorber.

As can be seen in Figure 3-4-1 the steel pieces are planned so that those above the core can be removed by the crane without removing any other steel. These steel pieces will be welded together, in groupings weighing less than 15 tons, so that their removal is simplified. Such removal is hopefully unnecessary, since it would take place only in the case of a failure in the integrity of the core cooling water system. The cooling piping for the core will be routed upwards, and then horizontally under the top layer of concrete, with

a disconnect prior to the horizontal run. Spacers will be used to create a channel for the horizontal run of pipe. Below the disconnect point the cooling piping will be rigidly attached to the inner core pieces, so that it accompanies the core if removal is necessary.

The riggers will first install the shield blocks forming the base of the absorber pile. Horizontal layers of continuous cast salvage (CCS) steel will be rigged into place in the front and middle sections of the absorber. The aluminum core will be rigged into place. The downstream steel core will be rigged into place. Electrical connections to temperature monitors will be made. The vertical, sidepieces of CCS steel will be rigged into place and assembled into a rigid unit on each side. The remaining CCS steel pieces will be rigged into place. Standard size concrete shielding blocks will be rigged in to complete the side shielding. The back concrete shielding blocks will be rigged into place. Water connections to the inner core piping will be made prior to putting on the top layer of concrete.

3.4.9 Commissioning Plan

3.4.9.1 Decay Region and Hadron Absorber

The active equipment in the decay region and in the Hadron Absorber is the equipment in water cooling systems and the vacuum pumps for the decay volume. The commissioning of the water cooling and vacuum systems will be described in Section 3-7.

3.4.9.2 Hadron Absorber

Temperature levels in the absorber core will be monitored during the initial operation of the RAW system cooling pumps, and later during the commissioning with beam. A radiation survey of the absorber pile and cavern after initial beam running will identify any places where shielding needs to be improved, such as around penetrations.

3.4.10 Performance Monitoring Plan

3.4.10.1 Decay Region and Absorber

The groundwater radionuclide activation will be monitored. The following paragraph is taken from the NuMI Environmental Assessment (dated 12/17/97, page 34)[10].

[10] This subject is also discussed in TM-2009, Opt. Cit.

"Two methods for monitoring the concentrations of radionuclides in the groundwater would be employed. One method would use standard monitoring wells placed near the tunnel, and at the depth of, three elements of the facility; the target hall, the most heavily grouted region of the decay tunnel, and the beam absorber. These wells would be designed to intercept the flow of groundwater from near the NuMI facility. These locations are those where the levels of activation of the rock surrounding the tunnel would be the greatest. The second method would take advantage of the fact that the proposed facility would be located directly in the aquifer and would have a net (albeit small) inflow into the tunnel. Small diameter holes would be drilled into the sides of the tunnel and fitted with taps and thus water samples could be taken directly from the rock just outside the shielding. These samples would be used to measure the radionuclide concentrations as close to the radionuclide production sources as possible. In the unlikely event that during the course of NuMI operations, radionuclide concentrations measured through either of these two techniques were found to be higher than anticipated, either the proton beam intensity would be reduced or the shielding configuration modified in order to prevent any of the regulatory limits from being exceeded."

3.4.10.2 Decay Region

Tunnel inflow water will be analyzed as a part of a routine monitoring program. The vacuum level in the decay pipe will be monitored by a set of vacuum gauges.

3.4.10.3 Hadron Absorber

Periodic radiation surveys and ground water monitoring will provide feedback on shielding efficacy. Regular sampling will be done for radionuclide levels in the closed loop RAW system serving the Hadron Absorber core. RAW water spills will be controlled by a combination of continuous water level sensing, along with secondary containment vessel collection and tightly controlled sump discharge. Temperature measuring instrumentation in the absorber will be monitored for any indication of temperatures rising to abnormal levels.

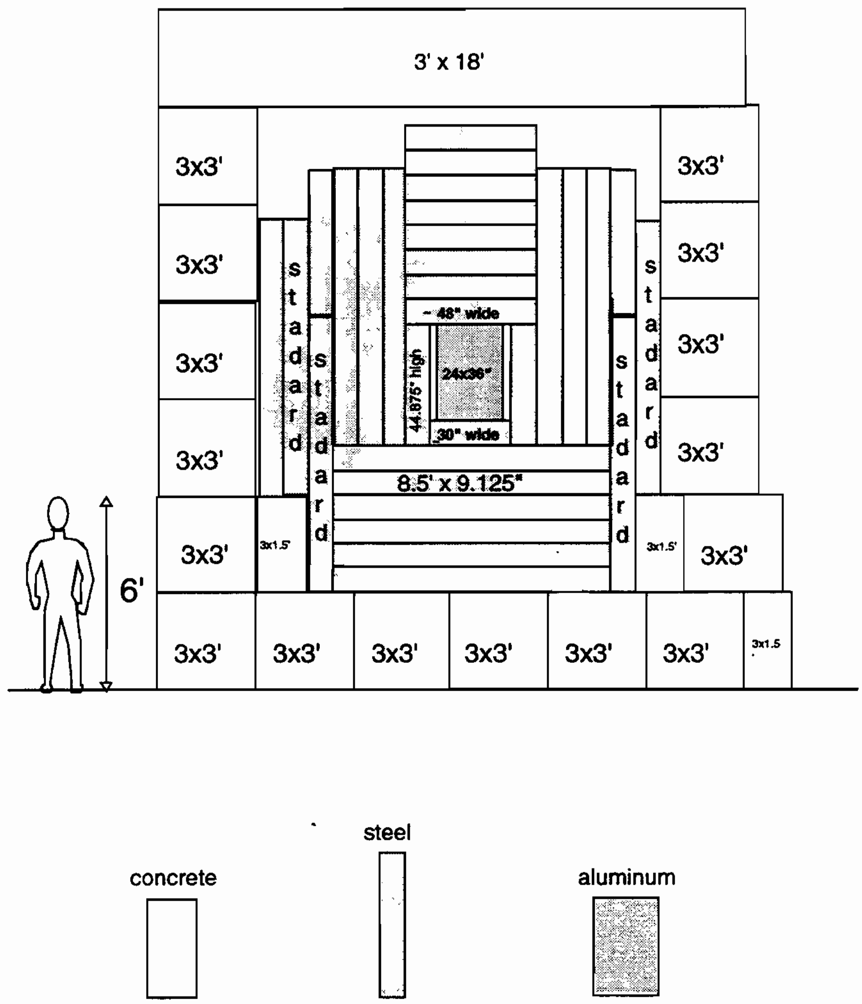

Figure 3-4-1 Hadron absorber, located at the end of the decay pipe.

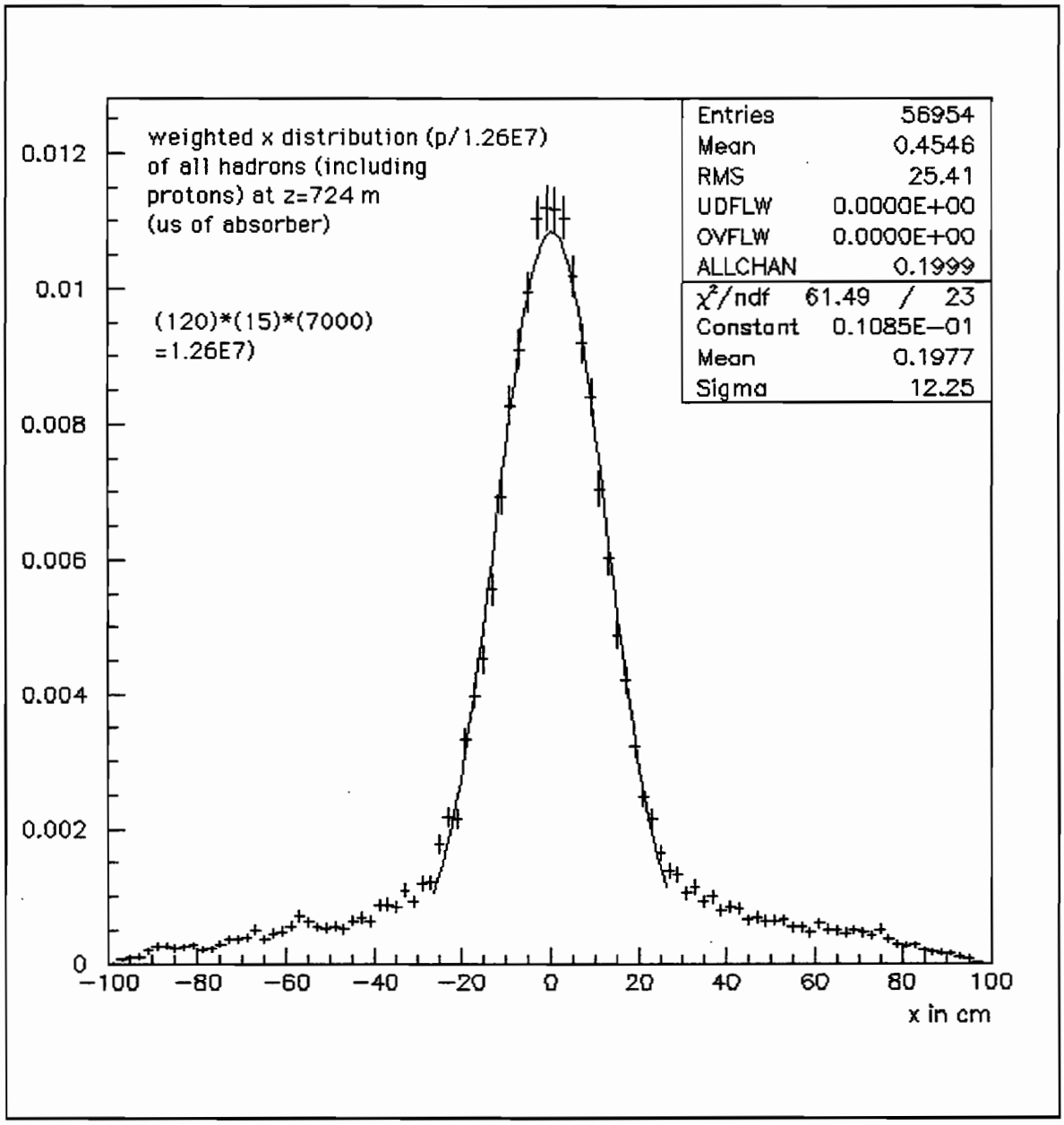

Figure 3-4-2 Momentum weighted distribution of hadrons incident on Absorber.

3.5 Neutrino Beam Monitoring (WBS 1.1.5)

Table of Contents

3.5 NEUTRINO BEAM MONITORING (WBS 1.1.5) 3.5-1

3.5.1 Introduction *3.5-4*

3.5.2 Design Assumptions *3.5-4*

3.5.3 Technical requirements and constraints *3.5-5*

3.5.3.1 Hadron Monitors: Overall Intensity Range 3.5-5

3.5.3.2 Hadron Monitors: Precision and Stability Requirements 3.5-6

3.5.3.3 Muon Monitors: Overall Intensity Range 3.5-7

3.5.3.4 Muon Monitors: Precision Requirements 3.5-8

3.5.3.5 Muon Monitors: Stability Requirements 3.5-9

3.5.3.6 Determination of the Physical Position of the Muon Slots 3.5-10

3.5.4 System Description *3.5-10*

3.5.4.1 Segmented Wire Ionization Chambers (SWIC) 3.5-11

3.5.4.2 Segmented Strip Ionization Chambers (SSIC) 3.5-13

3.5.4.3 Calibration of the Monitors 3.5-14

3.4.4.4 Gas System 3.5-15

3.5.5 Design Validation *3.5-15*

3.5.6 Construction Plan *3.5-16*

3.5.7 Installation Plan and Issues *3.5-16*

3.5.8 Commissioning Plan *3.5-16*

3.5.9 Monitoring the Monitors *3.5-16*

3.5.10 Prototype Testing *3.5-17*

3.5.10.1 Segmented Strip Ionization Chamber (SS250) 3.5-17

Table of Tables

Table 3-5-1 The integrated charged particle intensity (within a radius of 50 cm at DkU and a radius of 100 cm at DkD) and charged particle density within a diameter corresponding to the FWHM for nominal beam settings of all three beam configurations and the standard 1 ms spill of 4 x 10^{13} pot..... 3.5-18

Table 3-5-2 The integrated muon intensity and peak muon densities within one RMS of the mean position at five muon slot positions for the three beam configurations running at nominal horn position and current for the standard 1 ms spill of 4 x 10^{13} pot..... 3.5-19

Table 3-5-3 The mean of the muon x profile (cm) and the error on the mean for the statistics of the Monte Carlo for all three beam configurations at all five modeled muon-slot positions for horn 1 nominal and horn 1 offset by .4 cm 3.5-20

Table of Figures

Figure 3-5-1 Assuming nominal beam conditions with the PH2me-beam configuration, the profiles of the charged particles at DkU and DkD. The abscissa is in cm, the ordinate in particles per incident proton..... 3.5-21

Figure 3-5-2 Profiles with Horn 1 offset by 4 mm (cross) overlaid on nominal profiles (dashed line) at position DkU (top) and DkD (bottom). The abscissa is in cm, the ordinate in particles per incident proton. 3.5-22

Figure 3-5-3 The mean of the horizontal profile for all three beam configurations at position DkU as a function of the position of H1..... 3.5-23

Figure 3-5-4 The mean of the horizontal profile for all three beam configurations at position DkD as a function of the position of H1..... 3.5-24

Figure 3-5-5 The change in the mean of the x-profile for a given change in the horn 2 x position for the PH2me-beam at DkD..... 3.5-25

Figure 3-5-6 The change in relative intensity as a function of the relative change in horn current for the me beam at DkU and DkD positions. 3.5-26

Figure 3-5-7 The dependence of the relative intensity on the relative current delivered to the horns for the le-and-PH2he-beam configurations..... 3.5-27

Figure 3-5-8 The change in the ratio of intensities at DkU and DkD as a function of the relative current for the PH2me-beam..... 3.5-28

Figure 3-5-9 The profiles of muons reaching muon-slots 1-3 for the PH2me-beam. The abscissa is in cm, the ordinate in muons per incident proton..... 3.5-29

Figure 3-5-10 The change in the mean of the x-profile for a given change in the horn 1 x position for the PH2me-beam at all five modeled muon-slots. 3.5-30

Figure 3-5-11 The change in the mean of the x-profile for a given change in the horn 1 x position for the PH2he-beam at all five modeled muon-slots. 3.5-31

Figure 3-5-12 The change in the mean of the x-profile for a given change in the horn 1 x position for the PH2PH2le-beam at all five modeled muon-slots. 3.5-32

Figure 3-5-13 The relative intensity as a function of the relative current applied to the horns for the PH2PH2me-beam at the five muon-slots. 3.5-33

3.5.1 Introduction

The neutrino beam monitoring systems enable the beam users to control the quality of the neutrino beam being delivered to the experiments. This is accomplished by measuring the flux as well as the horizontal and vertical profiles of the secondary hadrons (and non-interacting primary protons) at various points along the secondary beam line and by measuring the flux and spatial distribution of the muons at various locations within the dolomite muon shield. Hardware problems with beamline and target components will be deduced from changes in the beam on a spill-to-spill basis. An alarm signal will be provided when performance is not nominal.

In order to detect variations, the secondary and muon intensity measurements are normalized both to the number of incoming protons and to each other, while the measured profiles are compared to nominal profiles. Since the intensity of the NuMI beam is quite high, the actual neutrino event rate and radial distribution in the on-site neutrino beam monitor (MINOS near detector) can be combined with the normalized measurements of the secondaries and muons to insure that the systems producing the neutrino beam are functioning correctly.

On a somewhat longer time-scale, the instrumented target section of the MINOS near detector will accumulate neutrino events at a rate of order 10 per spill (0.5 Hz). This will permit monitoring of the integrated rate and spatial distribution of neutrino events to the 1% level in the order of hours and the event energy distribution to similar accuracy daily.

Although secondary to monitoring the performance of the NuMI beamline, an important physics objective of the monitoring system will be to provide secondary intensity and spatial distribution input to determine the non-oscillated neutrino beam spectrum.

3.5.2 Design Assumptions

Integrity and alignment of the horn system are the most critical aspects of neutrino beam quality. The horn system goal for the far detector neutrino energy spectrum is contained in a study of alignment / control requirements[1]. Horn current and alignment deviations from nominal are limited to those that would cause a **2%** change in at least one 1-GeV energy bin within the neutrino energy spectrum at the MINOS far detector. The monitoring system must have redundancy to minimize

[1] Smart, W. NuMI-L-221, 31 Oct. 1996

systematic errors. Furthermore, the monitoring system must be able to meet these goals in all three different beam configurations - low energy (PH2le), medium energy (PH2me) and high energy (PH2he) - of the nominal 2-parabolic-horn beam.

The beam monitoring must be able to detect changes in horn current and horn misalignment. The neutrino energy tolerance translates into horn tolerances which state that the magnetic center of horn 1 should not move more than 0.75 mm and that the magnetic center of horn 2 should not move by more than 4.25 mm. The horn current should not change by more than 1.3%.

From previous experience, we know that the most sensitive indicator of the neutrino direction, intensity and energy on a spill-to-spill basis are monitors which measure the muons arising from the same decay of the secondary mesons which produce the neutrinos.

In addition to the muon monitors, a system that monitors secondaries between the second horn and the hadron absorber is also being designed. These monitors are required to provide feedback during beam start-up and to serve as a control of the muon monitoring system. The goal of the "spill-to-spill" NuMI neutrino beam monitoring effort is to have two independent monitoring systems which can be compared to each other, normalized to each other as well as to the number of protons on target and finally, combined in an on-line fit to ensure that all systems are performing nominally.

Monitoring of the performance must be in operation throughout the entire course of an experiment and there would be considerable radiation-handling and alignment difficulties in replacing monitoring devices. Dependability as well as redundancy is therefore an important design criterion.

3.5.3 Technical requirements and constraints

3.5.3.1 Hadron Monitors: Overall Intensity Range

Two locations have been considered for the placement of secondary monitors: after Horn 2 just upstream of the start of the decay pipe (DkU) and between the end of the decay pipe and the hadron absorber (DkD). Assuming nominal beam conditions with the PH2me-beam configuration, the intensities and profiles of the charged particles at these two locations have been generated using the GEANT Monte Carlo with the FLUKA 94 hadron production spectra.

The intensities and beam profiles are shown in Figure 3-5-1. It should be noted that the abscissa is in cm while the ordinate is the intensity of charged secondaries normalized to the number of

incoming protons (pot). As well, a p > 30 MeV cut was made on all particles at production however, once produced, particles were followed until p = 10 MeV for hadrons and 1 MeV for photons and electrons. A check was made on this 30 MeV cut by lowering the production cut to 10 MeV, which increased the Monte Carlo running time but did not change the results within the errors.

For the standard NuMI proton intensity of 4 x 10^{13} pot, the total number of charged particles traversing each of the locations over a 1 ms spill within an area of given radius for all three beam configurations is shown in Table 3-5-1.

3.5.3.2 Hadron Monitors: Precision and Stability Requirements

The precision required of the hadron monitors was determined by simulating non-nominal operating conditions of the NuMI beam line. Horn 1 and horn 2 were displaced by up to 10 mm in the x-direction simulating changes in the horn magnetic center which could be caused both by the horns physically moving through settling or mechanical deformation, or by the stripline failing to distribute a symmetric current to the horns. As a second test, the horn current was decreased by up to 25% of its nominal value. The changes in the intensity and means of the x-profiles were studied at both DkU and DkD locations in all cases. Figure 3-5-2 shows, for the PH2me-beam, the x-profile of charged particles at positions DkU (top) and DkD (bottom) when H1 has been shifted by 4 mm (crosses) overlaid on the nominal profile (dashed line).

Figure 3-5-3 and Figure 3-5-4 summarizes the situation for the for all three beam configurations by displaying the mean of the horizontal profile at, respectively, position DkU and DkD as a function of the position of H1, the most critical optical device. It can be seen from these figures that, for example, for the PH2me-beam, the "2% criteria" requirement of a maximum 0.75 mm displacement of H1 implies that we must be able to detect a change in the mean of the x profile at DkU of 3.5 mm. At the downstream position DkD, the movement of the mean of the x-profile is less sensitive resulting in a 1.5 mm shift for a 0.75 mm movement of H1.

The PH2me-beam configuration at DkU is the most responsive to movements of Horn 1. The shift of the profiles of the higher energy secondaries of the PH2he-beam follow the behavior of the PH2me-beam profiles but with a slightly reduced scale. The behavior of the PH2le-beam in this study mirrors other characteristics of the PH2le-beam. The profile of the PH2le-beam hadrons is dominated by a core of high energy hadrons, which pass essentially untouched by the PH2le-beam

horn configuration. This leads to a long high-energy tail in the neutrino event distribution and to an insensitivity of the PH2le-beam profiles to movements of horn 1.

Movement of H2 in the PH2me-beam, as seen in the downstream hadron detector at DkD, is summarized in Figure 3-5-5, **which** displays the mean of the horizontal profile at position DkD as a function of the position of H2. For a 4.25 mm displacement of H2 the mean of the profile at DkD changes by over 12 mm.

Turning now to the monitoring of the horn current, the change in intensity caused by a change in the current of the horns in the PH2me-beam is shown in Figure 3-5-6. The shape of the curves can be understood from the fact that as the horn current increases, the momentum selected also increases. Thus the number of particles exiting the train (Position DkU) decreases but the fraction that survive (do not decay or hit the walls) to the hadron absorber (Position DkU) increases. As can be seen from the figure, a change in horn current of 1.3 % (the 2%-criteria maximum allowed change) translates into a change in intensity of order 0.1% both at position DkU and DkD. Similar procedures were carried out for the other two alternative beam configurations; PH2le-beam and PH2he-beam. The corresponding 2% criteria for these two beam configurations are not yet available, but Figure 3-5-7 shows the dependence of the measured intensity on the current delivered to the horns. As with the mean of the secondary profiles, the PH2le-beam being dominated by high-momentum hadrons makes it less responsive to changes in horn current.

As is obvious from Figure 3-5-8, a more sensitive measure of the current is to take the ratio of intensities at the upstream and downstream ends of the decay pipe. However, even this procedure only roughly doubles the magnitude of change in intensity reflected by a 1.3% change in current for the PH2me-beam from $\approx 0.1\%$ to $\approx 0.3\%$.

In summary, to maintain the position and current of H1 and H2 to meet the "2% criteria" for the PH2me-beam, the profile monitor at DkU should be able to detect a change in a mean profile of 3.0 mm while the device at DkD should be able to detect a change in a profile of 10 mm. The stability of the devices needed to monitor the horn current has to be better than 0.3 %.

3.5.3.3 Muon Monitors: Overall Intensity Range

To understand how the muons traversing the muon shield downstream of the hadron absorber reflect non-nominal horn operating conditions, a study of the muon distributions at various locations within the dolomite muon shield has been performed (similar to that carried out for the previous

H66 3-horn beam [2]). In this study, muons were followed through the hadron absorber and the subsequent dolomite muon shield with all forms of energy loss included. At five locations along the path of the muons the intensity and spatial distribution of the muons were recorded. The five locations were chosen to reflect the energy spread of muons from all three beam configurations and were located after 0, 9, 23, 37 and 81 meters of dolomite. Since these locations follow 5 m of steel absorber, the average muon momentum required to reach the five locations is 8, 13, 18, 25 and 45 GeV respectively.

The muon profiles and intensities were determined for the nominal beam set-up and for perturbed situations, H1 and H2 displaced and non-nominal horn current, as in the above outlined hadron monitoring studies. The resulting profiles were binned in a manner consistent with the devices now under consideration (96-channel readout for each profile). As an example, Figure 3-5-9 shows the horizontal profile of muons in locations 1-3 with the nominal PH2me-beam configuration. Note that the error bars on the points as well as the errors on the mean reflect the Monte Carlo statistics corresponding to **2** x 10^6 protons or number of muons ranging from 130,000 to 7,000 in the slot locations. The predicted overall muon intensities at each slot for the standard 4 x 10^{13} pot, as well as the muon densities within a 1 sigma radius of the mean of the distribution are shown in Table 3-5-2. As can be seen, the error bars will be dominated by detector characteristics, not statistics.

Note that there is a halo of low energy electromagnetic particles surrounding the muons, which exit the absorbing material into the muon slots. This halo has not yet been included in this procedure. A study of the best way to eliminate these particles has just begun. This problem has been faced many times and, for example, was solved in the Fermilab E665 (Tevatron Muon) experiment by placing a material such as "wood" at the interface of the absorber. Space for this electromagnetic halo absorber must be included in designing the muon slots.

3.5.3.4 Muon Monitors: Precision Requirements

The procedure followed here is identical to that which was executed for the secondary monitoring system described above. Horn 1 and horn 2 were shifted and the current supplied to the horns was varied to determine the effect on the profiles and intensities at each of the five locations. Table 3-5-3 summarizes the mean and sigma at the 5 muon slot locations for the nominal positioning of the horns and for Horn 1 shifted by 4 mm in the PH2me-beam configuration. Note that again, the

---

[2] Wehmann, A. NuMI-B-369, 15 April 1998

errors quoted reflect the Monte Carlo sample corresponding to 2.2 x 10^6 protons. Scaling the errors to a standard spill reduces the statistical error on the mean by over 3 orders of magnitude so the statistical error on the mean from one spill's worth of muons is negligible and the limiting error in the comparison will be the resolution of the chosen detector.

Figure 3-5-10 is a graphical display of Table 3-5-3 with the addition of data from shifting horn 1 a full cm off axis, As can be seen, the profiles at slot locations 1 and 2 behave as expected with the magnitude of the shift in <x> of the profile for a given shift in horn 1 increasing as the lever-arm increases. This pattern is broken with the profiles at slot locations 3 - 5. This can be interpreted by noting that the average neutrino energy of the PH2me-beam is around 8 GeV, and the muons associated to these neutrinos have an average energy of just over 12 GeV. By the third slot (<P_loss> = 18 GeV) most of the muons associated with the PH2me-beam neutrinos have stopped and only the high energy core muons are left. Using the behavior of the <x> as a function of the shift in horn 1 demonstrated in slot locations 1 and 2, it can be seen that a 0.75 mm shift of horn 1 will manifest itself as a shift in the <x> of .98 cm and 1.35 cm respectively

Figure 3-5-11 and Figure 3-5-12 are similar displays of the <x> profile as a function of horn 1 offset for the PH2he-beam and PH2le-beam respectively. The PH2he-beam study yields consistent information through slot 4 while the PH2le-beam shows that even the profile of muons just after the absorber (slot location 1) is dominated by the high-energy core muons. Note that even the muons from the PH2he-beam have been mostly absorbed before slot 5. Once the 2%-criteria numbers for the PH2he-beam and PH2le-beam are available the required precision of the monitors can be determined from these two figures.

3.5.3.5 Muon Monitors: Stability Requirements

As in the secondary study the requirements for stability of the intensity measurements was determined by varying the horn current and determining the resultant change in intensity at each muon slot. Figure 3-5-13 shows the relative intensity at the five slot locations as a function of the relative current applied to the horns for the PH2me-beam. Using the results for slot location 2, a 1.3% drop in the current applied to the horns results in a 3.5% drop in the intensity of muons in slot location 2

This method of monitoring the horn current is, obviously, in addition to simple direct readings of the current being applied and will be primarily used as a control that the magnetic field of the horns is consistent with the current being supplied to them. In addition, once the neutrino event energy

spectra and intensity become available from the MINOS near detector these quantities will be the most sensitive control of actual horn magnetic fields. On a much longer time scale than the spill-to-spill measurements described here.

3.5.3.6 Determination of the Physical Position of the Muon Slots

The results of sections 3.5.2.3 through 3.5.2.5 can be used to determine the physical positions of the muon slots within the dolomite muon shield.

.

Specifically:

Using the muons to monitor the PH2le-beam can only be done with a detector directly following the hadron absorber. This requires providing sufficient room between the absorber and the start of the dolomite to place a 3m by 3m by 0.5 m detector. No separate "muon-slot" is required.

Muon monitoring of the PH2me-beam would be optimized by using the information of the detector just after the absorber and a detector placed around the 12 m of dolomite location. This location should improve sensitivity to horn current changes without the loss of sensitivity currently observed at the 23 m position.

Monitoring of the PH2he-beam only becomes reasonable at the 23 m and 37 m positions for horn 1 (with no information coming from the 81 m position) position and somewhere between the 37m and 81 m position for the variation in horn current. Muon slots at the 30m and 60m positions should allow monitoring of both horn 1 position and current fluctuations of the PH2he-beam.

In summary, a detector directly following the hadron absorber and detectors in three muon slots at 12m, 30m and 60m within the dolomite muon shield should permit sufficient monitoring of the horn position and horn current of all three beam configurations with the exception of the horn position in the PH2le-beam.

3.5.4 System Description

The above sections summarized the precision and stability required by the monitoring devices for the PH2me-beam. Although we must wait until the 2%-criteria numbers are available for the he-and-PH2le-beams to apply the requirements for all three beams, in this section we will describe relatively simple and straightforward detectors that meet the requirements of the PH2me-beam. For both "hadron" and muon locations, detectors have been chosen (and consequent costs determined) which were either used in the last fixed target run (1996-1997) or have been thoroughly researched by the CMS collaboration.

3.5.4.1 Segmented Wire Ionization Chambers (SWIC[3])

These ionization chambers are based on the standard Fermilab SWIC long used in both primary and secondary beamlines. To capture the extended size of the secondary beam in the NuMI beamline, these SWICs will contain a 90 cm x 90 cm active area (this active area will depend on the ultimately chosen geometry of the target/horn channel) and will be similar to the "Yard (37" x 37" active area) - SWIC" developed by the NuTeV experiment[4] and successfully used in the 1996/7 Fixed Target run. These large SWICs (designated SS90) measure horizontal and vertical profiles of the secondaries as well as the integrated intensity of the secondaries.

The large NuTeV SWIC was constructed using Al base plates with a large 3 ft. (NuTeV has always used English units) hole covered by a bonded Al + mylar window to form the gas box. The detector ran in the ionization mode, making it less sensitive to climatic fluctuations, with a gas mixture of 98% He / 2% H. The stability of the detector was tracked by measuring the recorded intensity of pions with respect to the incoming protons on target. This quantity was recorded with a variation in response of less than 3.0 % over the seven month run with no attempt made to minimize this variation. According to the authors of reference 4, most of this variation was probably due to the stability of the outdated electronics used for DAQ. The resolution of the chamber was measured both with the normal secondary spectrum during the run and with a special proton alignment beam at start-up. The result using the normal secondary spectrum was 0.7 mm while the special proton run yielded 1.0 mm. Both results safely meet the requirements specified above.

Although this large SWIC was operated at 300V across a 0.5 cm gap, it was found to be 98% efficient at 50 V during bench tests. At 300V it was able to record intensities of 5×10^{11} charged particles distributed over a spot size twice the width of the expected NuMI spot size over a spill (ping) of 5 ms duration without saturation. Direct scaling arguments can be used to relate the Yard-SWIC operating conditions and NuTeV beam characteristics to the expected NuMI beam conditions. The ratio R of space-charge field to the field of applied high voltage (a measure of saturation) is:

directly proportional to the intensity of the beam,
inversely proportional to the duration of spill,

---

[3] Tassotto, G., "Beam Profile Monitors Used in the Fermilab Fixed Target Beamlines", Fermilab-TM-1853, September 1993.

[4] Drucker, B. et al., FNAL - TM 2025

inversely proportional to square of the width,
inversely proportional to the square of the applied voltage.

To get a scaling factor for NuMI based on NuTeV, we apply appropriate scaling factors for intensity, spill, width and voltage, respectively:

$$R(NuMI)/\ R(NuTeV)=(200/1)\times(5/1)\times(4/1)\times(2500/\ V(NuMI)^2)$$

and indicates that the identical chamber operating at just over 3000 V would record the expected NuMI hadron intensities with 98% efficiency and without saturation. If, in addition, the gap is decreased to 3.5 mm on the NuMI SS90 we should be able to lower the voltage to around 1000 V. During bench tests this chamber ran at 2000 V without problems.

Smaller SWICs, based on the same technology, have withstood integrated intensities[5] of up to 5 x 10^{20} protons over an area of order 1 cm^2 without damage at CERN and at Fermilab. Studies done by various authors[6] have shown that the chamber being considered operating in the ionization mode using (primarily) He gas will safely withstand the flux of hadrons expected at the considered positions in the NuMI beamline.

A single SS90 will be located in the easily accessible position between the target/horn channel and the start of the decay pipe designated DkU in the above sections.

A larger ionization chamber (SS200) will be needed at the DkD position at the end of the 2m diameter decay pipe. This could be simply the SS90 design scaled up to the required 2m x 2m active area. However, extrapolating the structural requirements of mechanical stability for the wire tensions we are considering (500g for 5 mil wires) is subject to error. A chamber of the required size (2m x 2m active area) and with the required total wire tension (less tension/wire but many more wires) has been constructed and run as part of the KTeV TRD[7]. This chamber is actually somewhat over-designed for the application we are considering but for reliability and initial costing purposes it is certainly adequate. A distance between the SS200 and the hadron absorber of 2 m is necessary to

---

[5] G. Tassotto, Fermilab, private communication

[6] Sauli, F. CERN Yellow Report 77-09, 1977

[7] Hsiung, Y.B. et al., KTeV TRD Design Report, KTeV Internal Note 185, Feb. 1994 and Graham, G.E. et al., NIM A367, 224, (1995).

reduce backscatter and minimize the effects of the high radiation environment associated with the Hadron Absorber.

3.5.4.2 Segmented Strip Ionization Chambers (SSIC)

These devices (SS250) operate on the same principle as the SWIC mentioned above and yield a horizontal and vertical profile as well as an integrated intensity. However, since these devices will be quite large (250 cm x 250 cm) and they will be located in the muon slots within the dolomite muon shield where the amount of material placed in the beam is unimportant, the device will be constructed with copper strips of varying sizes instead of individual wires. These devices will be a significantly improved version of the muon monitoring device[8] which was installed in the Fermilab neutrino beam in 1983 and was still operating and used by the E-815 experiment in the last fixed target run. In that run the muon monitor, operating in the ionization mode with Ar/CO_2 gas and 2500 V across a 10 cm gap, yielded a 1 ma signal while successfully giving the profiles for total muon intensities of 1×10^9 per 5 ms ping. Extrapolating from NuTeV conditions to those expected for NuMI in Muon Slot 5, there should be no problem accumulating sufficient charge to measure the $O(1 \times 10^{10})$ muons expected in the last muon slot (60m of dolomite) over the 1 ms NuMI spill.

We quite recently became aware of the R&D program being carried out by a CMS group on Cathode Strip Chambers for the Endcap muon detectors. This group has chosen[9] a copper clad FR4 (fire-resistant fiberglass epoxy) attached to either side of a polycarbonate honeycomb filler. The FR4 skins are 1.6 mm thick with 34 μm copper and the overall density is 80 kg/m^3. This construction has tremendous structural strength and can be etched into any geometry (strips or pads of any desired shape) required by the situation. The pattern of choice and connector artwork are milled directly on the panels by computer controlled machines available at Fermilab. Either a 2-D plotter fitted with a milling head, the Gerber, or a 3-D router , the Axxiom machine can be used to process the planes. A significant advancement in this technique was developed by CMS when they discovered that a specially developed cutter tilted at a 45° to the panel plane makes a smooth groove free of the burrs which would otherwise cause electrical discharges. The cost of these FR4 planes is competitive with hand placed strips and has the added advantage of easy replacement, strong mechanical strength permitting less massive frames and a complete, well developed and documented

---

[8] Auchincloss, P. et al., FERMILAB-FN-0382, Mar 1983

[9] CMS Collaboration, The Muon Project Technical Design Report, CERN/LHCC 97-32, CMS TDR 3, Pg. 141-247, 15 December 1997,

R&D program These CMS strip planes are currently the technology of choice for the muon SS250 planes and have been used in the costing of these devices.

If radiation damage tests of these planes, currently underway at CERN by a CMS collaboration sub-group, shows that the structures can withstand the expected intensities, an SS250 will be located between the end of the decay pipe and the hadron absorber to monitor the hadrons replacing the SS200 wire chamber described above.

Four SS250, one directly following the absorber and one in each of three muon slots, will be used to monitor the muons. In these positions, the intensity of muons varies from 2.0×10^{12} just after the hadron absorber to 1.0×10^{10} in muon-slot 3 with densities varying from 2.0×10^{8} to 1.0×10^{6} over the 1 ms spill. As shown above, these instantaneous intensities are sufficient to operate in the ionization mode with possibly the same He/H mixture and certainly with a non-explosive gas such as Ar/CO2. A test of a reduced size prototype SS250 to study the response and stability of these large chambers (i.e. to various gas mixtures) will be carried out as described in section 3-5-9.

3.5.4.3 Calibration of the Monitors

The question of whether a separate calibration system is required for the system of muon monitors is still under study, but has been included in the scope of the NuMI project. The argument for no calibration system being needed is that all four detectors will be operating with the same gas system, all will be experiencing the same temperature and pressure differentials (a separate climatized enclosure will be required for all four positions to reduce the ambient humidity to reasonable operating limits) and there will be a negligible number of hadrons (from muon and neutrino interactions within the dolomite) interacting with the chambers.

If further study of this question results in the need for a separate calibration method due to the high degree of stability required by the system, a relatively simple calibration device employing silicon has been considered and costed. A chamber construction using the double sided CMS polycarbonate planes will serve as an example of how this Si-based calibration system would work. The chamber would contain two polycarbonate planes with four sides of copper all sharing the same gas environment. The first two copper planes would be etched to yield x and y profiles. The third plane would be the total intensity plane. The fourth plane would be the calibration plane and would have several etched pads each equal in area to a Si diode which would be placed on the outside of the gas box. The etched pads/Si-diodes would be placed at positions where the integrated muon intensity would not necessitate changing the Si more than once a year. These calibration points

would act as reference for all planes within the common gas box. A movable calibration box containing a Si diode would be manually moved from slot to slot to cross calibrate the detectors. This is a very simple adaptation of the intricate CERN system.

3.4.4.4 Gas System

The gas supply system for all monitoring devices will be the basic gas supply system developed for the E-815 Yard SWIC and based on the standard Fermilab SWIC gas system. The SS90 and SS200 upstream of the hadron absorber will each have their own gas supply (98% He/2% H_2). The four-muon SS250 monitors will have a common gas supply system (most likely the same He/H_2 gas) to insure minimal differences in the gas mixture to each of them. The distances involved - order 100 meters - are considerably smaller than the SWIC gas systems used in the Fixed Target areas. The system is comparatively simple and will be recycled from currently existing gas systems. It will consist of a large reservoir located centrally for the four monitors to be fed by pre-mixed gas located at the surface. The temperature and pressure will be monitored at each location and recorded as part of the DAQ system. Television cameras will provide visual monitoring of the reservoir area as well as each monitoring device.

3.5.5 Design Validation

The design of the monitoring system is being primarily validated through the use of the GNuMI Beam Monte Carlo. This Monte Carlo will become an even more accurate representation of reality as refined input becomes available. Currently it is thought that the hadron production model (FLUKA 92) overestimates integrated pion production by about 15%. Without having access to FLUKA 97.5, which includes data from the CERN SPY experiment to correct hadron production, a rough correction was made to the low-momentum spectra to see if such an increase might change any of the conclusions made in this report. It was noted that the changes are minimal and tend to change the scale but not the point-to-point behavior of the response to perturbations of the nominal beamline.

A prototype of the SS250 will be studied in the next Fixed Target run to examine the response to varying muon intensities and confirm that these devices can be used in the ionization mode in the muon pits.

3.5.6 Construction Plan

The SS90, SS200 (if needed) and SS250 will be constructed at the Fermilab Lab 6 Wire Chamber Construction Facility where the E-815 "Yard-SWIC" and the KTeV TRD chambers were constructed. The complexity and size of the monitors described here are not exceptional and similar devices have been successfully manufactured for several earlier experiments.

If the decision is taken to use the CMS double sided copper planes then negotiations with CMS will be necessary to obtain the necessary machine time on the Gerber milling machine to process the planes.

3.5.7 Installation Plan and Issues

The SS90 located just upstream of the decay pipe entrance should not be installed before the target hall shielding is completed and the decay pipe has been commissioned. To be part of the modular structure now being considered for the target/horn channel (similar to AP-0), a special element to include the SS90 has to be designed and fabricated. The SS200 between the decay pipe and the hadron absorber should be installed only when the neighboring massive devices have been installed and commissioned. The SS250 used in the three muon slots have no special installation requirements. As mentioned above, provisions for local humidity control need to be included in the facility plans.

3.5.8 Commissioning Plan

The commissioning of the beam monitoring system will be closely linked with the commissioning of the neutrino beam elements - target plus horns. After each of the monitoring elements has been declared operational, sufficient time must be allotted, during low intensity running, to simulate various non- nominal running scenarios such as target misalignment, horns at the wrong current, horn 1 misalignment or a failed horn. Noting what each of the monitoring devices reads during these scenarios will prove most helpful in quickly determining the source of a problem when one arises.

3.5.9 Monitoring the Monitors

The performance of the system will be monitored by checking the SS90, hadron SS250 and the muon monitoring system against each other with all devices normalized to the incoming proton intensity and to each other.

3.5.10 Prototype Testing

3.5.10.1 Segmented Strip Ionization Chamber (SS250)

The four large Segmented Strip Ionization Chambers with 250 cm x 250 cm active area, although similar to the detector now in place in the NuTeV beam line, need to be studied for response, stability and saturation effects.

The upcoming 800 GeV Fixed Target Experiment run is scheduled to start sometime in 1999 and run for six months or so. Although there may be other sources of intense muon beams that we are not yet aware of, one source of muons to study these large chambers will be available in PWest which will be running foe the E-872 experiment. In this experiment, downstream of the muon identification components, there is a very intense muon beam and space available to mount an SS250. Plans are currently being made to test a reduced size SS250 with representatives of the BD Instrumentation Department and those familiar with the CMS strip chambers.

Beam	Position	Charged Particles / spill	Peak density (FWHM) / spill
PH2he	DkU	1.2×10^{14}	4.8×10^{11} / cm^2
	DkD	5.0×10^{13}	1.3×10^{10} / cm^2
PH2me	DkU	1.3×10^{14}	1.7×10^{11} / cm^2
	DkD	4.3×10^{13}	9.1×10^{9} / cm^2
PH2le	DkU	1.7×10^{14}	1.8×10^{12} / cm^2
	DkD	4.3×10^{13}	1.7×10^{10} / cm^2

Table 3-5-1 The integrated charged particle intensity (within a radius of 50 cm at DkU and a radius of 100 cm at DkD) and charged particle density within a diameter corresponding to the FWHM for nominal beam settings of all three beam configurations and the standard 1 ms spill of 4 x 10^{13} pot.

Meters of Dolomite	Beam	Mean (cm)	RMS (cm)	Sum Muons (r = 150 cm)	Peak density / cm^2
0.0	PH2he	.05	50.6	2.0×10^{12}	1.7×10^{8}
	Ph2me	0.1	52.2	2.5×10^{12}	2.0×10^{8}
	PH2le	.43	53.3	2.4×10^{11}	1.9×10^{7}
9.0	PH2he	.007	55.2	1.7×10^{12}	1.2×10^{8}
	Ph2me	-0.19	55.4	1.1×10^{12}	7.8×10^{7}
	PH2le	.7	54.9	1.2×10^{11}	8.3×10^{6}
23.0	PH2he	.12	54.6	7.6×10^{11}	5.5×10^{7}
	Ph2me	0.22	58.2	1.2×10^{11}	7.4×10^{6}
	PH2le	.84	57.1	5.9×10^{10}	3.9×10^{6}
37.0	PH2he	-.012	57.3	2.8×10^{11}	1.8×10^{7}
	Ph2me	-0.44	59.2	3.6×10^{10}	2.2×10^{6}
	PH2le	-.12	58.9	3.2×10^{10}	2.0×10^{6}
81.0	PH2he	-.168	62.2	1.1×10^{10}	6.3×10^{5}
	Ph2me	-.54	62.1	3.6×10^{9}	2.0×10^{5}
	PH2le	-2.4	62.7	4.0×10^{9}	2.2×10^{5}

Table 3-5-2 The integrated muon intensity and peak muon densities within one RMS of the mean position at five muon slot positions for the three beam configurations running at nominal horn position and current for the standard 1 ms spill of 4×10^{13} pot.

Meters of Dolomite	Beam	Profile <x> H1x = 0	RMS / √n H1x = 0	Profile <x> H1x = .4 cm	RMS / √n H1x = .4 cm
0.0	he	.06	.11	5.68	.11
	me	.10	.15	5.32	.16
	le	.44	.20	.13	.20
9.0	he	.05	.13	7.28	.13
	me	-.19	.23	7.02	.24
	le	.70	.3	.03	.29
23.0	he	.12	.2	12.48	.21
	me	.23	.7	-3.6	.72
	le	.84	.43	1.1	.43
37.0	he	-.01	.33	12.16	.33
	me	-.44	1.29	-2.94	1.26
	le	-.12	.59	-.21	.59
81.0	he	-.17	1.7	-2.63	1.7
	me	-.53	3.95	-3.15	4.0
	le	-2.37	1.68	.31	1.67

Table 3-5-3 The mean of the muon x profile (cm) and the error on the mean for the statistics of the Monte Carlo for all three beam configurations at all five modeled muon-slot positions for horn 1 nominal and horn 1 offset by .4 cm

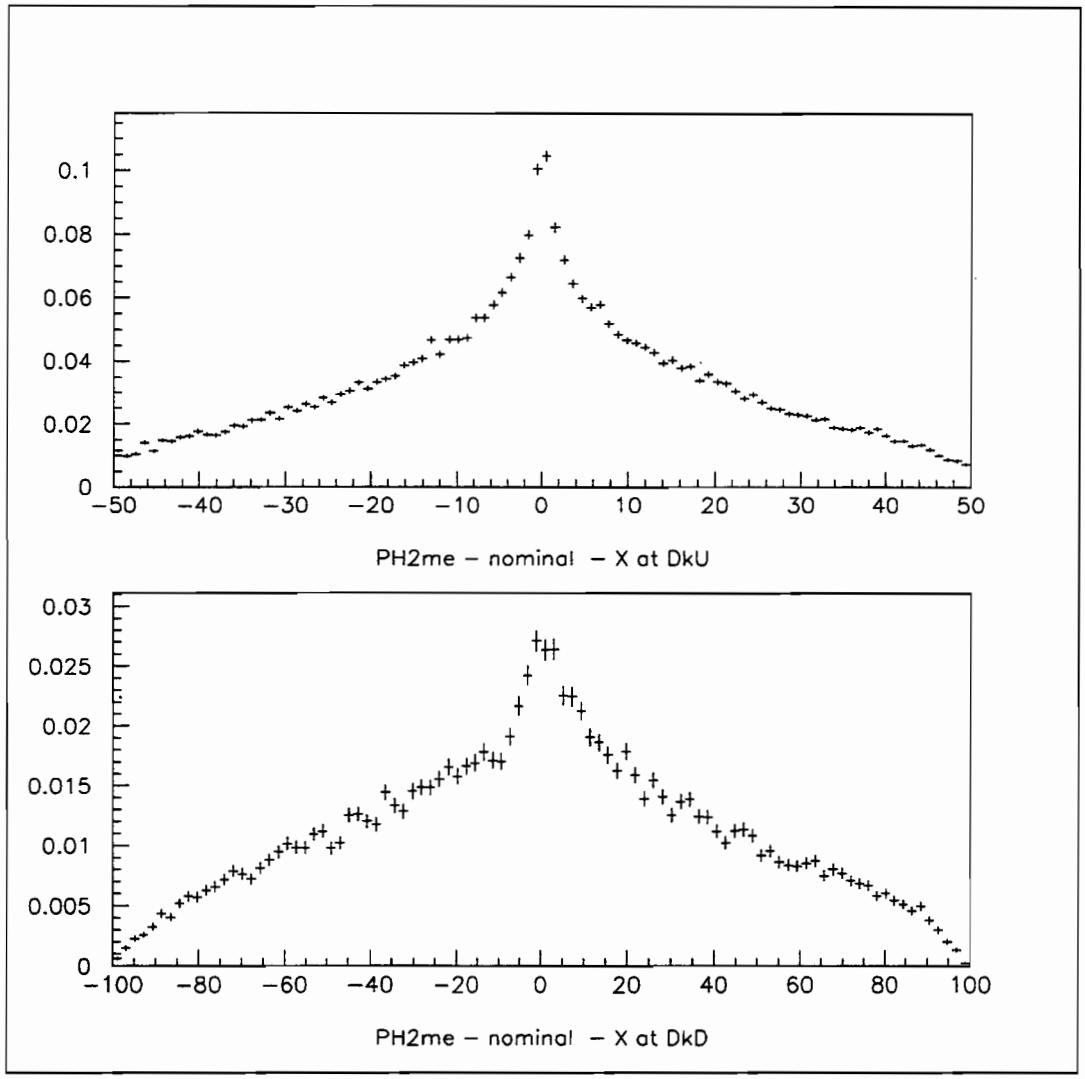

Figure 3-5-1 Assuming nominal beam conditions with the PH2me-beam configuration, the profiles of the charged particles at DkU and DkD. The abscissa is in cm, the ordinate in particles per incident proton.

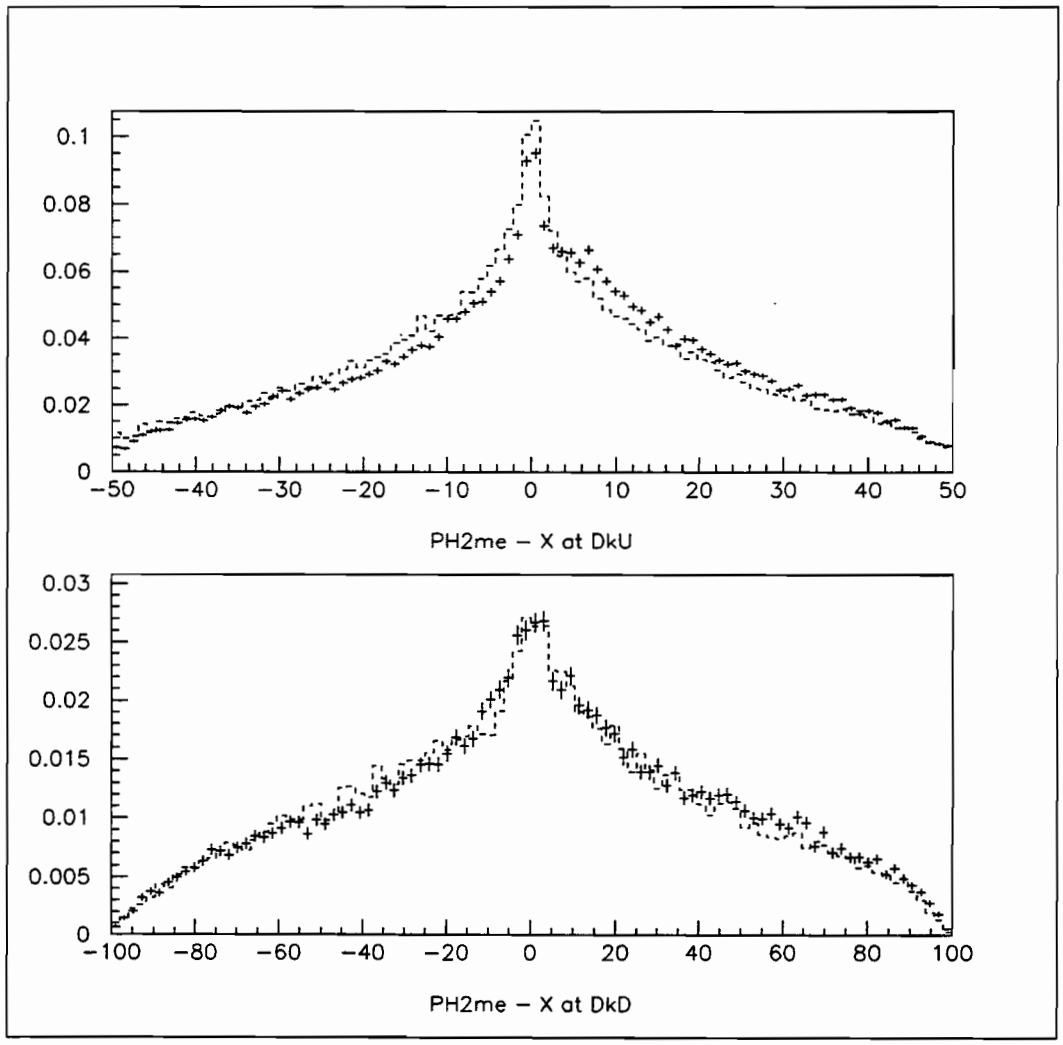

Figure 3-5-2 Profiles with Horn 1 offset by 4 mm (cross) overlaid on nominal profiles (dashed line) at position DkU (top) and DkD (bottom). The abscissa is in cm, the ordinate in particles per incident proton.

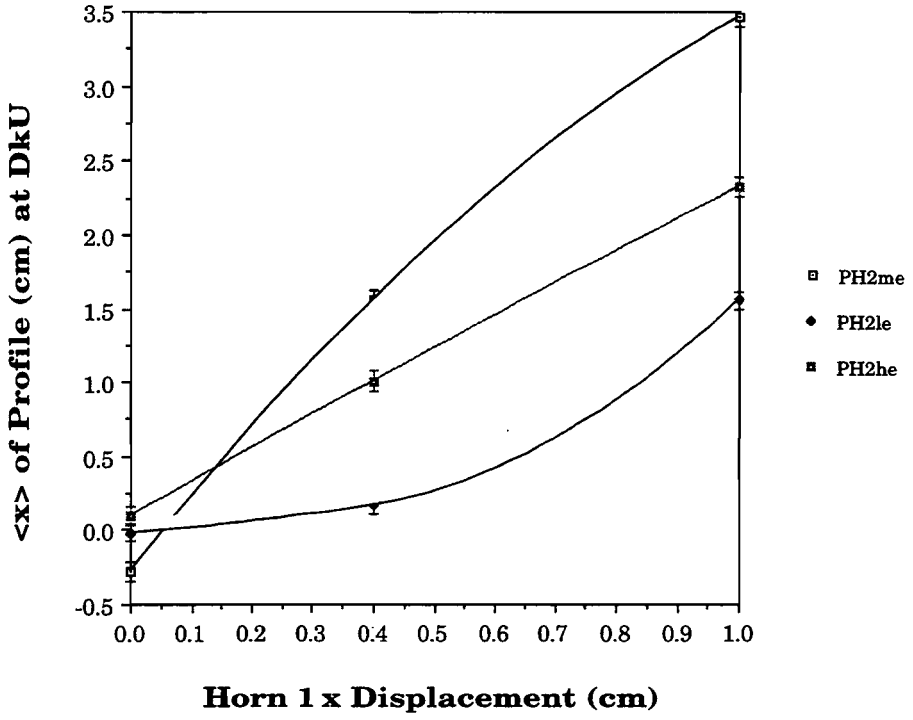

Figure 3-5-3 The mean of the horizontal profile for all three beam configurations at position DkU as a function of the position of H1.

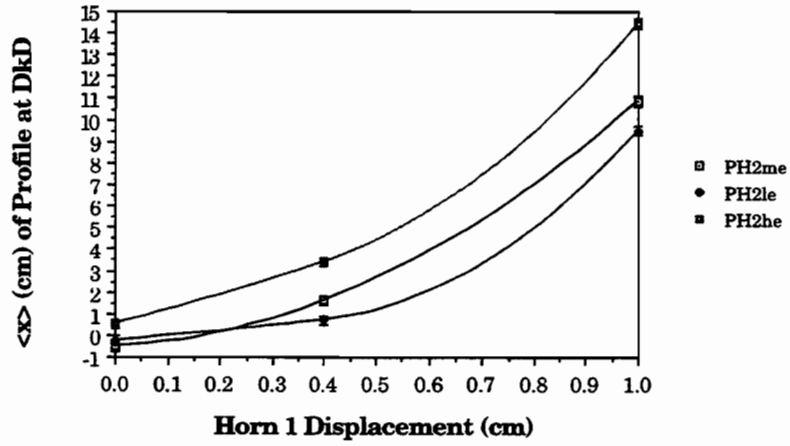

Figure 3-5-4 The mean of the horizontal profile for all three beam configurations at position DkD as a function of the position of H1.

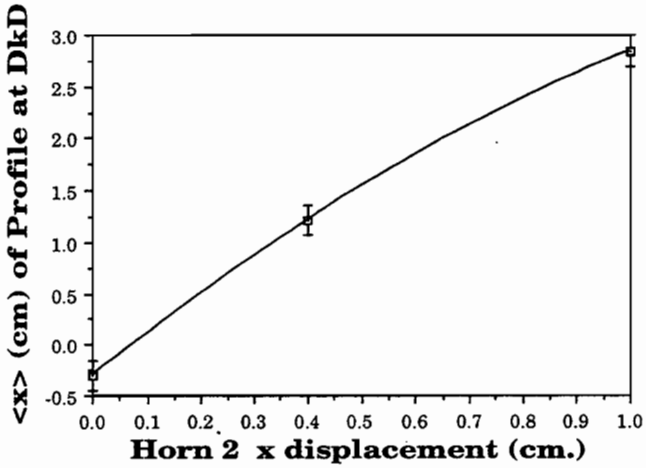

Figure 3-5-5 The change in the mean of the x-profile for a given change in the horn 2 x position for the PH2me-beam at DkD.

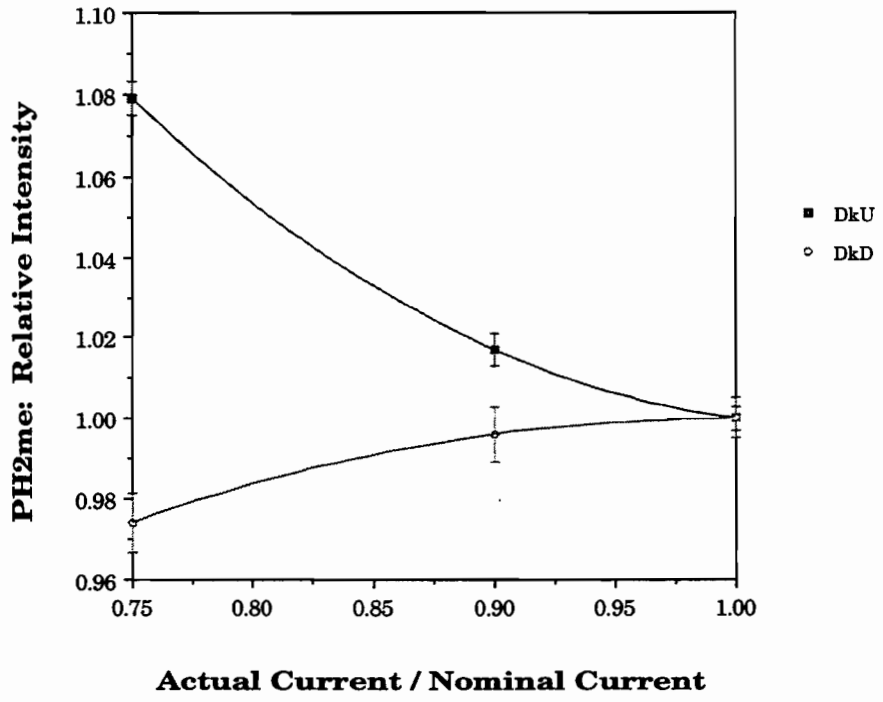

Figure 3-5-6 The change in relative intensity as a function of the relative change in horn current for the me beam at DkU and DkD positions.

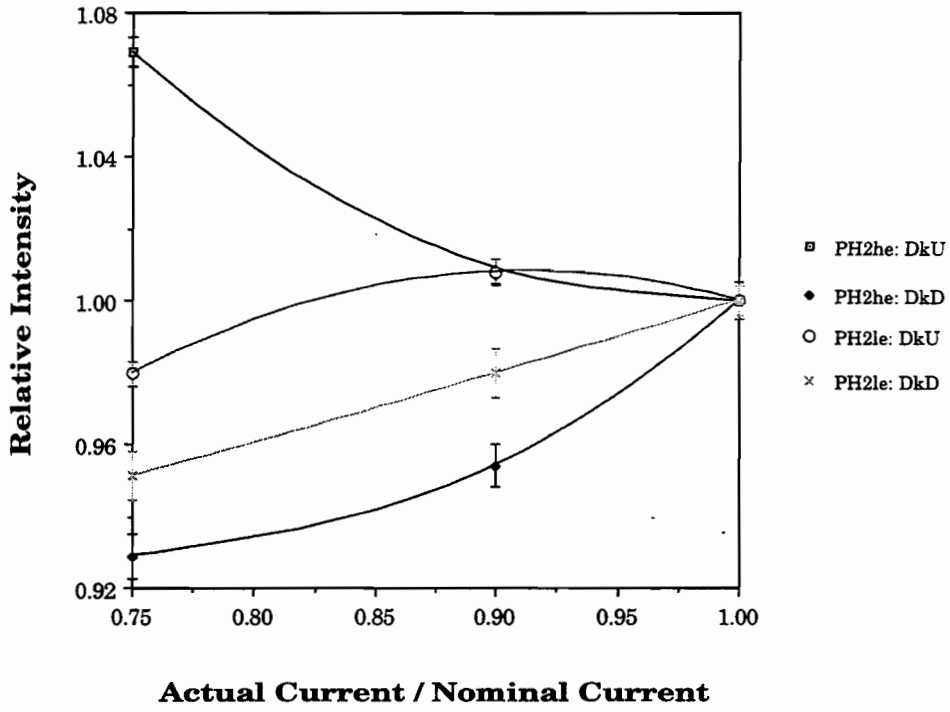

Figure 3-5-7 The dependence of the relative intensity on the relative current delivered to the horns for the le-and-PH2he-beam configurations.

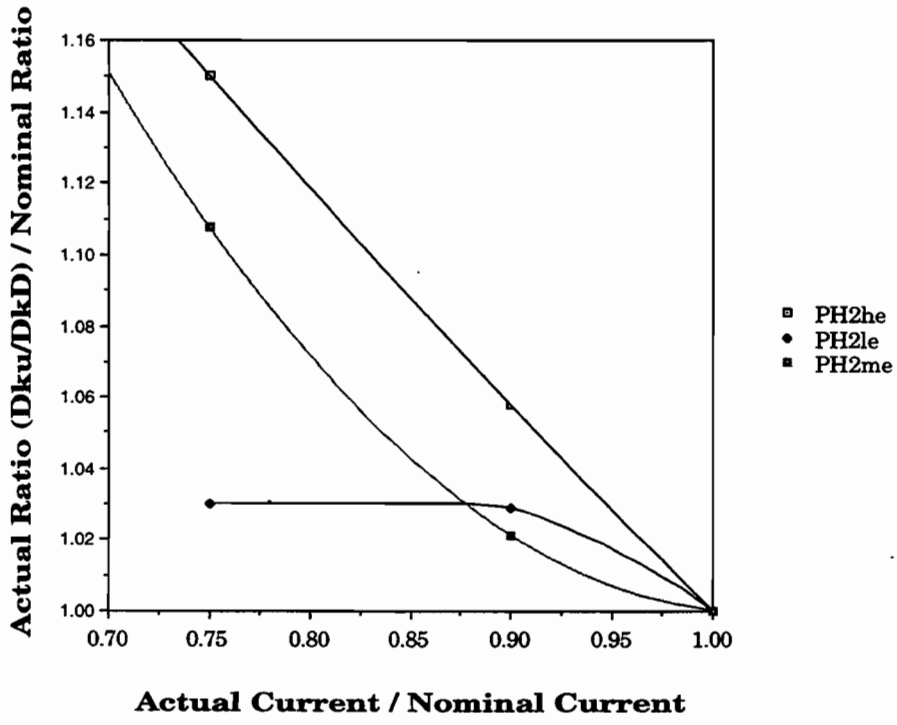

Figure 3-5-8 The change in the ratio of intensities at DkU and DkD as a function of the relative current for the PH2me-beam.

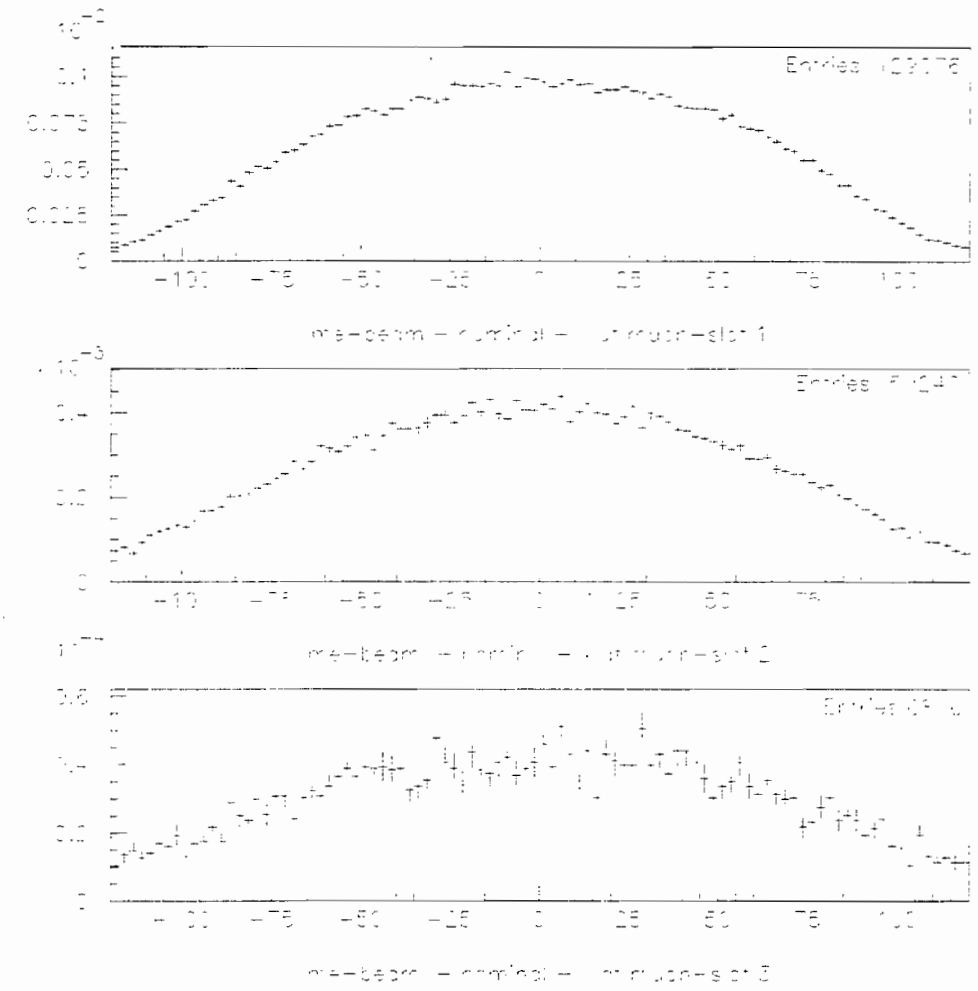

Figure 3-5-9 The profiles of muons reaching muon-slots 1-3 for the PH2me-beam. The abscissa is in cm, the ordinate in muons per incident proton.

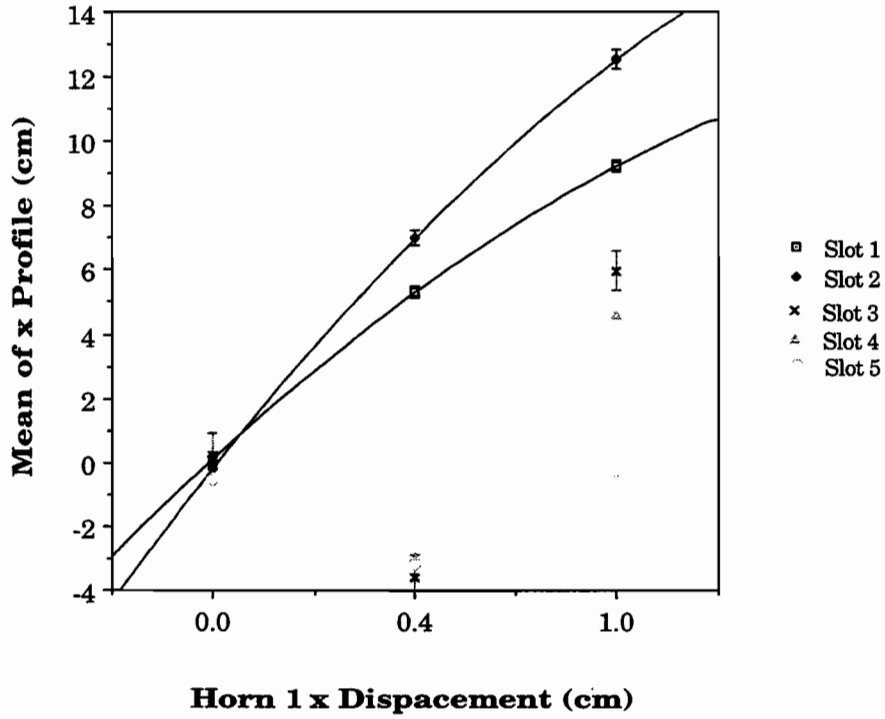

Figure 3-5-10 The change in the mean of the x-profile for a given change in the horn 1 x position for the PH2me-beam at all five modeled muon-slots.

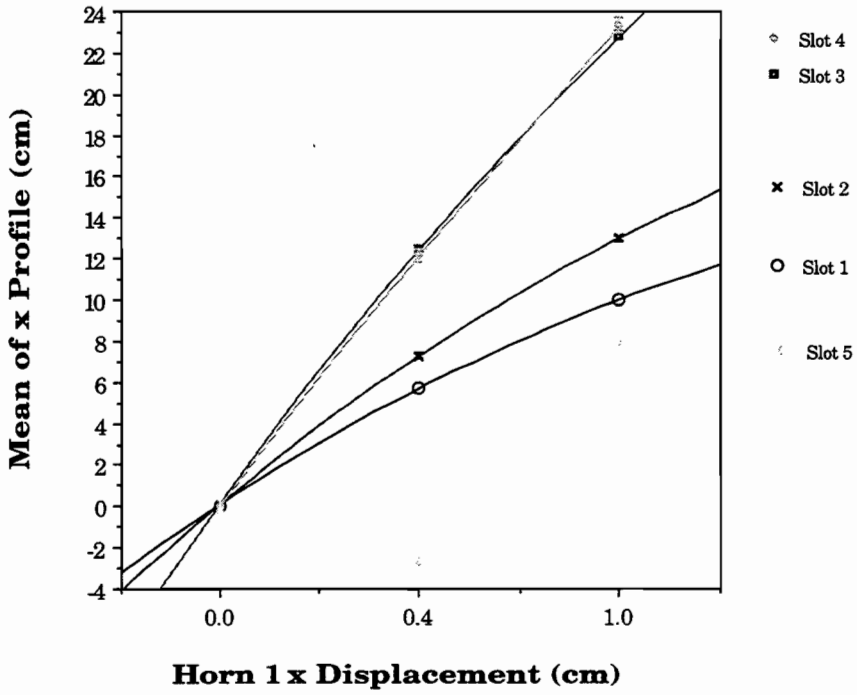

Figure 3-5-11 The change in the mean of the x-profile for a given change in the horn 1 x position for the PH2he-beam at all five modeled muon-slots.

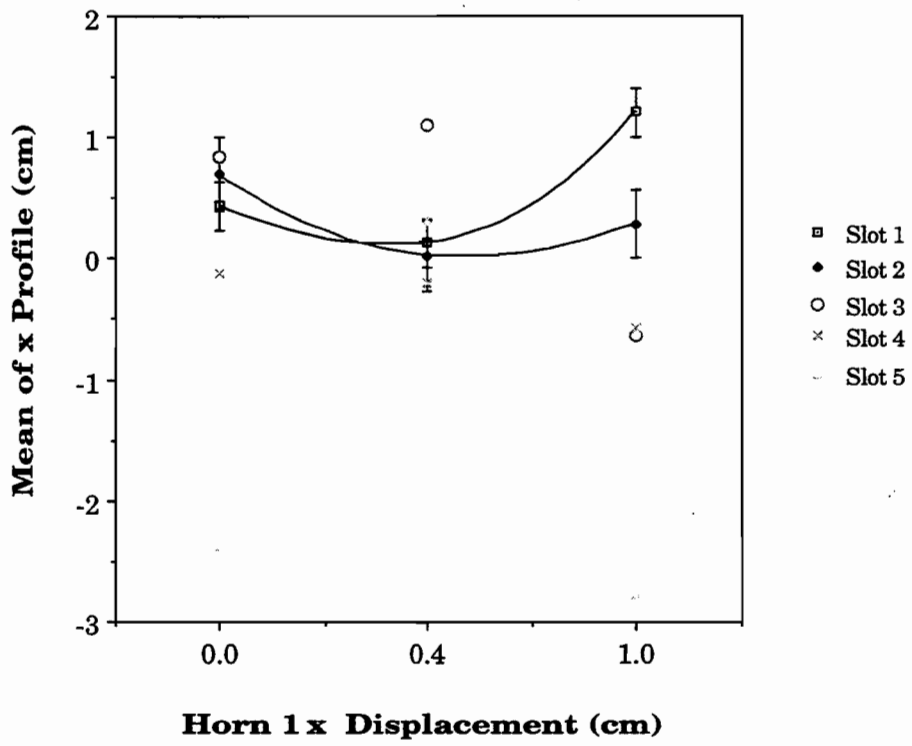

Figure 3-5-12 The change in the mean of the x-profile for a given change in the horn 1 x position for the PH2PH2le-beam at all five modeled muon-slots.

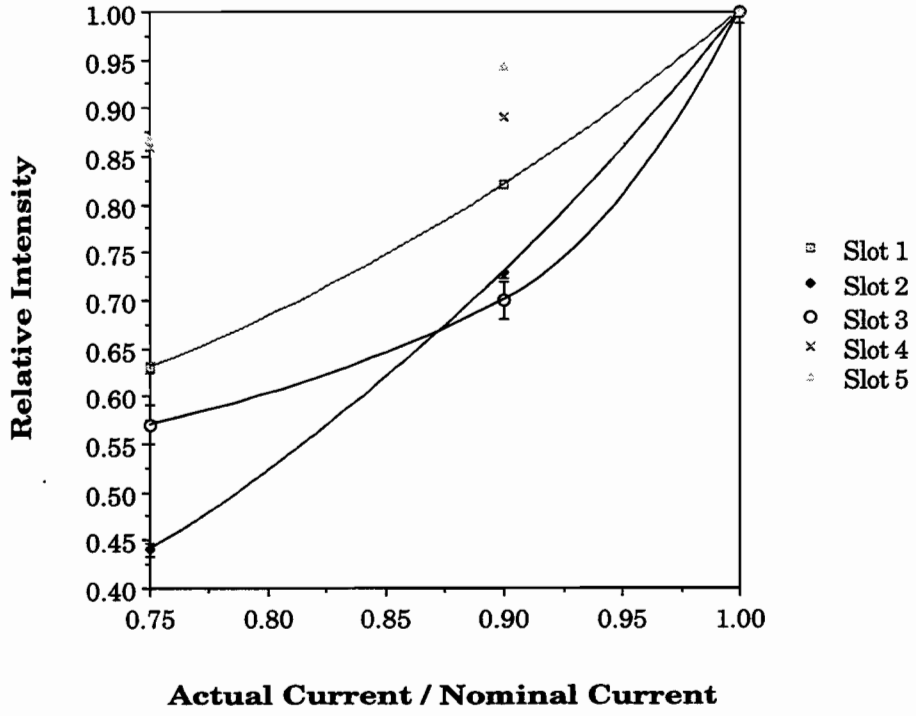

Figure 3-5-13 The relative intensity as a function of the relative current applied to the horns for the PH2PH2me-beam at the five muon-slots.

This Page Intentionally Left Blank

3.6 Survey, Alignment, and Geodesy (WBS 1.1.6)

TABLE OF CONTENTS

3.6 SURVEY, ALIGNMENT, AND GEODESY (WBS 1.1.6) 3.6-1

3.6.1 Introduction *3.6-3*

3.6.2 Primary Objectives *3.6-3*

3.6.3 Technical Requirements and Constraints *3.6-4*

3.6.3.1 Determining the Line from Fermilab to Soudan 3.6-4

3.6.3.2 Beam line element accuracy requirements 3.6-5

3.6.4 Design Assumptions *3.6-9*

3.6.5 System Design *3.6-9*

3.6.6 Design Validation *3.6-10*

3.6.7 Construction Plan *3.6-10*

3.6.8 Installation Plan and Issues *3.6-11*

3.6.9 Commissioning Plan *3.6-11*

3.6.10 Performance Monitoring Plan *3.6-11*

TABLE OF TABLES

Table 3-6-1 Alignment tolerance requirements for the two parabolic horn wide band neutrino beam in the medium energy configuration..... 3.6-12

TABLE OF FIGURES

Figure 3-6-1 Transverse distribution of the NuMI neutrino beam at the far detector as a function of energy. Note that the low energy neutrino beam is several kilometers wide..... 3.6-13

Figure 3-6-2 CORS (Continuously Observed Reference Station) network. GPS data are recorded for over 100 accurately known locations in the United States, including 4 in Wisconsin..... 3.6-14

Figure 3-6-3 Effect of a 4 mm offset of horn 1 on (top) the far detector flux, (middle) near detector at 300 m beyond the end of the decay pipe, (bottom) far over near ratio(RR)..... 3.6-15

Figure 3-6-4 Fits showing the peak at 12 GeV in RR for a horn 1 transverse shift (bottom section of Figure 3-6-3) requires terms up to shift to the fourth power..... 3.6-16

Figure 3-6-5 Effect of a 4 mm horn 1 transverse offset on the flux in the near detector as a function of neutrino energy..... 3.6-17

Figure 3-6-6 Largest contributions to errors in neutrino flux spectrum (see Table 3-6-1). Errors in the top two graphs have been multiplied by $\sqrt{2}$ to account for both horizontal and vertical misalignments... 3.6-18

3.6.1 Introduction

For a long-baseline neutrino experiment, properly aligning the two parabolic horn wide band neutrino beam, configured for medium energy, to hit the far detector 735 km away is clearly important. Actually the NuMI beam, for low neutrino energies, is several kilometers wide (see Figure 3-6-1) and modern geodetic survey techniques, especially the Global Positioning System (GPS) satellites, make hitting the far detector, at least with some neutrinos, relatively straightforward.

The neutrino energy spectrum physics test, which has the potential to measure oscillation parameters, is much more demanding, since it requires predicting far detector energy spectrum from measurements in the near detector to 2% or better in the worst 1 GeV energy interval. To help accomplish this, we plan to align the neutrino beam center to be within 100 meters of the far detector. This section spells out the alignment program designed to achieve this goal.

Internal alignment of the two detectors inside their caverns is not covered under WBS 1.1.6; it is included in the installation tasks of those detectors. The design phase part of the alignment program includes the survey tasks needed to specify the neutrino beam centerline at both Fermilab and Soudan before construction starts on the beam tunnel and far detector cavern.

3.6.2 Primary Objectives

One primary objective is to align the neutrino beam so the center passes within 100 meters of the far detector at the Soudan mine. We must accurately determine the line from Fermilab to Soudan and align the beam line elements to required accuracy (see Table 3-6-1), and also provide alignment monuments in both experimental caverns which are tied into the beam axis.

The second primary objective is, at the request of the Fermilab site construction coordinator, to check locations determined by the contractor during the construction phase of the NuMI facility at Fermilab. This practice leaves the responsibility for correctly locating the structures with the contractor, but Fermilab can closely monitor locations, and,

for example, warn the contractor to recheck the locations of his forms before the concrete is poured.

3.6.3 Technical Requirements and Constraints

3.6.3.1 Determining the Line from Fermilab to Soudan

The relative positions of Fermilab and Soudan on the surface will be determined by making simultaneous measurements using the Global Positioning System (GPS) satellites. These satellites, which contain extremely accurate atomic clocks, send out a time stamped radio signal that is detected by the GPS receiver at the point being measured. The receiver contains an accurate clock and records the arrival time of the signal; the time difference measures the distance to the satellite. The satellite signal also includes information specifying its position. The signals from four satellites must be received, one to determine the receiver clock offset, and three to measure the three spatial coordinates of the receiver position. If additional satellites are above the horizon, their signals provide redundancy and increase the accuracy of determining the unknowns in the fit. Errors in the satellite positions and clocks, and variations in the signal propagation speed through the atmosphere will degrade the accuracy of the measurement.

Prior to 1998, GPS measurements of Fermilab and Soudan were made at different times; these have a relative accuracy of 1 part in 10,000 (0.1 milliradian) or 75 meters in the horizontal transverse position. The study described in the next subsection shows that this error would use up much of our alignment tolerance budget. Making simultaneous GPS measurements at both Fermilab and Soudan will improve the relative accuracy both by reducing the effect of satellite position and clock errors (they will be the same position and have the same time, even if these are not exactly known, when the measurements are made) and because the atmospheric conditions are more likely to be similar. Taking GPS data continuously for an extended period provides information from a larger selection of satellites to help reduce these errors and provide redundancy. We plan to record simultaneous GPS data at both Fermilab and Soudan for two 24-hour periods.

The accuracy and reliability can be greatly improved by making use of the CORS (Continuously Observed Reference Station) network data, which records GPS data for over 100 accurately known locations in the United States, including 4 in Wisconsin (see

Figure 3-6-2). The data for the CORS network are processed and their positions fitted daily by NGS (National Geodetic Survey). Typically, horizontal positions of these points repeat to better than 1 cm over periods of several weeks. We are working on an agreement with NGS whereby we would make the GPS observations of Fermilab and Soudan according to their rules (use two separated GPS receivers at each site, record atmospheric conditions frequently) and provide them with our data and our analysis. The NGS would include our points in their global fits of the CORS points for the period of our observations and provide us with the results.

This plan provides many checks and improvements for this vital measurement. Several sources of GPS error are eliminated or reduced by simultaneous observations, and the CORS data confirm that GPS is functioning accurately and permit detailed corrections to the satellite positions, clocks, and atmospheric propagation. NGS, by including our data in the CORS fit, will provide the best possible external check of the geodetic calculations.

3.6.3.2 Beam line element accuracy requirements

The neutrino energy spectrum physics test, which has the potential to measure the coupling strength ($\sin^2 2\theta$) and mass difference (Δm^2) oscillation parameters, requires predicting far detector energy spectrum from measurements in the near detector to 2% or better in the worst 1 GeV energy interval. The neutrino flux energy spectra are different at the near and far detectors for two main reasons. First, the meson decays, which yield the neutrinos, are distributed along the length of the decay pipe. This is a line source for the near detector, but essentially a point source for the far detector. Secondly, for decays which occur at large radii in the decay pipe, the angle between the parent meson direction and the direction of a neutrino which will hit the near detector is much larger than the corresponding angle of a neutrino which will hit the far detector. Both the probability of such a decay occurring and the resulting neutrino energy are steeply falling functions of this angle. The difference between the far and near detector spectra increases as the near detector is moved closer to the end of the decay pipe.

The Monte Carlo program PBEAM_WMC (See NuMI Note L-221 for more details), was developed to calculate neutrino flux spectra in the far and near detectors. This program distributes primary beam protons in the production target and interacts them, to yield secondary π and K mesons distributed according to published experimental data. Each meson is stepped through the magnetic fields of the focussing horns and propagated

through drift spaces between the horns and through the decay pipe until it is lost in the walls of the target enclosure or decay pipe, reaches the dump and is lost, or decays. From the decay point, the probability the neutrino will go through the center of the detector and the corresponding neutrino energy are calculated. These are accumulated for a large number of mesons into a histogram to form the neutrino flux spectrum for that detector. Interactions of the parent meson in the production target and interactions and multiple scattering in the horns are included by weighting these probabilities. Neutrinos from muon decay or from scraping (any hadron interaction other than the primary beam proton in the target) are not included, but these have only a small effect on the muon neutrino spectrum above a few GeV. The program was designed to be fast, so the spectra can be calculated with good statistical accuracy in a reasonable amount of computer time.

With this weighting scheme, the neutrino flux is calculated at a point in the detector (in this study, at r = 0 in the near detector). This is good for the far detector and studying variations with distance from the beam axis in the near detector, but would require further calculation to find the average flux over a finite area in the near detector.

Using FAR and NEAR to represent the muon neutrino flux in those detectors we can predict the flux in the far detector (if there are no neutrino oscillations) by:

$$\text{FAR(predicted)} = \frac{\text{FAR(0)}}{\text{NEAR(0)}}\text{NEAR(measured)}$$

Where FAR(0) and NEAR(0) are the spectra calculated with PBEAM_WMC assuming that all the neutrino beam line elements are in their correct positions. If one element is displaced by X, the far detector spectrum calculated with the above equation will be in error, since the calculated ratio FAR(X)/NEAR(X) should have been used instead. The required correction factor is RR:

$$\text{RR} = \frac{\text{FAR(X)} / \text{NEAR(X)}}{\text{FAR(0)} / \text{NEAR(0)}} = \frac{\text{FAR(X)} / \text{FAR(0)}}{\text{NEAR(X)} / \text{NEAR(0)}}$$

The deviation of RR from 1.0 measures the error induced in FAR(predicted) by the displacement X of the beam line element.

Detailed design of NuMI wide band neutrino beam requires calculating the size of deviations of various beam element parameters (see Table 3-6-1) from nominal that can be

allowed without significantly affecting the result of the neutrino energy spectrum oscillation test. PBEAM_WMC is first run with all beam elements at their nominal values and positions ("on axis"). Next we select a parameter to investigate and vary it from its nominal value. For this example, we move both the upstream and downstream ends of the first focussing horn 4 mm in the same direction transverse to the beam axis ("Horn 1 X shift of 4 mm"), and calculate the resulting spectra at both detectors.

Since it is difficult to make quantitative assessments directly from flux plots, we divide the far detector flux (displaced) by the flux (on axis) for each one GeV neutrino energy interval and display the quotient in Figure 3-6-3a. A dashed line has been drawn for a flux ratio of 1.0, which would be the result if there were no change in the flux. It is now easy to pick out the largest fractional difference (in the interval 1 to 20 GeV), which occurs at about 19 GeV. Figure 3-6-3b is a similar graph for the center (i.e., at a radius of 0 in the transverse direction) of the near detector (300 m beyond the end of the decay pipe). The ratio of these ratios, RR, is shown in Figure 3-6-3c. The peaks at 19 GeV in the far and near detectors have cancelled in RR, leaving the peak at 12 GeV as the largest effect.

Since the deviations found for a 4 mm shift are all much larger than our desired limit of 2%, similar calculations were made for several horn 1 X shifts of and the resulting spectra analyzed as above. The value of RR in the peak at 12 GeV is shown in Figure 3-6-4 plotted against the horn 1 X shift in millimeters. The fits to these data show the RR deviation is more complicated than proportional to the square of the horn X shift; a term in shift to the fourth power is required. Odd power terms are required to be zero, since RR must be symmetrical about zero shift.

Beam element changes which break the azimuthal symmetry of the WBB, such as this horn 1 X shift, should be measurable in the near detector. The Lego plot in Figure 3-6-5 gives the ratio of flux with a horn 1 X shift of 4 mm to flux with horn 1 on axis for each of 21 bins along the x axis (i.e., transverse to the neutrino beam direction) of the detector. The effect at 12 GeV varies as you move across the detector along the direction of the horn shift. Such an azimuthal asymmetry should clearly identify a large misalignment of a beam line element.

Most beam element changes are proportional to their shift squared, without the fourth order term required for horn 1 X. However, the effective radius of the decay pipe, which is reduced from nominal radius by pipe being out of round and misalignment between pipe

sections, has a different dependence, since it is not required to be symmetrical about the nominal radius. In this case, the height of the peak in RR was found to be linear in the radius reduction.

Alignment tolerances must be allocated to the many beam line elements so they are both achievable for each element and their combined effect meets the goal. This NuMI alignment tolerance budget is given in Table 3-6-1. The estimated tolerance for the measurement of the parameter is given in the first column (A). The second column (B) contains the parameter deviation that will cause a 2% error in the worst 1 GeV neutrino energy bin of the predicted (without oscillations) far detector energy spectrum. This value was found by the procedure outlined in the example above.
The next column, $C = 2\% \times \left(\frac{A}{B}\right)^2$ (unless a different dependence is indicated by a footnote), is the percentage error in the worst 1 GeV bin in the predicted far detector energy spectrum caused by this estimated error in this parameter. The dependence was found in the study described above. Finally, $D = C^2$, the percentage error squared. In rows labeled Sum, the sum of the numbers above the line is entered in column D and the square root of this sum is entered in column C in italics. This column C entry is not the sum of the numbers above it in column C, but the sum of those numbers added in quadrature (i.e., the square root of the sum of the squares), which is the formula for adding independent errors.

In the table, angle parameters are expressed by a single linear distance; the downstream end of the device is displaced by this amount and the upstream end is displaced by an equal amount in the opposite direction. These two displacements are what is actually measured by the surveyors. The length of the device, in meters, is given in square brackets after the description.

The first four entries in the table concern the proton beam and the target. These are most critical in achieving the goal and special measures are used for three of them to augment the optical alignment. The beam on target X (transverse) shift tolerance comes from the displacement which would cause the neutrino and muon fluxes per incident proton to fall by 2%. It is assumed that this ratio will be monitored throughout the run, and a 2% drop quickly noticed, resulting in the proton beam being retuned to hit the target precisely. The angles of the proton beam are measured in two devices separated by an 18 meter long magnetic field free baseline, which greatly reduces the effect of transverse position errors in

aligning these devices. The actual target position is used to define the transverse position of the beam axis.

The three largest contributors to Table 3-6-1 are shown in Figure 3-6-6, as a function of neutrino energy.

3.6.4 Design Assumptions

The neutrino energy spectrum test for oscillations requires predicting the far detector energy spectrum (without oscillations) from the measured energy spectrum in the near detector. The combined effect of all alignment errors must cause less than a 2% change in any 1 GeV energy interval in this prediction.

Alignment of the experimental detectors is not included in WBS 1.1.6. It is to be included in the installation of those detectors.

3.6.5 System Design

The design phase program will provide detailed specifications for the alignment network to be used at Fermilab. Design phase alignment tasks, WBS 1.1.6.1 (EDIA). are included at this early stage to provide a confirmation of the neutrino beam line before construction starts. The increased accuracy of these measurements will be required when the neutrino beam elements are installed at Fermilab.

Survey monuments have been installed on the surface at Soudan and we plan to relate them to the 27^{th} level at the mine bottom using existing data from mine surveys and measurements made to determine the position of the Soudan 2 detector. We will perform a variety of auxiliary measurements to verify the existing data; these will include existing survey marks and cross checking with existing data.

During a planning trip to the Soudan mine, Fermilab surveyors selected locations for the new surface monuments, but discovered that a single measurement down the full length of the mine shaft with our Geodometer (an automatic survey instrument to measure both angles and distance using an infrared beam) is not practical due to deviations of the shaft from a straight line and fog generated as the cool, humid mine air rises to the surface. Preliminary gyro-theodolite (measures angles with respect to true north, which is found

from an internal gyrocompass) measurements confirmed the angle between the surface and the 27th level to better than 8 arc minutes (small compared to the 3.3 degree vertical angle deviation we have accepted by choosing to make the far detector axis level). The surface to 27th level elevation difference of 2340 feet was confirmed to within 10 feet by barometric pressure measurements. Fortunately, as can be seen in Table 3-6-1, transverse errors of 10 or even 20 meters at Soudan make a very small contribution to the overall effect of alignment errors.

The accurate Fermilab surface to Soudan surface GPS measurement described above will be done before underground construction starts at Fermilab to provide a final confirmation that we are building on the correct line to the future position of the MINOS far detector at Soudan. The NuMI neutrinos will also illuminate the existing Soudan 2 detector, which is only 46 meters off the beam center line.

3.6.6 Design Validation

The Fermilab surface and target hall alignment networks will be analyzed for predicted accuracy before field measurements are begun. This should result in good, accurate results the first time a network is measured. We will use professional (Fermilab and outside) surveyors with experience making the same type of measurements and calculations we require.

3.6.7 Construction Plan

Alignment tasks during the construction phase (WBS 1.1.6.2) are to insure the Fermilab target hall, tunnels, and decay pipe are built on the correct line, and to install and tie in alignment monuments after the target hall and experimental caverns are complete.

Transferring the horizontal angle of the line from Fermilab to Soudan from the surface to the target hall alignment network will be the most critical task during the construction phase, so two independent survey techniques will be used. A sight riser will be constructed at the downstream end of the target hall. Conventional survey techniques will be used through this sight riser and the access shaft at the upstream end of the target hall to establish two points in the target hall separated by about 50 m in the beam direction at both the floor level (for aligning the final two proton beam measuring devices) and the top of the

shielding (for aligning the target and horns). Secondly, a gyro-theodolite accurate to 15 microradian, will be used to transfer this angle from the surface to the target hall.

3.6.8 Installation Plan and Issues

There are several alignment tasks that must be accomplished during the installation phase (WBS 1.1.6.3). Many of the proton and neutrino beam elements and monitoring devices must be fiducialized, i. e., measure their active elements with respect to fiducial marks on the outside which are visible after installation. These items must be correctly positioned in their final locations, which will require the highest accuracy. Also we will recheck the position of the underground monuments in the target hall and experimental caverns after major weight has been moved in.

3.6.9 Commissioning Plan

Most of the alignment tasks will be completed before commissioning. If a problem is observed which may be due to incorrect alignment; for example, if there are about the expected number of events in the near detector, but too few neutrino beam events in the far detector over a broad energy range, we would first make timing and sensitivity checks of the far detector. If the alignment were still suspect, we would first re-measure the target and horn 1 relative to the target hall network and the network relative to the Fermilab surface monuments. Next, we would check the GPS geodetic calculations and repeat the GPS Fermilab to Soudan measurement. Finally we would re-measure horn 2 relative to the target hall network, and the near detector transverse position.

3.6.10 Performance Monitoring Plan

Accuracy monitoring of measurements will be accomplished by the standard techniques developed by surveyors at Fermilab and elsewhere in the practice of their profession: These include redundant and repeated measurements, using alternate measurement techniques, independent duplication of critical calculations, and measurements of known points, together with unknown points. An additional check for gross errors in aiming the neutrino beam at the far detector should come from off axis beam monitors in the Soudan mine. When inaccurate measurements are found with these techniques, blunders will be removed and the measurements repeated or additional measurements made with alternate techniques.

	PH2me	**Medium**	**Energy**	**Beam**
	A	B	C	D
	estimated accuracy	Will cause 2% error	error in worst energy bin	error squared
At Fermilab	(mm)	(mm)	(%)	(%)
Position of Beam on Target	0.38	1.20	0.201	0.040
Angle of Beam on Target [18.13m]	0.71	8.16	0.015	0.000
Target X	0.50	-	0.000	0.000
Target Angle [1.0m]	0.71	1.67	0.362	0.131
Horn 1 X &	0.50	0.89	0.645	0.416
Horn 1 Angle [3.0m]	0.71	1.69	0.353	0.125
Horn 2 X	1.00	4.28	0.109	0.012
Horn 2 Angle [3.0m]	0.71	23.00	0.002	0.000
Decay Pipe [675m]	25.00	270.00	0.017	0.000
Downstream End				
Near Detector	25.00	209.00	0.029	0.001
Sum			*0.851*	0.724
Times root 2, since two transverse planes			*1.204*	1.449
Decay Pipe effective radius #	20.00	43.80	0.913	0.834
Sum			*1.511*	2.283
To Soudan	(m)	(m)		
Horizontal	12.00	167.00	0.010	0.000
Vertical	4.00	167.00	0.001	0.000
Sum			*1.511*	2.283

Linear dependence

& Fourth Order Term Included

Table 3-6-1 Alignment tolerance requirements for the two parabolic horn wide band neutrino beam in the medium energy configuration.

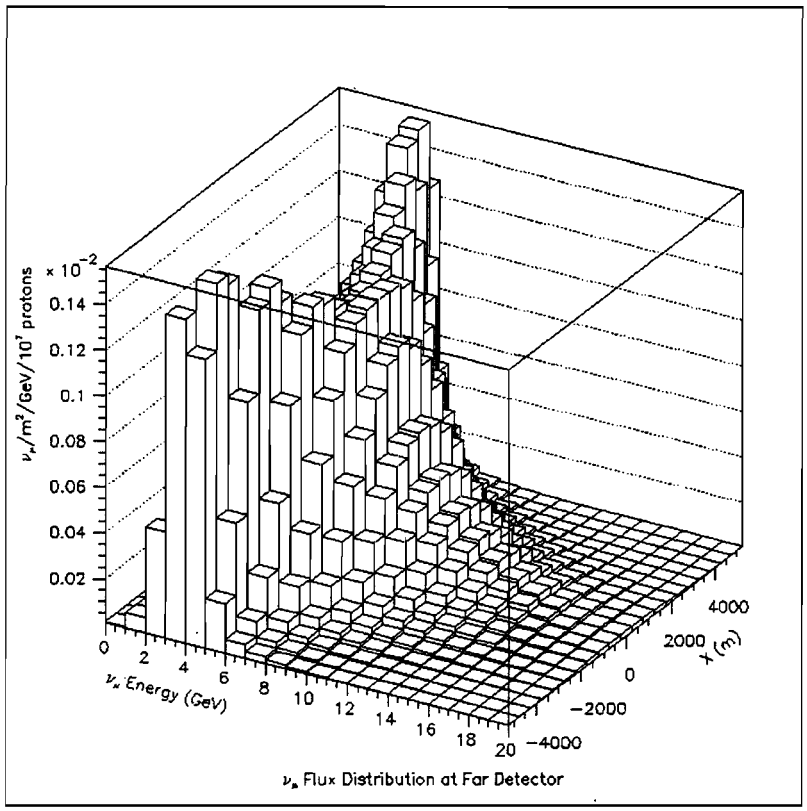

Figure 3-6-1 Transverse distribution of the NuMI neutrino beam at the far detector as a function of energy. Note that the low energy neutrino beam is several kilometers wide.

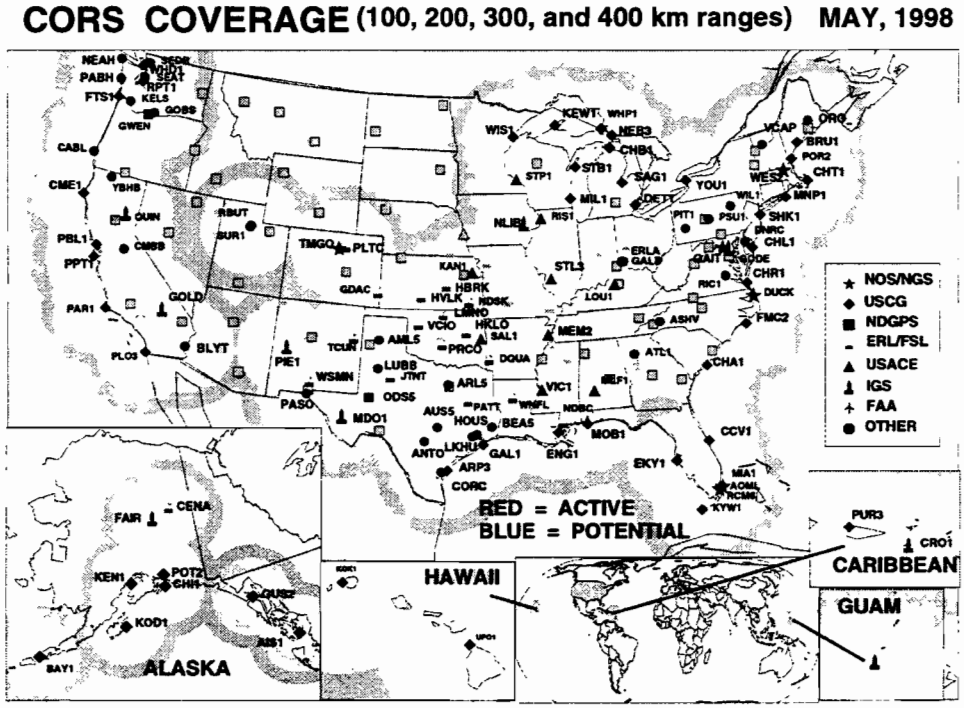

Figure 3-6-2 CORS (Continuously Observed Reference Station) network. GPS data are recorded for over 100 accurately known locations in the United States, including 4 in Wisconsin. (Source: National Geodetic Survey www page: http://www.ngs.noaa.gov/CORS/Maps/cors_coverage.ps)

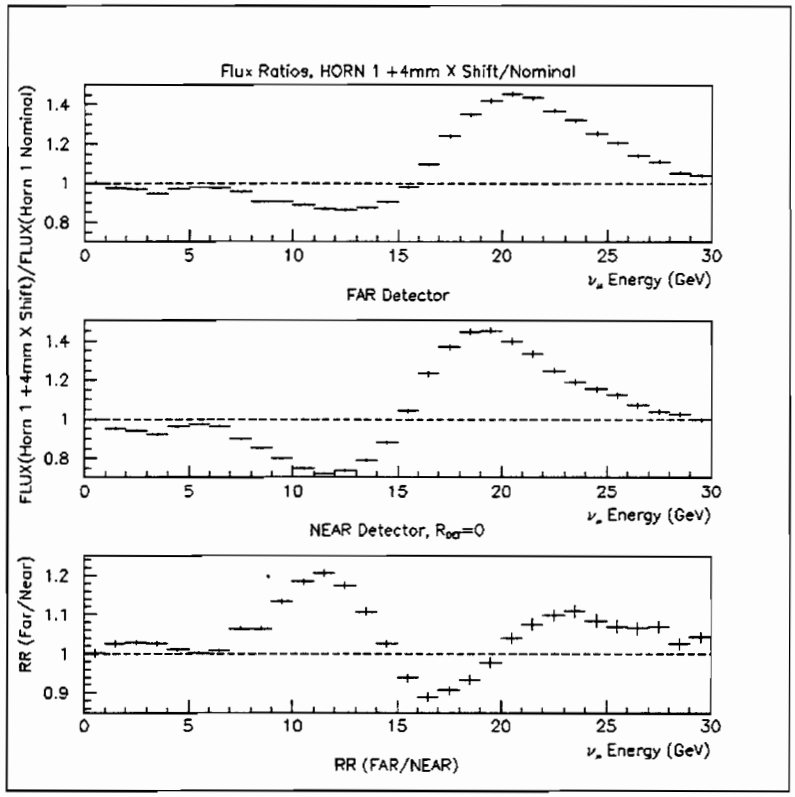

Figure 3-6-3 Effect of a 4 mm offset of horn 1 on (top) the far detector flux, (middle) near detector at 300 m beyond the end of the decay pipe, (bottom) far over near ratio(RR).

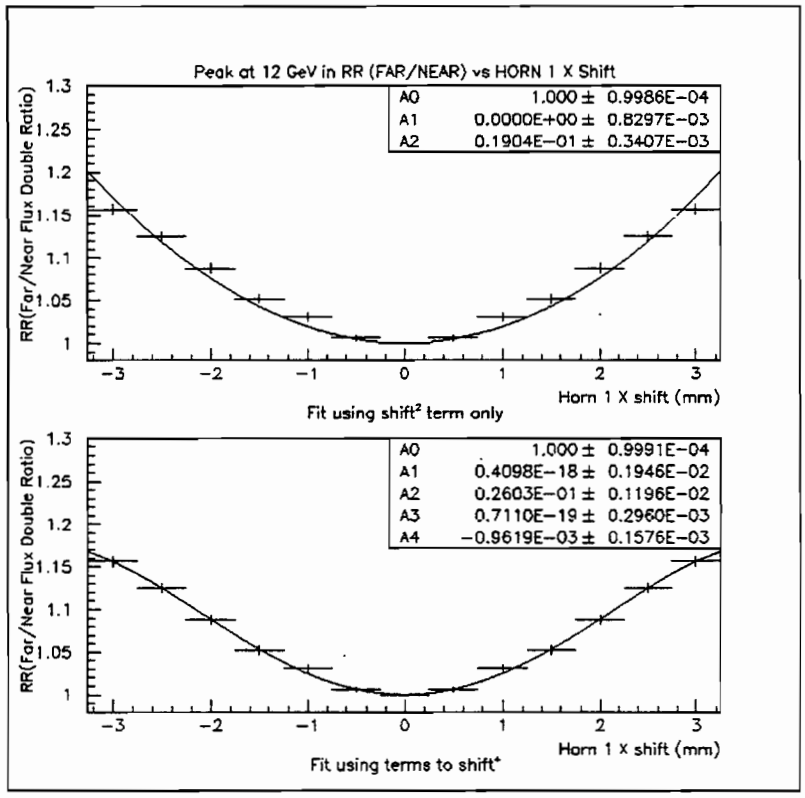

Figure 3-6-4 Fits showing the peak at 12 GeV in RR for a horn 1 transverse shift (bottom section of Figure 3-6-3) requires terns up to shift to the fourth power.

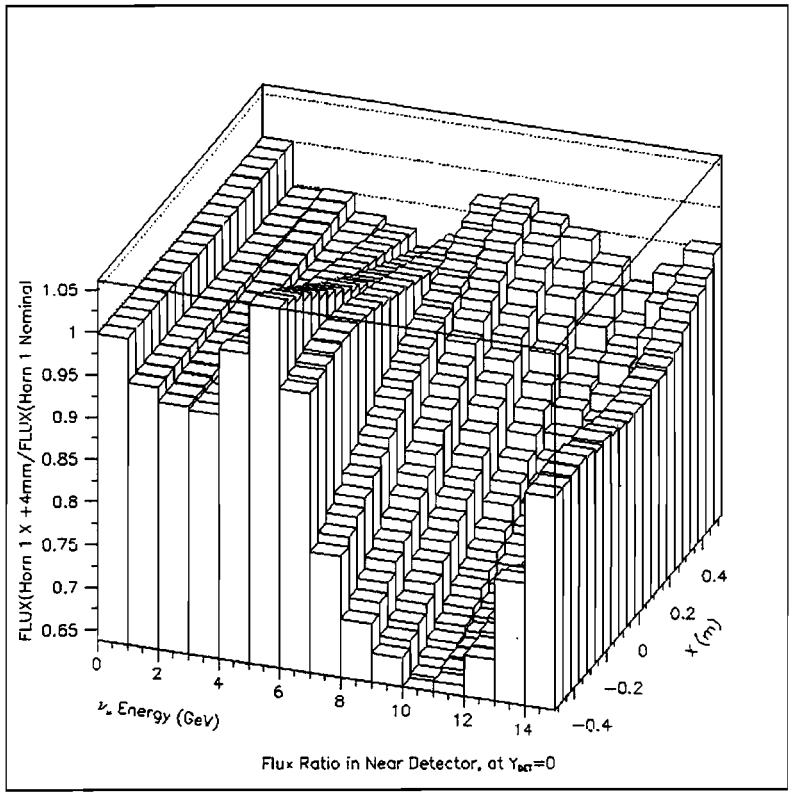

Figure 3-6-5 Effect of a 4 mm horn 1 transverse offset on the flux in the near detector as a function of neutrino energy.

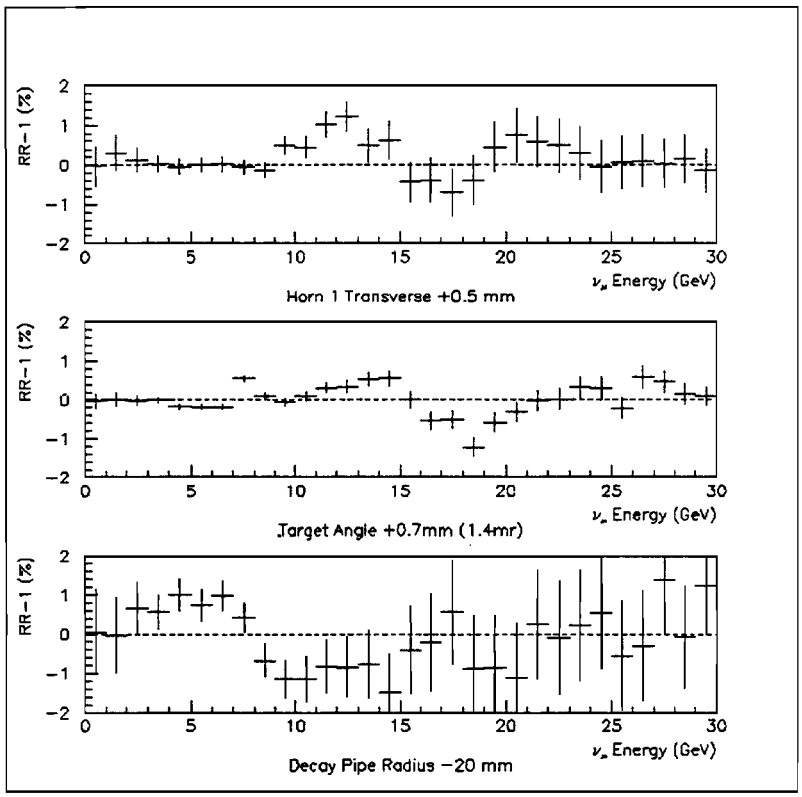

Figure 3-6-6 Largest contributions to errors in neutrino flux spectrum (see Table 3-6-1). Errors in the top two graphs have been multiplied by $\sqrt{2}$ to account for both horizontal and vertical misalignments.

3.7 Utilities – Water, Gas and Vacuum Systems (WBS 1.1.7)

Table of Contents

3.7 UTILITIES – WATER, GAS AND VACUUM SYSTEMS (WBS 1.1.7) 3.7-1

3.7.1 Introduction *3.7-3*

3.7.1.1 Water 3.7-3

3.7.1.2 Gases 3.7-4

3.7.1.3 Vacuum 3.7-4

3.7.2 Primary Objectives *3.7-4*

3.7.2.1 Water 3.7-4

3.7.2.2 Gasses 3.7-5

3.7.2.3 Vacuum 3.7-5

3.7.3 Technical Requirements and Constraints *3.7-5*

3.7.3.1 Water 3.7-5

3.7.3.2 Gasses 3.7-6

3.7.3.3 Vacuum 3.7-6

3.7.4 Design Assumptions *3.7-7*

3.7.4.1 Water 3.7-7

3.7.4.2 Gasses 3.7-7

3.7.4.3 Vacuum 3.7-7

3.7.5 Design *3.7-7*

3.7.5.1 Water 3.7-7

3.7.5.2 Gasses 3.7-8

3.7.5.3 Vacuum 3.7-8

3.7.6 Design Validation *3.7-9*

3.7.7 Construction Plan *3.7-9*

3.7.7.1 Water 3.7-9

3.7.7.2 Gasses 3.7-9

3.7.7.3 Vacuum 3.7-9

3.7.8 Installation Plan and Issues *3.7-9*

3.7.8.1 Water 3.7-9

3.7.8.2 Gasses 3.7-10

3.7.8.3 Vacuum 3.7-10

3.7.9 Pre-commissioning *3.7-10*

3.7.10 Performance Monitoring Plan *3.7-10*

Table of Figures

Figure 3-7-1 Schematic block diagram of the NuMI target station ICW, LCW and RAW systems. __3.7-12

Figure 3-7-2 Schematic block diagram of the NuMI downstream caverns ICW, LCW and RAW systems. _____3.7-13

Figure 3-7-3 A schematic drawing of the NuMI beamline gas system. Premixed Ar/CO_2 gas is flowed from bottles in the upstream service building (upper box of broken lines) to SWICs in beamline enclosures underground (lower box of broken lines) The solid lines represent the gas piping and arrows indicate the direction of flow. After passing through the SWICs the gas is vented through bubblers. _____3.7-14

3.7.1 Introduction

In this section are grouped together details of the various utilities required for the NuMI beams. Water and gas would normally be expected to fall under the heading of utilities, and for NuMI it has been decided to include vacuum as well.

3.7.1.1 Water

Cooling water at Fermilab falls into three categories – Primary Cooling Water, Low Conductivity Water (LCW) and RadioActive Water (RAW). These systems are needed to remove directly or indirectly the heat generated by the operation of electrical devices and to dispose of the energy deposited in various components by high energy beams. Without functional cooling systems, many beamline components would be damaged and fail due to excessive thermal buildup

Ultimately the energy absorbed by cooling water system of any type is transferred to the primary cooling water system and thence to the atmosphere. The primary cooling water system is part of the Fermilab infrastructure and includes cooling ponds, cooling towers and pumps. The pond water (PW) circulating through the primary cooling water system is not suitable for direct use in beamline components such as magnets or power supplies due to its high electrical conductivity. Therefore a separate system, of LCW, is required. The LCW system forms its own closed loops and includes heat exchangers, LCW pumps, DeIonization (DI) bottles, plumbing and the components to be cooled. The DI bottles bring the electrical conductivity of the LCW to a low enough level that it is suitable for use within electrical conductors.

The baffles, target, horns and absorber operate in an extremely high radiation level environment. The radiation level is high enough both that the devices must be cooled against radiation induced heating and that this water itself becomes activated, particularly with tritium. Therefore dedicated RadioActive Water (RAW) systems are required to cool these components. A RAW system contains many of the same components as are found in an LCW one but forms its own isolated closed loop. The heat that is absorbed by a RAW system is transferred through a heat exchanger to an LCW system, from there through another exchanger to an ICW system and finally to the atmosphere.

Fermilab has had long experience with ICW, LCW and RAW systems. However NuMI will contain the first Fermilab beamlines operated deep underground, more than 250' in the case of the hadron absorber. Since some parts of the cooling system will be on the surface while others will be at beamline level, the plumbing, the pumps, the heat exchangers and some other components will have to be designed to handle the higher pressures caused by this hydraulic head.

3.7.1.2 Gases

Requirements for two types of industrial gasses in the beamlines have been identified. The first is for helium, to fill voids inside the shielding in the vicinity of the target and horns. As is discussed in detail elsewhere in this report, this helium is used to displace air in regions of extreme radiation, as it is less susceptible than air to being activated. The gas will be in nominally closed containers, so that normal flow rates will need to counteract only small leakage. However it will occasionally be necessary to vent these containers during accesses, and refilling will then be required before continuing with operations.

The other gas required will be a mixture of argon and carbon dioxide (Ar/CO_2), for use in SWICs (Segmented Wire Ionization Chambers) which have been specified for both the primary proton and secondary hadron beams. Small amounts of gas flow constantly through these devices and are then vented into the tunnel. It is required that this flow be uniform so that the devices will operate in a stable fashion.

3.7.1.3 Vacuum

Transport of the NuMI proton and hadron beams will require that various levels of vacuum be established in the MI tunnel, extraction stub, carrier pipe, pretarget area and decay pipe. Since the NuMI beamlines are single pass, requirements are not so stringent as they are in a circular machine. The novel feature is the 675 m long decay pipe, which has a very large evacuated volume.

3.7.2 Primary Objectives

3.7.2.1 Water

The primary objective of the water systems is to provide sufficient heat rejection for the following devices:

- primary beam magnets (LCW)[1]

[1] LCW is Low Conductivity Water. All heat from LCW systems is rejected to ICW

- magnet power supplies (LCW)
- primary beam baffles (RAW)[2]
- target (RAW)
- horns (RAW)
- horn power supply (LCW)
- beam absorber (RAW)
- vacuum pumps (if cooling is needed) (clean ICW)
- MINOS near detector magnet (LCW)
- MINOS near detector magnet power supply (LCW)

A further requirement is that the system be sufficiently robust to be fully functional, and responsible for absolutely minimal downtime during scheduled operations.

3.7.2.2 Gasses

The objectives of the gas systems are to provide helium to the containers in the vicinity of the target and to provide Ar/CO_2 to the SWICs and downstream beam monitoring instrumentation in a steady flow.

3.7.2.3 Vacuum

The objectives of the system are to provide reliable vacuum at the specified levels.

3.7.3 Technical Requirements and Constraints

3.7.3.1 Water

The technical requirements of the LCW and RAW systems can be stated in terms of the flow rate and pressure differential for each of the components to be cooled. For the magnets these values are given in Fermilab-TM-623. As an example EPB dipoles, the most frequently used magnets in the primary proton line, require a flow rate of 1072 liters/hr at a pressure of 7.03 kg/cm^2. The values for the various power supplies to be employed are similarly available (see Appendix V of the Tevatron II Facilities Handbook Vol. 2 and the manufacturers' name plate data). For other devices to be cooled similar requirements must be determined as part of design. The list of such devices consists of carrier pipe and horn

[2] RAW is Radioactive Water. All heat from RAW systems is rejected to LCW

protection baffles, target, horns (cooled by sprayed water), horn power supply, beam absorber and MINOS near detector magnet.

The ICW must ultimately be able to remove all the energy created in these beamlines by both electrical and radiation heating. To set the scale, the magnets of the primary proton beam would generate 1.75 MW of heat if they were operated DC, in practice generating this amount reduced by some factor dependant on how rapidly they can be ramped. The beam power absorbed by various components totals approximately 300KW.

3.7.3.2 Gasses

The helium system must be able to supply enough gas to maintain approximately 46,000 liters at 1" water column pressure relative to atmosphere. The Ar/CO_2 flow required 10-20 ml/minute for each of the SWICs in the primary beamline, with a somewhat greater amount for those large ones in the hadron beam. Downstream beam monitoring instrumentation will require a mixture of helium and hydrogen (98% He, 2%H) for the instrumentation just upstream of the hadron absorber and an Ar/CO_2 mixture for the instrumentation in the Muon slots.

3.7.3.3 Vacuum

As the NuMI beam passes through the Lambertsons it shares a pipe with the MI beam and thus is in a region of vacuum of 10^{-8} Torr, maintained as part of the MI system. At such a point as the beam occupies its own pipe, a vacuum thin window will be installed, downstream of which less stringent criteria pertain, and a value of 10^{-3} Torr is sufficient. It is intended that this level be maintained from the main injector to the target, although 10^{-2} Torr in the carrier pipe, which has been achieved in similar pipes with conventional mechanical pumps, would meet the minimum beam transport requirements. At the locations of the primary beam instrumentation, pressures below 10^{-3} Torr would prevent charge affects from adversely affecting the primary beam instrumentation. This locally lower pressure will be provided by either turbo pumps or existing ion pumps recycled from the main ring.

The required vacuum in the decay region is 100 microns to 1 Torr (1×10^{-1} to 1 Torr) as is specified in Fermilab-TM-2018. This vacuum can be achieved with mechanical pumps. Given a 675 meter long decay pipe, 6 feet in diameter, a 400 cfm (cubic foot per minute) mechanical vacuum pump can evacuate the 62,600 cubic foot volume from atmosphere to 1 torr in approximately 12 hours.

3.7.4 Design Assumptions

3.7.4.1 Water

As stated in the Introduction to this section, pressures and flow rates are understood for most of the primary beamline devices, and will be determined as part of the design process of the hadron beam absorber. The assumption going into the design of the overall water system is that these requirements may increase, and that the system, pumps and heat exchangers, must be sized accordingly. The conversion to a narrow band beam in the future will entail both the installation of more magnets and the need to stop more beam in the target region. Both of these changes will require increased water flow. There is a further assumption that the RAW system will not be designed from scratch, but will be an appropriately sized copy of one already existing at Fermilab. (Such existing systems are rated at 11, 60 and 220KW.)

3.7.4.2 Gasses

There are two reasons for using helium. The first is that it serves to displace air in void regions inside the target pile and as such reduces the production of activated air. The second is that the helium serves as a substitute for vacuum in the regions between the horns. The assumptions based on these uses are that ultra pure gas is not a requirement and that in some regions a slight positive pressure with respect to atmosphere is required. As to the Ar/CO_2, the assumption is that it will be required only for SWICs, so that the mixture ratio (80% Argon 20% CO_2), required purity and flow rate are all known.

3.7.4.3 Vacuum

Thin windows can be installed as required for the separation of vacuum levels between portions of the beam pipe with different vacuum requirements.

3.7.5 Design

3.7.5.1 Water

The design methodology for the water system is the following:

- The Level 3 Manager for each system determines accurate values for the heat loads, pressure drops and flow rates for the devices of that system. In particular these values are well known for the magnets of the primary proton beam and for standard power supplies.

- With this information the water system engineer creates first a Piping and Instrumentation Diagram (P&ID) schematic and then a detailed Process Flow Diagram (PFD). On this latter schematic the pressures, temperatures, heat loads and flow rates at key points in the water system are indicated. Figures 3-7-1 and 3-7-2 are very preliminary P&IDs for the target station and downstream cavern water systems.
- The sizes of heat exchangers are determined from heat loads.
- From the required flow rates the pipes are sized and the pressure drops calculated from the Darcy and/or Hazen and Williams formulas.
- From pressure drops the Total Developed Heads (TDHs) for pumps are determined and pump parameters specified.
- The ICW piping and ICW to LCW heat exchanger are included in facilities design.

3.7.5.2 Gasses

In the case of the $ArCO_2$ for the SWICs little new is being done and existing designs can by-and-large be duplicated. A possible exception would be the use of new large SWICs in the hadron beam, SWICs whose properties might be unique.

The use of helium inside the target pile entails a few distinct scenarios. These include initial filling of the containers, likely very slow gas flow during operational periods, venting to prevent activation build-up and refilling after venting. During the design phase of the gas system, the pressures and flow rates will be calculated and the system components appropriately sized.

3.7.5.3 Vacuum

The vacuum system design methodology is:

- With well understood statements of the required vacuum in the different parts of the system, the types of pumps to be utilized are determined.
- The vacuum P&ID schematics are prepared.
- From these and the physical dimensions of each vacuum pipe, the gas loads are calculated.
- With these results the pumping system is sized. This system includes both the pumps and the piping between pumps and beam pipes.

3.7.6 Design Validation

The validations of the designs of all these utility systems are performed in the same manner. The diagrams and calculations that model the final system design are checked in detail by a second engineer.

3.7.7 Construction Plan

3.7.7.1 Water

The parts of the water system in the MI enclosure and the NuMI Stub will involve connection to MI water. In the pretarget Hall LCW will be required for the proton line magnets, while in the adjacent Target Hall RAW will be required for the equipment inside the target pile. All the parts of the RAW system will be carefully tested off line for integrity, and then the system basically assembled in place in the hall. Construction in the downstream region, serving the hadron absorber through to the MINOS near detector, must take account of the large head that will exist, as was noted above. This area is near no major water source or system, so construction of the piping from a source requires civil construction and is discussed in the civil portion of this report.

3.7.7.2 Gasses

The SWIC gas system will be constructed in place. This type of work has been done often before and does not present any particular problems. The helium containment volumes will be constructed in a shop and tested thoroughly for integrity before being taken to the Target Hall.

3.7.7.3 Vacuum

The major items of the vacuum system are various types of pumps, which are manufactured commercially. The major construction effort involves the beam pipes plus other piping required to connect the vacuum pumps thereto.

3.7.8 Installation Plan and Issues

A number of utility systems similar to those required for NuMI have been installed at Fermilab, so the installation procedure is well understood. The plans follow.

3.7.8.1 Water

- Install ICW - connect heat exchanger and ICW piping to existing pond pumps; install related instrumentation and test operation. Civil contractor.

- Install LCW piping in Pretarget Hall, power supply room, near detector cavern. Mechanical contractor.
- Install polishing loops, pumps and instrumentation on LCW skids. BD/Mechanical.
- Install polishing loops (as required), pumps, heat exchangers and instrumentation on RAW skids. BD/Mechanical.
- Install LCW and RAW skids in power supply room and downstream mechanical area, connect wiring and piping, test operation. Mechanical Contractor.
- Instrument RAW system. BD/Mechanical.
- Wire power to LCW and RAW skids. Electrical contractor.

3.7.8.2 Gasses

- Install gas lines, connect $ArCO_2$ to SWICs, and test. BD/Instrumentation.
- Install helium vessels as part of target pile construction. Mechanical contractors.
- Connect helium sources to vessels and test. BD/Mechanical.

3.7.8.3 Vacuum

- Locate, refurbish, and instrument existing vacuum pumps. BD/Mechanical.
- Receive, prepare, and instrument new vacuum pumps. BD/Mechanical.
- Install vacuum pumps in enclosures. BD/Mechanical.
- Wire power to vacuum pumps. Electrical Contractor.
- Connect vacuum pumps to beam pipes. BD/Mechanical.
- Connect vacuum instrumentation. BD/Electrical.

3.7.9 Pre-commissioning

The utility subsystems can all be thoroughly tested and made functional without beam. This precommissioning will include instrumentation, control system connections, readbacks and alarms. Cooling water for power supplies and magnets can be tested with powered systems. However beam is required for a thorough check of the cooling of radiation heated components.

3.7.10 Performance Monitoring Plan

There is considerable experience in using the ACNET control system to monitor utilities. Variables to be monitored include water temperatures, pressures and flow rates, gas flows

and vacuum levels. Additionally one can monitor the temperatures of magnet coils and power supplies with klixons, and use the klixon output to shut down the device if safe operating temperatures are being exceeded. The primary purpose of the helium gas is to keep air out of the ultra-high radiation area inside the target pile. Monitoring of airborne radionuclides in the hall provides a check that this subsystem is functioning as designed.

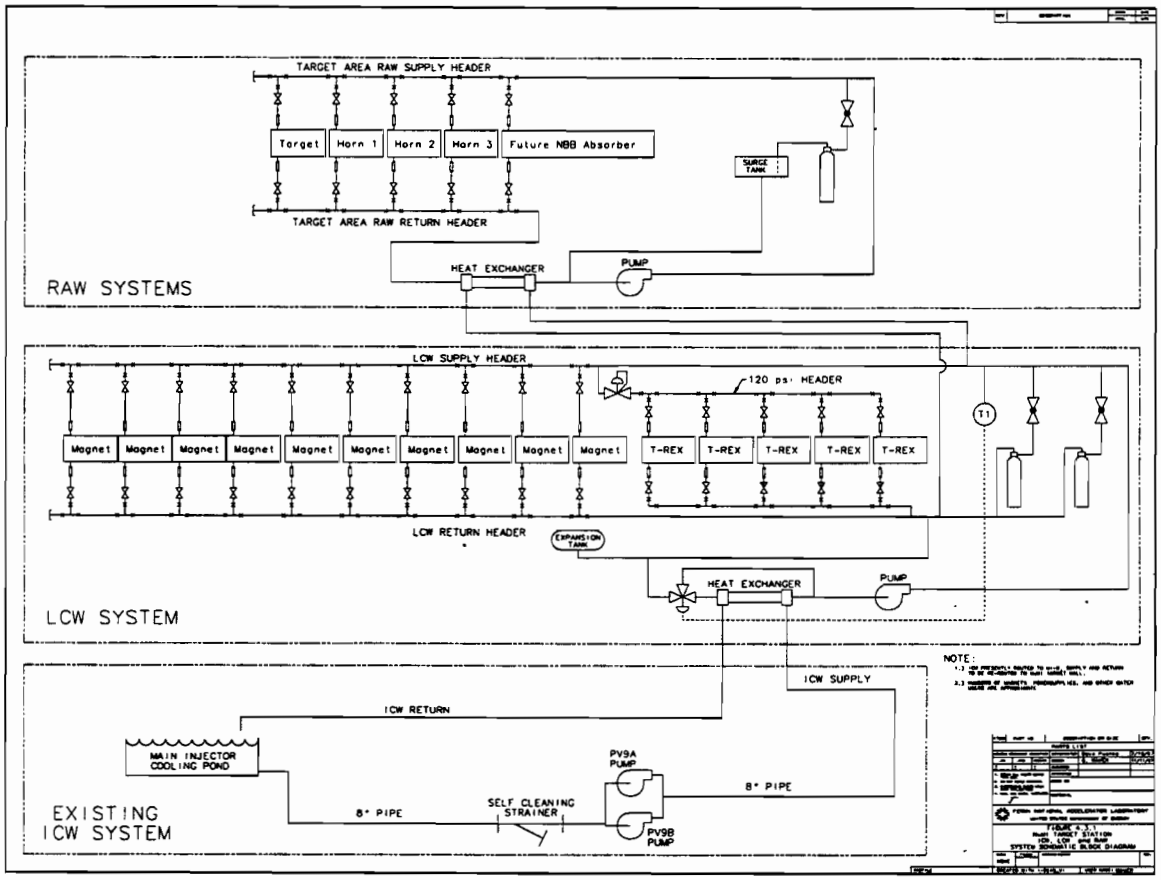

Figure 3-7-1 Schematic block diagram of the NuMI target station ICW, LCW and RAW systems.

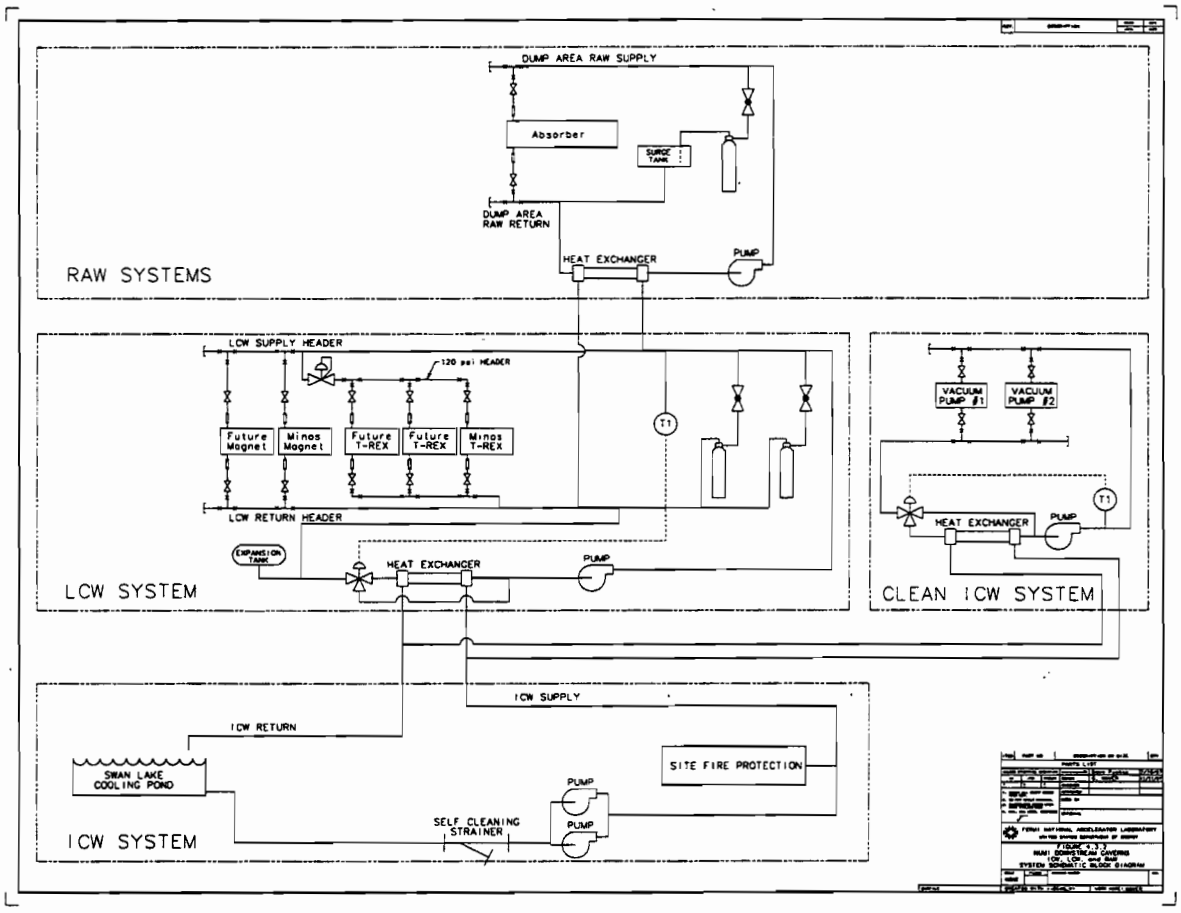

Figure 3-7-2 Schematic block diagram of the NuMI downstream caverns ICW, LCW and RAW systems.

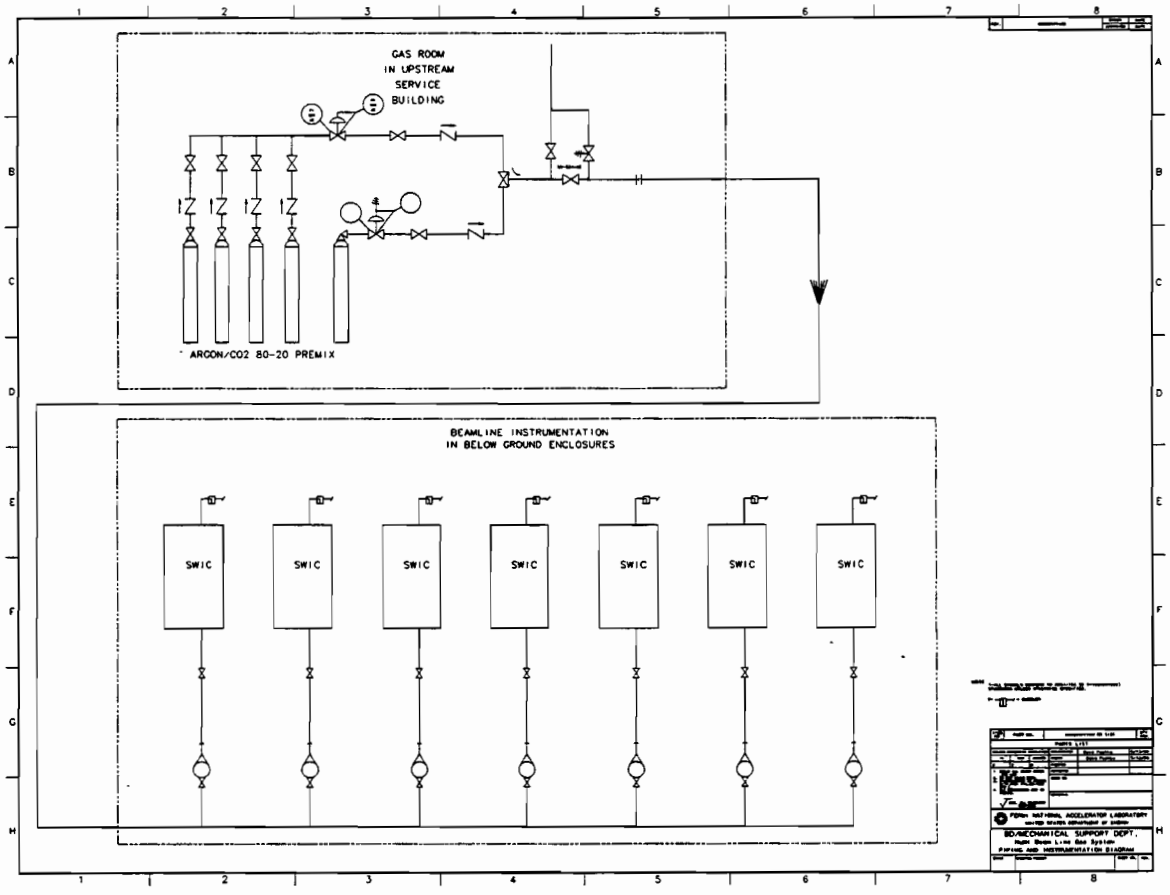

Figure 3-7-3 A schematic drawing of the NuMI beamline gas system. Premixed Ar/CO_2 gas is flowed from bottles in the upstream service building (upper box of broken lines) to SWICs in beamline enclosures underground (lower box of broken lines) The solid lines represent the gas piping and arrows indicate the direction of flow. After passing through the SWICs the gas is vented through bubblers.

3.8 Systems Installation and Integration (WBS 1.1.8)

Table of Contents

3.8 SYSTEMS INSTALLATION AND INTEGRATION (WBS 1.1.8) 3.8-1

3.8.1 Introduction *3.8-3*

3.8.2 Integration for NuMI Facility and Beam Systems *3.8-3*

3.8.2.1 Integration Function 3.8-3

3.8.2.2 Integration Design Validation 3.8-4

3.8.2.3 Integration Construction Plan 3.8-4

3.8.2.4 Installation Plan and Issues 3.8-4

3.8.2.5 Integration Performance Monitoring Plan 3.8-5

3.8.3 Control System *3.8-5*

3.8.3.1 Control System Technical Requirements and Constraints 3.8-5

3.8.3.2 Control System Design Assumptions 3.8-6

3.8.3.3 Control System Description 3.8-6

3.8.3.4 Control System Design Validation 3.8-8

3.8.3.5 Control System Construction Plan 3.8-8

3.8.3.6 Control System Installation Plan and Issues 3.8-9

3.8.3.7 Control System Pre-commissioning Plan 3.8-9

3.8.3.8 Control System Performance Monitoring Plan 3.8-10

3.8.4 Radiation Safety System *3.8-10*

3.8.4.1 Radiation Safety System Technical Requirements and Constraints 3.8-10

3.8.4.2 Radiation Safety System Design Assumptions 3.8-11

3.8.4.3 Radiation Safety System Description 3.8-12

3.8.4.4 Radiation Safety System Design Validation 3.8-13

3.8.4.5 Radiation Safety System Construction Plan 3.8-13

3.8.4.6 Radiation Safety System Installation Plan and Issues 3.8-14

3.8.4.7 Radiation Safety System Pre-commissioning Plan 3.8-14

3.8.4.8 Radiation Safety System Performance Monitoring Plan 3.8-14

3.8.5 Cable System *3.8-15*

3.8.5.1 Cable System Technical Requirements and Constraints 3.8-15

3.8.5.2 Cable System Design Assumptions 3.8-15

3.8.5.3 Cables System Description 3.8-15

3.8.5.4 Cable System Design Validation 3.8-15

3.8.5.5 Cable System Installation Plan and Issues 3.8-16

Table of Tables

Table 3-8-1 Standard Controls Items ____ *3.8-17*
Table 3-8-2 NuMI Specific Controls. ____ *3.8-18*
Table 3-8-3 CATV, CCTV and FIRUS Controls Items. ____ *3.8-18*
Table 3-8-4 NuMI Cable Estimates ____ *3.8-19*

Table of Figures

Figure 3-8-1 Systems Integration Overview. ____ *3.8-20*

3.8.1 Introduction

Systems Integration provides for the integration of activities for each of the NuMI Facility systems at the points of interface with other systems to ensure that they are brought together in a manner which will meet the NuMI Project's design goals. These include:

- integration efforts at the boundaries of the technical Level 3 systems presented in this chapter,
- coordination of specifying technical criteria needs for the Facility civil construction,
- provision of common services including beamline controls, portions of the beamline cabling, and certain radiation protection and monitoring systems,
- integration of installation efforts requiring common services and facilities, such as use of the underground access shafts,
- integration of the Facility technical and civil construction schedules, and
- quality assurance and review oversight as requested by Project Management.

An overview of Systems Integration responsibilities is displayed in Figure 3-8-1.
The following four sections 3.8.2 - 3.8.5 describe the overall system integration planning, the controls system, radiation protection and monitoring, and cables, respectively.

3.8.2 Integration for NuMI Facility and Beam Systems

3.8.2.1 Integration Function

Significant functions of Systems Integration are to maintain an awareness and understanding of the requirements of the technical component systems, to prevent interference between technical systems by providing integration across interface boundaries, and to provide common services as described in subsequent sections.

Technical requirements and constraints for Systems Integration are to help each subsystem meet its individual technical requirements and constraints. Two major tasks for this system are coordinating the technical criteria requirements for the facility civil construction, as detailed in Chapter 5 of this TDR, and preparing a bottom up installation schedule.

Part of System Integration is a process rather than hardware. As such, the design of the facility, cost and schedule, and installation plans and the execution of these plans are main elements of this WBS element.

3.8.2.2 Integration Design Validation

Validation of system integration planning, cost and schedule and the installation plan will be done by peer review. Key planning criteria are to minimize interference between systems, and to maintain a high level of overall efficiency. These plans are dynamic in nature to quickly accommodate and react to schedule changes. Validation of changes to the plans will be commensurate with the scope and significance of the change.

3.8.2.3 Integration Construction Plan

While the word 'construction' normally applies to hardware, the following paragraphs describe the construction or development of the integration process and installation plan.

The integration process requires that the staff responsible for this WBS element have a good understanding of the design and issues for each of the other Level 3 systems in the technical components, and the interface with the facility civil construction. From a detailed understanding of the design, physical characteristics, utility requirements, alignment requirements, installation needs, cable plant needs, etc. of each element in the other systems, the scope fine tuning, design modifications, consolidation of efforts with other systems, and other integration activities can be performed. Examples include interfacing primary beam and target hall technical requirements with civil construction method optimization described in Chapter 5.1, planning the technical installation sequence, coordinating pulling of cables used by several systems into a single contract, or understanding where the hoses that connect the magnets to the water system exist in the Project.

The initial development of the installation procedure will result in a top down schedule that sets the desired completion date for items in each system and provides an initial identification of critical paths. As progress is made within each system, the schedule information is fed back into the installation plan that will result in the actual bottoms up installation sequence.

3.8.2.4 Installation Plan and Issues

A significant responsibility of systems integration is to develop the integrated installation plan. Coordination with Main Injector shutdown times must be carefully planned for installation of upstream primary beam components. Coordination for joint system use of

the two access shafts for component installation must also be carefully planned and scheduled.

This system integration does not include installation of items in the far MINOS cavern. It will include some beamline controls items (TV systems, computer networking), the near MINOS magnet power supply, and utilities for the near MINOS cavern. Coordination of installation scheduling for the MINOS near detector and beam technical components using the same access shaft is included.

3.8.2.5 Integration Performance Monitoring Plan

The best measure of performance will be adherence to schedules with minimal rework requirements, minimal cost overruns, and a successful and efficient beam system commissioning.

3.8.3 Control System

The primary objective of the beamline control system is to provide the supporting technical infrastructure that will make the smooth operation of the NuMI beamline possible. This includes CAMAC and VME systems for the operation of beamline devices, transmittal of accelerator clock signals, a television system for monitoring the beamline and accelerator operations, extension of the FIRUS alarm system into the appropriate NuMI areas and networking in support of experimental data acquisition.

3.8.3.1 Control System Technical Requirements and Constraints

The control system backbones will be CAMAC and Ethernet links connecting all areas where NuMI electronics is housed. The CAMAC link will connect standard hardware, such as that of most of the primary proton beam, while the Ethernet link will connect VME and other more sophisticated processor-based controls. The CAMAC link will be driven by a dedicated front-end computer. Other standard infrastructure components – racks, crates, repeaters and CAMAC cards - will be included. The Ethernet link will also be used to support ACNET consoles, which will be utilized in service buildings during installation, and permanently if desired. Also required will be a means of transmitting accelerator information to Soudan. As much as possible of the CAMAC and VME etc. equipment will be attached to the existing base of software tools through entries in the ACNET database.

Controls also include the television system. Television signals are distributed around the laboratory utilizing CATV/CCTV technology. Information sent includes accelerator operation status from the Main Control Room and the data from certain beamline instrumentation, in particular SWICs. It is also used to provide a fire watch on unoccupied beam enclosures.

It is traditional at Fermilab to include under Controls FIRUS (Facility Incident Reporting and Utility System), the lab-wide fire and utility alarm system. FIRUS is a (redundant and robust) computer network that serves to notify the Operations Center and other locations of facility related alarms – including those for fires, burglary and such as sump pump failure. The general rule is that FIRUS must be operational in any new building or enclosure before beneficial occupancy can commence.

For the NuMI project it is also necessary to provide computer networking for the experimental data of the MINOS near detector. Future experiments will have the ability to transfer via network some or all of their data to the Feynman Computing Center for rapid analysis. Since the detector hall is in a previously undeveloped part of the laboratory, it is necessary to provide the appropriate networking infrastructure to it. This work will be costed and managed as part of Controls.

3.8.3.2 Control System Design Assumptions

Beamline controls at Fermilab have traditionally been shared between two separate systems: ACNET (Accelerator Controls Network) of the former Accelerator Division and EPICURE of the former Research Division. It is now policy that only ACNET be supported for future developments. We assume that the integration of the two systems will be complete well before the start of NuMI commissioning. Thus the control system will be available to aid the NuMI work, and will not itself be commissioned simultaneously. As noted above the control system includes TV, computer networking for MINOS, and FIRUS. Civil work provides for fire panels and sensor cables for FIRUS.

3.8.3.3 Control System Description

ACNET is modular at the hardware level but generic at the user interface; thus it is a straightforward matter to attach a new major system such as NuMI. Most equipment to be installed for NuMI will be similar to that of other beamlines, so that most controls will be relatively standard. The Fermilab central host system currently consists of a number of

DEC-VAX computers. They are used for software development by programmers, for logging of considerable controls related data by operators and for a variety of real time tasks. The most important single task is operation of database software, which contains addressing and scaling information for all attached hardware of the accelerator and beamline complex. NuMI equipment will be added to the database with the result that all data passing through standard interfaces will become widely available with little additional effort. NuMI will have to provide the front-end computer, one or more consoles for monitoring controls data and software related to any non-standard equipment. All control room consoles will also be able to monitor and control the NuMI beamline.

There are two major categories of NuMI controls hardware. The first contains those items that are "standard" - in use in other areas of the accelerator/beamline complex. While NuMI may need to purchase some hardware to extend these standard items into the new beamline, no new software development will be required to implement them. Furthermore hardware will be recycled wherever possible. Such standard items include controls for instrumentation and power supplies; provision of timing signals, alarms and datalogging and generic application software. The second category contains nonstandard items, generally of a more advanced nature, such as involving VME or programmable logic controllers (PLC). Insofar as possible NuMI is specifying such hardware in accordance with planned controls directions in an effort to avoid NuMI specific hardware and, more critically, software development. The components listed in Tables 3-8-1 through 3-8-3 represent the present understanding of requirements.

The major piece of new infrastructure required in the construction of the NuMI control system involves the cabling, primarily with fiber optic cables, and this is covered in the section on cables.

All new buildings and the tunnel will have connections to the lab wide system for fire alarms and, where appropriate, for security alarms as well. There will also be at least one FIRUS display console installed in the NuMI control room. FIRUS concentrated network access points (minis) will most likely be located in the upstream and downstream service buildings, the power supply room and the MINOS hall.

Several channels of CATV will be run along the beamline and connected to control areas. Some channels will convey beam diagnostic signals such as display of scope traces and fluorescent screens, and others will provide live observation of remote locations for

security purposes. In total this TV system will provide information both on the operation of the NuMI beam to operations and on Main Injector beam to NuMI.

Also required will be a means of synchronizing data acquisition in Soudan with the accelerator clock. Methods of accomplishing this are under study. One possibility is a video control modem that has telephone access capabilities and thus would be a means of sending signals long distances. Presently such a system is being used for FNAL site gate access.

3.8.3.4 Control System Design Validation

The control system hardware and software design, construction and installation validation/review will be performed by Beams Division engineers and technicians as described below.

Those parts of the controls installation that are standard design will not require separate review. One validation that must be done is to ensure that the bandwidth installed, for both communications and computers, is adequate for the anticipated information flow. As to the more novel installations, such as pertaining to the horn power supply and the hadron beam beyond the target, validations of a more serious nature are required. The engineer in charge of the equipment being controlled must confirm that the controls designed will provide the functionality and bandwidth that his/her system requires. Similarly software personnel must assure that any hardware being installed will not induce any undue software burden. An overall formal review of the control system will occur when the system design is nearly complete.

3.8.3.5 Control System Construction Plan

The control system will be constructed in place, so that what is normally referred to as construction – putting of various pieces together – by-and-large takes place in the installation phase.

The NuMI target hall control system will include CAMAC, VME and PLC systems. The horn power supply will use CAMAC based alarm, readback and controls. The target and horn motion controls will be VME based. The water system, target, and horn components will use a local PLC control system that transfers readback and alarm block data to the

VME front end via Ethernet. VME front-end interfaces to ACNET are supported by the Controls Department and will be the standard by the time NuMI comes on-line.

A database entry containing the details (location, function, scale factors, timing) of any particular piece of controls hardware represents what is required to add that equipment to ACNET. A systematic naming convention for NuMI devices will have to be developed and careful records kept by personnel who move (recycle) or add hardware. For console applications, "Parameter Pages" will need to be set up in order to view easily certain combinations of parameters often studied or set together. This, though, does not require new software.

3.8.3.6 Control System Installation Plan and Issues

Primary in the installation of the control system is the fiber optic cable carrying all information for links (CAMAC, timing etc.) and networks (VME subsystems, consoles). Once the fiber optic cable is installed and instrumented, installation of other pieces of equipment involves their connection to it. An advantage to this is that each new piece can be tested as it is installed. With the ability to have controls consoles at the vicinity of the installation work, it is possible to immediately examine the results of installing any new equipment. Testing in such a form includes hardware, software and database.

FIRUS signals are traditionally transmitted over CATV hardline cables and thus the installations of the FIRUS and TV systems are closely related. The working FIRUS connection requirement for beneficial occupancy of any new structure sets the installation schedule.

3.8.3.7 Control System Pre-commissioning Plan

The FIRUS system must be operational before beneficial occupancy can occur; thus it will be one of the first systems precommissioned. All power supplies will have an extensive power test before commissioning beam. This will point out any problems with power supply monitoring devices and cables. Water for magnet and power supply cooling will have to be operational at this point. The control system will be fully functional before commissioning, with data-logging, alarms and power supply adjusting available. Indeed one of the important requirements of a good control system is that it be operational to aid in the pre-commissioning of a number of other subsystems.

3.8.3.8 Control System Performance Monitoring Plan

As noted above, all of the control system data will flow over an optic fiber backbone that must be installed and tested. Since controls are not installed in radiation areas optic fibers can safely be used. (The instrumentation cables that connect to the control system are copper.) Typical installation contracts include terminating of fibers and testing of their connections for integrity. Fermilab has equipment appropriate to confirm these testing results. Once information is flowing, several ACNET diagnostic programs can be run which monitor the performance of the network, the front end and the CAMAC link. These will quickly point out any off nominal behavior. The entire fire alarm system is periodically tested with FIRUS being used for transmission of test results. Thus FIRUS is implicitly tested also on a regular and scheduled basis.

3.8.4 Radiation Safety System

3.8.4.1 Radiation Safety System Technical Requirements and Constraints

All requirements for personnel safety interlock systems (electrical and radiation) are stated in the Fermilab Radiological Control Manual (FRCM, 1998)[1] which is part of the Fermilab ES&H Manual (FESHM, 1998)[2]. They are based on the Code of Federal Regulations, Title 10, Part 835 (10 CFR 835)[3] and Fermilab experience. Three specific examples are given here. First, the circuits must be redundant which means that two independent methods or circuits are used to detect specific conditions. Secondly, the design must be fail-safe. Hardware circuits will use active high for loop and permit signals and the

---

[1] Fermilab Radiological Control Manual, January 1997 edition. This document contains Fermilab's policies for assuring worker safety and protection of the public and the environment from sources of ionizing radiation. It is part of the Fermilab Environment, Safety, and Health Manual (see FESHM, 1998).

[2] "Fermilab Environment, Safety, and Health Manual", January 1997 edition. This document contains Fermilab's policies for assuring worker safety and protection of the public and environment in accordance with Federal, State, and Local Regulations and good management practices.

[3] Code of Federal Regulations, Title 10, Part 835, "Occupational Radiation Protection".

programmable logic controller (PLC) will use an external alternating heart beat signal. Thirdly, there must be additional safety circuits such as an emergency off circuit, a ground fault detection circuit and a PLC controlled circuit for search and secure sequence functions. "Search and secure" requires two people to search the area visually and in the process make up an electronic circuit by turning keys in key boxes in a specified sequence. The sequence ensures that no one enters the area while the "search and secure" is in progress without breaking the interlocks. The safety system will use standard Fermilab safety system hardware, which is reliable and well understood.

Requirements for groundwater are that the groundwater limit for radionuclide content does not exceed the values in the Fermilab Radiological Control Manual (FRCM, 1998). These values are based on Chapter 77 of the Illinois Administrative Code Part 920 (77IAC 920).

Limits on the emissions of airborne radioactivity are specified in 40 CFR Part 61, National Emissions Standards for Hazardous Air Pollutants (NESHAPS), and in Fermilab's emissions permit from the Illinois Environmental Protection Agency (IEPA).

3.8.4.2 Radiation Safety System Design Assumptions

The safety interlock system will use standardized Fermilab safety system hardware. It will consist of several interlocked areas: the pretarget and target hall, the decay region, the absorber region and the muon monitoring caves. Beam loss monitors, beam position monitors, and other instrumentation will be interfaced to the control system and are not included in the personnel safety interlock system. Maintenance activities in the pretarget and target areas while the MI is running will use lockout of NuMI critical devices to keep personnel in those areas safe.

Three groundwater monitoring wells and approximately 20 sampling ports will be installed in order to ensure that the regulatory limits are not exceeded.[4] There is also a Fermilab environmental monitoring strategy that specifies the Fermilab environmental monitoring program, of which NuMI will become a part. The well locations will be based on MARS simulations of the beamline (see Chapter 4) and rock conditions discovered during tunneling. The sampling ports, drilled from inside the tunnel, are costed in the civil estimate (WBS 1.2).

---

[4] DOE/EA-1198, Environmental Assessment – Proposed Neutrino Beams at the Main Injector Project, December, 1997.

The NuMI design assumes that the mitigation of radioactivated air is driven by environmental protection rather than personnel protection, since the areas where activated air is present will generally be unoccupied or minimally occupied. The ventilation system will be such as to keep activated air away from the Experimental Hall (See Chapter 4). Fermilab's permit with the IEPA allows an average emission of 100 Ci/year. It is estimated that NuMI's emissions will comprise approximately 45% of the Laboratory's total.[5] Therefore the design goal is to keep emissions below 45 Ci per year. Stack monitors will be used to monitor performance.

3.8.4.3 Radiation Safety System Description

If the beam is on, a potentially lethal dose of radiation could occur to anyone in the NuMI beam enclosures. Consequently, these enclosures will be interlocked to prevent such an accident. Before the interlocks are made up to permit the beam to be turned on, these areas must be searched and secured to ensure no one remains inside. The same safety interlock system also disconnects power to major devices (e.g. magnets, focusing horns) when enclosure access is enabled.

Several dozen such interlocked areas have been used successfully at Fermilab for over 25 years, all using standardized, well-developed, redundant, fail-safe hardware and procedures. Specific system requirements and procedures are documented in the Fermilab Radiological Control Manual (FRCM, 1998).

There will be several separately interlocked areas in the hadron section of the NuMI tunnel - pretarget and focusing horn area, decay pipe, and hadron absorber area. This design will help minimize the number of time-consuming searches of the 675-meter long decay pipe area, where only infrequent accesses are expected. The muon monitoring areas located between the hadron absorber and the near detector experimental hall will also be separately interlocked.

Considerable work has been done in design of the NuMI beamline to minimize groundwater activation (see Chapter 4 and Fermilab TM 2009). Groundwater monitoring will include three wells located at areas with the greatest potential for groundwater activation, based on MARS calculations and examination of the rock along the beam

---

[5] *Ibid.*

enclosures. These wells will be drilled and monitored before NuMI receives any beam in order to obtain background samples. The initial monitoring frequency will be quarterly, with modification as necessary. Several sampling ports (~20) will also be drilled out from the tunnel walls. Water collected from these will provide calibration for shielding calculations and early indication of immediate area activation (within the calculation zone). This monitoring program will also be adopted into the Fermilab Environmental Monitoring Strategy.

Air activation will occur at beam loss points and in regions where the beam passes through air, especially in the Target Hall and the Hadron Absorber. Design of the ventilation system brings air in through the upstream and downstream shafts so as to move air through these regions away from occupied areas and toward the middle of the decay tunnel. Here the air will be vented to the surface through ventilation shafts. This will maximize the time before venting the radionuclides, which are short-lived, and thus minimize the radioactivity released. Stack monitors at these locations will monitor releases.

3.8.4.4 Radiation Safety System Design Validation

The radiation safety system design, construction and installation validation/review will be performed by engineers, Beams Division/FNAL technicians, and ES&H personnel. The safety interlock system will have an internal Beams Division design review and a required formal review (FRCM, 1998) by the Fermilab Interlock Coordinator. A formal safety interlock system test is also required before commissioning (FRCM, 1998). The air activation and groundwater monitoring systems will also have an internal Beams Division design review and a required formal review (FRCM, 1998 and FESHM 8011) by Fermilab ES&H Personnel.

3.8.4.5 Radiation Safety System Construction Plan

The personnel safety interlock system will use standard Fermilab safety hardware. This provides great cost savings in both materials and labor since much of the equipment will already exist and be well understood. The devices that need to be constructed for the personnel safety interlock system will be made from standard Fermilab safety system hardware.

3.8.4.6 Radiation Safety System Installation Plan and Issues

The personnel safety interlock system is a small labor item and should easily fit into the installation schedule. Gates and barriers for the personnel safety interlock system will be installed last in order not to interfere with other installations. Wiring for this safety system can be done in advance and terminated at the locations of the gates; thus easing final installation requirements.

The ground water monitoring wells will be installed after the tunnel has been excavated, but well in advance of the onset of beam. Installation will be by conventional drilling methods and according to regulations (77IAC 920). The stack monitors for air activation will also be installed well in advance of the onset of beam so that they can be tested.

3.8.4.7 Radiation Safety System Pre-commissioning Plan

The personnel safety interlock system must go through a formal pre-commissioning test before beam is enabled. The critical devices, alarm system, sequence system and all access points are tested as required by the FRCM (FRCM). The personnel safety interlock system can not be fully tested until the critical devices are installed and operational. Groundwater monitoring wells and sampling ports will be installed and background samples taken. Similarly the stack monitors will be tested.

3.8.4.8 Radiation Safety System Performance Monitoring Plan

The personnel safety interlock system is connected to a Status System which monitors the status of many parts of the safety system. Also, personnel safety interlocks must be tested every 6 months. The Status System, logged data and biannual tests will point out required repairs. Since spare parts exist and the system is standard, repairs should not be difficult.

Groundwater will be monitored frequently in the sampling ports and quarterly in the wells as NuMI begins beam operation. The groundwater monitoring program and procedures will be outlined in the Fermilab Groundwater Protection Procedures Manual, the Fermilab Groundwater Protection Management Plan, and the Fermilab Environmental Monitoring Strategy. Similarly the stack monitors will be used to determine the level of activated air released by NuMI. Trend analysis of the sampling results will be used at an early stage to project levels for sustained high intensity operation.

3.8.5 Cable System

3.8.5.1 Cable System Technical Requirements and Constraints

A requirement for cables is that those for power supplies, communications and controls be isolated as necessary. Cable selection will consider radiation levels and voltage drop in choosing cable type, gauge and noise reduction requirements. Cables should not present any performance limits, as specifications will be based on EIA/TIA standards. Note that the costs and installation of the power supply cables are covered in WBS 1.1.3.

3.8.5.2 Cable System Design Assumptions

It is assumed that the civil construction provides cable trays as described in Chapter 5, along the beamline, except in the MI and NuMI Stub enclosures. Cable requirements are based on the NuMI beamline described in this report. Control and communication cables are included in this system. Power supply cables are covered in WBS 1.1.3. Cable trays will need to be added to the MI and NuMI Stub areas and the NuMI service buildings. Where it is sensible, TV, computer networking and FIRUS cables will all be run along the same route with the beamline power.

3.8.5.3 Cables System Description

The cables for the NuMI beamline consist of control cables, communication cables, power supply cables, etc. These cables will be procured, installed, and terminated as necessary. Much of the cabling work will be done under contract. Table 3-8-4 summarizes the cables needed for the various systems. The schedule increases these determined cable lengths by 20% and includes the extra manpower to cover this. Power supply cables are not included in WBS 1.1.8, but are included in the table for completeness.

3.8.5.4 Cable System Design Validation

The cables system design and installation validation/review will be performed by engineers and/or Beams Division/FNAL technicians. A labeling system and database will be used for NuMI cables, accessible by NuMI personnel. Level 3 managers will determine their systems cabling needs, these needs will then be checked first informally and then formally as a cable system review. A specification sheet will be written describing how the cables are to be installed and tested, and this sheet will be reviewed with the cabling contractor.

Fermilab will then assign a task manager/coordinator to the contract to oversee and witness the installation and testing of the cables.

3.8.5.5 Cable System Installation Plan and Issues

Termination of cabling of power supplies, beamline devices and controls can only occur once the devices the cables are to be connected to are installed. Cabling will probably be done first in the existing enclosures, depending on accessibility, and later in the new construction.

Cables will be pre-commissioned as magnets, instrumentation, power supplies and the controls system are pre-commissioned, thereby pointing out any cabling problems. Sufficient spare cables will be laid to accommodate foreseeable problems.

Item	Count/Description
Water System monitors	ICW, LCW, RAW
Vacuum System controllers	Digital interfaces (CIA crates included in utilities)
Thermocouple readouts	About 60 required
Loss Monitor readouts	20 presently specified
Power Supply controllers	Standard ramp cards with power supply interface
BPM controllers/readouts	7 H/V pairs; several types of interface are available
Primary Beam SWIC controllers/readbacks	5 required
Super SWIC 90 controller/readback	Similar controllers exist
Super SWIC 250 controller/readback	May require expanded readback capability
SEED controllers/readbacks	2 required
Horn Field monitors	B-dot coils; new instrumentation but standard controls
Accelerator Clock modules	Receivers, fanouts, timers. Some required in all control locations including MINOS cavern
Relay racks, CAMAC crates	Presently ~21 relay racks and 6 CAMAC crates
Repeaters	Both fiber and copper; as required for all links including clocks
Stepping Motor controls	16 channels required for target station
Horn Power Supply controls	7 C-series in house cards
Target Station Component interlocks	2 in house boxes

Table 3-8-1 Standard Controls Items

Item	Resources required
Fast pulse capability in QXR	1 month programmer
Target Station PLC controls	1 PC, ~10 electronics cards attached thereto 1 month programmer
Toroid Monitor current readout/display and cross calibration	1 month programmer
Transmission of appropriate digital, timing and TV information to Soudan	2 months engineer
Implementation AUTOTUNE for NuMI primary beamline	2 months beamline physicist
Console schematic beamline displays	6 months physicist/programmer

Table 3-8-2 NuMI Specific Controls.

Item	Count/Description
Remote control color cameras	7, for fire watch
Fixed black & white cameras	4, for technical beam information
Monitors and keyboards	8 monitors, 4 keyboards, for CCTV
TVs	Approximately 9, in various NuMI locations
FIRUS minis	4

Table 3-8-3 CATV, CCTV and FIRUS Controls Items.

Table 3-8-4 NuMI Cable Estimates (See insert).

	MI60 Service Building			MI62 Service Building			Target Hall Service Buildi		
	Cable	Material Cost	Labor Cost	Cable	Material Cost	Labor Cost	Cable	Material Cost	Labo
Cable Type	(No. of)	($)	($)	(No. of)	($)	($)	(No. of)	($)	(
leutrino Monitoring Cables	0	0	0	0	0	0	5	2,300	
nstrumentation Cables	65	9,900	28,100	37	11,700	18,300	50	12,800	2
ower Supply Power Cables	39	21,800	33,900	36	31,400	43,600	21	12,400	2
Controls Cables	17	500	1,100	22	800	1,600	74	4,400	1
Cable Tray									
Vacuum & Water									
V Systems									
(mainly hardline cable)									
Computer Networking									
(mainly optic fiber cable)									

ice Building		Downstream Service Building			Total				
ost	Labor Cost	Cable	Material Cost	Labor Cost	Cable	Material Cost	Labor Cost	Total Cost	Contingency
	($)	(No. of)	($)	($)	(No. of)	($)	($)	($K)	
00	3,000	81	46,800	100,400	86	49,100	103,400	152,500	10%
00	26,700	6	3,400	8,400	158	37,800	81,500	119,300	10%
00	23,800	2	1,400	3,500	98	67,000	104,800	171,800	10%
00	11,500	2	100	200	115	5,800	14,400	20,200	30%
						27,200	27,200	54,400	50%
						63,500	49,500	113,000	30%
						9,600	33,600	43,200	30%
						46,000	28,000	74,000	30%

Table 3-8-4

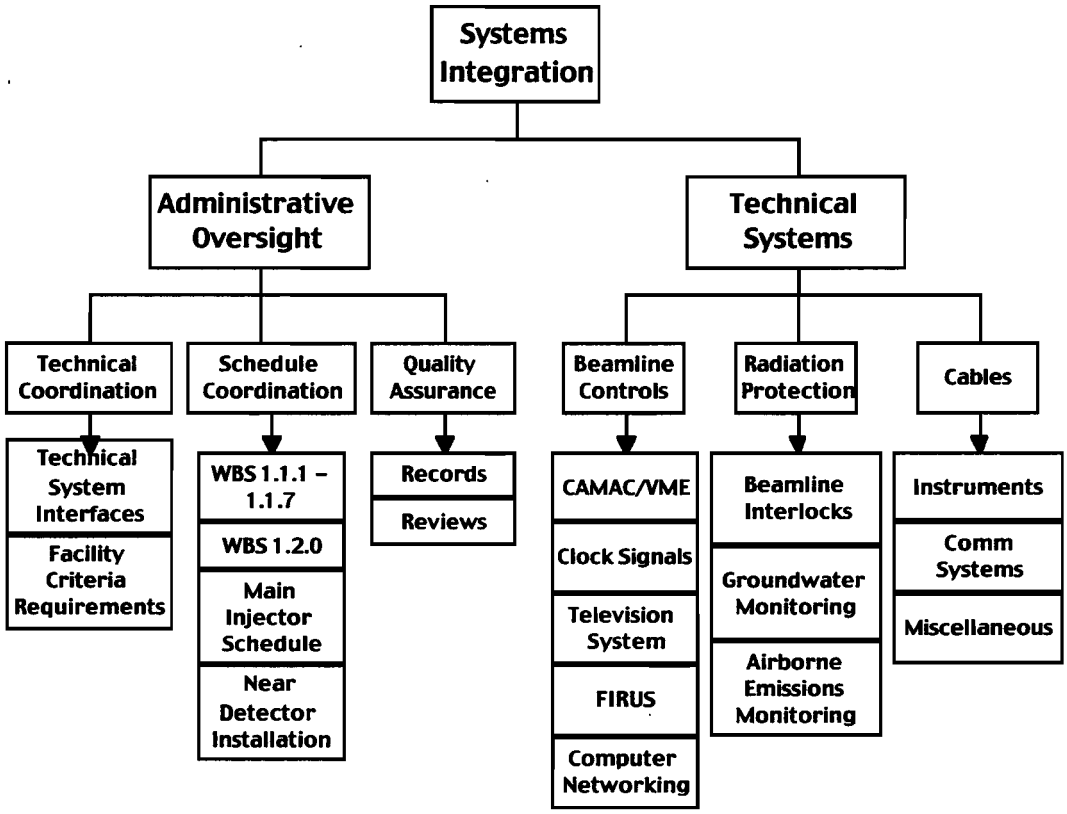

Figure 3-8-1 Systems Integration Overview.

4.0 Radiation Safety

Table of Contents

4.0 RADIATION SAFETY 4-1

4.1 INTRODUCTION 4-4

4.2 TYPES OF RADIATION AND METHODS OF MITIGATION AND EVALUATION 4-5

4.2.1 Types of Radiation 4-5

4.2.2 Regulatory Limits 4-6

4.2.2.1 Methods of Mitigation 4-8

4.2.3 Methods of Evaluation 4-9

4.2.3.1 Prompt Radiation 4-10

4.2.3.2 Residual Radiation 4-12

4.2.3.3 Airborne Activation 4-13

4.2.3.4 Groundwater Irradiation 4-14

4.3 EVALUATION METHODS FOR NUMI 4-18

4.3.1 Prompt Radiation 4-18

4.3.2 Residual Radiation 4-20

4.3.3 Airborne Activation 4-21

4.3.4 Groundwater Irradiation 4-23

4.3.4.1 The local geology 4-23

4.3.4.2 The Hydrogeology Factor, Fi , revisited 4-24

4.3.4.3 Direct Production of ^{3}H 4-25

4.4 CONCEPTUAL DESIGNS OF THE NUMI SHIELDING 4-27

4.4.1 Target Hall 4-28

4.4.2 Decay Tunnel and Beam Absorber 4-28

4.4.3 Options for Facility Reconfiguration 4-29

4.4.4 Groundwater Monitoring 4-29

4.5 CONCLUSION 4-29

Table of Tables

Table 4-1 Summary of area posting requirements ____ *4-31*

Table 4-2 Summary of "beam-on" prompt radiation protection requirements ____ *4-31*

Table 4-3 Regulatory limits on allowed radionuclide concentrations in groundwater and surface water. Units are in pCi/ml. ____ *4-31*

Table 4-4 Densities of materials to be used in or around the NuMI Facility ____ *4-32*

Table 4-5 Conversion factors (simulation output to dose equivalent) for prompt and residual radiation. The conversion factors for residual dose are for the conservative case of infinite irradiation, zero cool down. ____ *4-32*

Table 4-6 Groundwater leachability factors used in NuMI shielding analysis. ____ *4-32*

Table 4-7 Determination of S_{avg} and G for each region of the facility for the baseline medium energy beam. Similar calculations have also been done for the low and high energy options. ____ *4-33*

Table of Figures

Figure 4-1 Flow chart of radiation protection analysis procedure. ____ *4-34*

Figure 4-2 Concentration "build-up" vs. time for ^{22}Na and ^{3}H. ____ *4-35*

Figure 4-3 Schematic illustration of the parameters required to calculate the "average" star density in the 99% volume. R represents the radial extent over which the volume is averaged. ____ *4-36*

Figure 4-4 Radial fall-off of star density for two values of z along the decay pipe. ____ *4-37*

Figure 4-5 Illustrative example of leaching curves showing the saturation as a function of the weight of water passing through the medium. (The curves are drawn to guide the eye). ____ *4-38*

Figure 4-6 Weighted sum of the build-up of the radionuclide concentration vs. running time for several values of the average star density. ____ *4-39*

Figure 4-7 Comparison of the concentration (per unit volume) of tritium from direct production vs. leaching. ____ *4-40*

Figure 4-8 Separate concentrations for sodium and tritium where the tritium concentration has been derived for the maximum probability of direct production. The consequence is that the limit on the average allowable star density is reduced by a factor of 3. ____ *4-41*

Figure 4-9 Results of the MARS simulation used to determine the amount of shielding required in the Target Hall for the medium energy beam configuration. ____ *4-42*

Figure 4- 10 Conceptual Design cross section of a radiation shielding "module" for regions of the Target Hall containing the active elements (target and horn). 4-43

Figure 4-11Conceptual Design cross section of a radiation shielding "module" for regions of the Target Hall not containing the active elements. 4-44

Figure 4-12 Results of the MARS simulation used to determine the amount of shielding required in the decay tunnel and beam absorber hall for the PH2ME (medium energy) beam configuration. The configuration of the shielding used in the simulation is also shown. 4-45

Figure 4-13 Attenuation of the star density as a function of the thickness of the concrete shield. 4-46

Figure 4-14 Results of the MARS simulation used to determine the amount of shielding required in the Target Hall for the PH2LE (low energy) beam. 4-47

Figure 4-15 Simulation results for the low energy beam showing the resulting star density compared to the allowable limits as determined for the range of G factors for the decay tunnel. 4-48

Figure 4-16 Comparison of the star density for the medium energy beam configuration as compared to predicted residual dose rates (closed target pile). 4-49

4.1 Introduction

Chapter 3 of this Report presented technical designs for each of the subsystems required to produce the neutrino beam for the NuMI physics program. Inherent in the designs is the fact that radiation protection is of the greatest importance in both primary and secondary beam areas. The purpose of this Chapter is to present the various radiation-related matters and to explain the methodology that has guided the designs of the radiation protection systems in the project. It should be noted that at this stage of the project we have attempted to address all of the major issues that have an impact on determining a baseline design for the facility construction project. There are however, a number of topics that continue to be studied. These include radiation protection issues associated with the Main Injector extraction, quantitative evaluation of the level of airborne activation expected in the target hall and finally a quantitative assessment of potential activation from the direct production of tritium in the groundwater in the vicinity of the underground facility.

The design of the Fermilab Main Injector permits the acceleration of numbers of protons previously unthinkable in the energy regime above 100 GeV. The design of the NuMI Facility assumes that Main Injector protons will be transported to the target at an average intensity of 4×10^{13} protons every 1.9 seconds. Physics goals of the MINOS experiment assume a value for beam on target of 3.7×10^{20} protons per year. To set the scale, this annual value is comparable to the total accumulated protons on all Fermilab target stations, including antiproton, since the founding of the laboratory. For the purposes of designing radiation protection for the NuMI Facility, the above intensities translate to an instantaneous proton rate of 2×10^{13} protons per second and an annual "dc" average of $\sim1\times10^{13}$ protons per second.

The extraction for the primary proton beam to NuMI will take place within the Main Injector enclosure and the first phase of the beam transport will be in the NuMI Extraction Stub. Both of these regions will be located in the glacial till, and prompt radiation concerns are primarily addressed by the use of earth shielding. Downstream of the NuMI Extraction Stub the primary proton beam will be transported through a carrier tunnel, which will penetrate through the till/dolomite interface. The majority of the NuMI Facility will be located in dolomite bedrock, which, by state regulations, is a Class 1 groundwater aquifer.[1] This requires particular concern in the design of the shielding, which must be adequate to meet standards applicable to potential sources of potable water.

---

[1] Illinois Administrative Code Environmental Regulations, Title 35 - Environmental Protection, Subtitle F - Public Water Supplies, Chapter I - Pollution Control Board, Part 620 – Groundwater Quality

As discussed in Chapter 2, an important consideration in the design of the NuMI Facility has been the desire to maintain the flexibility to accommodate a variety of neutrino beam configurations. This flexibility includes designing a target hall in which the location of the beam line components such as the target and the focusing horns may vary depending on the desired range of neutrino energy. Also, an option for a future configuration of the beam may be for a narrow band beam, which would require the installation of a primary beam dump in the mid-section of the target hall. Maintaining this flexibility has an impact on the design of the radiation shielding because of the desire to minimize the reconfiguration of the target hall shielding after the facility has begun operation.

4.2 Types of Radiation and Methods of Mitigation and Evaluation

4.2.1 Types of Radiation

There are four types of radiation which are of concern in the design of a facility such as NuMI. These are 1) the prompt radiation field, 2) the residual radiation field, 3) airborne activation and 4) groundwater irradiation.

The *prompt radiation field* at particle accelerators and beam lines exists only while they are in operation. In general, the higher the energy of the particles accelerated and transported, the more complex the character of the prompt radiation field will be. Depending on the configuration of the facility and its components, the nature of the prompt radiation fields may include thermal neutrons, fast neutrons, photons or muons.

The *residual radiation field* is that which remains or lingers after the beam has been shutdown. This remnant radiation field results from the decay of radioactivity induced in the facility structure and its components by the interaction of the constituent particles of the prompt radiation field. Its precise characteristics will depend on many factors such as the type and energy of the particles, the beam intensity and the nature of the materials irradiated by the primary and secondary particles. In most situations at Fermilab, the residual radiation field is almost exclusively gamma rays, with the occasional presence of beta rays near a contaminated surface.

Airborne activation results from the interaction of primary and secondary particles directly with constituent target nuclei of the air or other gaseous medium which later mixes with the air. A secondary source of airborne activity is dust, formed by natural erosion or wear or by work on radioactive accelerator components. The third and final source of airborne radioactivity results from the emission of gaseous radioactivity from liquids irradiated in the accelerator produced radiation

environment. Activities in radioactive air consist primarily of ^{11}C, ^{13}N, ^{15}O sometimes with a little ^{41}Ar; all with relatively short half-lives.

Groundwater irradiation can occur due to the fact that radionuclides produced in the soil or rock surrounding an accelerator or beam line enclosure have a finite probability of leaching into water passing through the soil or rock, and that water later migrates to or mixes with a potential source of potable water. The production of these radionuclides is dependent on the beam parameters such as energy, particle type, intensity and target configuration, while the soil or rock activation and migration to groundwater is dependent upon the details of the local hydrology. Knowledge of media constituents, possible activation products, and a number of published leaching analyses of activated soil and rock samples has shown that the only two radionuclides that require consideration in the environment surrounding Fermilab are ^{3}H and ^{22}Na.

4.2.2 Regulatory Limits

The level to which these types of radiation must be controlled is determined by requirements that consist of regulatory guidelines from various governmental agencies, internal Fermilab rules (expressed in the Fermilab Radiological Control Manual[2] (FRCM)) and commonly accepted guidelines and work practices. The Laboratory has monitoring programs in place to assure that the requirements are met. In general the purpose of such programs is to provide an early warning that a specific limit might be approached and to lead to a curtailment of the activity leading to the problem. There are programs in place to monitor radiation exposures to personnel and the general public and to check for radionuclides in groundwater. Occupational radiation exposures must be controlled in accordance with the Federal Regulation 10CFR835[3]. The chief statement in this regard is that all workers dealing with activated components keep their exposures ALARA (As Low As Reasonably Achievable). The specific requirement on exposures to general employees is a limit of 100 mrem/yr. For radiation workers this limit is 5 rem/year. However, by Laboratory policy the Laboratory Director's approval is required before any individual is allowed to surpass 1.5 rem/yr.

The posting of radiation areas is discussed in Article 234 of Chapter 2 of the Fermilab Radiological Control Manual, and the requirements are summarized in Table 4-1 of this Chapter. The definition of a radiation area corresponds to the presence of dose rates between 5 and 100 mrem/hr; localized areas

---

[2] Fermilab Radiological Control Manual (formerly known as the Fermilab Radiation Guide); copies are available from the Fermilab E,S&H Section.

[3] Reference 10CFR835

are to be identified with an exposure rate sticker/label if they exceed 20 mrem/hr. Regulatory limits on radiation exposure to either the general public or radiation workers require that the prompt radiation field be evaluated for both normal operating conditions of the accelerator and/or beam lines and for potential accident conditions. The limits on the radiation doses and corresponding classifications of areas that are allowable for each of these conditions are summarized in Table 4-2.

Controlling the rate of residual radiation is important to minimize exposure to personnel when entering an enclosure after beam has been turned off. In many cases the chief source of such residual radiation is the shielding itself which surrounds highly activated components such as targets, focusing elements and beam absorbers. Work in areas containing levels in excess of 200 mrem/hr requires approval of a Radiation Safety Officer.

Fermilab is required to comply with the National Emissions Standards for Hazardous Air Pollutants (NESHAPS) as set forth in 40 CFR Part 61. Among other things, this regulation sets forth the requirements for monitoring airborne radioactivity. Off-site releases of airborne radionuclides from the entire Laboratory are limited by the Laboratory's permit application to 100 Curies/year average and 900 Curies/year maximum. The maximum off-site dose equivalent at any given point is limited to 10 mrem/year, and if the dose equivalent at the point of maximum exposure were to exceed 0.1 mrem/year the Laboratory would be required to implement an "EPA-approved" continuous monitoring program.

There are also regulations controlling occupational radiation exposures to airborne radionuclides.[4] The Derived Air Concentrations (DACs) for ^{11}C, ^{13}N and ^{15}O are $4x10^{-6}$ μCi/ml, applicable to radiological workers. The DAC is that concentration of a radionuclide in air which, in a 2000 hour working year, would deliver an annual exposure limit (internal or external) to the worker. However, since workers at Fermilab do not work full time in areas that have such potential concentrations the actual limits do not come into play. Rather, the DACs do require the Laboratory to post notification of an airborne radioactivity area in any regions where the concentration is >0.1DAC.

Limits on the radionuclide concentrations in groundwater and surface water are found in Chapter 11 of the Fermilab Radiological Control Manual. The ^{3}H and ^{22}Na concentrations come from two different regulations – DOE Order 5400.5 and 40 CFR 141. The standards, though differing somewhat from each other, are designed to limit doses to users of the water as their source of drinking water to 4 mrem per year. The concentration limits turn out to be 20 pCi/ml of ^{3}H or 0.4

---

[4] 10CFR835

pCi/ml of ^{22}Na. Additionally, the regulatory limit on the weighted sum of the concentrations in the groundwater is not to exceed unity, i.e.:

$$\frac{C_f(^3H)}{C_{reg}(^3H)} + \frac{C_f(^{22}Na)}{C_{reg}(^{22}Na)} \leq 1,$$

where C_{reg} (^{A}Z) is the regulatory limit on the concentration for isotope ^{A}Z. (For surface water the limit goes up to 100 mrem/year, with a corresponding increase in the allowable concentrations.) These requirements pertain to amounts of isotope built up in the groundwater resource over time, not to a rate of production. The current regulatory limits for both groundwater and surface water discharge are summarized in Table 4-3.

4.2.2.1 Methods of Mitigation

The most straightforward and common way to implement radiation protection in an accelerator facility is through the use of shielding. While one could consider a variety of dense materials to be used for passive shielding, experience has shown, that particularly for economic reasons, only three are normally considered, namely, earth, concrete and steel. Occasionally, for some special circumstances such as attenuation of very low energy neutrons or gamma rays borated polyethylene or lead may be used. A summary of these typical shielding materials is given in Table 4-4.

Ordinary concrete is an inexpensive, easily handled material whose nuclear properties are good enough, taken in conjunction with its excellent structural properties, to make it desirable as a shielding material. Concrete may be used either in the form of modular blocks or as reinforced concrete to be poured or pumped into place to create an immobile and essentially inflexible structure. The use of concrete blocks to construct shield walls and roofs adds an essential degree of flexibility, especially if a change in the shield design and configuration is necessary. A typical value for the density of concrete is 2.35 g/cm^3, though it can be obtained with densities varying by as much as ±20% of this average value.

The use of special, low sodium aggregates may be used to reduce thermal neutron induced radioactivity of concrete and consequently residual radiation levels after the beam is turned off. The same result may be obtained by addition of boron compounds.

The use of steel is particularly advantageous when space considerations require compact shielding. Its relatively high density, which is roughly three times that of ordinary concrete, facilitates great savings in space. As with the case of earth and concrete, the density of steel materials can vary. A low-grade cast iron may only have a density of 7.0 g/cm^3, but typical steel used for shielding has a density of 7.8 g/cm^3.

General guidelines that are used in the design of shielding are that one foot of steel will reduce a radiation field by a factor of 10 and is equivalent to three feet of concrete. The specific choice and arrangement of materials for a given beam line configuration are generally determined by space and financial considerations.

In addition to the use of shielding as a passive way to provide radiation protection, there are several common circumstances where it is more appropriate and practical to use a more "active" method of mitigation. The most common of these is the use of interlocked radiation detectors. An interlock system can remove beam in a fail-safe manner from any enclosure when the beam-on rate exceeds a pre-determined threshold.

4.2.3 Methods of Evaluation

When high energy particles strike an object, there is a shower that builds up and then diminishes. The build up will generally occur within the shielding of the protected region. Beyond shower maximum in the unprotected region, the fall-off in the radial and longitudinal dimensions varies exponentially. The nature of this fall-off is dependent on the particular geometry of the beam and shielding being used. To study the build-up, fall-off and methods of attenuation, Monte Carlo programs are used. A short review of these simulation programs has been given by Mokhov and Cossairt.[5] These programs simulate the particle interactions and can be used to determine how much shielding is required to protect personnel and the environment. Because modeling the paths and interactions of each individual particle through bulk shielding is very "CPU" intensive, approximations are devised. The most common one is to select a representative set of particles produced in the initial interaction and weight them according to data on the inclusive production of those particles. For example, a proton hitting a target creates five pions of varying energies and directions. The five particles are simulated by creating one pion with an energy and direction made

[5] N, V, Mokhov and J. D. Cossairt, Nuclear Instruments and Methods in Physics Research A244 (1986) 349-355.

from a weighted combination of the real ones. This "new" pion is then assigned a weight greater than one, to be used in subsequent calculations.

Prior to the spring of 1998, Fermilab used a program called CASIM[6] for this task. CASIM proved to be sufficient for the bulk shielding design for high energy (> 50 MeV) particles. Recently however, for a variety of reasons, the program MARS[7] has been adopted. The baseline design of the NuMI shielding, which is described below, is based on the use of the MARS simulation. MARS and CASIM both use the inclusive approximation, but MARS tracks a subset of different types of particles with a range of energies, whereas CASIM just tracks one particle, typically the highest energy one. For this reason MARS agrees with data over a wider range of energies than does CASIM.

The "output" of the Monte Carlo calculations is either a particle flux (particles/cm^2/incident proton) or "star" (i.e. nuclear interaction) density (stars/cm^3/incident proton). Particle fluxes or star densities are subsequently converted to activation or dose equivalents or used to determine the probability of radionuclide production in the air, soil or rock in which the nuclear interactions occur. These doses can then be compared to the various regulatory limits for each type of radiation exposure. For example one must compare the level of radiation in the groundwater produced by a certain beam line and shielding configuration to that which would lead to a residual radiation problem inside that same hall. A simple flow chart outlining the radiation protection analysis procedure is presented in Figure 4-1. The simulation output to dose rate conversion factors for prompt and residual dose rates are summarized in Table 4-5. The methodologies for using each of these as well as the way to convert stars or flux to dose for airborne or groundwater radiation are described in the sub-sections below.

4.2.3.1 Prompt Radiation

As stated above the prompt radiation field must be predicted and mitigated for both normal operations and accident conditions. In addition to evaluating the radiation field outside of enclosures which are normally embedded and/or covered by bulk shielding comprised of rock and/or soil, one must also evaluate the "leakage" of radiation through labyrinths and penetrations which connect the source of radiation to the unprotected regions of the surrounding environment. While the methods and

---

[6] A. Van Ginneken, "Weighted Monte Carlo Calculations of Hadronic Cascades in Thick Targets", NAL-FN-250 (1972).

[7] N. V. Mokhov, "The MARS Code System User's Guide",Fermilab-FN-628 (1995); Update Version 13(98), February, 1998

$$H = \frac{N_p H_0 E_p^m}{r^2} \exp(-\beta\theta)\exp(-d(\theta)/\lambda)$$

calculations are different for these two situations the requirements outside of the facility are the same. Both a qualitative and quantitative evaluation of the amount of bulk shielding, d, which will attenuate a prompt radiation field is given in terms the dose rate, H, outside for the shield by Moyer[8], where

N_p	Number of protons
E_p^m	energy of the protons and m is the scaling power
r	is the distance from the source to the beginning of the shield
θ	is the angle of the particle shower, with respect to the beam direction
β	is the "relaxation parameter" related to the fall of the radiation around $\theta = \pi/2$
λ	is the interaction length of the shielding medium

For calculations of the required amount of bulk shielding it is appropriate to use the results which have been well established by the simulations done for a relevant set of case studies. These results are documented[9,10] and accepted for use in the design of bulk shielding at Fermilab.

The prompt radiation field must also be evaluated outside of penetrations into enclosures in which there is prompt radiation being produced. Such penetrations include entrance ways (generally constructed in the form of labyrinths), conduits or ducks, as well as cracks. The methodology used to evaluate and design penetrations is based on a two step approach – evaluation of the source strength, followed by determination of the attenuation through the penetration. The source term is given by the following equation:

$$\phi_n = N_p \frac{1}{4\pi r^2} E_p^{0.8}$$

where again

---

[8] A summary of the Moyer Model is presented in Appendix 4A of Radiological Safety Aspects of the Operation of Proton Accelerators, R.A. Thomas and G.R. Stevenson, *Technical Report Series* No. 283, International Atomic Energy Agency, Vienna, 1988.

[9] A. Van Ginneken and M. Awschalom, "High Energy Particle Interactions in Large targets", Fermilab, 1975, (available from the Publication's Office).

[10] J. D. Cossairt, "A Collection of Casim Calculations", TM-1140, October 22, 1982.

N_p Number of protons
E_p energy of the protons

The flux is converted to dose equivalent using the conversion factor 3×10^7 neutrons/cm^2-rem. Attenuation curves for both the first and subsequent legs of the penetration are summarized in Thomas and Stevenson[11].

4.2.3.2 Residual Radiation

The dose rates due to residual activation of shielding and other beam line components can be estimated from the results of the same Monte Carlo simulation used to determine the prompt radiation shielding. The rates depend on assumptions about typical irradiation and cool-off times as well as the type of activated material. The most conservative assumption is that of infinite irradiation and zero cool-off times, which results in the highest estimated levels of activation. The method of dose rate estimation is summarized in the Fermilab Radiological Control Manual and is based on the work of Barbier[12]. The dose rate is given by:

$$\frac{dD(\vec{r})}{dt} = \frac{\Omega}{4\pi}\frac{dS(\vec{r})}{dt}\omega\left(t_i, t_c\right) = \frac{\Omega}{4\pi}\cdot\Phi(E)\cdot d\left(t_i, t_c\right),$$

where

$$\frac{dS(\vec{r})}{dt} = S(\vec{r})\cdot N_{protons/spill} / \Delta t_{spill}$$

Particle flux is related to the star density by:

$$\Phi = \frac{\lambda}{\rho}S$$

[11] Op. Cit. Thomas and Stevenson, pp. 274 and 276.

[12] M. Barbier, "Induced Radioactivity", North Holland Publishing Company, (1969)

The radiological conversion factors ω and d are likewise related:

$$\omega = \frac{\lambda}{\rho} d$$

$\Omega/4\pi$ is the fractional solid angle subtended by the source at the measurement location

$\omega(t_i, t_c)$ is the material-dependent conversion factor, for an irradiation time of t_i and cool-off of t_c, that converts star density at the surface of the material to dose rate.

$S_{surface}$ is the calculated star density at the surface of the material of interest

N_p is the number of protons

Δt_s is the duty cycle

During the design of the "TeVII" facilities at Fermilab, steel target pile shielding was designed so that the residual dose rate at the outer surface of the shield would be no more than 100 mrads per hour, and significantly lower in areas where it is anticipated that frequent access for maintenance and repair will be required.

4.2.3.3 Airborne Activation

Air activation can be estimated using the following well-established formula for the concentration per unit volume:

$$C = \sum_i \sum_j N_j \sigma_{ij} \phi \left(1 - e^{-\lambda_i t}\right)$$

where

N_j is the partial density of the target atom j being irradiated

σ_{ij} is the cross section for producing nuclide i from target j

ϕ is the flux density of the particles through the air or gas volume

λ_i is the decay time of the radionuclide i

t_{ir} is the irradiation time

Once the concentration of the relevant nuclides has been determined, the volume of air that may become activated must also be determined. This must then be compared to the volume of air within the enclosure which is not directly activated, but with which the activated air can mix, taking into account the relative frequency with which the air exchanges take place. This final concentration then becomes the concentration of interest when evaluating the exchange of this larger volume of air with the outside environment.

4.2.3.4 Groundwater Irradiation

Analysis of potential irradiation of the groundwater is done using the Groundwater Radionuclide Concentration Model[13] , which was developed principally to apply to the case of a near-surface target station located in the glacial till several meters above a groundwater aquifer. The model was adopted at Fermilab in 1993 to replace the Single Resident Well Model (SRW).[14] At that time it was noted that application of the new model to a situation such as NuMI would require some modifications to the model. These modifications will be described below. To clarify their motivation we briefly describe the basic principles of the standard concentration model. The model very conservatively assumed that radioactivity builds up to its saturation value in soil surrounding a target station or beam dump without any removal due to flowing water. (For ^{3}H this only occurs after 50 years of continuous irradiation, with no removal.) After the buildup to saturation levels, water is assumed to pass through the soil and leach out the radioactivity. In this model the initial concentration, C_o of a particular radionuclide, i, C_{oi} (in picoCuries per milliliter per year) in water close to the target station or dump is given by :

$$C_{oi}\left(\frac{pCi}{ml-yr}\right)=\frac{1}{0.037}N_P S_{avg}\frac{K_i L_i}{\rho_s w_i}$$

---

[13] A.J. Malensek, et al., "Groundwater Migration of Radionuclides at Fermilab", TM-1851, August 1993

[14] Environmental Protection Note 8, "Use of a Concentration-Based Model for Calculating the Radioactivation of Soil and Groundwater at Fermilab", J. Donald Cossairt, December 1, 1994

The factor (1/0.037) is the conversion factor required to convert disintegrations per second to picoCuries. The other factors in the equation are defined below. The first two are directly related to the design and operating parameters of the facility, whereas the later four are determined by the geological medium in which the facility is located, and later grouped into a single parameter labeled F_i.

N_p is the number of incident protons per second

S_{avg} is the average star density (in stars/cm^3) per incident proton in a region of unprotected soil or rock close to the source of the production.

K_i is the radionuclide production probability per star

L_i is the leachability factor for the radionuclide

ρ is the material density

w_i is the weight of water divided by the weight of soil needed to leach 90% of the leachable radioactivity that is present

The final concentration in the groundwater, C_f, for a particular radionuclide is related to the initial concentration by :

$$C_f = C_i \cdot R_{till} \cdot R_{mix} \cdot R_{dolomite}$$

where R_{till} is a reduction factor in the model that takes into account the migration of radionuclides downward through the soil (glacial till) to an underlying aquifer and includes dispersion and radioactive decay en route. R_{mix} is a reduction factor that takes into account concentration reduction due to mixing in the transition region at the aquifer boundary where the flow changes from vertical to horizontal, and $R_{dolomite}$ is a reduction factor that takes into account dispersion and radioactive decay in the horizontal flow of the aquifer en route to some distant location, e.g. the site boundary or nearest drinking water well.

Several modifications to the basic concentration model have been included for the design of the NuMI facility. Since the NuMI design locates the target station and the decay tunnel in dolomite bedrock below the region of glacial till no credit can be taken for concentration reduction due to vertical migration through the till or for mixing at the till-dolomite interface, hence we conclude that the final concentration is simply equal to the initial concentration, $C_f = C_i$.

On the other hand we have removed the assumption that the radionuclide concentration has actually built up to saturation before leaching into the groundwater would begin. Rather, the actual "build-up factor" related to the mean lifetime of the nuclides is taken into account, giving the modified equation below. The build up for sodium and tritium are shown in Figure 4-2.

At the end of a run of time t_{ir}, $C_i(t)$ is given by:

$$C_{oi}\left(\frac{pCi}{ml-yr}\right)=\frac{N_p S_{avg} K_i L_i (1-e^{-t/\tau_i})}{0.037 \rho_s w_i}$$

λ_{he} is the inverse mean lifetime of radionuclide i, measured in units consistent with those of time t_i

The Number of Protons, N_p

The proton intensity is expressed in protons per second, taking into account the average number of protons delivered to the target per cycle as well as an overall efficiency factor for operation of the beam line. The value of N_p chosen should be representative of the average annual proton delivery. Given the nature of the Fermilab operations cycle, it is recommended that this average be taken over a three-year period. For the NuMI Project it has been assumed that an average intensity of 4×10^{13} protons per 1.9 second cycle time will be achievable at an overall efficiency between 50 and 60%. For ease of calculation we have chosen to use a "dc" rate of 10^{13} protons per second for use in the groundwater radiation protection calculations.

The Average Star Density, S_{avg}

The average star density can be obtained from star density contour plots in r and z, by going "out" in r and z from their values for the star density S_{max} at the boundary of the protected to unprotected region (in most cases this is just outside the enclosure) to those radial and longitudinal values at which S has dropped to 1% of its maximum value. The total stars in this volume can be obtained by multiplying the stars in each bin (radial or longitudinal) by the volume of the bin and summing over the number of the bins within that region. S_{avg} is then equal to the total stars within that region divided by the volume enclosed by the limiting values of r and z. This concept is illustrated schematically in Figure 4-3. It is reasonable to use an average over a distance that is of the order of a few meters because the initial distribution is dispersed as water migrates through the region. In the region outside the "99% volume", the production of radionuclides is essentially zero. A quantitative plot of the radial fall off for two different values of z along the decay tunnel is shown in Figure 4-4.
We can determine the average star density within our averaging volume :

$$S_{avg} = S_{\max} \cdot G_{region}$$

Alternatively, the average star density can be related to the maximum star density that is produced just outside the protected region. The "geometry factor", G, is specific to the configuration of the protected regions and the shape of the fall off of the star density. For a very simple geometry such as

a beam dump G can be calculated analytically, however in general it must be derived for each specific configuration which is modeled. This is done using the following relationship.

$$G_{region} = \frac{S_{Tot}}{V_{99\%} \cdot S_{\max}}$$

Once G has been determined, it can be used to define the relationship between the average star density and the maximum star density in the region. This is advantageous from the standpoint of simulation

$$S_{\max}^{\lim} = \frac{S_{avg}^{\lim}}{G_{region}}$$

and analysis time. Additionally, G can then be used to determine the relationship between the allowable limit on S_{avg} and a corresponding limit on S_{max}.

The Hydrogeology Factor, F_1

As groundwater percolates through the irradiated soil or rock, some ^{22}Na dissolves in the water and is transported along with it. ^{3}H ions exchange with hydrogen in the natural groundwater and move along in the same way as the non-irradiated water. The amount of radioactivity leached out of a material (clay, sand, till, rock) is a function of (a) the amount of water that has moved through the material, and (b) the grain size of the material. As more water is added, more activity is leached. However, not all of the activity produced is picked up and transported by groundwater. Illustrative leaching curves for a medium of sand and gravel are shown in Figure 4-5. The curves show that saturation is achieved very quickly. By taking the 99% point on the curves one obtains w_i (weight of water/weight of soil) for each of the radionuclides. The following relationships are useful to illustrate how the factors of volume, density and water weight are related.

$$C_{oi}\left(\frac{pCi}{ml-yr}\right) = \frac{A_i(pCi/cm^3 - yr)V_s(cm^3)L_i}{V_w(ml)}$$

$$\frac{V_w}{V_s} = \left(\frac{W_w}{\rho_w}\right)\left(\frac{\rho_s}{W_s}\right) = \rho_s\left(\frac{W_w}{W_s}\right) = \rho_s w$$

The Irradiation Time, t_{ir}

Taking into account the radionuclide buildup factors for ^{3}H and ^{22}Na shows that reaching the limit is a function of how long the facility has been operating. The weighted sum of the concentrations as a function of time is shown in Figure 4-6 for several values of S_{avg}. The determination of a reasonable

value of the irradiation time t_{ir} must be based on judgement as to a reasonable lifetime of the particular facility.

4.3 Evaluation Methods for NuMI

This section describes the evaluation of the radiation issues described above specifically applied to the design of the NuMI beam and facility. Evaluation of the radiation protection requirements for the NuMI facility has resulted in the driving factors being either protection against residual dose rates when entering an enclosure for maintenance or repair or protection of the groundwater. The former is true for the shielding required in the Target Hall and the Hadron Absorber Enclosure, while the latter is true for the shielding of the decay tunnel. These evaluations form the basis for the shielding designs described in Sections 3.2 and 3.4 and the interlock system described in Section 3.8.

4.3.1 Prompt Radiation

Since most of the NuMI Facility lies deep underground there are only a few areas where the issue of prompt radiation must be considered. In particular, these include the regions of the Main Injector where the NuMI extraction devices are located and the NuMI Extraction Stub. It is strongly desired that surface areas above all Main Injector related beams be classified as Unlimited Occupancy, and additionally that they not have radiation posting.

Another area that might be subject to prompt beam-on radiation is that which contains the power supplies for the horns and other Target Hall equipment. The current design has this adjacent to the Target Hall. If no posting is present then the requirements are the same as for those on the surface. If this area is instead acceptable for unlimited occupancy but posted as a Controlled Area, then the requirements relax to 0.25 mrem/hr normal and 5 mrem/hr accident. Higher levels are acceptable if the people who work there are classified as Radiological Workers and the area is classified as a Radiation Area.

The earth or equivalent shielding over all NuMI components in the Main Injector Enclosure and NuMI Stub is included as part of the Main Injector project. All such MI shielding has been built to the standard that all surface areas in the vicinity remain suitable for unlimited occupancy. This condition requires, as noted above, that any dose received be less than 1 mrem/hour for accident conditions and 50 μrem/hour for chronic losses. This shielding is mostly in place and is in the process of being formally assessed (as of September 1998). The applicable criterion applied to the MI indicates the need for 24.5 feet of soil equivalent over most of the enclosure and 25 feet over extraction regions,

with stairways, cable penetrations etc. being treated separately. This level assumes the possibility of full 8 GeV beam loss at any point (120 GeV in extraction regions), with cycle time as little as 1.9 seconds and intensity of up to 3×10^{13} protons per pulse. The as-built drawing which includes the MI-60 extraction region and the NuMI Stub[15] shows that the stated criteria have been satisfied.

There is a concern that muons, resulting from interactions of primary protons in the upstream part of the line, might be directed toward the horn power supply room located adjacent to the Target Hall. Preliminary studies of this matter are in progress and indicate that the potential for a problem depends in a detailed way on the location of this construction. The intention is that the horn power supply room be located such that the unlimited occupancy designation will pertain, during MI operations.
The Pretarget Hall will be built at an elevation low enough that the natural overburden, without construction of a berm, provides the required shielding. Thus, except for surveying to assure that conditions are as believed, no specific action will be required.

There is an outstanding question on the matter of required earth shielding. As noted above, the Main Injector is assessed for beam intensity of 3×10^{13} protons per pulse. However it is presumed that the intensity delivered to NuMI will be in the range $4\text{-}6\times10^{13}$. At such a time as these latter intensities become reality, some change in classification of the Main Injector complex itself will be required.
The primary critical device for NuMI will be the Lambertson string (L6081-3) located in MI-60. The secondary will be the set of bend magnets V105. The personnel safety interlock system will also "request" the abort signal, required to stop NuMI extraction in those situations when a radiation or critical equipment protection limit has been exceeded.

The NuMI safety interlock system will prevent personnel access when the beam is enabled to the Pretarget and horn area, decay pipe tunnel, hadron absorber area and muon slots. There will also be an interlocked detector(s) that will remove beam if the radiation levels become too high in the power supply room. Other interlocked detectors may be deemed necessary once the shielding design is completed.

Finally, we must address the issue that arises when Main Injector is operating and access to the Pre-target Enclosure is required (i.e. during NuMI construction). A preliminary analysis indicates that a "plug" equivalent to 15 to 25 feet of earth equivalent will be required. A detailed calculation and design are in progress.

---

[15] Radiation Safety 9667-C7

4.3.2 Residual Radiation

Our goal is to provide shielding for personnel protection so that the residual dose rates in the enclosure (with all shielding in place) do not exceed the ALARA trigger thresholds, initiating a radiological review of the scheduled work. We believe that our baseline design will meet this goal. In particular, when the target pile is closed we predict residual radiation levels in the hall will be significantly less than 10 mrem/hr. In contrast, special procedures and the review will have to be carried out when the shielding pile is opened up to work on the components that are enclosed in it.

The design of the Target Hall shielding pile is modular in the vicinity of active components, so that these components may be extracted easily. The active components include the target, focusing horns and beam instrumentation. The experience gained with the Fermilab Anti-Proton Production Target at AP0 is being used extensively in the design of this shielding pile. Remote handling capability and the use of shielding materials in selected locations that have reduced activation potential and more rapid decay properties (such as marble), the use of temporary shielding and lead coffins for storage and transport of components are all methods that can be used to mitigate personnel exposures.

Each active component will be mounted on either a single or double AP0-style universal module. Careful planning will precede removal or reconfiguration of activated components. Once shielding has been removed to make the top of a module accessible, the utility connections at the top of the module will be undone enabling the entire assembly to be lifted out of the vault. Possible destinations for the assemblies that must be removed (due to failure) would be the hot storage area or the hot repair area located in the Target Hall.

It is important that the top of the module remain as non-activated as possible since technicians must make/break connections there for water, electrical lines and component support. The purpose is to minimize personnel exposure rates during beam-off jobs. To minimize irradiation of the top of the module through penetrations water lines and electrical penetrations are functional, but narrow. The trace elements in the steel used in the manufacture of modules will be chosen to minimize potential long-lived radionuclides.

The target will be hermetically sealed. This will minimize the potential spread of radioactive materials from broken target segments during operation and transport. Examination of the target to determine its integrity will be possible through a remotely removable window.
For most component failures it will be necessary to temporarily store that failed component until the activation level is diminished. At that time the complexity of the necessary repair may be analyzed and one can either make the repair or declare component mortality. The design of the repair area will be tailored to the design of horns. There will be many points of removable shielding so that interested

parties can physically access the components. The use of lead glass will be integral, to permit visual observation.

4.3.3 Airborne Activation

The NuMI beam has two distinctive characteristics that bear heavily on the problem of air activation control and monitoring. The first is the high beam intensity. The second is the large volumes of air (or gas) within the target hall that surrounds the irradiated target and horns. Both of these factors will lead to production of radionuclides in the air or other gas volumes (i.e. He) used to surround the components. Control of the production and release of them needs to be addressed during the course of detailed facility design. The radionuclides produced by beam interactions in air and the relative amounts in which they are produced are fairly well understood from previous measurements at Fermilab and elsewhere. The task of characterization for NuMI is twofold. The first part is to determine the absolute amount of radioactivity produced in various regions of the beamline. The main areas of production will be the target hall and the beam absorber, although some air activation will undoubtedly be produced in the pre-target and decay areas as well. Secondly, the activity must be characterized at the exhaust stack(s) for specific configurations of the NuMI ventilation system. These quantities may be estimated via basic calculations but these will be supported by detailed Monte Carlo simulations. It is assumed that the ventilation will be such as to keep radioactive air away from the experimental hall. In order to minimize buildup of airborne radionuclides, as much open space as possible in the target station will be filled with ^{4}He or vacuum. In ^{4}He, only the production of ^{3}H (tritium) is of concern. For ^{3}H, which would be built up in the helium containers, the occupational concentration limit is 0.5 μCi/ml. This radioactivity would not be routinely released, but would have to be addressed whenever the helium containers were vented. The helium containers should be broken up into manageable segments to avoid releasing the gas all at once, whether accidentally or intentionally. Studies of the radiation environment within the target hall, along with consideration of the mitigation methods given below are underway, the results of which will be incorporated into the facility designs. The HVAC systems for the facility will be arranged to avoid sending activated air toward the occupied areas such as the experimental hall.

A single monitoring ventilation stack will be incorporated into the facility design. This would become essential if an EPA-certified monitoring system were ever deemed to be needed. The ventilation system will be designed to minimize leaks that result in the monitored radionuclides bypassing this stack; a negative pressure configuration could be used to accomplish this. Provisions will be made to monitor the emissions from this stack on a permanent basis by logging the data on the Laboratory's

MUX system, or whatever equivalent exists at that time. Preparations will also be made to monitor the release of ^{3}H whenever the need arises to reconfigure the helium containers. There are several options for mitigation of short-lived radioactive gases which may be implemented in the design of NuMI if the calculations deem it necessary These methods span a range of complexity and potential expense and include :

Delayed ventilation is the simplest method and the one historically used at Fermilab. Since the vast majority of the radioactive atoms produced are short lived (20.5 minutes for ^{11}C), a delay time of one hour from production to exhaust will reduce the radioactivity by roughly one order of magnitude at the stack. However, there are several potential drawbacks of relying on this method for NuMI. First, the construction of a built-in delay (e.g., a holding tank) might be problematic, given the expense of underground construction. Secondly, reduction (or stoppage) of the air flow in NuMI might adversely affect other technical areas, such as ventilation for life safety, radon mitigation, or heat rejection or possibly lead to corrosion problems. Finally, given the intensity of the NuMI beam, the air activation levels might be such that reduction by an order of magnitude is insufficient.

Adsorption beds using a material such as activated charcoal is another method that may be considered. Such a system was considered for LAMPF (now LANSCE) but was never actually tested. Activated charcoal adsorption beds present have both advantages and disadvantages. The advantage is that activated charcoal is very effective at adsorbing CO_2. Since a large fraction of the air activation at the stack is anticipated to be in this form, such a system could potentially effect a significant reduction in NuMI's emissions. However, the disadvantage is that in time the beds become saturated and have to be regenerated or replaced. Regeneration involves heating the charcoal in vacuum or inert gas after the radioactivity has been allowed to decay. Concern over the potential complexity and expense of the regeneration system dissuaded the Los Alamos group from proceeding with this method. If NuMI proceeds with an adsorption system, other adsorbents, such as silica gel, could be considered, but these would have similar drawbacks.

Scrubbing would entail an additional water system. In such a system, the radioactive gases are bubbled through water that is slightly basic, e.g., through the addition of a small amount of NaOH. The gases are absorbed in the water, which is then held for decay. When the radioactivity has decayed, the water is neutralized, e.g., through the addition of a small amount of HCl, and released or re-used. An additional benefit of this method is that, while relatively little tritium is present in the air activation products, the scrubbing system will remove virtually all of it.

4.3.4 Groundwater Irradiation

The NuMI primary proton beam at its downstream end, and the secondary hadron beam over its entire length, must be directed toward the MINOS far detector in Soudan, implying a 58 mradian slope. Although this consideration does not fix the depth below grade of the target itself, it does imply that most of the hadron decay region and all facilities downstream thereof will lie at the level of the local aquifer. This has led to careful consideration and analysis of the processes that might lead to potential contamination of the groundwater resources. The key issue for NuMI is that radionuclides produced in the rock surrounding the beam line have no chance to decay before possibly leaching into the groundwater resource, as they do for facilities not constructed so deeply. Several early analyses and designs have been documented and lay the groundwork for further refinements of the model and methodology which has resulted in the understanding of the problem as summarized in the following sub-sections[16,17].

4.3.4.1 The local geology

The Chicago area is one of the most favorable regions in the state for groundwater production. It is underlain at depths of 500 feet or more by sandstone aquifers that have been prolific sources of water for over 130 years. At lesser depths the area is underlain by sand and gravel deposits and fractured dolomite that are locally excellent sources of groundwater. Three major aquifer systems are present, although not necessarily all together at any given location. From shallowest to deepest, these are the sand and gravel aquifers within the glacial drift, the upper bedrock aquifer and the deep bedrock aquifer system. A fourth major aquifer, the basal Elmhurst-Mt. Simon, is present throughout the area, but, due to the tendency of wells penetrating it to gradually encounter saline water, has increasingly been plugged off from those wells. These layers are shown on Figure 1-1.

Historically, the importance of these three aquifer systems as sources of water has been in the reverse order from that given above - that is, from deepest to shallowest. Prior to the switch-over of many communities from aquifers to Lake Michigan as their source of water, for every gallon pumped from glacial deposits in northeastern Illinois three were pumped from the shallow bedrock and five from the deep bedrock. With the switch to lake water, however, significantly less pumpage has been taking place from the deep aquifers. At Fermilab no significant aquifers have been encountered, or are believed to exist, in the glacial deposits, and thus concern centers only on the deeper structures.

---

[16] B. Freeman, "A NUMI Wide-Band Beam Shield Design That Meets the Concentration Model Groundwater Criteria, NuMI-B-155, June 13, 1995.

[17] A. Wehmann,et.al.,"Groundwater Protection for the NuMI Project, FERMILAB-TM-2009, October 10, 1997.

Silurian Age dolomitic bedrock is generally encountered at depths ranging between 60 and 75 feet below grade. These Silurian strata are marine sediments that were deposited in a shallow interior sea. Groundwater in the Silurian rocks occurs in joints, fissures, solution cavities and other openings. Two dominant joint sets, one striking approximately northeast and the other northwest, have been identified in northeastern Illinois. Most of the joints noted in Chicago area boreholes and rock quarries are nearly vertical; 75 to 85 percent of all those in the dolomites have dip angles greater than 70^0. Permeability measurements on the upper 6 to 12 feet of the bedrock suggest weathering is present. The bedrock at Fermilab possesses several zones that are intensely fractured and/or solutioned.

The Silurian Age bedrock, as well as the upper Ordovician formations, appear to be hydraulically interconnected and therefore to behave as a single aquifer system. The estimated thickness of this aquifer is 230 feet, and this is where most of the NuMI tunnels will be constructed. (See Figure 1-1) It is believed that the shale bedrock present in the lower part of the Scales formation functions as an aquitard. Regional references also indicate that the Maquoketa Group shale formation, in combination with the Galena-Platteville dolomite, functions as a confining layer for the underlying Cambrian-Ordovician sandstone aquifer.

Based on the available groundwater characterization data, the proposed NuMI tunnel system, if left totally unlined, would have an estimated inflow of several hundred to a few thousand gallons per minute. Experience has shown that high initial inflows tend to decrease with time and to stabilize at lower sustained levels. Inflow into the NuMI tunnel can be substantially reduced by grouting fractures. Further discussion of the implications of groundwater inflow is continued in Chapter 5, *Civil Construction*.

4.3.4.2 The Hydrogeology Factor, Fi , revisited

Since the writing of TM-2009 in Summer, 1997 Cossairt & Cupps [18] have refined the values that make up the factor F_i.. New values for K_iL_i and for ρ have been obtained using rock samples taken from test borings made in the same geological units through which the decay tunnel will be excavated. The rock samples were irradiated with hadrons by placing them on top of a Lambertson magnet[19] at F17 in the Fermilab Main Ring. The mass of each of the rock samples ranged between 31 and 39 grams. Each was covered with 120 cm^{-3} of distilled water and kept in that condition for a suitable period of time for radionuclide leaching into the water to occur. The water was then drained

---

[18] D. Cossairt and V. Cupps, *Parameters for NuMI Groundwater Protection, DRAFT*, March, 1998

[19] The Lambertson magnet was part of the extraction system to the antiproton target.

and analyzed for ^{22}Na and ^{3}H in Fermilab's Activation Analysis laboratory[20]. The results obtained from four samples are:

$$\rho = 2.74 \pm 0.03 \text{ (g/cm}^3\text{)}$$

$$K_3L_3 < 5.1 \times 10^{-4} \text{ (atoms/star)}$$

$$K_{22}L_{22} = 1.2 \times 10^{-4} \pm 2.27 \times 10^{-5} \text{ (atoms/star)}$$

The test boring report[21] gave the porosities, p, of the three principal geological formations in the path of the NuMI tunnel. These were found to be 0.19, 0.17 and 0.22, for the Silurian Dolomite, the dolomite Scales Formation and the shaley Scales Formation, respectively. These values average to 0.19±0.03. These values are averages for the stated geological units and are larger than the intrinsic porosities of the rock (typically about 0.05). Based on the STS report it is reasonable to assume that these "voids" will be filled with water when the rock is in place in the geological unit.

4.3.4.3 Direct Production of ^{3}H

Since the measured upper limit for K_3L_3 is $< 5.1 \times 10^{-4}$ (atoms/star), whereas the value for K_3L_3 used in TM-2009 was 0.03, we were led to consider whether or not the direct production of tritium in the water present in the "voids" or fractures in the rock is represented by the newly available value for K_3L_3. The mechanism for the direct production of ^{3}H in water is spallation reactions on the oxygen in the water molecules. (^{22}Na cannot be produced by this mechanism and neither radionuclide of interest can be produced by high energy interactions with hydrogen. One can produce ^{3}H by means of successive captures of thermal neutrons on protons but this process would have a completely insignificant cross-section.).

It is possible to estimate the production rate of ^{3}H directly in water, using the production cross section (σ_3) of 33 mb from the $^{16}O(p, {}^{3}H)X$ spallation reaction. Cossairt & Cupps[22] give the result of such a calculation as 0.093 ^{3}H atoms/star in water. For the number of ^{3}H atoms produced in water by each star in a cm^{-3} of rock they find

$$0.093 \times 0.43p = 0.04p = 7.6 \times 10^{-3}$$

---

[20] V. Cupps, private communication.

[21] STS Consultants, Ltd., *Hydrogeological Evaluation Report, Fermi National Accelerator Laboratory, Neutrino Main Injector (NuMI)*, April, 1997.

[22] Ibid., Cossairt & Cupps

(where $S_{water} = 0.43\ S_{rock}$, obtained from the flux density expression , and S_{rock} is the star density in the rock obtained from the Monte Carlo simulation). This value of 7.6×10^{-3} for ^{3}H atoms per star in rock is considerably larger than the upper limit measured from the rock samples from the boring holes, and is hence a conservative approach to making the estimates.

As an alternative way to evaluate the effect of direct production of ^{3}H in the groundwater one can consider an argument following the results of Borak et. al.[23] In measurements of activation and leaching of samples of Fermilab glacial till they also included samples of water in the exposure. They report that the concentration of tritium measured in the water samples after exposure was 1/3 that of the concentration of tritium in the water extracted from the samples of glacial till. They concluded that tritium was being produced in both the water and glacial till, and noted that the measurement technique could only measure that tritium which came out of the samples in water-either by heating and distillation, or by leaching. To account for direct production in the NuMI evaluation we have assumed that the concentration of ^{3}H will be 1.3 times the estimate for leaching alone.

Finally one needs to determine the value of the parameterw_i to estimate the radionuclide concentrations. It is well known that in a.given sample of irradiated environmental media, either soil or rock, the leaching process eventually saturates. That is, the rinsing of the sample by more and more water removes less and less radioactivity. A new development for the value to use for w_i is the publication of the results of studies Baker, et.al. of radionuclide production and leaching for the SSC sited in Texas[24]. Their publication provides leaching curves for ^{3}H in crushed chalk and ^{22}Na in crushed chalk and unfractured chalk. These new leaching curves have been compared with the sand and gravel leaching curves used in TM-2009 and new values for w_i for 90% leaching result. These values, along with new values for K_iL_i and the resulting F_i are summarized in Table 4-6.

The K_3L_3 value calculated by Cossairt is consistent with the assumption made in TM-2009 that the groundwater is static, and makes the further assumption that in order to remove it and the tritium it contains, additional water (represented by w_i) must be involved. If the groundwater present in the rock were in motion and not static, then it would spend less time in locations near the tunnel wall where the star density (and hence the radionuclide production) in the rock is at a maximum. The tritium concentration would then necessarily be less than that for the static assumption. Furthermore, a likely direction of motion would be into the NuMI tunnel, where the water will be collected and any

---

[23] Borak, T. B., et. Al., "The Underground Migration of Radionuclides Produced in Soil Near High Energy Proton Accelerators", *Health Physics*, 23 (November 1972), pp. 679-687.

[24] S. I. Baker, et.al., "Leaching of Accelerator-Produced Radionuclides", *Health Physics* 73 (1997) 912-918.

tritium concentration in it will be subject to surface water limits-which are much higher than groundwater standards.

Credit for this reduction in activation is not taken in the calculation, since we can not rely on sufficient water movement everywhere along the NuMI tunnels; actual flow rates will vary widely depending on the amount of fracturing of the rock, matrix conductivity and also any grouting done on the tunnel walls.

Finally one additional point is worth noting. It should be made clear that the values used for the probability of tritium being in the groundwater has been derived using the probability of leaching, modified for the probability of direct production. The upper limits we have used come from data obtained by studying the case of water and soil rather than water and rock, which would be more applicable to the case of NuMI. Though we don't believe that this would produce any major change in our designs, since we have been quite conservative in many assumptions However, we are continuing to develop a better and more accurate understanding of the impact of direct production with in the cracks and voids within the dolomite. Since the concentration of tritium from direct production within the water will dominate from the concentration from leaching, this understanding will be important when considering future intensity upgrades of NuMI or new facilities at Fermilab. Preliminary results of this analysis are presented in Figure 4-7 and Figure 4-8. The major factor that has not yet been taken into account in this analysis is the factor related to the actual amount of water that is subject to direct production (volume of the voids) and the velocity of the water as it passes through the rock. Both of these factors will reduce the actual concentration. For the present time we have assumed that our baseline design described below, along with this reduction, is adequate to maintain the concentration levels below the regulatory limits.

4.4 Conceptual Designs of the NuMI Shielding

In this sub-section we summarize the results of the Monte Carlo simulations that have been done to model the NuMI beam configuration. We also present a conceptual design of a radiation shield around the components in the Target Hall, the Decay Tunnel and the Hadron Beam Absorber. It should be noted that it is not necessary for the design of the shield in the simulation to be exactly the shield required to provide adequate attenuation of the radiation. Rather, the simulation provides a baseline prediction for the amount of radiation that would penetrate or be attenuated by the modeled shield. Along with the basic scaling guidelines for the use of steel and concrete shielding, we have used these results to determine which regions of the facility will require more shielding and where less could be used. For protection of the groundwater we use the results of the simulation which

provide the total star density in the 99% volume. These are summarized for each of the regions of the facility in Table 4-7.

We then provide a conceptual design of the cross sections of those shields for relevant locations down the length of the facility. In designing the shielding we have chosen the two horn medium energy configuration as the baseline and have insured adequate shielding. As a secondary goal we have incorporated some additional requirements driven by the low energy beam configuration. Specific technical designs of the shielding are found in the discussions of these areas in Chapter 3.

4.4.1 Target Hall

The results of the Monte Carlo simulation in the region of the Target Hall are given in As a result of this simulation we see that for the two horn medium energy beam configuration the star density peaks in the two areas of the hall which contain the active beam devices. Between the devices and downstream of the second horn it can be seen that the star density falls by nearly two orders of magnitude. Because of this large difference between the regions of the hall containing components and the rest of it, we have considered a shielding design in which the star density (either outside of the enclosure or on top of the shielding pile) is made more uniform by trading steel for concrete in the low radiation regions. A cross section of the shield for the "component regions" is shown in Figure 4- **10** and the cross section for the non-component regions is shown in Figure 4-11.

4.4.2 Decay Tunnel and Beam Absorber

The results of the Monte Carlo simulation in the region of the decay tunnel and Beam Absorber and are given in Figure 4-12. As a result of an earlier simulation with uniform shielding along the decay pipe (66" thickness) we found that for the two horn medium energy beam configuration the star density was higher at the upstream end of the decay tunnel and gradually decreased along the length. In our subsequent simulations we added additional concrete (using the guidance learned from the study summarized in Figure 4-13. Additionally, for the low energy beam the star density deposition at the upstream end of the tunnel is about two to three times larger than for the medium energy configuration. Because adding additional shielding for the low energy beam at a later date would be very difficult the proposed design accommodates the required amount for both beams from the beginning. In an attempt to economize we have used the fact that less shielding is actually required at the downstream end to narrow the tunnel and save money on excavation and shielding.

4.4.3 Options for Facility Reconfiguration

The shielding arrangements presented in the preceding two sections have been designed so that they provide adequate protection for either the medium or low energy beam. This can be seen in the analysis of the Target Hall shielding for the low energy beam presented in Figure 4-14. Accommodation of either the two horn high energy beam or the narrow band beam will require some modification to the target hall shield. (The decay pipe shielding has been designed to be adequate for any of the beam configurations discussed in this report.)

4.4.4 Groundwater Monitoring

While the shielding designs presented in the preceding sections are designed to maintain groundwater radionuclide concentrations below regulatory limits, operation of the NuMI Facility will be included in the comprehensive laboratory monitoring program. Wells are an integral part of the Fermilab environmental monitoring strategy. The unique element of NuMI wells is that they can be located in the regions near to where radionuclide production occurs, i.e. directly in the aquifer. Two wells for this purpose are planned. They will be located down gradient of, and at the same depth as, the Target Hall and the beam absorber. A third could possibly be located along the decay tunnel, again down gradient from and at the same depth as that point where the heaviest grouting was required during tunnel boring. Typically, samples of 125 ml are taken to measure the radionuclide concentrations in the monitoring well water. Samples would initially be examined every month, with the sampling rate eventually being reduced once NuMI has reached steady-state operation.

In addition, we have incorporated monitoring ports along the length of the decay tunnel where we will be able to sample the groundwater directly and make comparisons between predictions and measurements. Regular sampling will also be done for radionuclide levels in cooling water systems, including both the closed loop RAW system serving components experiencing higher activation levels, and the LCW cooling system serving conventional beam transport elements. RAW spills are controlled by a combination of continuous water level sensing, secondary containment vessel collection and tightly controlled sump discharge.

4.5 Conclusion

Planning for the high intensities at which the NuMI Facility will operate has had a major impact on the design phase of this project. In most areas, the radiological concerns associated with the NuMI project are no different than those that have been handled successfully at Fermilab in the past. Prompt radiation dose rates will be mitigated by the depth of the beam below ground and the

production of airborne radionuclides will be carefully monitored as part of the lab wide monitoring program. Extra care has been taken in regard to the issues of groundwater protection and residual dose rates. Extensive shielding in both the target hall and the decay tunnel are an integral part of the facility design. Recognition of the radiation environment which personnel might encounter when needing to work within the facility structures has played an integral part in the design of the mounting and handling fixtures for the targets and focusing horns.

Posting	**Dose rate limits**
Radiation area	> 5 mrem/hr < 100 mrem/hr
Unlimited occupancy - controlled area	> 0.05 mrem/hr < 5 mrem/hr
Unlimited occupancy - no controls	< 0.05 mrem/hr

Table 4-1 Summary of area posting requirements

	Normal operating	**Accidental Beam loss**
Unlimited occupancy - controlled area	<0.25 mrem/hr >0.05 mrem/hr	<5mrem/hr
Unlimited occupancy - no controls	<0.05 mrem/hr	1 mrem/hr

Table 4-2 Summary of "beam-on" prompt radiation protection requirements

	^{22}Na	^{3}H
Groundwater	0.4	20
Surface Water	10	2000

Table 4-3 Regulatory limits on allowed radionuclide concentrations in groundwater and surface water. Units are in pCi/ml.

Material	Density (g/cm^3)
Earth	2.24
Dolomite	2.67
Steel	7.60
Concrete	2.40

Table 4-4 Densities of materials to be used in or around the NuMI Facility

Type of Radiation	**Star to dose conversion factors**
Prompt Radiation (outside bulk shield)	18 mrem/hr per star/cm^3-sec
Residual radiation (outside of an iron shield)	9×10^{-3} mrad/hr per star/cc^3-sec
Residual radiation (outside of a concrete shield)	8×10^{-3} mrad/hr per star/cc^3-sec

Table 4-5 Conversion factors (simulation output to dose equivalent) for prompt and residual radiation. The conversion factors for residual dose are for the conservative case of infinite irradiation, zero cool down.

	TM-2009 (October 1997)	**Cossairt & Cupps** (March 1998)
K_3L_3	2.7×10^{-2}	$7.6\times10^{-3}\pm7.9\times10^{-4}$
w_3	2.7×10^{-1}	$3.25\times10^{-1}\pm4.9\times10^{-2}$
F_3	3.75×10^{-2}	$7.68\times10^{-3}\pm1.39\times10^{-3}$
$K_{22}L_{22}$	2.0×10^{-4}	$1.20\ 10^{-4}\pm2.27\times10^{-5}$
w_{22}	5.2×10^{-1}	$6.60\times10^{-1}\pm1.1\times10^{-1}$
F_{22}	1.44×10^{-4}	$5.99\times10^{-5}\pm1.51\times10^{-5}$

Table 4-6 Groundwater leachability factors used in NuMI shielding analysis.

Region	S_{TOT} (stars/cm^3-p)	**99% Volume** (cm^3)	$S_{average}$ (stars/cm^3-p)	**Geometry Factor, G**
Target Hall	1.03e-2	2.4e+9	4.3e-12	0.07
Decay Region	2.2e-1	3.1e+10	7.1e-12	0.10
Beam Absorber	6.0e-3	6.2e+8	9.7e-12	0.16

Table 4-7 Determination of S_{avg} and G for each region of the facility for the baseline medium energy beam. Similar calculations have also been done for the low and high energy options.

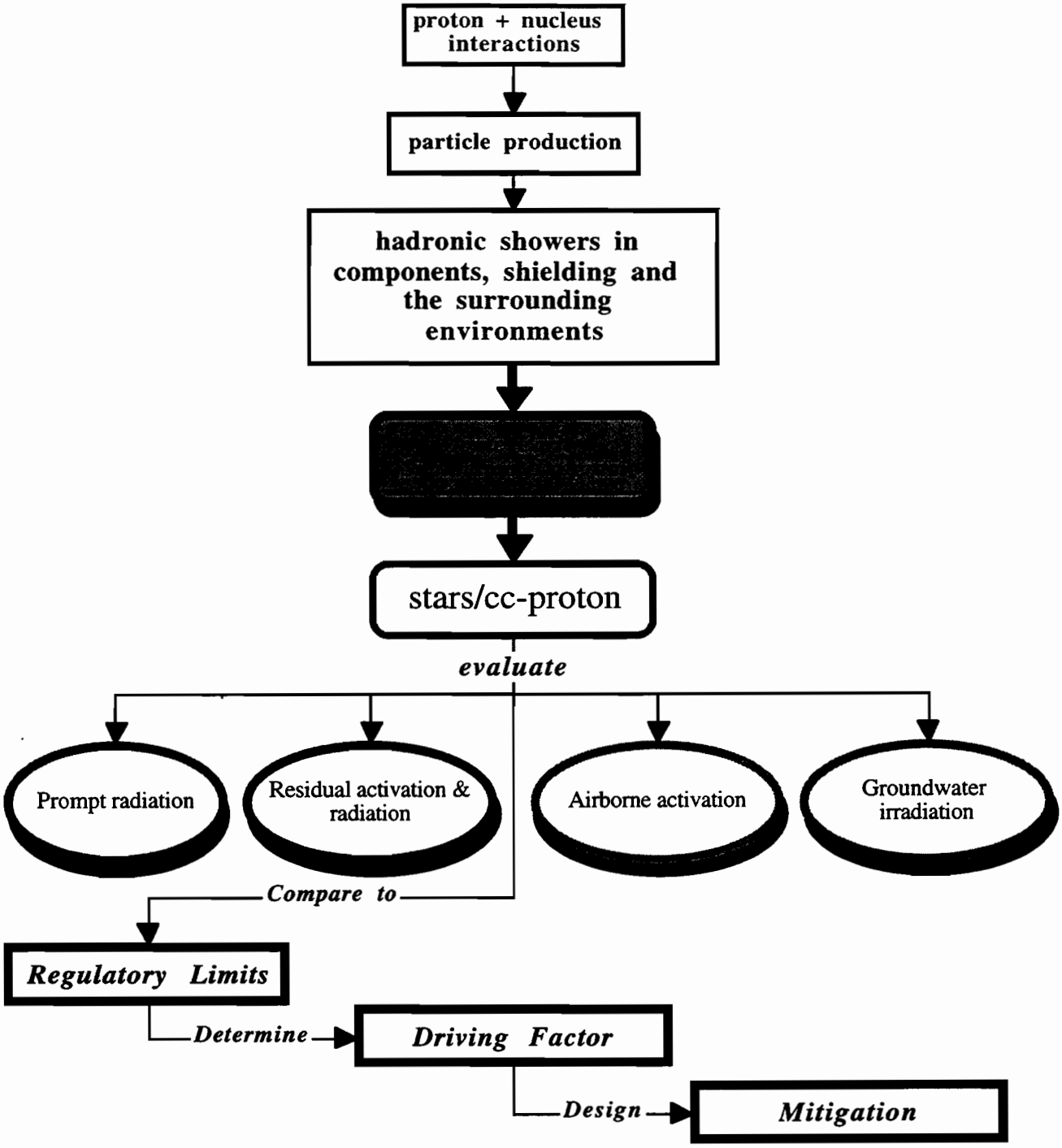

Figure 4-1 Flow chart of radiation protection analysis procedure.

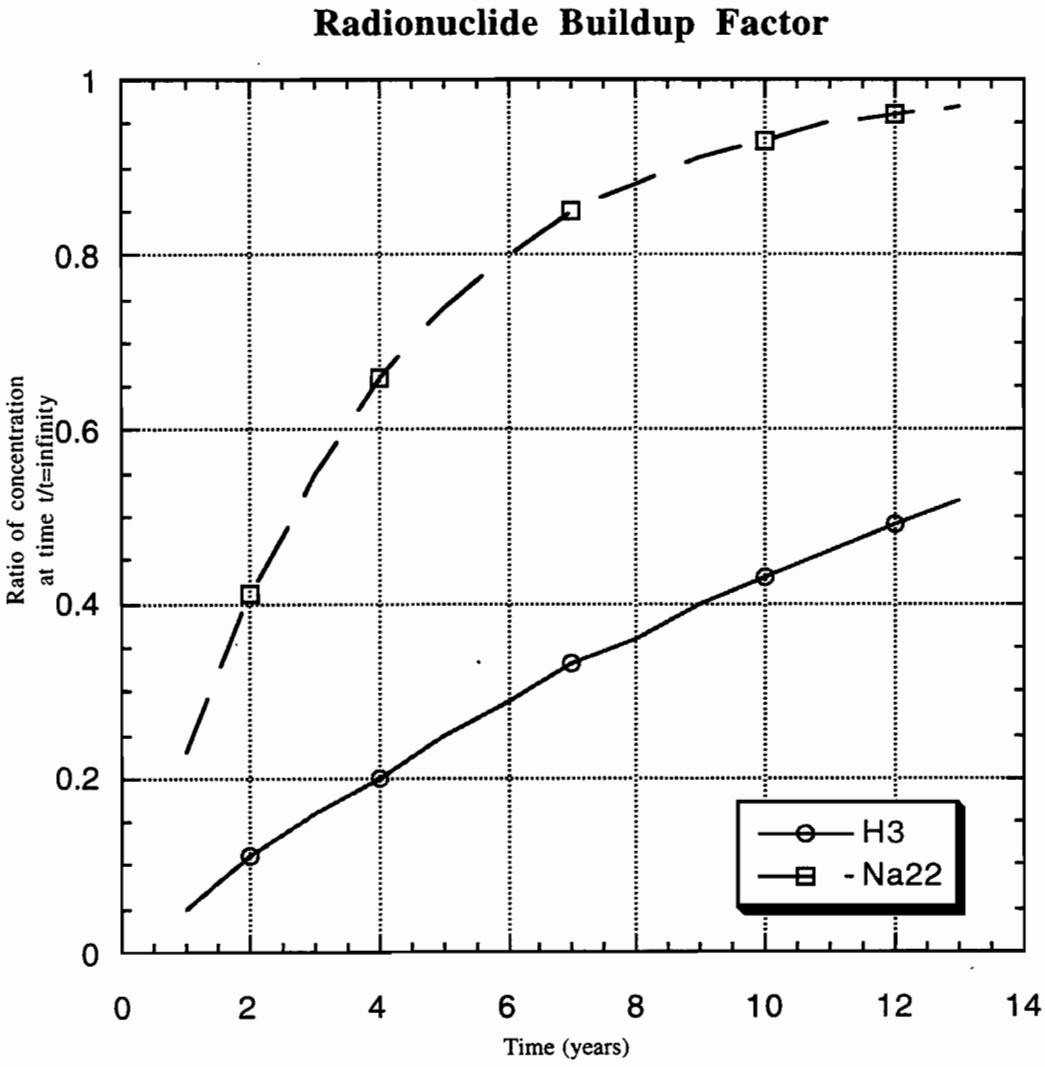

Figure 4-2 Concentration "build-up" vs. time for ^{22}Na and ^{3}H.

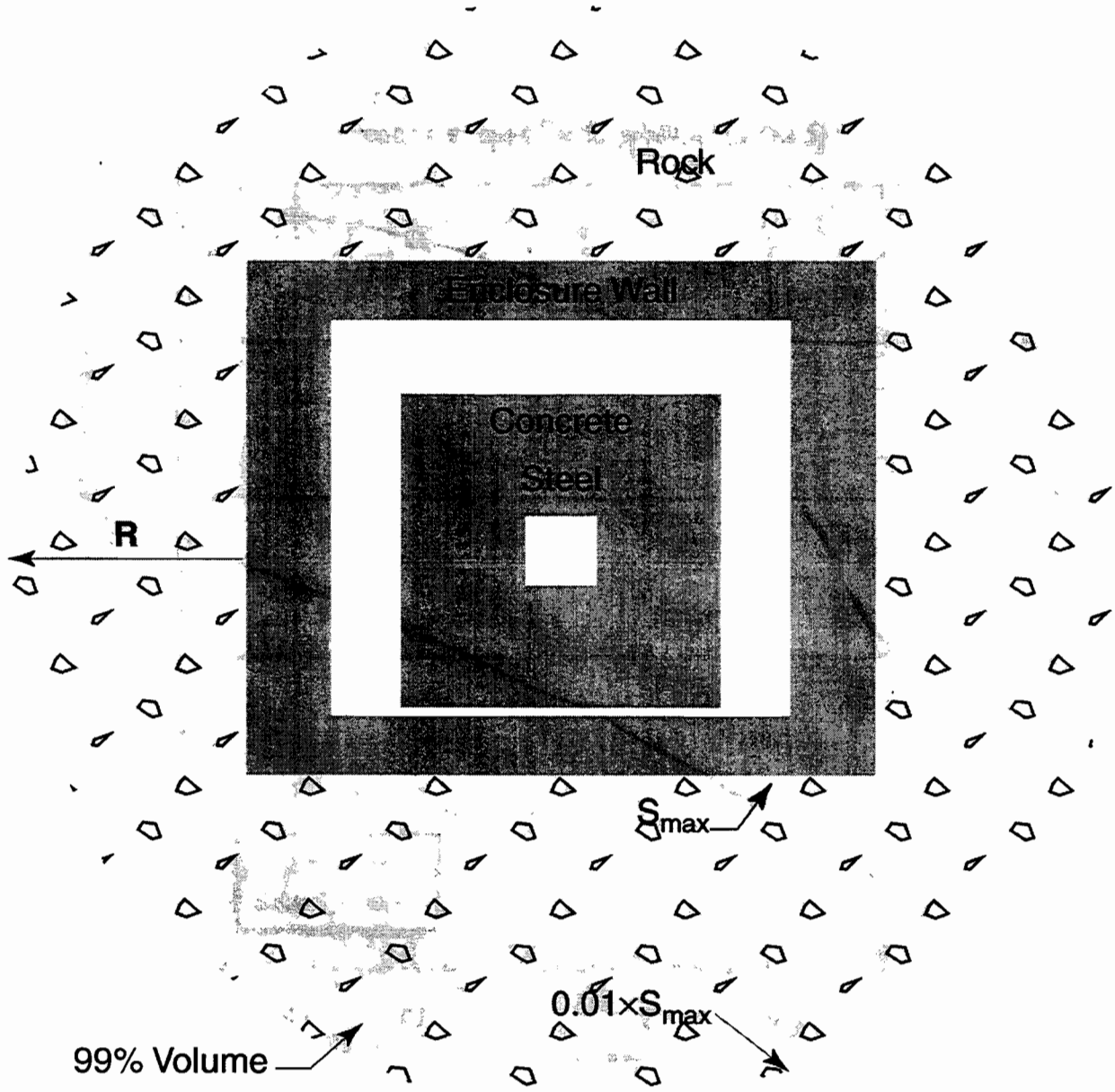

Figure 4-3 Schematic illustration of the parameters required to calculate the "average" star density in the 99% volume. R represents the radial extent over which the volume is averaged.

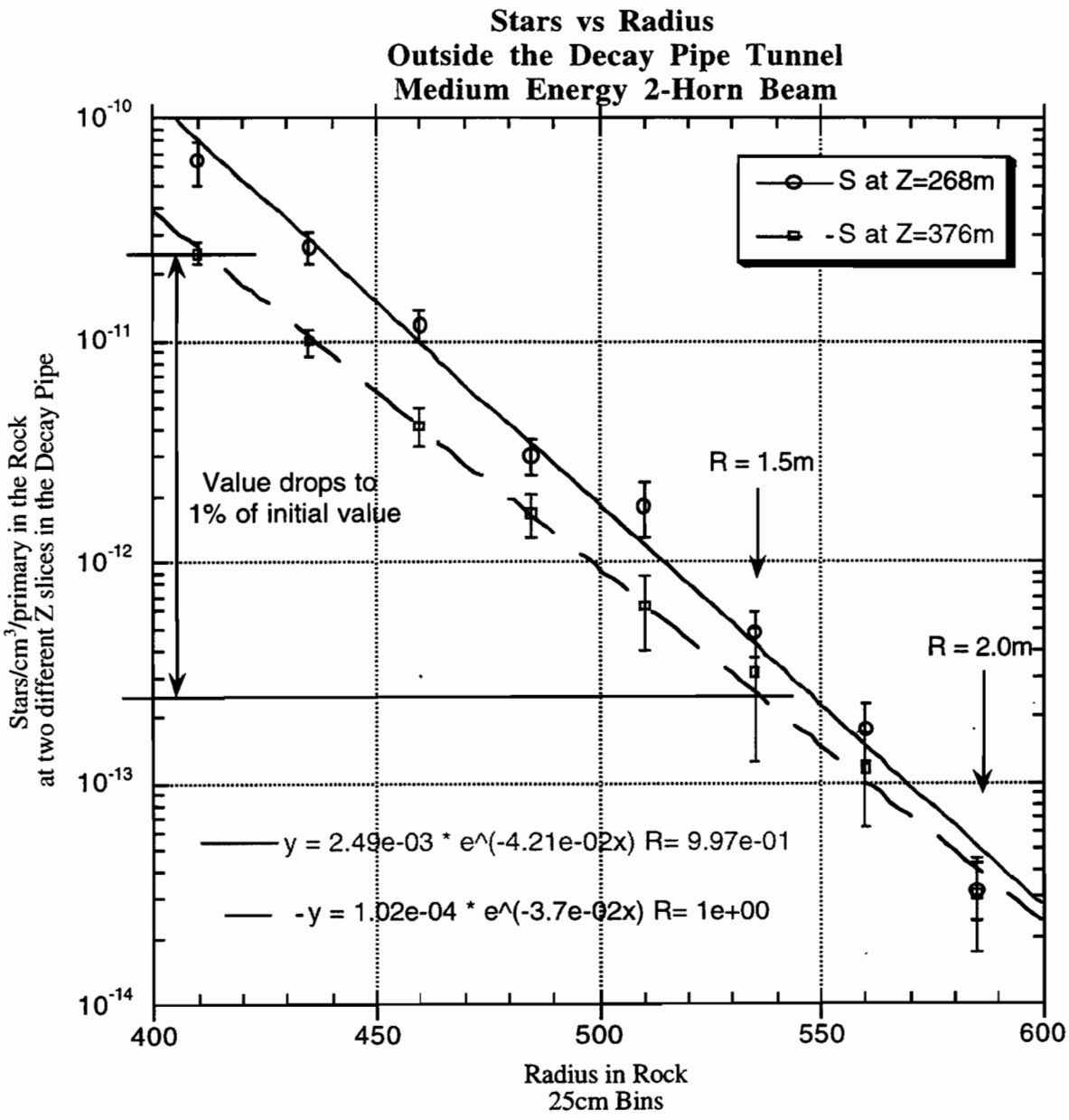

Figure 4-4 Radial fall-off of star density for two values of z along the decay pipe.

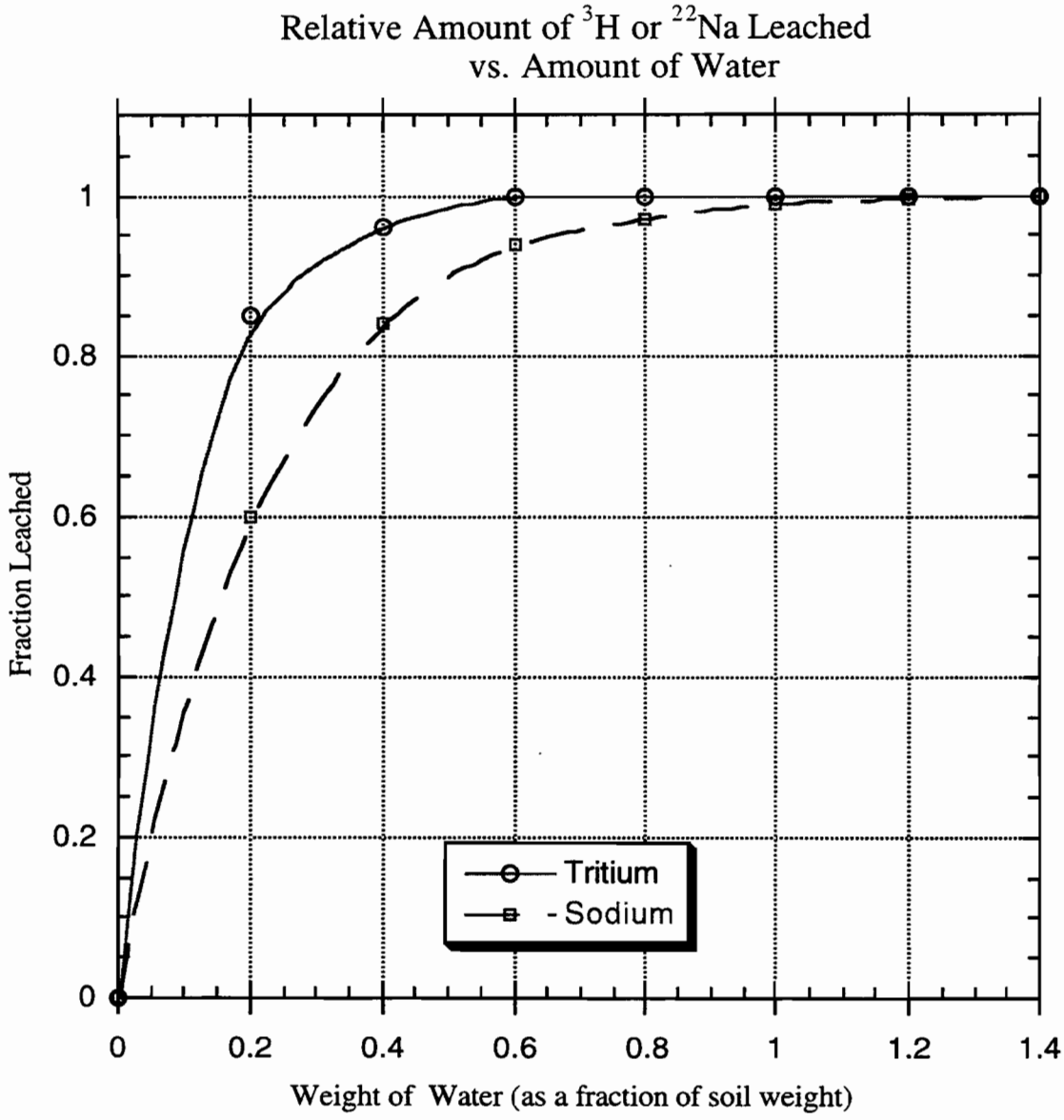

Figure 4-5 Illustrative example of leaching curves showing the saturation as a function of the weight of water passing through the medium. (The curves are drawn to guide the eye).

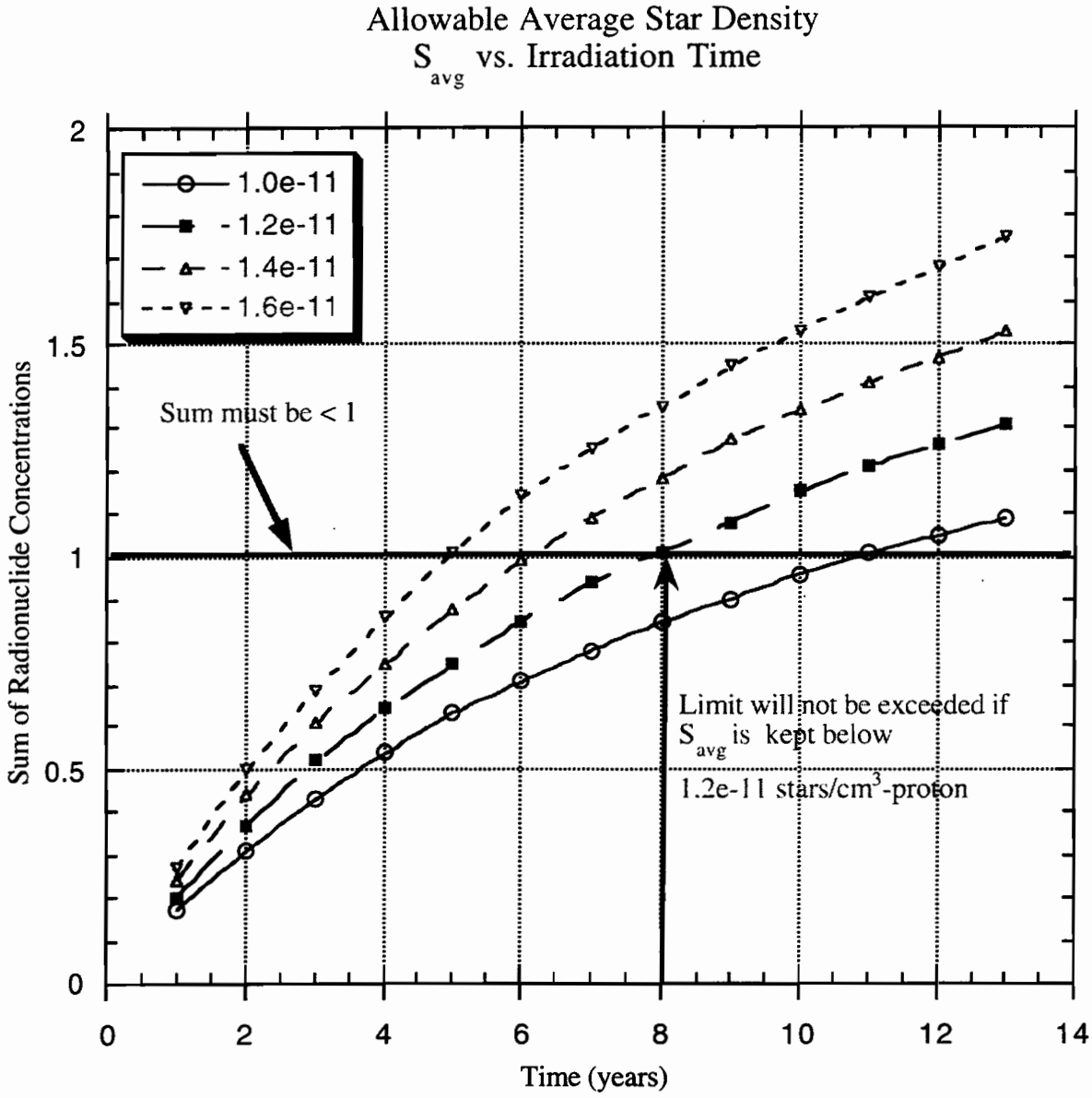

Figure 4-6 Weighted sum of the build-up of the radionuclide concentration vs. running time for several values of the average star density.

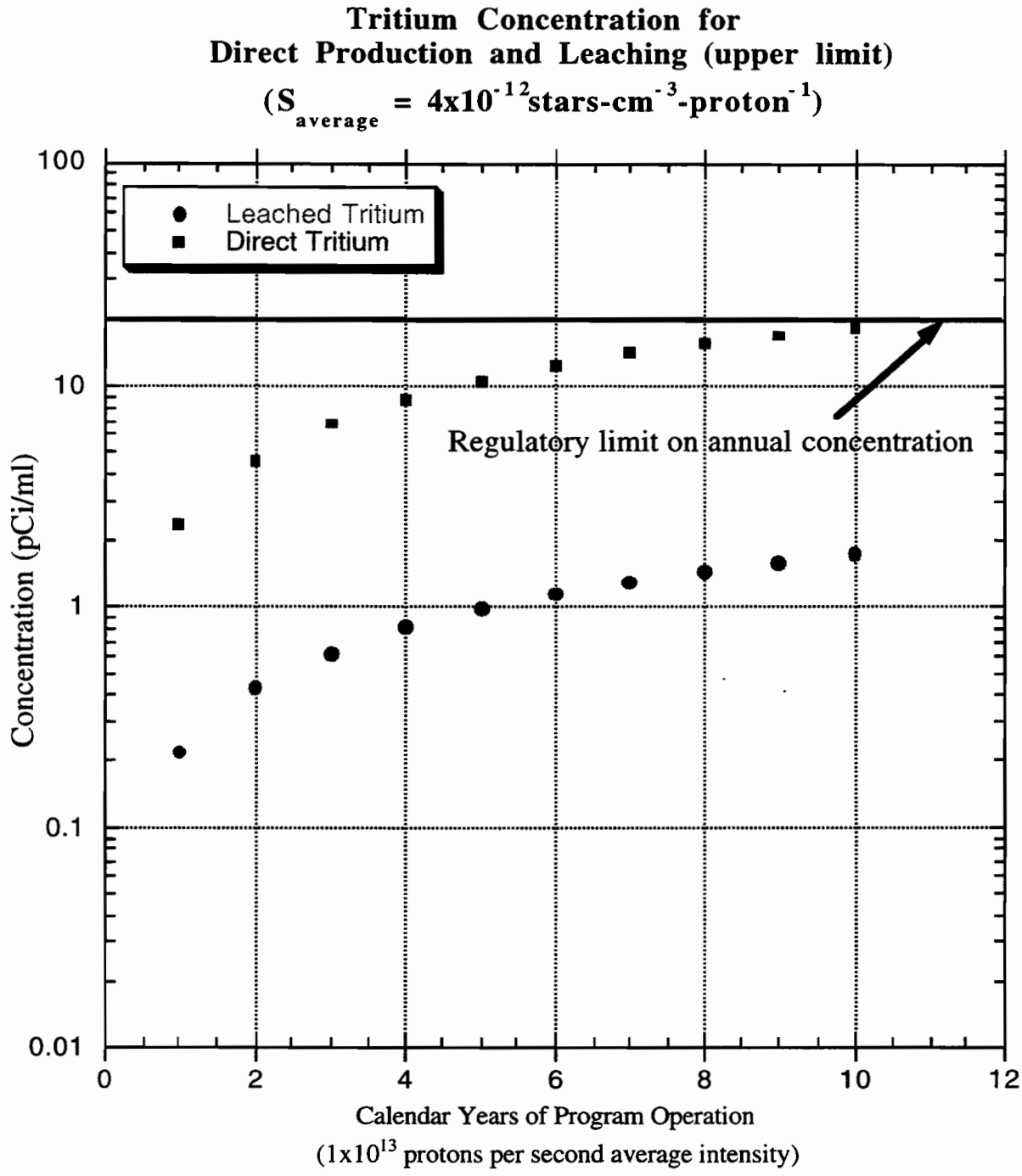

Figure 4-7 Comparison of the concentration (per unit volume) of tritium from direct production vs. leaching.

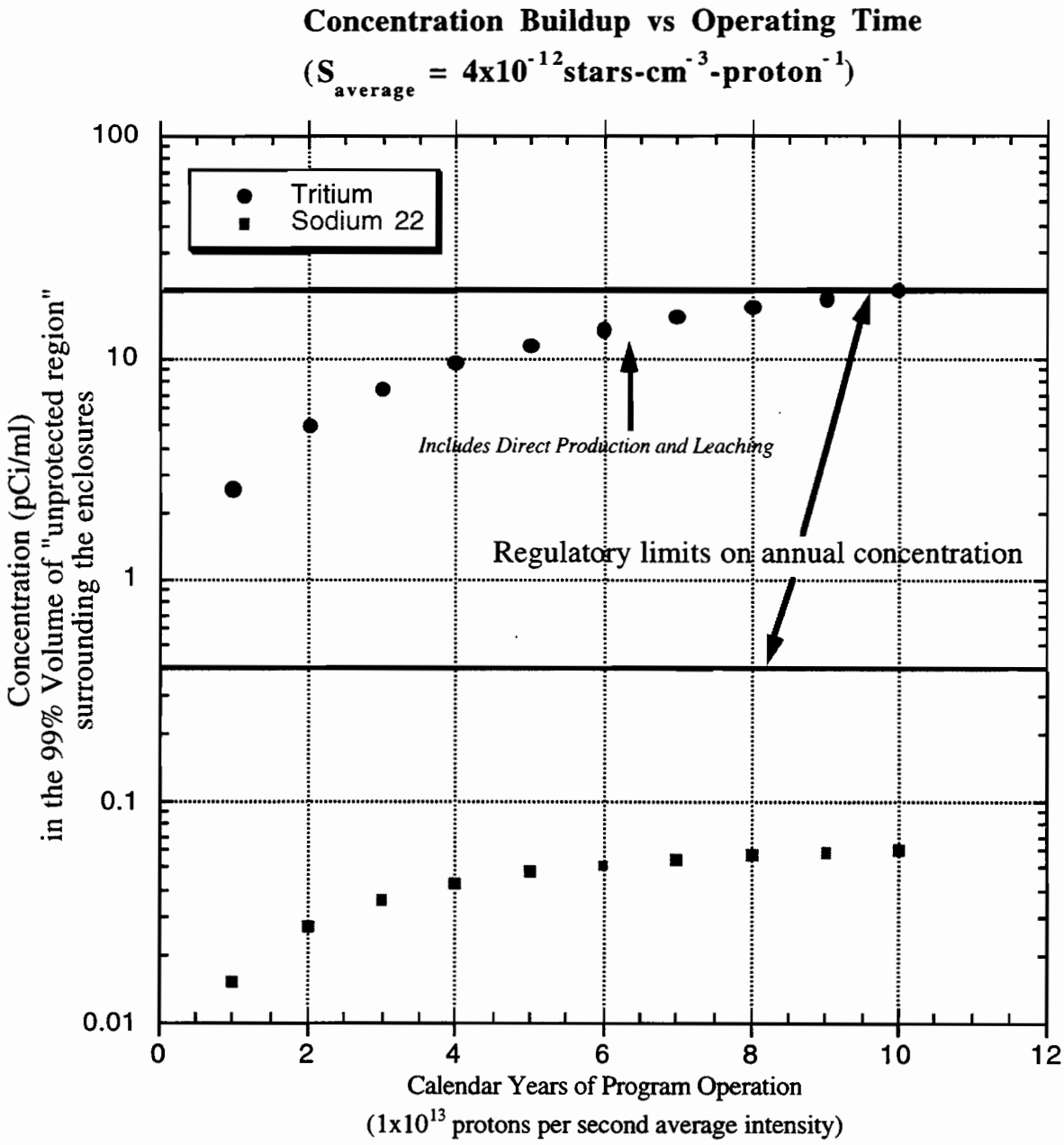

Figure 4-8 Separate concentrations for sodium and tritium where the tritium concentration has been derived for the maximum probability of direct production. The consequence is that the limit on the average allowable star density is reduced by a factor of 3.

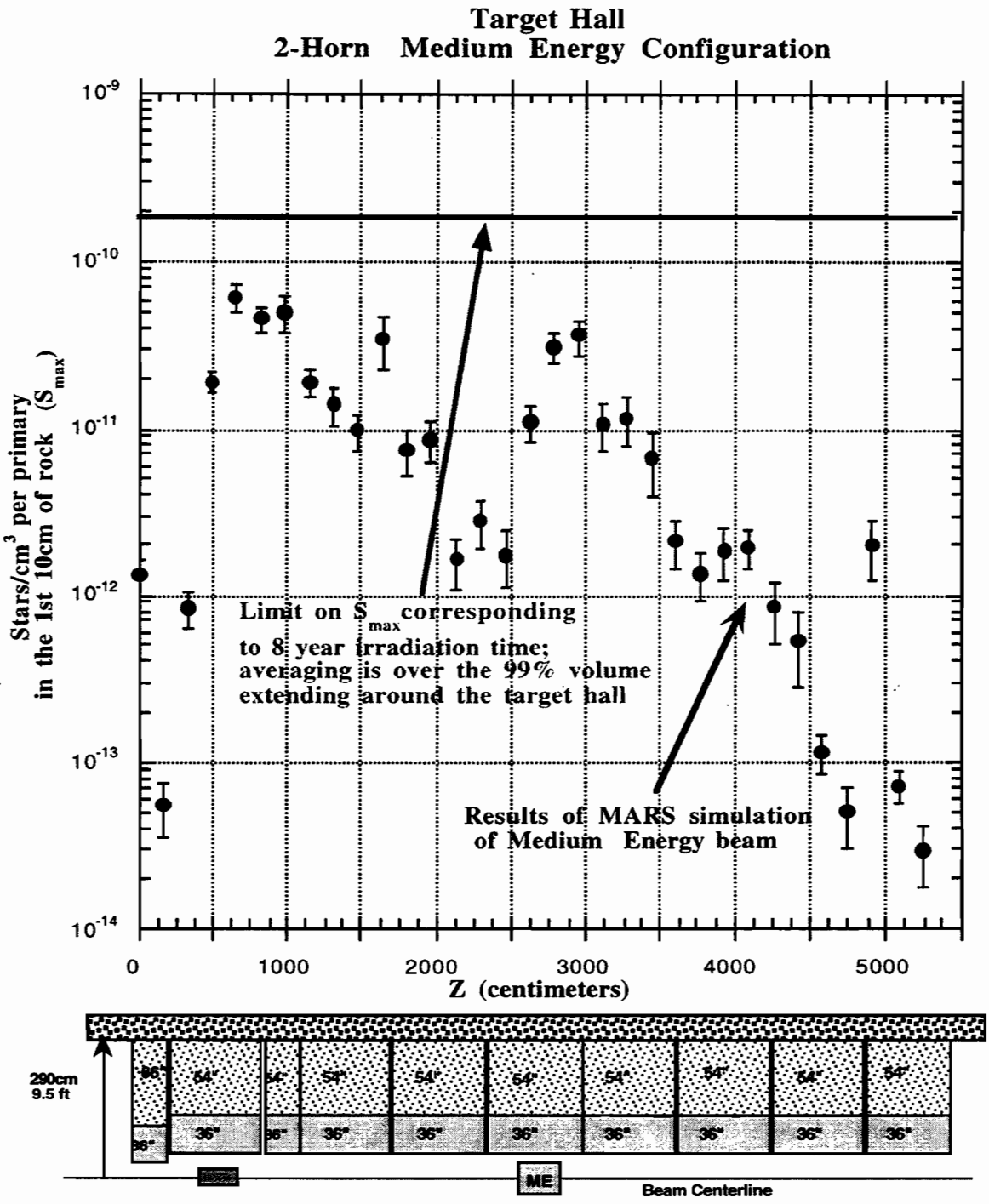

Figure 4-9 Results of the MARS simulation used to determine the amount of shielding required in the Target Hall for the medium energy beam configuration.

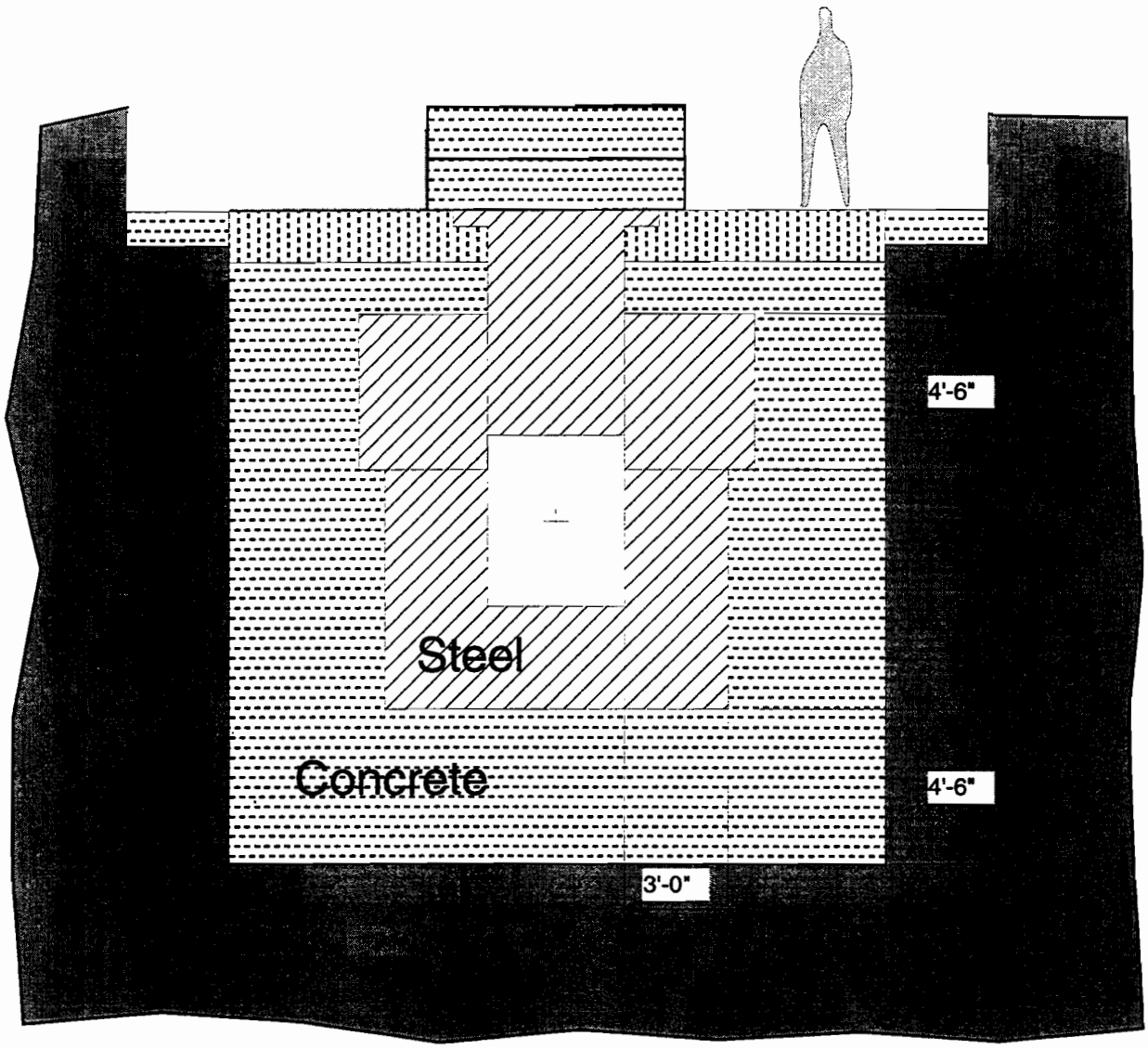

Figure 4- 10 Conceptual Design cross section of a radiation shielding "module" for regions of the Target Hall containing the active elements (target and horn).

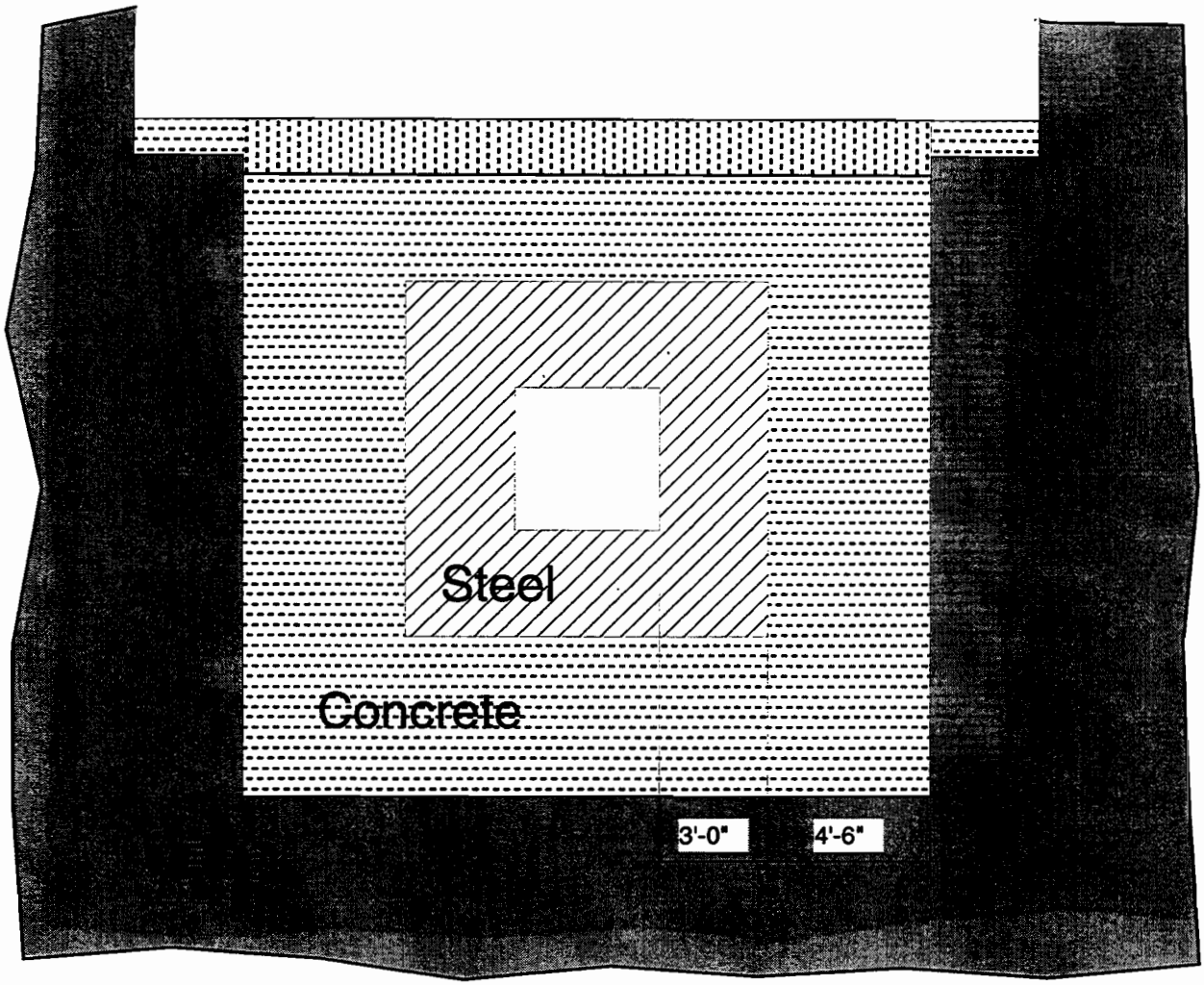

Figure 4-11 Conceptual Design cross section of a radiation shielding "module" for regions of the Target Hall not containing the active elements.

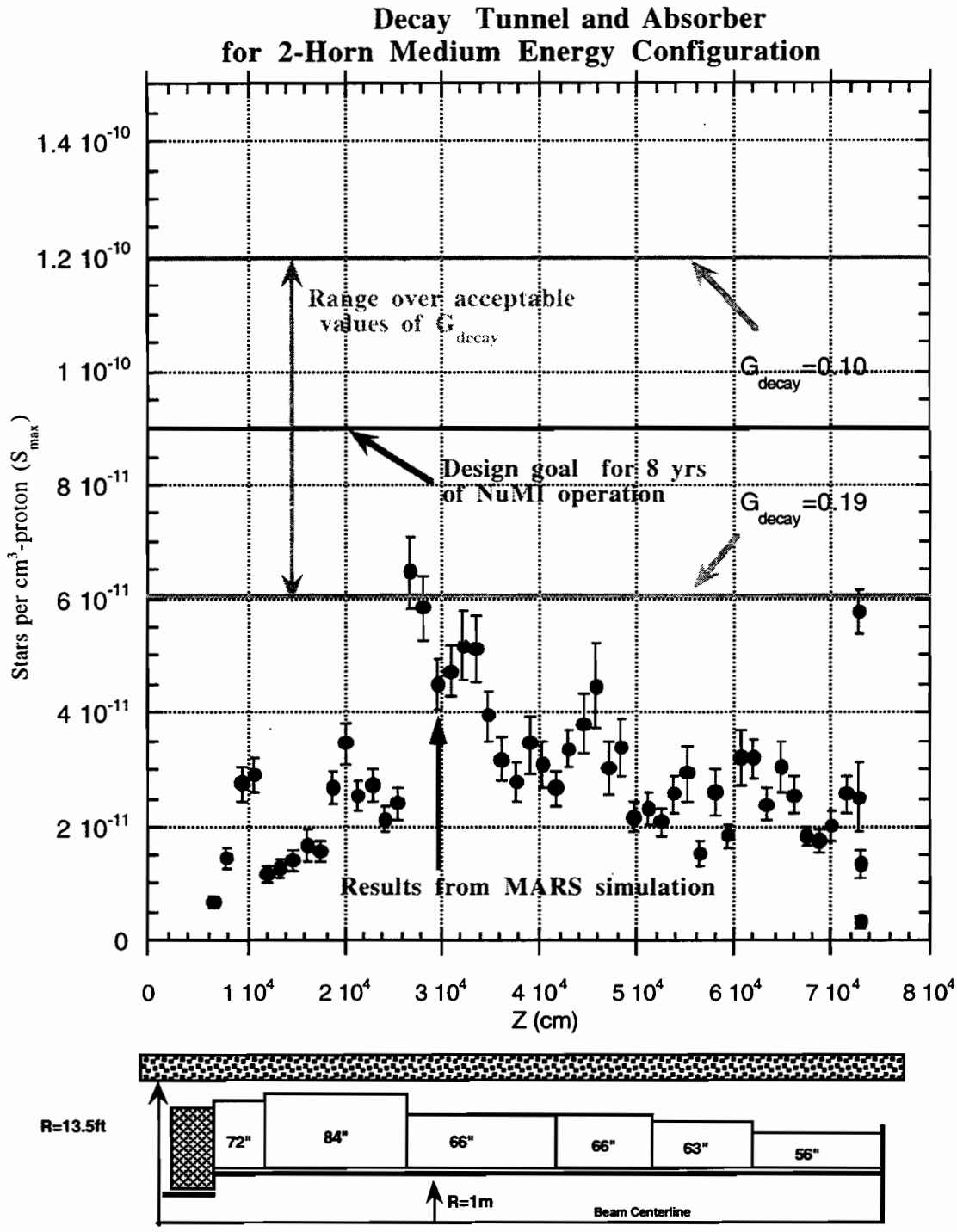

Figure 4-12 Results of the MARS simulation used to determine the amount of shielding required in the decay tunnel and beam absorber hall for the PH2ME (medium energy) beam configuration. The configuration of the shielding used in the simulation is also shown.

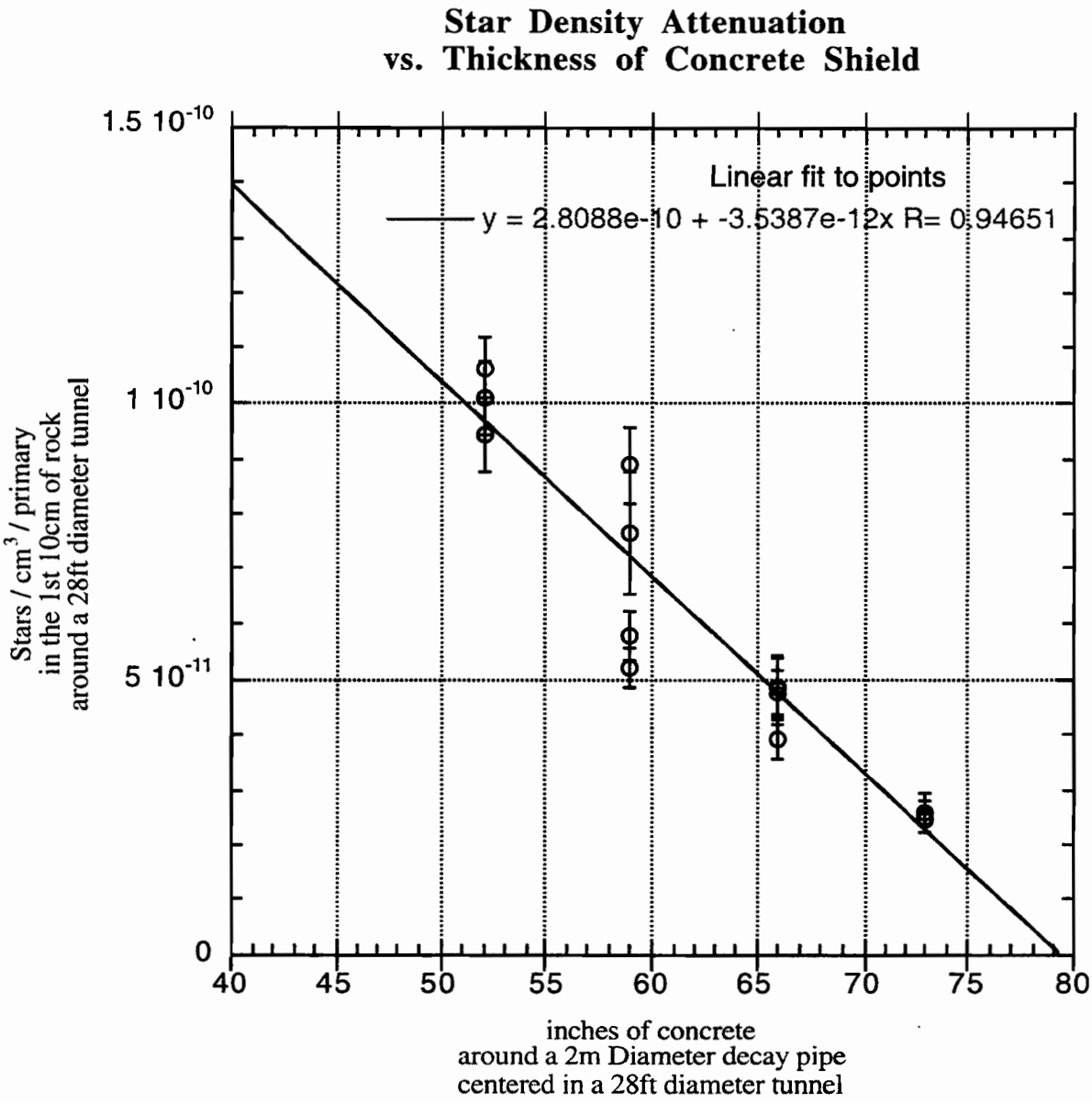

Figure 4-13 Attenuation of the star density as a function of the thickness of the concrete shield.

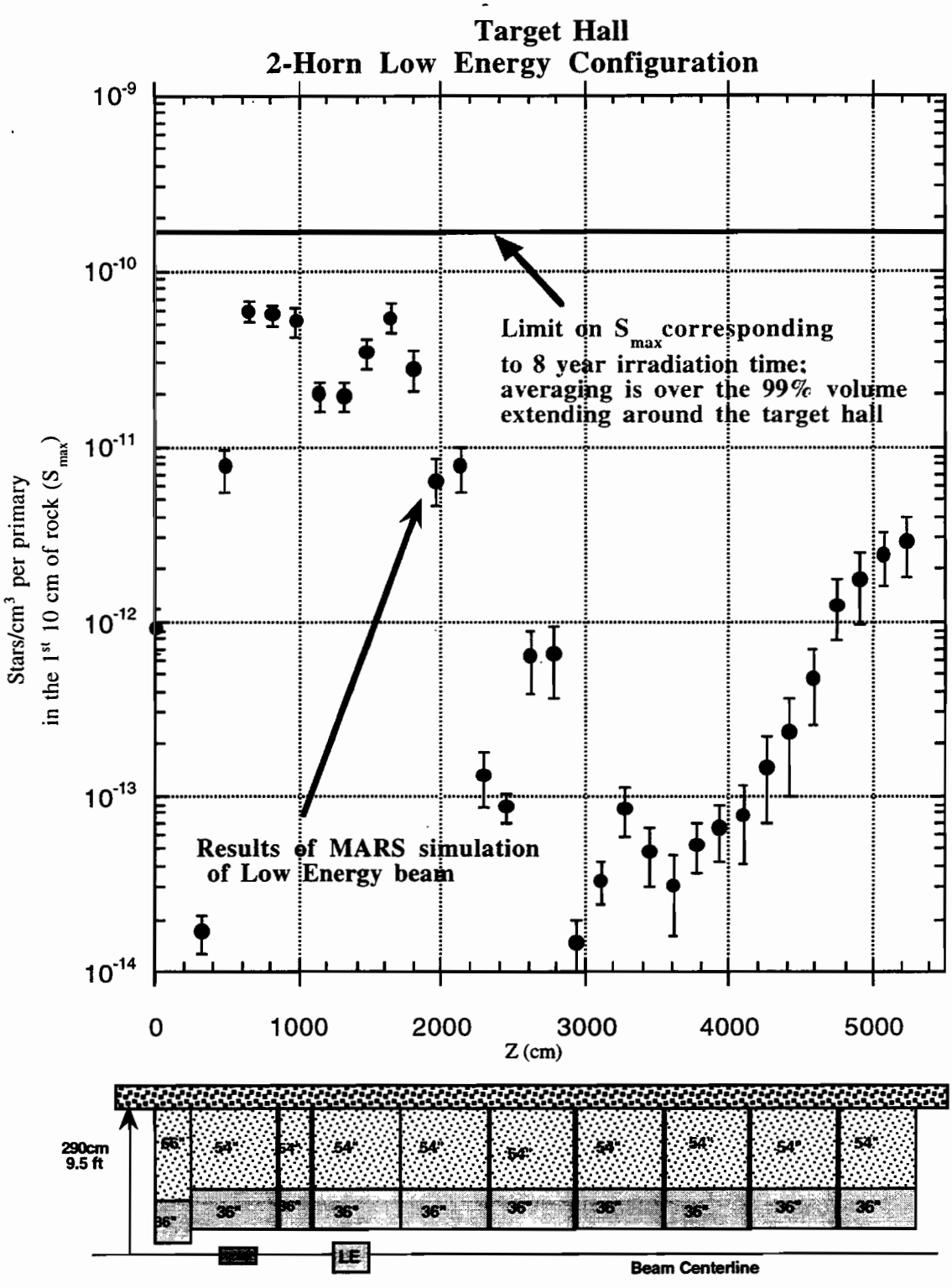

Figure 4-14 Results of the MARS simulation used to determine the amount of shielding required in the Target Hall for the PH2LE (low energy) beam.

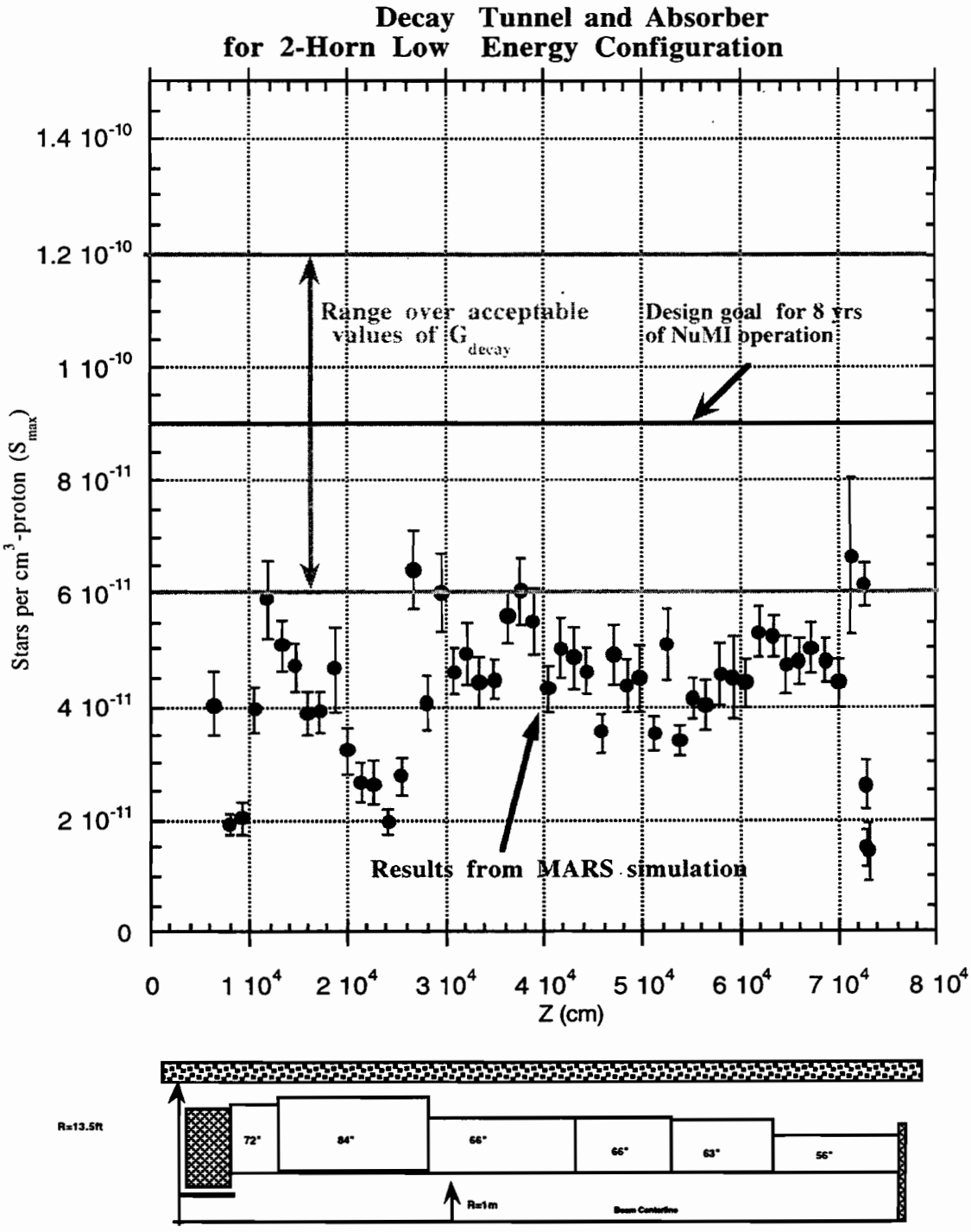

Figure 4-15 Simulation results for the low energy beam showing the resulting star density compared to the allowable limits as determined for the range of G factors for the decay tunnel.

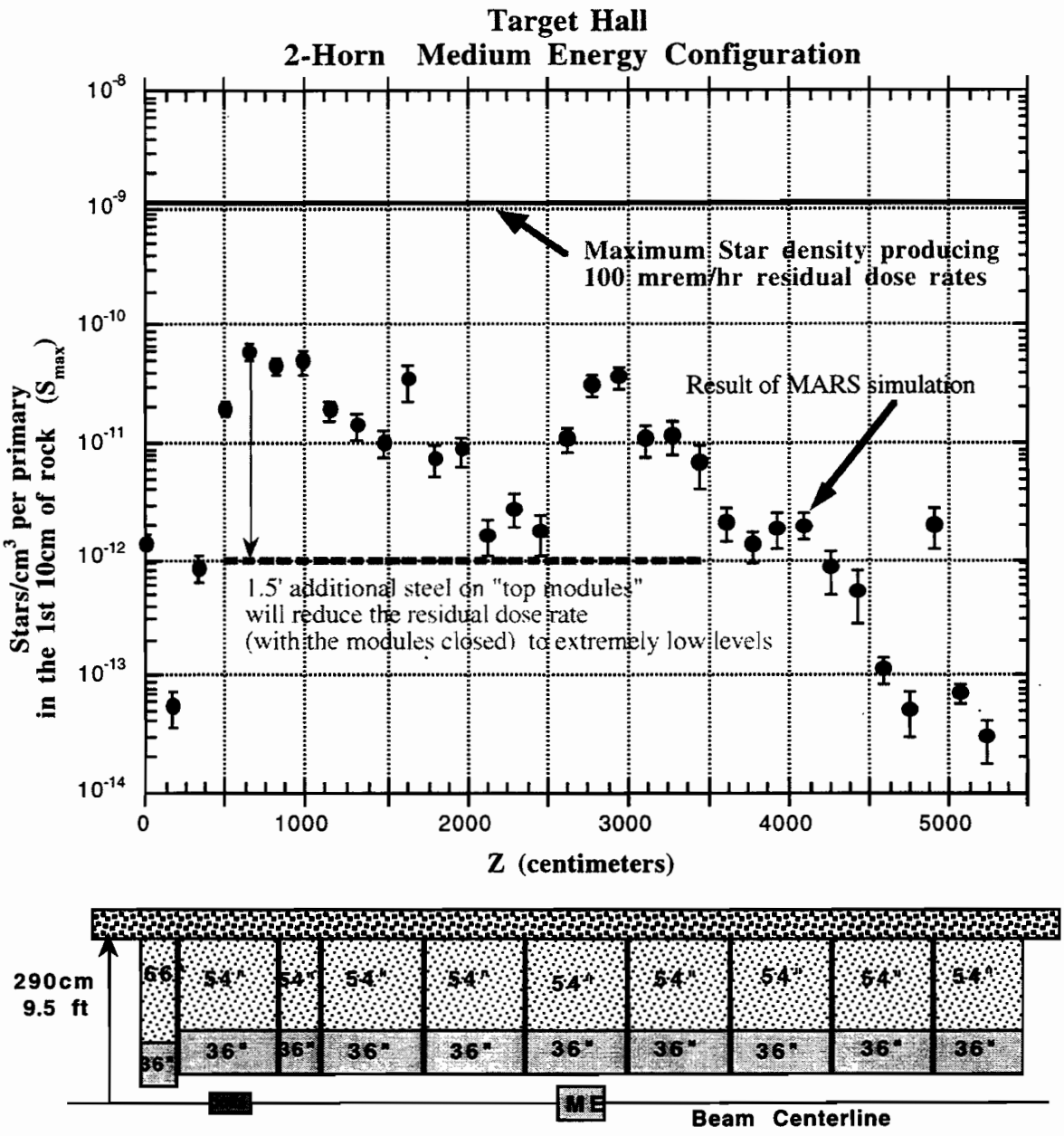

Figure 4-16 Comparison of the star density for the medium energy beam configuration as compared to predicted residual dose rates (closed target pile).

This Page Intentionally Left Blank

5.0 Civil Construction

Table of Contents

5.0 CIVIL CONSTRUCTION.....5-1

5.1 CONVENTIONAL FACILITIES..... 5-4

5.1.1 Overview..... 5-4

5.1.2 Conventional Underground Structures and Subsurface Setting..... 5-4

5.1.3 Conventional Surface Structures..... 5-5

5.1.4 NuMI Conventional Facilities Siting Criteria..... 5-6

5.1.4.1 Alignment Criteria..... 5-6

5.1.4.2 Underground Layout Criteria..... 5-6

5.1.4.3 Surface Layout Criteria..... 5-6

5.1.4.4 Excavation Criteria..... 5-6

5.1.5 Value Engineering of the Conceptual Design..... 5-8

5.1.6 Grouting and Ground Water Control Requirements.....5-10

5.1.7 Environmental Requirements.....5-10

5.1.8 Public Relations.....5-11

5.1.9 Positional Tolerances of the Underground Structures.....5-11

5.1.10 Design Life.....5-11

5.1.11 Contract Packaging.....5-12

5.1.12 Contract Provisions.....5-13

5.2 FACILITY SPACE AND HANDLING REQUIREMENTS.....5-14

5.2.1 Overview.....5-14

5.2.2 Carrier Pipe Tunnel.....5-14

5.2.3 Pretarget Tunnel.....5-14

5.2.4 Target Enclosure.....5-15

5.2.5 Target Enclosure Service Room.....5-16

5.2.6 Decay Tunnel.....5-16

5.2.7 Beam Absorber Enclosure.....5-17

5.2.7.1 Crane Capacity and Coverage in the Beam Absorber Enclosure.....5-17

5.2.8 Downstream Access Tunnel.....5-17

5.2.8.1 Muon Alcoves.....5-18

5.2.9 MINOS Enclosure.....5-18

5.2.9.1 Crane Capacity and Coverage in the MINOS Enclosure.....5-19

5.2.10 MI60 and MI62 Service Buildings (Existing).....5-19

5.2.11 Target Service Building and Access Shaft *5-20*
5.2.11.1 Crane Capacity for the Target Service Building and Access Shaft 5-20
5.2.12 MINOS Service Building and Access Shaft *5-21*
5.2.12.1 Crane Capacity for the Target Service Building and Access Shaft 5-21
5.3 UTILITIES 5-21
5.3.1 Electrical Utilities *5-21*
5.3.2 Cooling Water Utilities *5-22*
5.3.3 Anchorage for Utility Cable Trays and Ducting *5-23*
5.4 FACILITY ENVIRONMENTAL REQUIREMENTS 5-24
5.4.1 Overview *5-24*
5.4.2 Heating, Ventilation and Air Conditioning (HVAC) by Region *5-24*
5.4.3 Approximate Illumination-Level Requirements by Region *5-25*
5.4.4 Acoustic Control Measures by Region *5-25*
5.4.5 Telephone Service by Regions *5-26*
5.4.6 Door Lock Compatibility *5-26*
5.5 INSTALLATION 5-26
5.5.1 Pre-Target Elements *5-26*
5.5.2 Target Station Shielding *5-26*
5.5.3 Vacuum Decay Pipe and Shielding *5-27*
5.5.4 Beam Absorber *5-27*
5.5.5 MINOS Detector *5-27*
5.5.6 Alignment Requirements *5-28*
5.6 LIFE SAFETY 5-28
5.6.1 Overview *5-28*
5.6.2 Flammable Materials used in each Region *5-29*
5.6.3 Fire Protection Control Measures by Region *5-30*

Table of Tables

Table 5-1 NuMI Pretarget Beam Line Magnets. ____ *5-33*
Table 5-2 NuMI Power Supply Requirements. ____ *5-34*
Table 5-3 Summary of Components in the Target Hall Service Room. ____ *5-35*
Table 5-4 Summary of Components in the Upstream Service Building. ____ *5-35*
Table 5-5 Electrical Requirements by Region. ____ *5-36*
Table 5-6 Footnotes: Electrical Requirements by Region (KVA). ____ *5-37*
Table 5-7 Required Cable Tray Areas by Region. ____ *5-38*
Table 5-8 WBB Upstream Heat Loads. ____ *5-39*
Table 5-9 WBB Downstream Heat Loads ____ *5-40*
Table 5-10 NBB Upstream Heat Loads. ____ *5-41*
Table 5-11 NBB Downstream Heat Loads. ____ *5-42*
Table 5-12 Maximum Occupancy for Each Region. ____ *5-43*
Table 5-13 Heating, Ventilation and Air Conditioning (HVAC) by Region. ____ *5-44*
Table 5-14 Approximate Illumination-Level Requirements by Region. ____ *5-45*
Table 5-15 Acoustic Control Measures by Region. ____ *5-46*

Table of Figures

Figure 5-1 Extraction Enclosure Plan and Elevation (Title I Design Drawing C-14) ____ *5-49*
Figure 5-2 Carrier & Pretarget Tunnels (Title I Design Drawing C-15) ____ *5-49*
Figure 5-3 Target Enclosure and Access Shaft (Title I Design Drawing C-16) ____ *5-49*
Figure 5-4 Absorber Enclosure & Access Tunnel (Title I Design Drawing C-17) ____ *5-49*
Figure 5-5 Absorber Access Tunnel & MINOS Shaft (Title I Design Drawing C-18) ____ *5-49*
Figure 5-6 MINOS Enclosure Plan and Elevation (Title I Design Drawing C-19) ____ *5-49*
Figure 5-7 Upstream Tunnel Sections - Sheet 1 (Title I Design Drawing C-20) ____ *5-49*
Figure 5-8 Upstream Tunnel Sections - Sheet 2 (Title I Design Drawing C-21) ____ *5-49*
Figure 5-9 Downstream Tunnel Sections - Sheet 1 (Title I Design Drawing C-22) ____ *5-49*
Figure 5-10 Downstream Tunnel Sections - Sheet 2 (Title I Design Drawing C-23) ____ *5-49*

5.1 Conventional Facilities

This Section describes the baseline scope of the NuMI and MINOS Near Detector conventional facilities and the technical requirements on which they are based.

5.1.1 Overview

The NuMI/MINOS conventional facilities provide structures that are suitable for the installation, operation and maintenance of the technical and beamline components and experimental equipment of the NuMI project including; transfer line, target, decay region, beam absorber, muon detectors and Near MINOS detector.

The technical requirements and excavation criteria that have determined the alignment, size, shape, mechanical, electrical, and architectural scope of the conventional facilities are discussed in the text below by reference to a set of tables and figures, included at the end of this section. The tables summarize major component sizes, weights, power, airflow, lighting, communication, cooling, and occupancy requirements. The figures show the location of the underground housings in the subsurface, egress passage locations, the dimensions of major components and sizing of tunneled housings. The figures used in this chapter (Figure 5-1 through Figure 5-10) are reproductions of civil engineering drawings (C-14 through C-23) that form part of the Title I design drawing set.

5.1.2 Conventional Underground Structures and Subsurface Setting

The set of underground structures that house and provide tunnel access to the NuMI beamline elements are listed below:

Carrier Pipe Tunnel;
Pre-Target Tunnel;
Target Enclosure;
Target Access Shaft, including base of shaft, power rooms and access tunnels;
Decay Tunnel;
Absorber Enclosure;
MINOS Access Shaft, including base of shaft;
MINOS Access Tunnel;
Muon Alcoves (3);
MINOS Enclosure.

These underground facilities are sited in the soils and bedrock that underlie Fermilab. The Fermilab site is situated in a region of relatively flat terrain, with subsurface conditions typical of those encountered in the region. Glacial sediments or till form a relatively thick mantle, some 60 to 70 feet in thickness, overlying a bedrock that consists of a sub-horizontally bedded sequence of dolomite, dolomitic limestone and shale layers.

The series of tunneled structures that house the NuMI beamline will be excavated at an angle of approx. 7 degrees through the till and descend at a reduced angle of approx. 3 degrees in to the sequence of sedimentary rock layers. The upper section of the Carrier Tunnel, which connects with the existing Main Injector Extraction enclosure, is housed in glacial till; all other NuMI beamline structures are housed in the bedrock.

The sequence of rock units and the location of the NuMI structures within them is shown on the longitudinal cross-section in Figure 1-1. The Pretarget Tunnel, Target Enclosure and upper section of the Decay Tunnel are housed in the predominantly dolomitic limestones of Silurian age. Geologic units mined in this upper section include, from youngest to oldest (top to bottom), Joliet, Kankakee, Elwood and Wilhelm formations. The lower section of the Decay Tunnel, Beam Absorber Enclosure, Muon Alcoves, Access Tunnel and MINOS Enclosure are excavated in interbedded shale and dolomitic limestone layers of the Ordovician age, known collectively as the Maquoketa Formation, which include, from youngest to oldest, the Brainard, Fort Atkinson and Scales members. The general stratigraphy and specific geologic characteristics of the rock units and members in which the NuMI tunneled structures will be mined are described in detail in Williams et al[1]. At the base of the MINOS near detector hall, the floor of the excavation is located approximately 326 feet (99 meters) below natural ground surface.

Access to the underground NuMI beamline structures and components will be provided by two shafts and a connecting tunnel system.

5.1.3 Conventional Surface Structures

At each shaft, a grade-level service building will be constructed to support the unloading and transfer of components and equipment underground. These shafts will also house a significant portion of the electrical and mechanical systems required to support the operation and maintenance of the completed underground facilities.

---

[1] Williams et al, "Handbook of Illinois Stratigraphy," Illinois State Geological Survey, Bulletin 95, 1975.

5.1.4 NuMI Conventional Facilities Siting Criteria

The criteria and principal constraints used in establishing the location of the NuMI surface and underground structures are discussed below.

5.1.4.1 Alignment Criteria

Upstream of the Target station the beam alignment has been fixed to allow for a maximum length of beamline housing to be sited in competent bedrock. Downstream of the Target Station, the alignment must be such that it intersects both the Near (Fermilab Site) and Far (Soudan Mine Site) MINOS detectors. Details of the beam alignment are described in Section 3.6. The coordinates of the beam are given in Appendix A to this report.

5.1.4.2 Underground Layout Criteria

The layout and outfitting of the NuMI shafts and tunnels are designed to provide for installation, replacement and servicing of all NuMI components during operation and maintenance of the facility. Life safety measures have been incorporated into the design to ensure safe egress under operation and maintenance.

5.1.4.3 Surface Layout Criteria

The above grade buildings, located above the two NuMI access shafts, have been located to cause minimal disturbance to Fermilab's natural setting. The chosen sites minimize the need for any construction through the wetlands, and eliminate the need for any permanent above-grade structures to be constructed to the North of Eastbound Pine Street [2,3].

5.1.4.4 Excavation Criteria

The baseline design of tunneled structures has been influenced by both the end user requirements and the methods and means of construction. During the conceptual deign a viable excavation method (Tunnel Boring Machine) was selected and compatible excavation cross-sections developed. To support this design, a preliminary site investigation program was undertaken that identified the main geotechnical and hydrogeological characteristics of

---

2 Brunton, R. "Initial Review and Project Definition," Meeting Minutes NuMI 001, January 4, 1996.

the soil and rock, at depth, along the NuMI alignment. The results of this investigation are summarized in reports by STS Consultants Ltd. [4, 5] and an interpretation of the hydrologic portion of the investigation, conducted by the designer[6]. This investigation confirmed that the ground mass and groundwater conditions were similar to those encountered in the region. Indeed, the series of host geologic units in which NuMI will be housed have been excavated by Conco-Western Stone at a location some five miles from the proposed Fermilab site. Additionally, these units have been mined for extended distances in the construction of tunnels and pump houses for the Chicago Tunnel and Reservoir Plan (TARP)[78]. The designer's subcontractor (Harza) has been able to draw extensively up on experience gained on the mining of these tunnels and caverns in developing the NuMI design, schedule and budget.

To support the final design of the rock structures a detailed site investigation campaign has been performed.[9] Within the scope of this campaign a seismic survey was conducted to determine the soil-rock contact elevation along the full tunnel alignment. In addition, a drilling program, consisting of five holes, was carried-out to aid in the characterization of the ground mass conditions adjacent to the principal engineering structures. Drill holes were made at the following locations:

- a vertical hole drilled between the Main Injector stub and the Pretarget Tunnel to investigate till, weathered rock and groundwater conditions adjacent to the mixed face portion of the carrier pipe tunnel;

---

[3] Brunton, R. "NuMI Phase 2 Underground Facilities Review," Meeting Minutes NuMI 004, April 15, 1996.

[4] STS Consultants Ltd., "Subsurface Exploration and Geotechnical Data Report for the NuMI Project, STS Project No. 12050-CG," Transmittal Date: December 22, 1993.

[5] STS Consultants Ltd., "Hydrogeological Evaluation Report Neutrino Main Injector NuMI," STS Project No. 12050-DL, Volumes I and II, April 2, 1997, Addendum and Review Report, June 16, 1997.

[6] Fluor Daniel and Harza Engineering, "Review of the STS Hydrogeological Evaluation Report for the NuMI Project, Dated April 2, 1997, and Initial Discussion of Expected Inflows into the NuMI Tunnel," May 30, 1997.

[7] Cikanek, E.M. and Goyal, B. "Experiences from Large Cavern Exvation for TARP." Proceedings on large Rock Caverns, Helsinki, 1986, pp. 35-46.

[8] Harza Engineering Company and Fluor Daniel, "NuMI Project Tunneling Considerations," Chicago, Illinois, January 26, 1996.

[9] "Proposed Geotechnical Investigation and Testing Program," Fluor Daniel/Harza, April 17, 1998.

• one vertical borehole to investigate till, weathered rock and groundwater conditions at the Target Shaft;

• one vertical borehole to investigate till, weathered rock and groundwater conditions at the MINOS Shaft;

• two inclined holes drilled to investigate rock mass and groundwater conditions at the Target Enclosure; and

• one inclined hole to investigate rock mass and groundwater conditions at the MINOS Enclosure.

Inclined holes (angled at 30 degrees to vertical) were drilled at the enclosure locations to improve characterization of the rock mass by increasing the likelihood of intersecting the sub-vertical jointing that constitutes the dominant form of rock mass fracture in the region.

5.1.5 Value Engineering of the Conceptual Design

The preliminary site investigation data and TARP tunneling experience formed the basis for developing the NuMI Project Conceptual Design Report (CDR)[10]. This report was subjected to a value engineering (VE) review conducted by three well-established tunneling contractors. The contractors, Frontier-Kemper Constructors, Inc., Kenny Construction Company and J.F. Shea Company, Inc. were provided with summaries of the CDR and asked to comment on a number of design issues pertaining mainly to constructability, including selection of methods and means, utility needs and general cost-effectiveness of the design. Full-day workshops were held with each contractor and minutes taken on the feedback provided [11, 12, 13].

A consensus, developed from these VE reviews, led to changes being made to the CDR design. Some of the more significant changes resulting from the VE reviews are noted below:

---

[10] "NuMI Project, LBL MI-60, Civil Construciton Conceptual Design Report, June 1997.

[11] Fluor Daniel/Harza, "Meeting Minutes from the NuMI Constructability Workshop No. 2 - Frontier Kemper Constructors, Inc.", held on April 9, 1998, at Fermilab (draft copy referenced, 5-11-98).

[12] Fluor Daniel/Harza, "Meeting Minutes from the NuMI Constructability Workshop No. 3 - Kenny Construction Company", held on April 17, 1998, at Fermilab (draft copy referenced, 5-11-98).

• The contractors all identified drill and blast excavation as being a more cost-effective method of rock excavation than Tunnel Boring Machine (TBM), as adopted in the CDR. Two contractors, who already owned TBM equipment that could mine the tunnel as designed, noted that the cost of refurbishment, mobilization and demobilization made the use of a TBM on a tunnel of NuMI's length non-competitive with drill and blast. Additionally, contractors noted that the slope of the NuMI tunnel was high for the operation of rail-mounted equipment, as often used in conjunction with the TBM operation.

• To mine the glacial till, contractors who had recent firsthand experience in the mining of soils (Kenny and Shea) recommended the adoption of pipe jacking and/or hand mining techniques. In particular, they emphasized the high risk of encountering boulders in glacial deposits and were concerned that microtunneling equipment, as adopted in the CDR, would not be able to negotiate boulders larger than 1/3 the diameter of the tunnel. If such conditions were encountered "rescue shafts" would be required to provide face access to remove or break-up larger boulders, adding significantly to the costs of a given section of tunnel. Hand mining or pipe jacking techniques would allow for personnel to reach such obstructions through the tunnel and reduce the risks associated with the tunneling operation.

• The contractors all preferred the adoption of a lower alignment that allowed for the NuMI underground structures sited preferentially in the bedrock. In particular, all the contractors preferred the "Superlow" scheme, as presented to them as an option during the workshop, because it allowed the target hall to be constructed as a mined structure.

Based on the consensus reached on this set of basic engineering issues the NuMI design was changed to reflect the contractors' recommendations, notably adjusting the sizes and shapes of the mined structures to be compatible with the drill and blast excavation method while maintaining the space requirements discussed below. Additionally, to reduce the risks of ground instability being encountered in the Target and MINOS Enclosures the crown spans were reduced to provide for the excavation of narrower and more similar cross-sections [14].

---

[13] Fluor Daniel/Harza, "Meeting Minutes from the NuMI Constructability Workshop No. 1 - J. F. Shea Company", held on March 27, 1998, at Fermilab (draft copy referenced, 4-13-98).

[14] MacPherson, H.H. "Preliminary planning considerations for NuMI Underground Facilities." Intra-Company Correspondence, Files Project 5800G 202, March 27, 1996.

The methods and means selected to support the baseline scope, cost and schedule are all practiced in the region and considered to represent proven relatively low-risk construction methods well adapted to the site conditions.

5.1.6 Grouting and Ground Water Control Requirements

There is no specific technical requirement for the NuMI structures to be completely watertight. All subsurface NuMI facilities are designed to collect, drain and evacuate post-grout levels of water inflow, using a combination of channels, drip shields, floor drains and pumps. Drainage systems will be sized to allow access for general maintenance and clean-up/removal of debris or calcium carbonate build-up. Sumps are located at the base of the two access shafts. In general, the tunnel structures will be provided with a sprayed concrete (shotcrete) lining that will be locally backed with drainage panels to direct any groundwater inflow to floor drainage channels. Additional water control measures will be employed locally, either where the residual water inflow is likely to be most pronounced (shafts) or to protect the more sensitive components of NuMI/MINOS equipment. In the Shafts, Power Room and Target Enclosure crown, cast-in-place linings will be used in combination with full water drainage membranes. In the Absorber Enclosure, Detector Enclosure and Counting Room areas, drip shields will be placed to prevent any groundwater from dripping from the crown directly on to the housed equipment.

5.1.7 Environmental Requirements

All contractors will be required to respect the regulatory limits that are placed on construction activities, notably those relating to noise, vibration, soil erosion, water discharge regulations and air-borne dust. Vibration and noise levels will be imposed upon all NuMI blasting operations. Vibration levels will be monitored to ensure that specified limits are not exceeded, either on Fermilab structures or on residential housing located in proximity to the NuMI blasting site(s). Specific requirements for controlled blasting measures will be specified in the excavation of the more critical rock structures, notably for the excavation of the Target Enclosure crown. Ambient construction noise and air over-pressures resulting from blasting, will be monitored at the Fermilab site boundary to ensure compliance with statutory noise limits. Shaft blasting will be restricted to day light hours.

The noise and vibration limits proposed for the NuMI project are those that have already been used on other projects undertaken in residential areas of Chicago[15, 16].

5.1.8 Public Relations

Prior to undertaking NuMI construction work, the surrounding communities will be briefed on the nature and extent of the work itself. The impacts of NuMI construction on specific neighborhoods will be discussed in detail at a series of meetings organized in conjunction with the Fermilab Public Relations Department.

5.1.9 Positional Tolerances of the Underground Structures

It is important that the NuMI facilities constructed by the underground contractor be aligned with sufficient accuracy to ensure that the NuMI beamline components and utilities can be installed efficiently using normal accelerator alignment techniques. To this end, Fermilab will periodically check the survey coordinates used to guide the excavation of the underground structures.

After hole-through of the Decay and Carrier Tunnels, and prior to installation of the beamline floors and beam pipes (decay and carrier); Fermilab will conduct precise surveys, recalculate survey monuments' coordinates and check that the excavations profiles conform to the contract tolerances. Normal engineering tolerances for excavation and the placement of concrete and shotcrete (ACI) will be specified.

5.1.10 Design Life

A nominal design life of 25 years[17] is projected for the NuMI facilities. At the end of this period provision may be made for the detailed inspection and renovation of structures. Operational and maintenance issues associated with Life Cycle Costs will be addressed during the detailed design of the facilities.

---

[15] Brunton, R.. "Typical Noise and vibration Levels from Underground Excavation Activities." Letter Report, June, 1996.

[16] MacPherson, H.H. "Typical Range of Freqeucies for Blasting Vibrations." Intra-Company Correspondence, Files Project 5800G 202, July, 1998.

[17] Brunton, R. "NuMI Phase 2 Underground Facilities Review." Meeting Notes NuMI 004, April 15, 1996.

5.1.11 Contract Packaging

The integrated schedule calls for the NuMI conventional facilities to be built in four major construction packages. The main scope items of each of these packages is outlined below:

• Site Preparatory Work - to include the clearance, construction and/or upgrading of the NuMI access roads and provision of construction utilities;

• Underground Construction - to include excavation and support the underground openings, installation of construction elevators, sump pumps and piping, ventilation fans and ducting, and pipe and shielding installations;

• Target Service Building - to include construction of the building, completion of utilities, surrounding landscaping and the electrical, mechanical, architectural finish-out of the underground openings upstream of the Decay Tunnel; and

• Minos Service Building - to include construction of the building, completion of utilities, surrounding landscaping and the electrical, mechanical, architectural finish-out of the underground openings downstream of the Decay Tunnel.

Additional contract packages will be required for the procurement of the decay pipe and other mechanical and electrical systems.

Detailed design work (Title II) will be tasked and undertaken separately for these packages. Final Title II deliverables will include a Geotechnical Baseline Report (GBR) for the underground contract, Drawings and Specifications. Intermediate Title II deliverables will include drafts of the final deliverables and notes addressing specific and critical design issues, notably pertaining to stability, blasting, grouting and water inflow control.

The VE conducted on the CDR led to significant economy being garnered for the NuMI project. A further independent VE review and an independent cost estimate will be undertaken once the results of the site-specific investigation campaign, and Title I back-up documentation of facility requirements are delivered. Fermilab will fix the final configuration of the underground structures based on the results of this VE exercise, which will include a review of the cost, schedule and safety impacts of any changes. This review will be completed prior to commencement of Title II design work. The draft Title II designs will also be subjected to VE review.

5.1.12 Contract Provisions

Provisions for the different contracts are not finalized. However, it is envisaged that Fermilab will employ standard contracting practices that include specific requirements for safety and quality construction management. Safety requirements specific to the NuMI project are also discussed in the Preliminary Safety Assessment Document (PSAD)[18]. Some additional provisions that are being considered for inclusion in the Underground Contract are listed below;

• a value engineering clause - to encourage the contractor to make constructive suggestions and provide economy to the project through the sharing of savings;

• a partnering scheme - to ensure an open relationship between contractor and owner, provide for clear definition of roles and responsibilities and, in particular, the definition of an hierarchy of contractual mechanisms by which disputes can be efficiently resolved;

• a differing site conditions clause - to reassure the contractor that the contract is to be administered fairly and that the owner will accept any cost and time penalties associated with ground conditions encountered being materially worse than those described in the Geotechnical Baseline Report (GBR). This clause consequently will allow the contractor to reduce the size of any "ground-related" cost contingency that would otherwise be built-in to his or her bid price;

• a limited set of unit prices for a "ground-related" bill of quantities - to provide some discretion or flexibility to the Contractor and Construction Manager, with regard to the selection of appropriate methods for the treatment, and support the ground mass and/or control of groundwater inflows.

• a contractual requirement for the compilation of a joint shift report to be countersigned (with or without reserve) by the owner's and contractor's site representatives on a daily basis - to ensure that the substance of any disagreement in attributing the cause behind a construction delay and/or an extra cost can be rapidly documented and communicated throughout the "project hierarchy". The end goal here is to ensure that any problem is rapidly defined and fixed and that its consequences to the project (time lost, costs incurred) are minimized.

---

[18] NuMI Project Team, "NuMI Project at Fermilab: Preliminary Safety Assessment Document." April 1998.

5.2 Facility Space and Handling Requirements

5.2.1 Overview

This section summarizes the space and handling requirements of the NuMI beam and MINOS Enclosure.

The beamline components are summarized in the Beam Sheet, which has been included in Appendix A to this Report. Locations and sizes for NuMI primary beam technical components are shown in Table 5-1. Upstream elements are to be located in the existing MI and linking NuMI extraction stub, while those primary beam components downstream of NuMI Station 939 feet are to be installed in the Pretarget Tunnel. The space requirements for the NuMI facilities are driven largely by the installed footprint of the components, utility runs, assembly areas, shielding and installation and egress passages. The size, shape and configuration of the underground structures have been engineered to optimize the constructability of the ensemble of tunneled structures, as discussed in previous sections.

5.2.2 Carrier Pipe Tunnel

An evacuated beam pipe of 18 inches diameter and 434 feet approximate length is required to transport the extracted Main Injector beam from the existing extraction enclosure, near MI-60, to the Pretarget Tunnel. This pipe is situated in the Carrier Tunnel as shown in Figures 5-1, 5-2, and 5-7. The civil construction requirements shown in these figures for the Carrier Tunnel are driven by the optimization of the construction approach through the different ground materials traversed (till, till/rock interface, rock) to reach the Pretarget Tunnel. Pipe-jacking was selected as the baseline method for excavation in the glacial till and hand-mining techniques adopted to mine through the rock-till contact (mixed face mining) into the unweathered rock material. Provisions for grouting and additional ground support are included in the baseline design in the mixed face zone. A hadron shield of approximate 25 feet length will be located in the MI extraction enclosure. This shield is required to provide radiation protection enabling NuMI access into the Pretarget Tunnel during Main Injector beam operation, see Chapter 4.

5.2.3 Pretarget Tunnel

The Pretarget Tunnel is 190 feet long and of sufficient cross-section to permit installation of a string of beamline magnets, instrumentation and other components along with the

necessary shielding and an emergency egress passage, as shown in Figures 5-2, 5-3 and 5-7. A minimum distance from the beam center-line will be maintained, to provide space for groundwater shielding along the beamline where potential beam loss points exist. An aisle along the west side of the beamline with a minimum width of 5 feet is necessary to provide space for replacing failed magnets. A separately ventilated egress passage is provided adjacent to this tunnel to allow for safe evacuation of personnel.

The tunnel is sized to allow for either carts or the existing Main Ring magnet mover to be used to move magnets up the inclined floor of the Pretarget Tunnel and install them. A safety anchorage will be installed at the upstream end of the tunnel to anchor any wheeled vehicles operating on the sloped floor. The tunnel floor will be rough broom finish concrete for improved traction.

Anchor points in the walls of the Pretarget Enclosure will be located every 8 feet along the beam. A maximum point load capacity for the anchors of 2000 pounds per running foot will be provided.

5.2.4 Target Enclosure

The NuMI Target Enclosure is shown in Figures 5-3, 5-7 and 5-8. The enclosure houses the primary target and focusing horns along with the shielding pile, needed to provide groundwater and residual activation protection from the primary beam targeting. The shielding pile is described in detail in Chapter 4 of this report. Internal dimensions of the Target Enclosure are 220 ft. in length, 27 ft. wide and of increasing elevation from 40 ft. at the upstream to 49.5 ft. at the downstream end. The roof is at a constant elevation, while the enclosure floor is sloped to match the downward 58 mrad. (3.3 deg) beam angle. Beam elevation at the target location is 626.8 ft. M.S.L., approximately 114 ft. below surface grade level.

Access for installation and removal of technical components is from the top of the shield pile. Components are supported in place below modular steel shielding sections that are installed and removed as complete units. This loading concept has worked well in the existing AP0 target hall.

5.2.3.1 Crane Capacity and Coverage in the Target Enclosure

A 25 ton overhead crane with a pendant connection is required in the Target Enclosure. The crane will have hand held radio control to provide for control of the three directions of motion.

This crane is to be utilized for installation of the target pile shield, and for installation and removal of technical components located within the shield. Crane coverage allows lifting of components from the floor area upstream of the shield pile to the top of the pile, and subsequent installation from that location. The work space downstream of the shield pile is also under crane coverage.

5.2.5 Target Enclosure Service Room

The Target Support Enclosure needs to be sufficiently shielded from the Target Enclosure that it can be occupied during beam on conditions. Location of the enclosure, at the base of the Target Access Shaft, is shown in plan and section views in Figure 5-3 and 5-8. The largest component located in this enclosure will be the horn capacitor bank (5.5 ft × 17.5 ft × 6.5 ft high). It is important to keep the capacitor bank close to the Target Enclosure so that the length of the stripline, used to carry the current to the horns, can be kept as short as possible. A minimum rock shield of 20 ft. is maintained between this enclosure and the Target Enclosure.

The power supply that is part of the NuMI horn system is located in this area adjacent to the capacitor bank for ease of troubleshooting. The space needed for the horn power supply area is 21 ft × 34 ft. The elements of this system will be installed using pallets. The Target Support Enclosure will also contain the pumps and heat exchangers of the radioactive (RAW) and low conductivity (LCW) water systems. Sizes of components to be installed in this enclosure are summarized in Table 5-3. Anchor points are needed in the concrete walls and ceiling of the enclosure located every 8 feet along its length. Allowable point load capacity for the anchors of 2000 pounds is required for both types. Needed space for these components is 24 ft × 34 ft.

5.2.6 Decay Tunnel

The 2215 foot (675 meter) long Decay Tunnel occupies a large part of the NuMI facility footprint, but has a simple geometry. The vacuum decay pipe and its shield are shown in Figure 5-3, 5-4 and 5-9. Contained in this tunnel is the vacuum decay pipe of 6.5 ft. (2.0 m) diameter, which is surrounded by a shield formed of low strength concrete. An access passage is provided to one side of the shield and an inspection gap to the other. The passage and air-gap are provided to allow for sampling of groundwater along the length of the decay region and visual inspection of an air gap respectively. The passage also

provides a secondary means of egress from the downstream enclosures in case of emergency.

5.2.7 Beam Absorber Enclosure

The Beam Absorber Enclosure is shown in Figure 5-4 and 5-9. The enclosure dimensions are 50 ft. long, 27 ft. wide, and approx. 36 ft. high. The Beam Absorber with shield has a gross weight of about 600 tons. The inner block assembly will be assembled outside of the enclosure and installed as a unit. The bulk shielding will be assembled in place from precast concrete blocks and steel plates, nine (9) inches thick. No element of the beam absorber will weigh more than 15 tons.

5.2.7.1 Crane Capacity and Coverage in the Beam Absorber Enclosure

An overhead lifting capacity of 15 tons is required in the enclosure with a crane hook coverage area of forty (40) feet long by eighteen (18) feet wide. The distance from the top of the absorber shielding to the crane hook at the top of its travel is seven (7) feet to provide sufficient room for attachments. Due to the radiation levels, the control panels will be removed during beam operations.

5.2.8 Downstream Access Tunnel

The Downstream Access Tunnel is shown in Figures 5-4, 5-5, 5-6 and 5-10. The tunnel provides access to the Beam Absorber and MINOS Enclosures through the MINOS Access Shaft. Between the shaft and the Beam Absorber Enclosure the tunnel is sloped at a gradient of approximately ten percent. Between the shaft and the MINOS Enclosure the tunnel floor is flat. The flat floor is designed to facilitate manipulation, transport and storage of MINOS detector equipment.

The Beam Absorber RAW pump system and Decay Pipe vacuum pump will be located in the upstream end of the Downstream Access Tunnel. Each of the two vacuum skids will occupy a footprint of approximately 4 ft wide × 6 ft long and will have a local electrical isolation switch, motor starter panel, and OSHA conforming clear area in front of it. A carbon steel duct six inches in diameter will conduct the vacuum pump exhaust from the skids to the MINOS access shaft and up to an exhaust point on the surface. The beam absorber RAW system skid will occupy a footprint 6 ft wide × 8 ft long, and include a local

electrical isolation switch, motor starter panel, and OSHA conforming clear area. Since the RAW system will become activated, shielding is necessary between the RAW system and the access route to it.

5.2.8.1 Muon Alcoves

Three (3) Muon Alcoves will extend from the Downstream Access Tunnel into the beam as shown in Figures 5-4, 5-5 and 5-9. Each alcove will be used to house equipment that will monitor the muons produced together with neutrinos in meson decays. Each muon alcove will be 12 ft. high × 12 ft. wide (transverse to the beam direction), centered on the beam line. The access passage to the muon alcove will be 10 ft wide.

The muon alcoves are spaced down the beam line to monitor the number of muons left after penetrating through various amounts of rock. The first alcove is located behind 33 ft.(10 m) of rock after the end of the Beam Absorber Enclosure. There will be 115 ft. (35 m) of rock between the first and the second alcoves, 246 ft. (75 m) of rock between the second and the third, and an additional 400 ft. (122 m) of rock between the third muon alcove and the start of the on beam line portion of the access passage to the detector hall.

The passageways to the alcoves will maintain a minimum height of 12 ft. and accommodate an 18 inch wide cable tray. The cable tray will accommodate 30 signal cables, 30 medium voltage bias cables (few hundred volts) and a temperature probe cable. The muon alcoves will be equipped with lighting and two 120 VAC, 20 amp circuits (each with two duplex outlets) for hand power tools and oscilloscopes.

5.2.9 MINOS Enclosure

The MINOS Enclosure, which is 150 ft. long × 30 ft. wide × 36 ft. high is shown in Figures 5-6 and 5-10. The upstream portion of the hall provides detector module assembly space. The upstream face of the assembled detector begins at 85.5 ft. from the upstream end of the enclosure. Beam center height above the hall floor is 10.0 ft at this upstream face. It should be noted that this location is slightly above the physical center of the detector at this upstream face.

The access passage from the downstream shaft to the enclosure is aligned to provide an open tunnel space of 6 ft. radius around the beam for a distance of 75.5 ft. upstream of the detector hall. This provides a beam cylinder region that is clear of rock for a 161 ft. distance upstream of the front face of the detector. The detector is oriented so that a square hole for the magnet coil is on the east side. The west vertical side of the detector is located 5.5 ft. from the beam center. Under catwalks to the detector sides is a minimum 3 ft. wide aisleway. The enclosure floor is level to aid in detector construction. An enclosed egress hallway is placed on the east side of the hall.

A data acquisition room, of size 12 ft. wide × 30 ft. deep × 12 ft. high, is located at the west side of the hall at the center of the detector. The power supply for the detector magnet will be located in the upstream region of the detector hall.

5.2.9.1 Crane Capacity and Coverage in the MINOS Enclosure

An overhead crane lifting capacity of 15 tons is required in this enclosure with crane hook coverage over the full area of the detector hall, except for nominal dead space distances on the sides and at the ends. Crane hook height is 26 ft. above the floor of the hall. The crane will have a hand held radio control for three directions of motion, and a provision for a pendant connection.

A second crane (7.5 tons) is needed in the upstream assembly area of the detector enclosure. The addition of this crane will significantly decrease detector module assembly times.

5.2.10 MI60 and MI62 Service Buildings (Existing)

The NuMI items to be installed in the existing Main Injector Service Buildings, MI60 and MI62, are described in this section. Three relay racks will be needed in each of these buildings for NuMI beamline instrumentation plus additional space for water and vacuum requirements. Table 5-2 shows the NuMI power supply requirements including the power supplies that will be located in these areas and the total power supply feeder loads. Water requirements can be met by the existing systems in these buildings. For supplying 480VAC power, the plan is to use an existing spare 13.8kV transformer pad at MI60 for locating a 1500 kVA substation. The substation and a 480VAC power panel in the MI60

building will be provided by NuMI. A 1500kVA substation connected to the beamline feeder and a 480VAC panel and cabling that can be used by the NuMI power supplies will be located at MI62 for the MI. Thus NuMI does not need to provide a substation or 480VAC power panel at MI62.

5.2.11 Target Service Building and Access Shaft

One pulsed power 1500kVA substation, one 750kVA substation, two 480VAC panels, and associated AC wiring will be needed at the Target Service Building.

The Target Service Building provides space for seven large power supplies. Three 500kW supplies and one 240kW supply (for the horn power supply system) are for the NuMI Baseline Beamline. Three additional large power supplies will be needed for the Narrow Band Beamline and space has been allowed for this.

The Target Service Building and Shaft will be the only means of access for bringing components into the target, pretarget and vacuum decay regions. Consequently, the access shaft needs to be sufficiently large to accommodate all of the components to be placed in the upstream subsurface structures. Items which will have to be brought down the shaft and which set requirements for the dimensioning of the shaft drop space are:

- Horn power supply system capacitor bank: 5.5 ft × 17.5 ft × 6.5 ft high.
- Main Ring B2 magnets 20.7 ft. long.
- Steel shielding of sizes to 20 ft. long and 23 tons.

Offloading/staging space of approximately 400 sq. ft. will be provided in the upstream service building under crane coverage for efficient installation of Pretarget Tunnel and Target Enclosure components.

5.2.11.1 Crane Capacity for the Target Service Building and Access Shaft

Overhead lifting capacity of twenty five (25) tons with crane hook coverage area that fully covers the adjacent loading dock space is necessary. Minimum distance from the top of the concrete at the loading dock to the crane hook at the top of its travel will be 17.5 ft to provide sufficient room for lifting components from a flatbed trailer.

5.2.12 MINOS Service Building and Access Shaft

The downstream above grade service building and access shaft will be the only means of bringing components into the MINOS Beam Absorber Enclosures and Muon Alcoves. Items that will have to be brought down the shaft and which set requirements for the access shaft dimensions are:

- Steel detector modules. These pieces set requirements for a minimum height of at least 18.5 ft. for the Downstream Access Tunnel between the shaft and the MINOS Enclosure.

- MINOS magnet coil. L-shaped pieces each 60 ft. × 12 ft. × 1.5 ft. There are two such pieces; one with the short leg of the "L" at the upstream side, and the other with it on the downstream side. The long side of the access hatch must be oriented along the axis of the tunnel to the Detector Hall. The shaft-tunnel intersection must accommodate the passage of these coil pieces.

Offloading/staging space of approximately 1000 sq. ft. will be provided under crane coverage for efficient installation of the detector components.

5.2.12.1 Crane Capacity for the Target Service Building and Access Shaft

Overhead lifting capacity of fifteen (15) tons with crane hook coverage area that fully covers the access shaft and adjacent loading dock space is necessary. The height from the top of the concrete at the loading dock to the crane hook at the top of its travel will be 17.5 ft. to provide sufficient room for lifting components from a flatbed trailer.

5.3 Utilities

5.3.1 Electrical Utilities

Electrical power usage falls into three primary categories: 1) building power which is used for lighting, HVAC equipment, convenience wall outlets, welding receptacles, overhead cranes, sump pumps, hoists and elevators, etc. 2) user utility power for magnet power supplies, or other user installed equipment and 3) user clean power for computers, electronics and other delicate or sensitive hardware specific to the experiments.

Loads from the first category (building power) will be calculated by the A&E and the distribution sized appropriately.

Loads for the second two categories (user utility and clean power) have been determined. Feeder loads are given in the last columns of Table 5-2 and are summarized for the service buildings that are being used by NuMI: MI60, MI62, the Target Service Building and the MINOS Service Building. A single 500kW power supply has been allocated for the MINOS power supply. Total electrical requirements by region are summarized in Table 5-5. Footnotes for this table are summarized in Table 5-6.

At Fermilab, cable trays are generally used in the below grade tunnels and experimental halls for routing magnet power leads and signal cables. Previous experience indicates minimal difference in the installed cost for 12 inch and 18 inch cable tray. Consequently, 18 inch is preferred. Conventional AC power is not to be run in these trays as they are for DC magnet power and signal cable. Cable trays between geographically adjacent regions will connect together at the intersection. PVC conduits will be oriented such that they align with the tray at the region boundary. Cable tray requirements by region are summarized in Table 5-7.

Ethernet cable will also be installed along the beam facilities as part of WBS 1.1.8; a description is given in Section 3.8.

An emergency gas generator will be installed adjacent to the MINOS service building. This generator will supply emergency power for critical services including the elevator, emergency lighting and ventilation systems and sump pumps.

5.3.2 Cooling Water Utilities

Three cooling water system will be used for NuMI. These are Industrial Cooling Water (ICW), Low Conductivity Water (LCW), and Radio Active Water (RAW) systems. These systems are needed to indirectly or directly remove the heat generated by the operation of electrical devices and to dispose the power deposited in various beam line components by the absorption of high energy beam particles.

Ultimately the energy absorbed by the cooling water system is transferred to the atmosphere. To accomplish this task the ICW system is used. Water circulating through the ICW system is not suitable for direct use in beam line components such as magnets and power supplies because of the high electrical conductivity of the ICW. Therefore, a separate system, the LCW system, is required, which forms its own closed loop. The main components of the LCW system are heat exchanger(s), LCW water pumps, De-Ionization (DI) "bottles", plumbing, and the components to be cooled. The function of the DI "bottles" is to treat the water to bring the electrical conductivity of the water to a very low level. Once the water has been treated, the electrical resistance of the water in the LCW

system is in the 4 to 10 megaohm range and is suitable for use within the electrical conductors. This LCW is then pumped through magnets, power supplies and other components where it absorbs the thermal energy from the components. The LCW is then cooled by the ICW system with the use of a heat exchanger. Given that the NuMI LCW system must cool devices in the Pretarget Tunnel and target enclosure areas, the absorber located 725 m downstream of the target, and the equipment in the MINOS detector hall located further downstream of the absorber, the LCW system will be separated into separate subsystems.

While most of the components that require cooling water operate in non-radiation or low radiation level environments, some of the NuMI components such as the target, horns, absorber(s), will have to operate in very high radiation level environments. The water cooling system for a very high radiation level environment is known as the RAW system. The main components of a RAW system consist of heat exchanger(s), pumps, DI-"bottles", plumbing, components to be cooled, and the containment system(s) to contain any significant leakage that might occur at especially vulnerable locations. As exposure of water to high radiation level environment results in water that contains radioactive isotopes, especially tritium, the RAW system forms its own closed loop. Heat absorbed by the water in the RAW system is removed through a heat exchanger, which transfers energy to the LCW system. Then the LCW system is cooled by ICW before the heat is finally dissipated into the atmosphere. Due to the significant distance between target and absorber enclosures, two separate RAW systems are required for NuMI.

Shown in Table 5-8, Table 5-9, Table 5-10 and Table 5-11 are the projected user heat loads for upstream and downstream service buildings with two different NuMI beam configurations: the Wide Band Beam (WBB) upstream and downstream and the Narrow Band Beam (NBB) upstream and downstream loads. The distribution of loads between upstream and downstream service buildings shifts greater than does the total load in switching from WBB to NBB configuration. The facility will be designed to accommodate either configuration.

5.3.3 Anchorage for Utility Cable Trays and Ducting

Utility runs are to be hung from brackets attached to insert placed in cast in place (shafts, target enclosure roof, power room) or pre-cast elements (carrier pipe) or attached to rock anchorage, drilled through shotcrete-supported tunnel sections. Preference will be shown for the use of bolt anchorage drilled horizontally or slightly downward through the shotcrete in to the rock sidewall. This orientation of anchorage bolting is chosen given the

high potential for vertical holes to conduct and drip water onto the underlying objects, floor or cable tray contents.

5.4 Facility Environmental Requirements

5.4.1 Overview

The majority of underground structures in which NuMI will be housed are situated below the water table. Although it is expected that grouting of the rock will significantly reduce the levels of water inflow and that drainage placed behind the cast-in-place and shotcreted lining will direct most remaining water inflows in to closed drainage channels, some water ingress into the underground openings is to be expected. To reduce the negative impact of water on the functioning of more delicate experimental apparatus and utilities special protective measures are employed locally, as noted in earlier sections of this Chapter. Additionally, the ventilation air will be dehumidified prior to circulation in underground areas. A target relative humidity of 10% for air introduced to the underground enclosures, has been specified in design to minimize the potential for condensation when the air is brought into contact with the excavation walls (ambient rock temperature estimated at 55 degrees Fahrenheit).

To ensure that the end user fully appreciates the ambient conditions they are likely to face during installation and operation of the NuMI facility, underground visits were organized to the Des Plaines tunnel and to the TARP Mainstream Pumping Station Underground Complex[19]. Requirements for the enclosure environments used in Title I design were finalized based on discussions held after these visits had taken place.

5.4.2 Heating, Ventilation and Air Conditioning (HVAC) by Region

Providing adequate ventilation, air conditioning (both cooling and humidity control), and temperature control is essential. While sufficient heating is generally provided by user loads, correct sizing of dehumidification capability to control condensation in critical underground enclosures is especially important. Table 5-13 presents the desired limits on the temperature and humidity for the various regions.

In designing the ventilation system for the below ground structures it is important to recognize that air in the beam absorber region, the target hall and to a lesser extent in the

vacuum decay and pre-target regions will become activated. Most of the isotopes produced in air activation decay within 20 minutes and thus the ventilation system is designed such that activated air has a minimum 30 minutes of transit time in the ductwork before being exhausted outside of the enclosure. An assessment of total activated air emissions is required to determine in detail the necessary air transit time. It is equally important that the relative pressure in occupied areas (target hall service room, access passage way, MINOS hall, and service buildings) be maintained at a fraction of an inch of water column (0.1 in. w.c.) above the pressure in the pre-target, target hall, vacuum decay, and absorber region, so that the possibility of activated air flowing into occupied areas is prevented.

5.4.3 Approximate Illumination-Level Requirements by Region

Adequate lighting is necessary for individuals expected to work in the various regions. However, not all areas will have the same requirements. Shown in Table 5-14 is a preliminary estimate of the appropriate level of illumination for each region based on installation, operational and safety requirements.

5.4.4 Acoustic Control Measures by Region

It is desirable during the design phase to identify user installed equipment that will require either hearing protection or acoustic control measures so that efficient solutions can be implemented. Estimates of maximum design sound levels are presented in Table 5-15 for below grade regions where sound mitigation is needed.

• The Target Support Enclosure will include DC power supplies plus RAW and LCW systems. Both the power supplies and the RAW system pumps will generate significant acoustic noise. These will either require a permanently installed noise absorption media or hearing protection for people working in this area. From a user's standpoint, the former is preferable and is planned.

• The Downstream Access Tunnel adjacent to the Beam Absorber Enclosure will include a RAW system and the vacuum pumps.

• A power supply will be located in the MINOS Enclosure.

---

[19] Anon. "Metropolitan Wqater Reclamation Dsictirct of Greater Chicago; Tour of Mainstream Pumping Station Undergorund Complex" (Briefing Document), August 6, 1998.

5.4.5 Telephone Service by Regions

Historically, telephone service has been installed in newly completed buildings after beneficial occupancy under a separate contract. Fermilab's telecommunication office has initiated contracts to outside vendors to pull cable from the telephone tie in location to a central telephone panel (usually a 4 foot by 8 foot plywood panel mounted on the wall in the enclosure and painted with fire retardant paint). From this point, the laboratory telephone service provider installs the telephones and wiring inside the building under a service agreement. In this project, it is beneficial for the building contractor to provides the central telephone panel and the trunk line from telephone tie in location to the panel. Terminations of this cable, interior building wiring and handsets will be provided by the service provider under the administration of Fermilab's telecommunication office. Anticipated telephone needs are summarized in Table 5-16.

5.4.6 Door Lock Compatibility

Locksets used on all doors in the project need to be compatible with the requirements of radiation safety. Prior to commencing facility operation, lock cores for interlocked areas will be changed to radiation safety cores.

5.5 Installation

5.5.1 Pre-Target Elements

Installation of pre-target elements will be accomplished using the Target Service Building Crane to lower components to the floor level of the Target Enclosure. Either the Main Ring magnet mover or wheeled carts will be used to transport the magnets from the enclosure up the inclined Pretarget Tunnel. Once a magnet is pulled to the proper location along the beam line, conventional rigging methods will be used to move it into position in the beamline.

5.5.2 Target Station Shielding

Installation of the target station shielding represents one of the largest installation endeavors included within the scope of the NuMI project. The baseline schedule calls for all of the steel and concrete shielding to be installed after beneficial occupancy of the Target Enclosure and Target Service Building. Each steel or concrete shielding element will be lifted off a flat bed truck in the loading dock area of the Target Service Building, lowered

down the vertical shaft, and moved to the upstream end of the Target Enclosure. From this position, the 25 ton target hall crane will move each element into position in the shielding station. It is anticipated that the installation of this target station shielding will occur after the vacuum decay pipe and its shielding is fully installed.

5.5.3 Vacuum Decay Pipe and Shielding

Installation of the vacuum decay pipe and its shielding is planned to take place before installation of the Target Enclosure shielding. The baseline schedule calls for sections of vacuum decay pipe to be prefabricated off site and transported to the Target Service Building area. They are to be lowered down the Target Shaft and positioned and welded together underground. The baseline program calls for the use of cast-in-place low strength (low cost) concrete to be pumped from surface, either using a pipeline passing through the Target Enclosure or through ventilation shafts drilled at the approximate midpoint of the Decay Tunnel (see Figure 1-1).

5.5.4 Beam Absorber

Under the baseline plan, installation of the absorber will be undertaken by passage of material (approximately 600 tons) through the MINOS Shaft and Downstream Access Tunnel.

A 15 ton crane in the absorber enclosure is used to assemble the absorber and its shield. Since space in this region is quite limited, items will need to arrive in the order used.

5.5.5 MINOS Detector

Installation of the near detector components will be via the MINOS Shaft. Approximately one week's worth of steel and scintillator are stored within the MINOS Service Building, and deliveries to this building will occur every few days to replenish the supply. Components are delivered underground when one of the two assembly areas in the near hall is ready to receive them. The smaller crane is used to place a steel plane onto a strongback at an assembly station. The larger crane is used to pick up a completed plane plus the strongback and position the plane on the detector. Either crane is used to pick up scintillator modules and place them on a plane being assembled, depending on which is free at the time. This process of detector assembly takes place for approximately one year after beneficial occupancy. The total amount of steel installed during that time is approximately 1200 tons.

5.5.6 Alignment Requirements

Alignment of individual elements in the pretarget primary beam, target station, muon alcoves, absorber region, and the detector hall is crucial to the success of the experiment. For example, it is a routine practice to position primary beamline magnets to accuracy better than 0.025 inches and expect their absolute position with respect to the nominal beamline not to vary by more than 0.010 inch due to temperature changes and settling of the enclosure. While preliminary evaluation of the soil and a rock in this area suggest that alignment requirements can be satisfied, attention to details during the design is essential to ensure that the alignment procedures are not compromised by design choices.

Site risers are vertical pipes which extend from the ceiling of a below ground structure to the surface and are usually positioned above a monument located on the floor of the enclosure. They are used to allow the surveyors to transfer the site alignment grid (frequently referred to as DUSAF coordinates) to the below ground structure. After the alignment grid is completed and before operation of the beam commences, these pipes are sealed on the bottom and filled with sand bags from the top to achieve the necessary shielding density. Vertical site risers are necessary at the upstream end of the pre-target region and near the downstream end of the target station. In addition, the vertical shafts for the upstream and downstream service buildings will also be used by the surveyors for the same purpose and must have clear sight lines from the surface to the floor of the below ground enclosure.

5.6 Life Safety

5.6.1 Overview

Particular attention must be paid to life safety considerations for the NuMI facility due to the deep underground location of the enclosures, limited number of access points and relatively cramped conditions under which all work will be performed. A key design consideration is that flammable gases will not be used for the MINOS detector or any part of the NuMI underground facility. Some oxyacetylene welding will be required in the MINOS Enclosure. A summary is provided in Table 5-17.

Life safety and fire protection measures of the final structures have been adopted to conform to the recommendation of an independent consultant, Gage Babcock.[20] In the review of safety issues for NuMI methods of egress, enclosure occupancy, ventilation design, fuel loads and fire detection and suppression systems were all considered by the independent consultant. One significant recommendation from the consultant was to locate the downstream shaft in close proximity to the MINOS Enclosure, a recommendation adopted in the current facility design.

Maximum occupancy projections for each enclosure are shown in Table 5-12, both during normal operation and maintenance periods. Also included is an estimate of access frequency, after an initial commissioning period, and the access mode expected for each enclosure.

5.6.2 Flammable Materials used in each Region

Pre-Target Tunnel: Potentially flammable materials in the pre-target region include the paint on approximately 800 square feet of carbon steel (10 magnets, magnet stands or other beamline devices, each painted with enamel paint), and approximately 6000 feet of 500 MCM insulated (type XHHW) cable.

Target Enclosure: Potentially flammable materials in the target station region include the paint on approximately 400,000 square feet of carbon steel, approximately 5000 feet of 500 MCM insulated cable, and approximately 10,000 feet of RG 59 coaxial cable. The bulk of the painted steel is encased by either a thick concrete shield or by other layers of painted steel.

Target Support Enclosure and Service Building: Potentially flammable materials in the power supply rooms include components within the DC power supplies, AC power cabling into the power supplies, DC output cable (500 MCM type XHHW insulation), rubber hoses for the power supply cooling and cabling for instrumentation.

Decay Tunnel: Potentially flammable materials in the vacuum decay region include the paint on approximately 12,000 square feet of the carbon steel of the vacuum vessel. This steel is encased in a thick concrete shield.

Beam Absorber Enclosure: Potentially flammable materials in the absorber region only include the paint on approximately 6000 square feet of shielding steel. This is encased in a thick concrete shield.

---

[20] Gage Babcock & Associates "Fire Protection/Life Safety Requirements", July 9, 1998.

Downstream Access Tunnel: Potentially flammable materials in the passageway include the vacuum pumps (motors, drive belts, vacuum pump oil (e.g. Leybold HE-150) and vacuum pump instrumentation wiring. Some instrumentation wiring from the muon pits will be routed through the passageway.

MINOS Enclosure: Flammable materials in the MINOS experiment cavern include about 185,000 pounds of plastic scintillator. Only a small amount of scintillator is exposed in the hall at any time during the detector assembly. After assembly the scintillator is encased in steel with only thin end faces exposed. Detector readout cables will be present and the insulation is potentially flammable. None of these cables will carry high current power. The DAQ room will contain racks holding CAMAC and VME type crates and these crates include high current DC power supplies. The supplies will be fused following FESS guidelines. A magnet power supply (and its associated cabling) will be located in the hall which contains potentially flammable materials.

5.6.3 Fire Protection Control Measures by Region

Fire protection is usually provided by water sprinkler systems and occasionally by inert gas discharge (formerly Halon, most recently Inergen) systems. Sprinklers are the default system of choice for almost all areas, while inert gas discharge systems are selectively used for computer rooms and other installations involving electronics. In the following paragraphs the reasoning behind limiting the level of fire protection in certain enclosures and tunnels of the NuMI facilities are noted.

The Pretarget Tunnel should not contain fire protection piping for several reasons. First, this area will transport primary beam and water contained within the fire protection system piping would become tritiated. Also, the combustible materials listed above represent a limited volume. Finally, given the relatively low value of the components (a typical magnet used in this area is approximately worth $80,000) with spares readily available, the value of including fire protection in the pre-target region is not worth the risk of discharging tritiated water.

The target hall region should not contain fire protection piping for the same reasons cited above. The most valuable components in the target hall region are the horns and target. These devices are buried deep within the target station shielding and contain little if any combustible material (organic materials tend to decompose in the highly radioactive environment within the target station shielding). This limited volume of combustible material and the fact that the most valuable equipment would not be protected by a water

based fire protection system indicate that installing fire protection in the Target Enclosure is not sufficiently beneficial to offset the risk of generating tritiated water.

For the same reasons the vacuum decay and absorber enclosures should not contain fire protection piping.

NuMI Pretarget Beam Line Magnets									
		Dimensions				Station	DUSAF		
location	type_code	width [in]	height [in]	length [in]	weight [lb.]	NuMI Coordinate [ft]	up stream end x [ft]	up stream end y [ft]	up strea end z [ft
Q607	3Q84-2	23.3	17.6	86.4	9000	-103.124	101422.8331	97191.4094	715.
C_608	MRHC	17.5	8.1	11.3	115	-59.267	101385.3322	97214.1489	715.
L6081	LAM_1	28.1	39	120.0	24000	-56.886	101383.2965	97215.3834	715.
Q608	3Q84-2	23.3	17.6	86.4	9000	-46.403	101374.3362	97220.8260	715.
L6082	LAM_1	28	39	120.0	2400	-37.538	101366.7614	97225.4314	715.
L6083	LAM_1	28	39	120.0	2400	-26.340	101357.1944	97231.2509	715.
V100	CMG_1	15.3	15.8	148.0	8000	-14.755	101347.2996	97237.2751	716.
HQ101	3Q120-2	17.0	15.0	125.9	6890	0.499	101334.2687	97245.2033	716.
HV1011	EPB	12.5	16	126.0	5640	25.129	101313.2331	97257.9954	717.
HV1012	EPB	12.5	16	126.0	5640	36.296	101303.6616	97263.7382	717.
HV1013	EPB	12.5	16	126.0	5640	47.463	101294.0288	97269.3775	717.
HV1014	EPB	12.5	16	126.0	5640	58.629	101284.3358	97274.9129	718.
HV1015	EPB	12.5	16	126.0	5640	69.796	101274.5836	97280.3439	718.
HV1016	EPB	12.5	16	126.0	5640	80.963	101264.7865	97285.6964	718.
HV1017	EPB	12.5	16	126.0	5640	92.129	101254.9562	97290.9916	718.
HQ102	3Q120-2	17.0	15.0	125.9	6890	110.476	101238.7438	97299.5791	718.
HQ103	3Q120-2	17.0	15.0	125.9	6890	126.476	101224.5927	97307.0454	718.
HC103	MRHC	17.5	8.1	11.3	115	141.333	101211.4523	97313.9785	718.
VC103	MRVC	10.5	5.25	11.4	115	142.824	101210.1334	97314.6744	718.
HQ104	3Q120-2	17.0	15.0	125.9	6890	297.919	101072.9611	97387.0489	718.

NuMI Pretarget Beam Line Magnets									
		Dimensions				Station	DUSAF		
location	type_code	width [in]	height [in]	length [in]	weight [lb.]	NuMI Coordinate [ft]	up stream end x [ft]	up stream end y [ft]	up strea end z [ft
HQ105	3Q120-2	17.0	15.0	125.9	6890	321.261	101052.3161	97397.9416	718.
V1050	B2	19.5	25.3	243.5	25200	332.178	101042.6609	97403.0359	718.
V1051	B2	19.5	25.3	243.5	25200	353.262	101024.0159	97412.8733	718.
V1052	B2	19.5	25.3	243.5	25200	374.346	101005.3846	97422.7035	717.
V1053	B2	19.5	25.3	243.5	25200	395.430	100986.7803	97432.5194	716.
V1054	B2	19.5	25.3	243.5	25200	416.513	100968.2164	97442.3141	714.
HQ106	3Q120-2	17.0	15.0	125.9	6890	437.681	100949.6331	97452.1190	711.
HC106	MRHC	17.5	8.1	11.3	115	448.538	100940.116	97457.1403	710.
VC106	MRVC	10.5	5.25	11.4	115	450.029	100938.8089	97457.8300	710.
HQ107	3Q120-2	17.0	15.0	125.9	6890	453.606	100935.6738	97459.4842	709.
HQ108	3Q120-2	17.0	15.0	125.9	6890	939.407	100509.8483	97684.1572	644.
HC108	MRHC	17.5	8.1	11.3	115	950.265	100500.3312	97689.1785	643.
VC108	MRVC	10.5	5.25	11.4	115	951.756	100499.0241	97689.8682	643.
HQ109	3Q120-2	17.0	15.0	125.9	6890	959.377	100492.3441	97693.3926	642.
V1090	EPB-R	12.5	16	126.0	5640	982.270	100472.2774	97703.9802	639.
V1091	EPB-R	12.5	16	126.0	5640	993.437	100462.4817	97709.1486	637.
V1092	EPB-R	12.5	16	126.0	5640	1004.603	100452.673	97714.3238	636.
V1093	EPB-R	12.5	16	126.0	5640	1015.770	100442.8524	97719.5054	635.
V1094	EPB-R	12.5	16	126.0	5640	1026.937	100433.0211	97724.6925	634.
V1095	EPB-R	12.5	16	126.0	5640	1038.103	100423.1802	97729.8847	633.
V1096	EPB-R	12.5	16	126.0	5640	1049.270	100413.3309	97735.0814	632.
HQ110	3Q120-2	17.0	15.0	125.9	6890	1067.082	100397.6071	97743.3776	631.
HC110	MRHC	17.5	8.1	11.3	115	1078.132	100387.8502	97748.5255	630.
VC110	MRVC	10.5	5.25	11.4	115	1079.623	100386.5335	97749.2202	630.

Note: Surveyor's 1 m = 39.37 inches is used above rather than 1 m = 39.370

Table 5-1 NuMI Pretarget Beam Line Magnets.

Table 5-2 NuMI Power Supply Requirements.

Ramp Cycle Time: 1.9 seconds

MI60 Power Supplies

CIRCUIT	MAGNET TYPE	# MAGs	PEAK FLD/GRD kG/(kg/m)	MAG. IND. (henry)	MAG. RES. (ohms)	CABLE TYPE kcmil	CABLE # 1 way	CABLE R/kFt ohms	CABLE L (ft)	CABLE RES. ohms	Total Res. ohms	PEAK CURR. (amps)
Septa	Septa	2				DS314	1		555			0.01
LAMB	Lamb.	3	8.93	0.017	0.013	500	5	0.026	155	0.001612	0.041	1506
CMAG	Cmagnet	1	10	0.002	0.007	500	6	0.026	165	0.00143	0.008	2786
Q1	3Q120	1	72.37	1.5	2.25	1/0	1	0.125	105	0.02625	2.276	35.2
BND1	EPB	7	14.15	0.03	0.0175	500	5	0.026	217	0.0022568	0.125	1449
Q2	3Q120	1	69.93	1.5	2.25	1/0	1	0.125	215	0.05375	2.304	34
Q3	3Q120	1	53.72	1.5	2.25	1/0	1	0.125	231	0.05775	2.308	26.13
MI62 Power Supplies												
Q4	3Q120	1	53.72	1.5	2.25	1/0	1	0.125	607	0.15175	2.402	26.13
Q5	3Q120	1	53.72	1.5	2.25	1/0	1	0.125	584	0.146	2.396	26.13
BND2	B2	5	17.64	0.008	0.00718	500	8	0.026	573	0.0037245	0.040	4589
Q6	3Q120	1	51.62	1.5	2.25	1/0	1	0.125	527	0.13175	2.382	25.1
Q7	3Q120	1	54.35	1.5	2.25	1/0	1	0.125	543	0.13575	2.386	26.4
TPS1	MR Corr.	1	?	0.1	6	10ga	1	1.2	764	1.8336	7.834	12
TPS2	MR Corr.	1	?	0.1	6	10ga	1	1.2	764	1.8336	7.834	12
TPS3	MR Corr.	1	?	0.1	6	10ga	1	1.2	764	1.8336	7.834	12
TPS4	MR Corr.	1	?	0.1	6	10ga	1	1.2	535	1.284	7.284	12
TPS5	MR Corr.	1	?	0.1	6	10ga	1	1.2	535	1.284	7.284	12
TPS6	MR Corr.	1	?	0.1	6	10ga	1	1.2	535	1.284	7.284	12
Upstream Service Building and Horn Power Supplies												
Q8	3Q120	1	82.8	1.5	2.25	1/0	1	0.125	498	0.1245	2.375	40.3
Q9	3Q120	1	97.94	1.5	2.25	1/0	1	0.125	478	0.1195	2.370	47.6
BND3	EPB	7	14.17	0.03	0.0175	500	4	0.026	435	0.005655	0.128	1493
Q10	3Q120	1	34.06	1.5	2.25	1/0	1	0.125	370	0.0925	2.343	16.6
TPS7	MR Corr.	1	?	0.1	6	10ga	1	1.2	487	1.1688	7.169	12
TPS8	MR Corr.	1	?	0.1	6	10ga	1	1.2	487	1.1688	7.169	12
TPS9	MR Corr.	1	?	0.1	6	10ga	1	1.2	487	1.1688	7.169	12
TPS10	MR Corr.	1	?	0.1	6	10ga	1	1.2	360	0.864	6.864	12
TPS11	MR Corr.	1	?	0.1	6	10ga	1	1.2	360	0.864	6.864	12
TPS12	MR Corr.	1	?	0.1	6	10ga	1	1.2	360	0.864	6.864	12
HORN PS	Horn	2		3.655	0.932	500	1	0.026	435	0.02262	0.001	300
MINOS Power Supply, located in the MINOS Hall												
MINOS PS		1	80	0.03	2.25	500	1	0.026	250	0.013	2.263	1000
Assume 1 240kW supply (no passive filter) and space for 2 relay racks.												
Upgrade with Most Addtional Magnets: Narrow Band Beam												
NBB1	EPB	2	14.17	0.03	0.0175	500	4	0.026	400	0.0052	0.040	1500
NBB2	NBR	1	80	0.03	2.25	500	4	0.026	400	0.0052	2.255	1500
NBB3	NBB	1	80	0.03	2.25	500	4	0.026	400	0.0052	2.255	1500

Notes:

1. Assumptions for transrex-type power supplies:
   - Regulation .05%
   - Water Flow 5gpm
   - PS losses 5% of load (80% of which is in water, remainder in air)
   - Line kVA 140% of calc. Load (assumes 860 A for 500kW supply)
   - PS Footprint 48.5" wide, 50" deep, 75" high
2. PEI 20kW power supplies are air-cooled
3. B2END (B2) and E{ BEND (EPB) dipoles have been increased 5% from Transport values as safety margin
4. Q1 through Q9 (3Q120) quad gradients have been incread by 20% from Transport values as safety margin
5. Q10 (3Q120) quad gradient has been increased by 100% from Transport values as safety margin
6. The septa for NuMI are located at the upstream end of MI60
7. Beamline elements updated: 1430, 21 May 98
8. The MINOS magnet coils have not been designed and the NBB NBR and NBN magnets are not well known. Estimates were put in the above table as to their resistance and inductance.

JIREMENTS

Min.		PEAK	RMS	PEAK	Power	Power Supply				RMS	Fdr	Peak
Curr.	dI/dT	VOLT.	CURR.	PWR	Supply	TYPE	Volt	Curr.	Losses	PWR	Load	Fdr
(amps)	(A/s)	(volts)	(amps)	(kW)	Location	#, Man./Pwr	(volts)	(amps)	(kW)	(kW)	kVA	kVA
0.01	0	125000	0	1	MI60N	1, Glassman	125000	0.016	0.06	1	2	2
0	1585	142	869	214	MI60N	1, Xrex/500kW	200	2500	8.69	39	243	422
0	2933	29	1608	82	MI60N	1, PEI/150kW	30	5000	2.41	24	68	117
35.2	0	80	35	3	MI60N	1, PEI/20kW	200	200	0.35	3	10	10
0	1525	501	837	726	MI60N	3, Xrex/500kW	600	2500	25.10	112	703	1217
34	0	78	34	3	MI60N	1, PEI/20kW	200	200	0.34	3	10	10
26.13	0	60	26	2	MI60N	1, PEI/20kW	200	100	0.26	2	7	7
						MI60N Power Totals:			37	184	**1040**	1783
26.13	0	63	26	2	MI62	1, PEI/20kW	200	100	0.26	2	7	7
26.13	0	63	26	2	MI62	1, PEI/20kW	200	100	0.26	2	7	7
0	4831	375	2649	1721	MI62	4, Xrex/500kW	400	5000	52.99	331	1484	2570
25.1	0	60	25	2	MI62	1, PEI/20kW	100	200	0.13	2	4	4
26.4	0	63	26	2	MI62	1, PEI/20kW	100	200	0.13	2	4	4
12	0	94	12	1	MI62	MR DipoleTrim	150	12	0.09	1	3	3
12	0	94	12	1	MI62	MR DipoleTrim	150	12	0.09	1	3	3
12	0	94	12	1	MI62	MR DipoleTrim	150	12	0.09	1	3	3
12	0	87	12	1	MI62	MR DipoleTrim	150	12	0.09	1	3	3
12	0	87	12	1	MI62	MR DipoleTrim	150	12	0.09	1	3	3
12	0	87	12	1	MI62	MR DipoleTrim	150	12	0.09	1	3	3
						MI62 Power Totals:			54	345	**1521**	2607
40.3	0	96	40	4	TH SB	1, PEI/20kW	200	100	0.40	4	11	11
47.6	0	113	48	5	TH SB	1, PEI/20kW	200	100	0.48	6	13	13
0	1572	521	862	778	TH SB	3, Xrex/500kW	600	2500	25.86	121	724	1254
16.6	0	39	17	1	TH SB	1, PEI/20kW	200	100	0.17	1	5	5
12	0	86	12	1	TH SB	MR DipoleTrim	150	12	0.09	1	3	3
12	0	86	12	1	TH SB	MR DipoleTrim	150	12	0.09	1	3	3
12	0	86	12	1	TH SB	MR DipoleTrim	150	12	0.09	1	3	3
12	0	82	12	1	TH SB	MR DipoleTrim	150	12	0.09	1	3	3
12	0	82	12	1	TH SB	MR DipoleTrim	150	12	0.09	1	3	3
12	0	82	12	1	TH SB	MR DipoleTrim	150	12	0.09	1	3	3
0	316	700	173	210	TH SB	1, PEI/240kW	800	300	6.93	162	194	336
				Upstream Service Building Power Totals:					34	301	**962**	1635
1000	0	200	1000	200	DS SB	1, Xrex/240kW	400	600	20.00	2283	560	560
				Downstream Service Building Power Totals:					20	2283	**560**	560
0	1579	155	866	233	US SB	1, Xrex/500kW	200	2500	8.66	39	242	420
0	1579	3430	866	5145	US SB	1, Xrex/500kW	200	2500	8.66	1700	242	420
0	1579	3430	866	5145	US SB	1, Xrex/500kW	200	2500	8.66	1700	242	420
		Additional NBB Upstream Service Building Power Totals:							26	3439	**727**	1260
		Upstream Service Building Power Totals (w/NBB):							60	3739	**1690**	2895

Table 5-2

Item	Quantity	Size (Height, ft, Width, ft, Depth, ft)	Approximate Weight (lbs.)
240kW Power Supply	1	6.0 by 3.5 by 3.3	4500
Horn Capacitor Bank	1	6.5 by 17.5 by 5.5	25000
Relay Racks	4	7.0 by 2.5 by 2.0	1000
Water Skids	2	7.0 by 8.0 by 6.0	3000
Interlock Relay Racks	2	7.0 by 2.5 by 2.0	1000

Table 5-3 Summary of Components in the Target Hall Service Room.

Item	Quantity	Size (Height, ft, Width, ft, Depth, ft)	Approximate Weight (lbs.)
500kW Power Supply	6	6.0 by 4.25 by 4.25	5000
240kW Power Supply	1	6.0 by 3.5 by 3.3	4500
Racks for PEI 20kW Power Supplies	2	7.0 by 2.3 by 2.0	500
Racks for Correction Magnet Power Supplies	3	7.0 by 2.5 by 2.0	100
Relay Racks	4	7.0 by 2.5 by 2.0	1000

Table 5-4 Summary of Components in the Upstream Service Building.

Upstream Area	Conventional Power[a] (KVA)	User Utility Power (KVA)	User Clean Power (KVA)
Pre-target	4	100	0
Target Hall	291	25	0
Power Supplies	0	962[b]	0
Upgrade N. B.	0	727 additional	0
Vacuum Decay	4	15	0
Target Enclosure Service Building	124	0	0
Upstream Totals	423	1778	0

Downstream Area	Conventional Power[a]	User Utility Power	User Clean Power
Beam Absorber	34	5	0
Passage	37	120[c]	0
Power Supplies	0	560	80
Downstream Service Building	88	0	0
MINOS Hall	126	0	0
Downstream Totals	275	545	80

Table 5-5 Electrical Requirements by Region.

a	estimate Only - A&E to re-calculate and confirm or adjust as necessary
b	from Average Power: 301 kW, Ave. Feeder Load: 962 kVA and Peak Feeder Load: 1635 kVA
c	assumes a 100 HP of vacuum pumps: 2 Skids ea. w/ a 30 HP mechanical pump and a 20 HP blower + 20 HP worth of pumps for the RAW system

Table 5-6 Footnotes: Electrical Requirements by Region (KVA).

Area	# of 18" wide trays	# of 5" PVC Conduits
Pre-Target	3 (4 w/NBB)	0
Target Hall	3 (4 w/NBB)	0
Target Hall Service Room	4 (5 w/NBB)	
Vacuum Decay	0	6
Beam Absorber	0	6
Passage	1	6
MINOS Cavern	4	0
U. S. Service. Bldg.	5 (7 w/NBB)	0
D. S. Service Bldg.	0	0

Table 5-7 Required Cable Tray Areas by Region.

Loads for NuMI WBB				
Area	Heat to RAW kW	Heat to LCW kW	Heat to Primary Cooling Water kW	Heat to Air kW
U.S. Total Load to Primary Cooling			674	183
U.S. Service Building Totals	0	34	0	10
Pre-Target Supplies	0	21	0	7.9
Horn Power Supply	0	13.4	0	2.4
Pre-Target Totals	10	496	0	26
Pre-Target Magnets	0	496	0	25
Baffles	10	0	0	1
TH Pump & PS Room Totals	13	144	674	11
Horn Power Supply Cap Bank	0	0	0	unknown
U.S. Raw System	0	80	0	4
U.S. LCW System	0	0	674	
U.S. Raw System Pump Motors	13	13	0	1
U.S. LCW System Pump Motors	0	50	0	6
Target Hall Totals	80	0	0	136
Baffles	10	0	0	1
Horns	60	0	0	0
Target	10	0	0	0
Target Hall Shielding	0	0	0	135
Vacuum Decay Totals	0	0	0	unknown
Beam Heating	0	0	0	unknown
* Denotes that the table values are in addition to the existing MI heat loads already present in these areas ** Denotes a conservative number chosen prior to determination of actual values Beam Heating Denotes Contribution made by the beam energy deposition in shielding				

Table 5-8 WBB Upstream Heat Loads.

Loads for NuMI WBB				
Area	Heat to RAW kW	Heat to LCW kW	Heat to Primary Cooling Water kW	Heat to Air kW
D.S. Total Load to Primary Cooling			711	43
Beam Absorber Totals **	135	0	0	0
Heat to the Absorber Core	135	0	0	0
Heat to the Absorber Shielding	0	0	0	unknown
Passage (Pump & P.S.) Totals	20	189	711	15
D.S. Raw	0	155	0	0
D.S. LCW	0	0	675	0
Vacuum Pumps	0	0	36	9
D.S. LCW System Pump Motors	0	34	0	4
D.S. RAW System Pump Motors	20	0	0	2
MINOS PS Totals **	0	11.5	0	2.9
MINOS Power Supply	0	12	0	3
MINOS Hall Totals **	0	475	0	25
MINOS Magnet Coil	0	475	0	25
D.S. Service Building Totals	0	0	0	0
* Denotes that the table values are in addition to the existing MI heat loads already present in these areas ** Denotes a conservative number chosen prior to determination of actual values Beam Heating Denotes Contribution made by the beam energy deposition in shielding				

Table 5-9 WBB Downstream Heat Loads

Loads for NBB				
Area	Heat to RAW kW	Heat to LCW kW	Heat to Primary Cooling Water kW	Heat to Air kW
U.S,. Total Load to Primary Cooling			897	205
U.S Ser. Bldg. Totals	0	34	0	10
Pre-Target Supplies	0	21	0	7.9
Horn Power Supply	0	13.4	0	2.4
Pre-Target Totals	0	496	0	26
Pre-Target Magnets	0	496	0	25
Baffles	unknown	0	0	1
TH Pump & PS Room Totals	13	367	897	22
Horn Power Supply Cap Bank	0	0	0	unknown
U.S. Raw System	0	303	0	15.15
U.S. LCW System	0	0	897	
U.S. Raw System Pump Motors	13	13	0	1
U.S. LCW System Pump Motors	0	50	0	6
Target Hall Totals	303	0	0	147
Baffles	10	0	0	1
Horns	60	0	0	0
Target	10	0	0	0
Target Hall Shielding	0	0	0	135
NBB Target Box Magnets	88	0	0	4.4
NBB Beam Absorber	135	0	0	6.75
Vacuum Decay Totals	0	0	0	unknown
Beam Heating	0	0	0	unknown

* Denotes that the table values are in addition to the existing MI heat loads already present in these areas
** Denotes a conservative number chosen prior to determination of actual values
Beam Heating Denotes Contribution made by the beam energy deposition in shielding

Table 5-10 NBB Upstream Heat Loads.

Loads for NBB				
Area	Heat to RAW kW	Heat to LCW kW	Heat to Primary Cooling Water kW	Heat to Air kW
D.S. Total Load to Primary Cooling			556	43
Beam Absorber Totals	0	0	0	0
Heat to the Absorber Core	0	0	0	0
Heat to the Absorber Shielding	0	0	0	0
Passage (Pump & P.S.) Totals	0	34	556	15
D.S. Raw	0	0	0	0
D.S. LCW	0	0	520	0
Vacuum Pumps	0	0	36	9
D.S. LCW System Pump Motors	0	34	0	4
D.S. RAW System Pump Motors	0	0	0	2
MINOS PS Totals**	0	11.5	0	2.9
MINOS Power Supply	0	12	0	3
MINOS Hall Totals**	0	475	0	25
MINOS Magnet Coil	0	475	0	25
D.S. Service Building Totals	0	0	0	0
* Denotes that the table values are in addition to the existing MI heat loads already present in these areas				
** Denotes a conservative number chosen prior to determination of actual values				
Beam Heating Denotes Contribution made by the beam energy deposition in shielding				

Table 5-11 NBB Downstream Heat Loads.

Area	Construction Phase	Normal Operations	Maintenance	Maintenance Frequency	Access Mode
Carrier Pipe	5	0	0*	< Bi-annual	* Confined space
Pre-target	5	0	5	Weekly	Interlock control
Target Hall	10	0	5	Bi-weekly	Interlock control
Power Supply	10	5	5	Daily	Open
Vacuum Decay	10	0	5	Bi-monthly	Limited access
Beam Absorber	10	0	5	Bi-weekly	Interlock control
Passage	10	0	5	Weekly	Interlock control
MINOS	20	4	10	Daily	Open
US. Service Bldg.	5	5	5	Daily	Open grade level
DS. Service Bldg.	5	5	5	Daily	Open grade level
Totals	90	19	50		

Table 5-12 Maximum Occupancy for Each Region.

Area	Temperature Range (Deg F)	Humidity Range (% RH)
Pre-Target	60 to 85 °F	0 to 80%
Target Hall	60 to 80 °F	0 to 60%
Target Hall Power Supply Room	60 to 80 °F	0 to 60%
Vacuum Decay	60 to 85 °F	0 to 80%
Beam Absorber	60 to 85 °F	0 to 80%
Passage	60 to 85 °F	0 to 80%
MINOS	65 ± 5 °F	0 to 60%
U. S. Serv Bldg.	60 to 80 °F	0 to 60%
D. S. Service	60 to 80 °F	0 to 60%

Table 5-13 Heating, Ventilation and Air Conditioning (HVAC) by Region.

Area	Illumination (foot candles)
Pre-Target	20
Target	75
Target Hall Power Supply	50
Vacuum Decay	15
Beam Absorber	20
Passage	15
MINOS	75
U.S. Service. Bldg.	30
D.S. Service. Bldg.	30

Table 5-14 Approximate Illumination-Level Requirements by Region.

Area	Sound level (dB)
Pre-Target	NA
Target	NA
Target Hall Power Supply	80
Vacuum Decay	NA
Beam Absorber	NA
Passage	80
MINOS Power Supply	80
U.S. Service. Bldg.	NA
D.S. Service. Bldg.	NA

Table 5-15 Acoustic Control Measures by Region.

Area	Lines	Number of Handsets	Number of Lines
Pre-Target	A	1	1
Target Hall	A	3	1
Power Supply	B	2	1
Vacuum Decay	C	10	1
Beam Absorber	D	1	1
Passage	E	1	1
MINOS	F,G,H,I	8	4
U.S. Service. Bldg.	J	1	1
D.S. Service Bldg.	K	1	1

Table 5-16 Telephone Service Needs by Region.

Area	Sprinkle (yes/no)	Inert Gas (yes/no)
Pre-Target	No	No
Target Hall	No	No
Power Supply	Yes	No
Vacuum Decay	No	No
Beam Absorber	No	No
Passage	Yes	No
MINOS	Yes	No
U.S. Service. Bldg.	Yes	No
D.S. Service Bldg.	Yes	No

Table 5-17 Fire Protection Control measures by Region.

Chapter 5 Drawing List (See inserts)

Figure 5-1 Extraction Enclosure Plan and Elevation (Title I Design Drawing C-14)

Figure 5-2 Carrier & Pretarget Tunnels (Title I Design Drawing C-15)

Figure 5-3 Target Enclosure and Access Shaft (Title I Design Drawing C-16)

Figure 5-4 Absorber Enclosure & Access Tunnel (Title I Design Drawing C-17)

Figure 5-5 Absorber Access Tunnel & MINOS Shaft (Title I Design Drawing C-18)

Figure 5-6 MINOS Enclosure Plan and Elevation (Title I Design Drawing C-19)

Figure 5-7 Upstream Tunnel Sections - Sheet 1 (Title I Design Drawing C-20)

Figure 5-8 Upstream Tunnel Sections - Sheet 2 (Title I Design Drawing C-21)

Figure 5-9 Downstream Tunnel Sections - Sheet 1 (Title I Design Drawing C-22)

Figure 5-10 Downstream Tunnel Sections - Sheet 2 (Title I Design Drawing C-23)

This Page Intentionally Left Blank

Figure 5-1

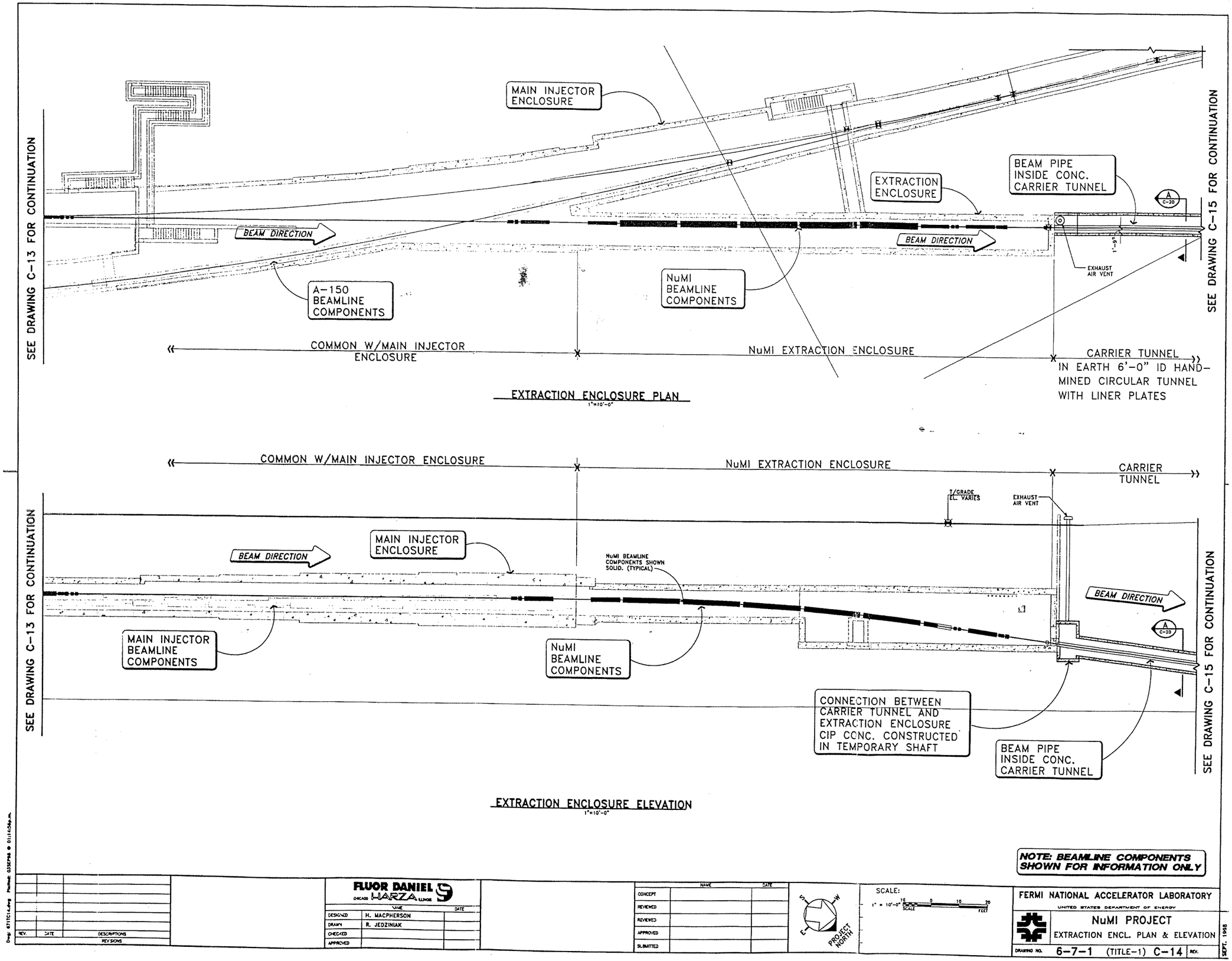
SEE DRAWING C-13 FOR CONTINUATION
MAIN INJECTOR ENCLOSURE
BEAM PIPE INSIDE CONC. CARRIER TUNNEL
EXTRACTION ENCLOSURE
BEAM DIRECTION
BEAM DIRECTION
A C-20
1'-9"
EXHAUST AIR VENT
A-150 BEAMLINE COMPONENTS
NuMI BEAMLINE COMPONENTS
SEE DRAWING C-15 FOR CONTINUATION
COMMON W/MAIN INJECTOR ENCLOSURE
NuMI EXTRACTION ENCLOSURE
CARRIER TUNNEL IN EARTH 6'-0" ID HAND-MINED CIRCULAR TUNNEL WITH LINER PLATES
EXTRACTION ENCLOSURE PLAN
1"=10'-0"
COMMON W/MAIN INJECTOR ENCLOSURE
NuMI EXTRACTION ENCLOSURE
CARRIER TUNNEL
T/GRADE EL. VARIES
EXHAUST AIR VENT
SEE DRAWING C-13 FOR CONTINUATION
BEAM DIRECTION
MAIN INJECTOR ENCLOSURE
NuMI BEAMLINE COMPONENTS SHOWN SOLID. (TYPICAL)
BEAM DIRECTION
A C-20
MAIN INJECTOR BEAMLINE COMPONENTS
NuMI BEAMLINE COMPONENTS
CONNECTION BETWEEN CARRIER TUNNEL AND EXTRACTION ENCLOSURE CIP CONC. CONSTRUCTED IN TEMPORARY SHAFT
BEAM PIPE INSIDE CONC. CARRIER TUNNEL
SEE DRAWING C-15 FOR CONTINUATION
EXTRACTION ENCLOSURE ELEVATION
1"=10'-0"
NOTE: BEAMLINE COMPONENTS SHOWN FOR INFORMATION ONLY
REV. DATE DESCRIPTIONS
REVISIONS
FLUOR DANIEL GTI CHICAGO HARZA ILLINOIS
DESIGNED H. MACPHERSON
DRAWN R. JEDZINIAK
CHECKED
APPROVED
CONCEPT
REVIEWED
REVIEWED
APPROVED
SUBMITTED
NAME DATE
PROJECT NORTH
SCALE: 1" = 10'-0"
10 0 10 20 SCALE FEET
FERMI NATIONAL ACCELERATOR LABORATORY
UNITED STATES DEPARTMENT OF ENERGY
NuMI PROJECT
EXTRACTION ENCL. PLAN & ELEVATION
DRAWING NO. 6-7-1 (TITLE-1) C-14 REV.
SEPT. 1998

Figure 5-3

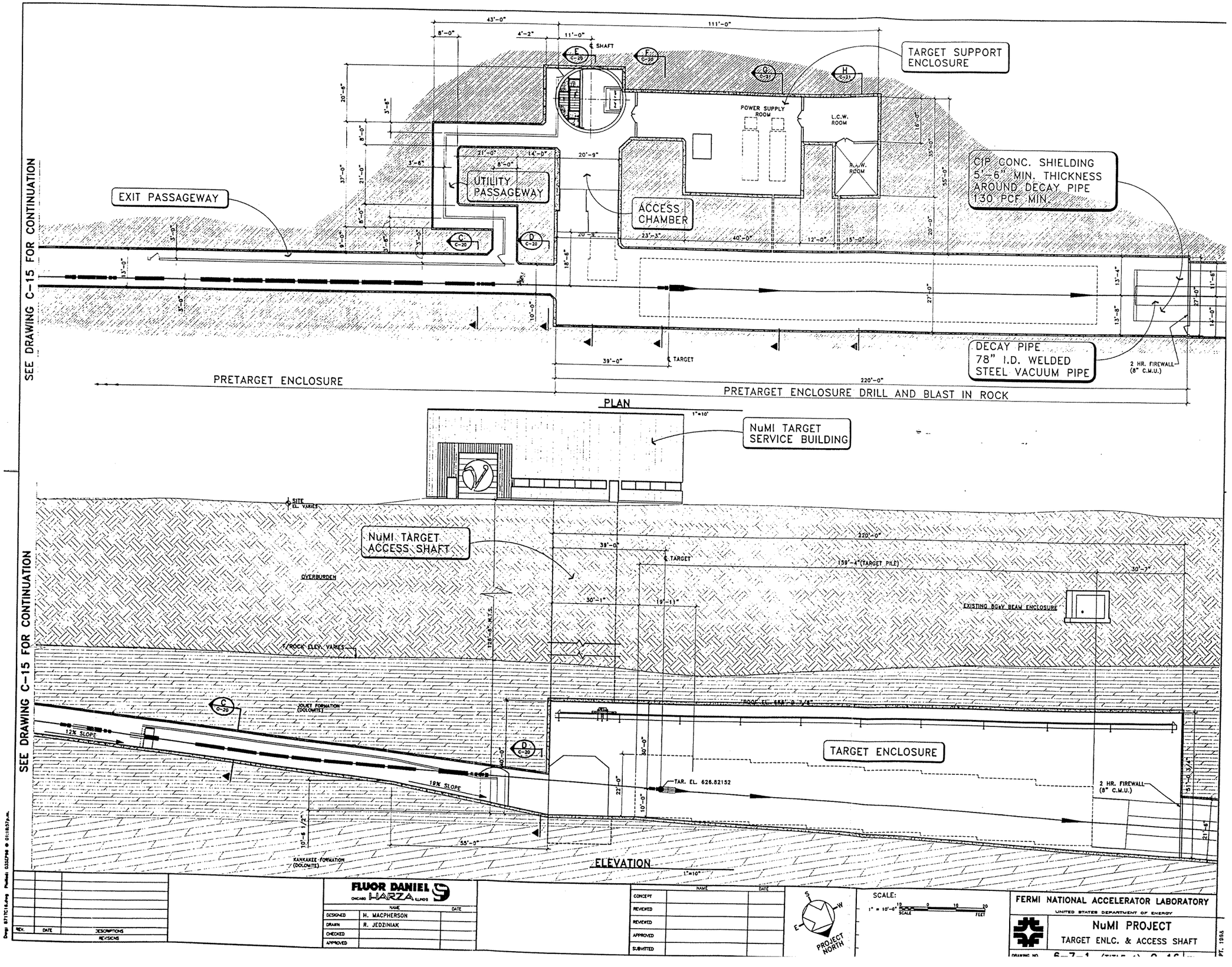
SEE DRAWING C-15 FOR CONTINUATION
EXIT PASSAGEWAY
UTILITY PASSAGEWAY
ACCESS CHAMBER
TARGET SUPPORT ENCLOSURE
POWER SUPPLY ROOM
L.C.W. ROOM
R.A.W. ROOM
CIP CONC. SHIELDING 5'-6" MIN. THICKNESS AROUND DECAY PIPE 130 PCF MIN.
DECAY PIPE 78" I.D. WELDED STEEL VACUUM PIPE
2 HR. FIREWALL (8" C.M.U.)
PRETARGET ENCLOSURE
PRETARGET ENCLOSURE DRILL AND BLAST IN ROCK
PLAN
NuMI TARGET SERVICE BUILDING
NuMI TARGET ACCESS SHAFT
OVERBURDEN
T/ROCK ELEV. VARIES
JOLIET FORMATION (DOLOMITE)
KANKAKEE FORMATION (DOLOMITE)
12% SLOPE
19% SLOPE
TARGET ENCLOSURE
TAR. EL. 626.82152
EXISTING 8GeV BEAM ENCLOSURE
ROOF EL. 668'-0 7/8"
ELEVATION
SHAFT
TARGET
SITE EL. VARIES
PROJECT NORTH
FLUOR DANIEL GTI CHICAGO HARZA ILLINOIS
DESIGNED H. MACPHERSON
DRAWN R. JEDZINIAK
CHECKED
APPROVED
CONCEPT
REVIEWED
REVIEWED
APPROVED
SUBMITTED
SCALE: 1" = 10'-0"
FERMI NATIONAL ACCELERATOR LABORATORY
UNITED STATES DEPARTMENT OF ENERGY
NuMI PROJECT
TARGET ENLC. & ACCESS SHAFT

Figure 5-4

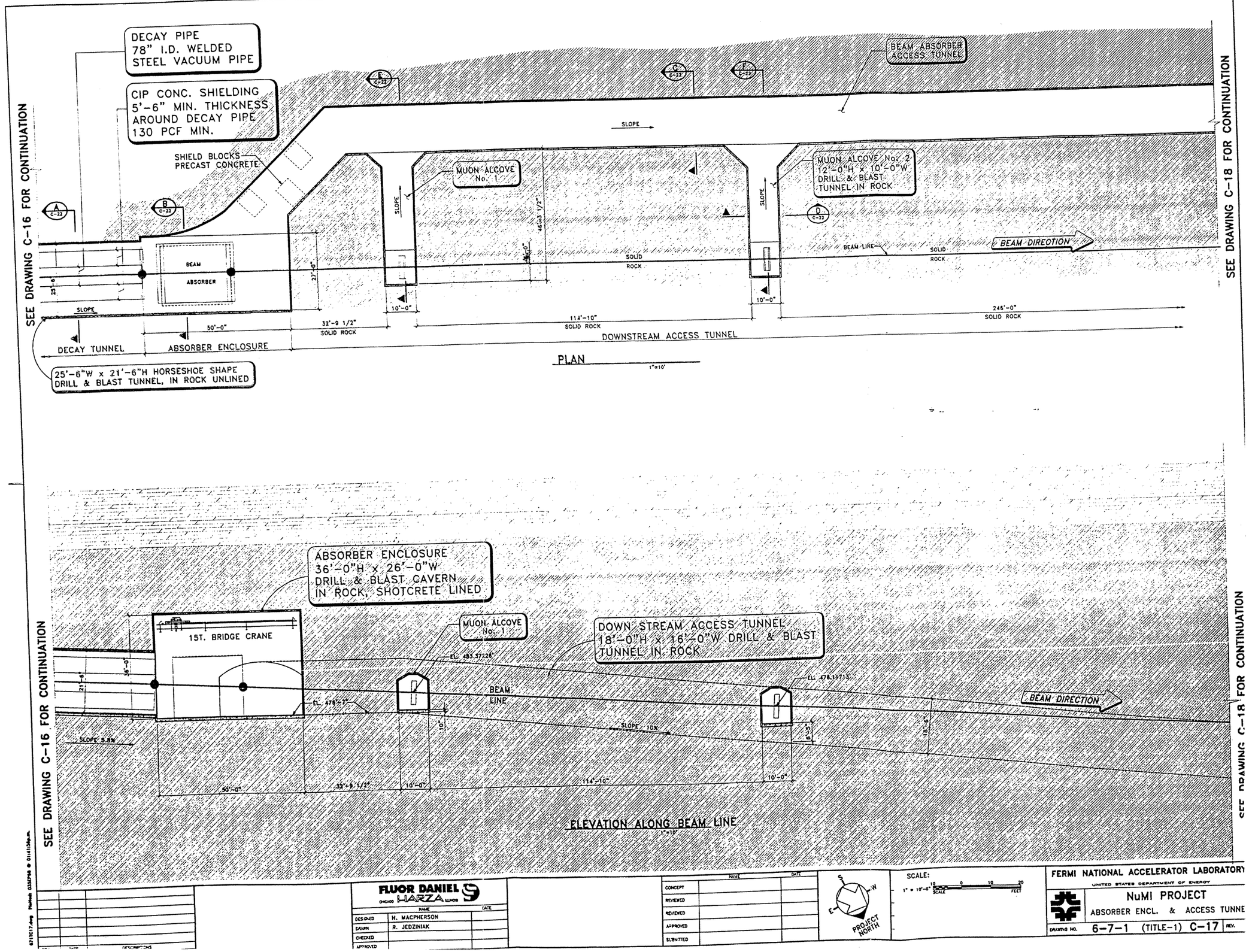
DECAY PIPE
78" I.D. WELDED
STEEL VACUUM PIPE
CIP CONC. SHIELDING
5'-6" MIN. THICKNESS
AROUND DECAY PIPE
130 PCF MIN.
SHIELD BLOCKS
PRECAST CONCRETE
BEAM ABSORBER
ACCESS TUNNEL
MUON ALCOVE
No. 1
MUON ALCOVE No. 2
12'-0"H x 10'-0"W
DRILL & BLAST
TUNNEL IN ROCK
SEE DRAWING C-16 FOR CONTINUATION
SEE DRAWING C-18 FOR CONTINUATION
BEAM
ABSORBER
SLOPE
SOLID
ROCK
BEAM LINE
BEAM DIRECTION
DECAY TUNNEL
ABSORBER ENCLOSURE
DOWNSTREAM ACCESS TUNNEL
25'-6"W x 21'-6"H HORSESHOE SHAPE
DRILL & BLAST TUNNEL, IN ROCK UNLINED
50'-0"
32'-9 1/2"
10'-0"
114'-10"
246'-0"
PLAN
1"=10'
ABSORBER ENCLOSURE
36'-0"H x 26'-0"W
DRILL & BLAST CAVERN
IN ROCK, SHOTCRETE LINED
15T. BRIDGE CRANE
DOWN STREAM ACCESS TUNNEL
18'-0"H x 16'-0"W DRILL & BLAST
TUNNEL IN ROCK
EL. 483.37126'
EL. 478.11713'
EL. 478'-7"
SLOPE 5.8%
SLOPE 10%
ELEVATION ALONG BEAM LINE
1"=10'
FLUOR DANIEL
CHICAGO HARZA ILLINOIS
DESIGNED H. MACPHERSON
DRAWN R. JEDZINIAK
CHECKED
APPROVED
CONCEPT
REVIEWED
REVIEWED
APPROVED
SUBMITTED
SCALE:
1" = 10'-0"
FERMI NATIONAL ACCELERATOR LABORATORY
UNITED STATES DEPARTMENT OF ENERGY
NuMI PROJECT
ABSORBER ENCL. & ACCESS TUNNE
DRAWING NO. 6-7-1 (TITLE-1) C-17 REV.

Figure 5-5

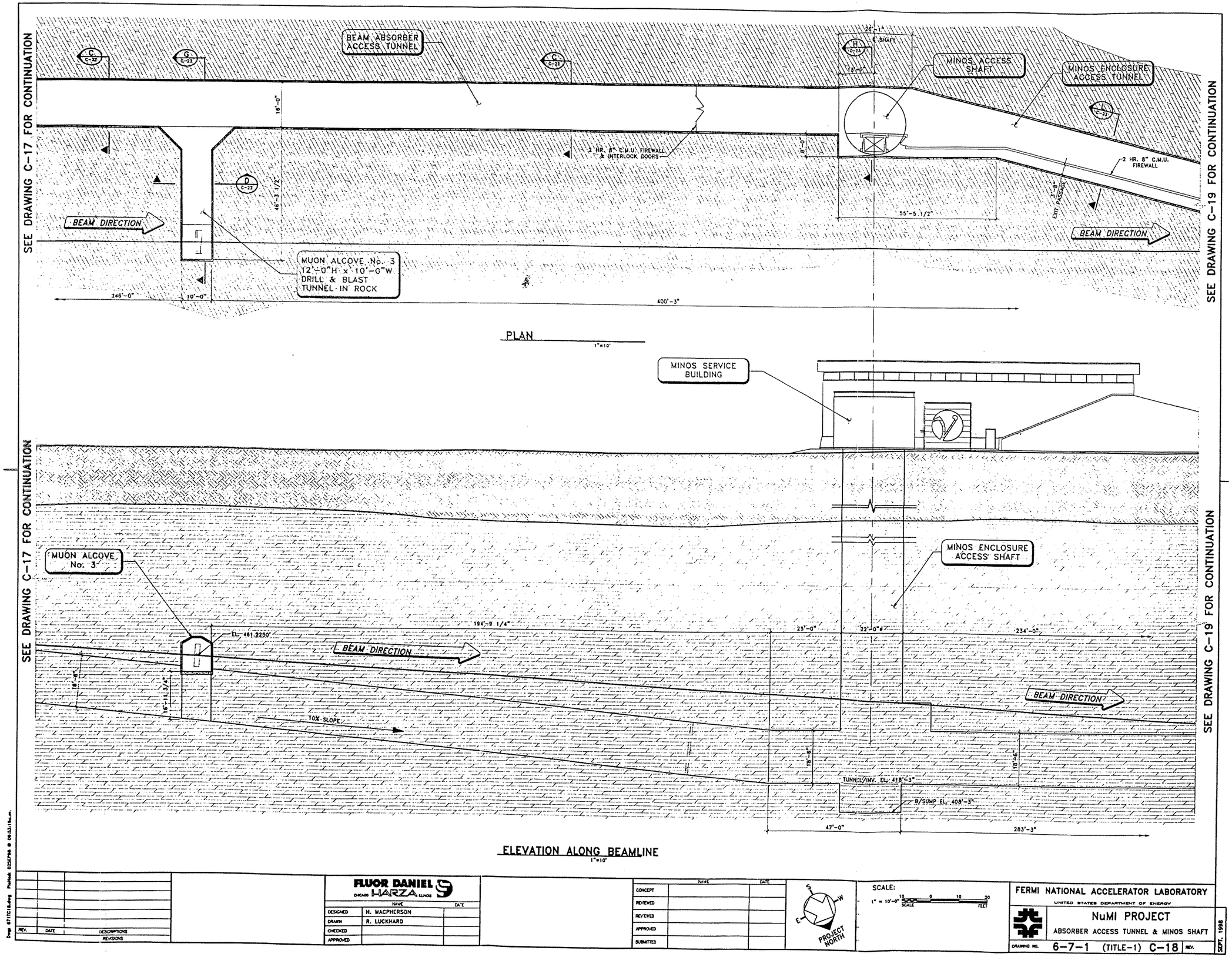

REV.	DATE	DESCRIPTIONS

REVISIONS

FLUOR DANIEL GTI CHICAGO HARZA ILLINOIS

	NAME	DATE
DESIGNED	H. MACPHERSON	
DRAWN	R. LUCKHARD	
CHECKED		
APPROVED		

	NAME	DATE
CONCEPT		
REVIEWED		
REVIEWED		
APPROVED		
SUBMITTED		

PROJECT NORTH

SCALE: 1" = 10'-0" (10 0 10 20 SCALE FEET)

FERMI NATIONAL ACCELERATOR LABORATORY
UNITED STATES DEPARTMENT OF ENERGY

NuMI PROJECT
ABSORBER ACCESS TUNNEL & MINOS SHAFT

DRAWING NO. 6-7-1 (TITLE-1) C-18 REV.

SEPT. 1998

Dwg: 671TC18.dwg Pltdat: 02SEP98 @ 08:33:18a.m.

Figure 5-6

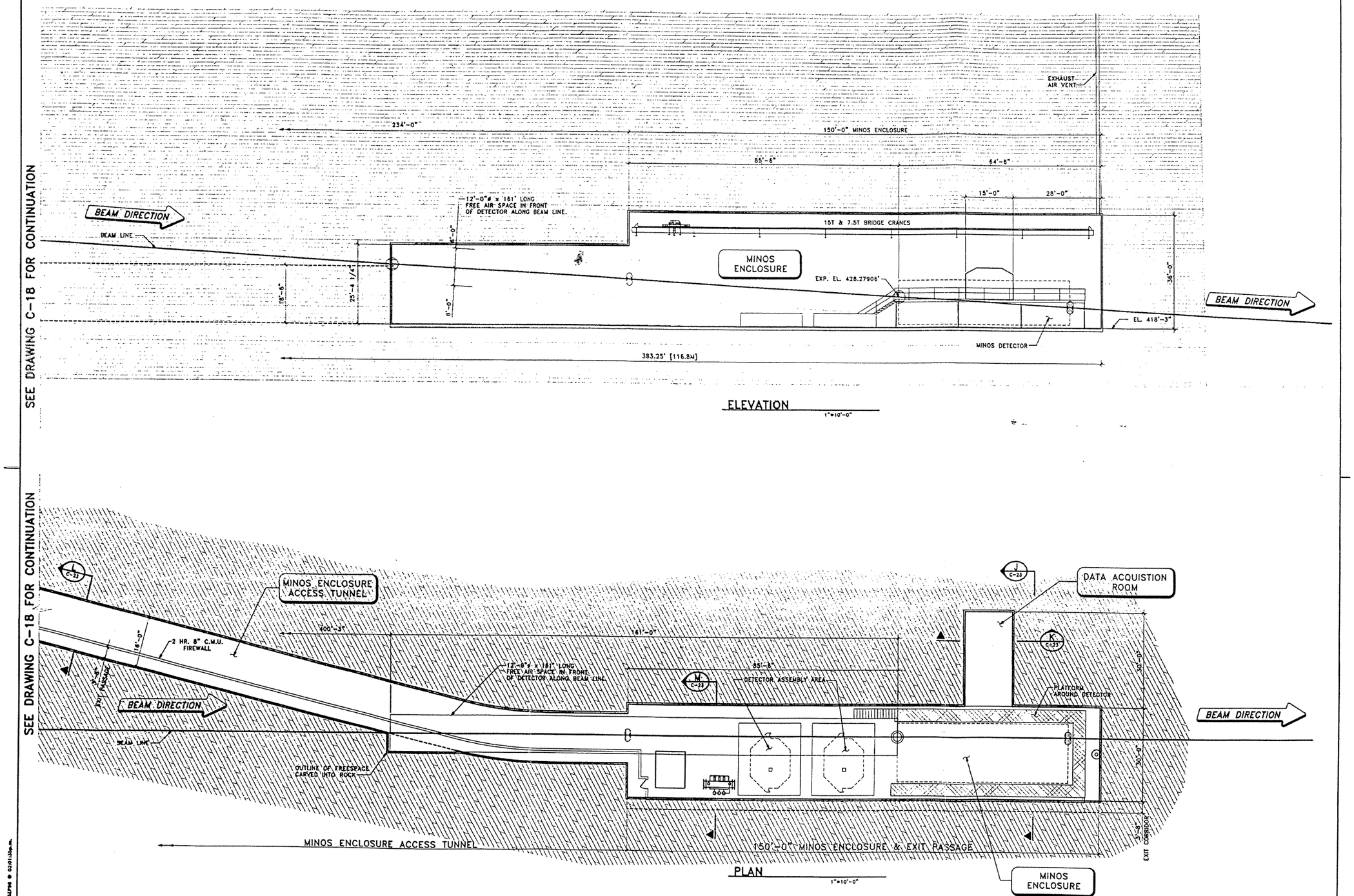

REV.	DATE	DESCRIPTIONS
		REVISIONS

FLUOR DANIEL / CHICAGO HARZA ILLINOIS

	NAME	DATE
DESIGNED	S. MACPHERSON	
DRAWN	Z. SILJKOVIC	
CHECKED		
APPROVED		

	NAME	DATE
CONCEPT		
REVIEWED		
REVIEWED		
APPROVED		
SUBMITTED		

PROJECT NORTH

SCALE: 1" = 10'-0" (10 0 10 20 SCALE FEET)

FERMI NATIONAL ACCELERATOR LABORATORY
UNITED STATES DEPARTMENT OF ENERGY

NuMI PROJECT
MINOS ENCLOSURE PLAN AND ELEV.

DRAWING NO. 6-7-1 (TITLE-1) C-19 REV.

SEPT. 1998

Dgn: 971C19.dwg Pltdate: 03SEP98 @ 02:01:33p.m.

Figure 5-7

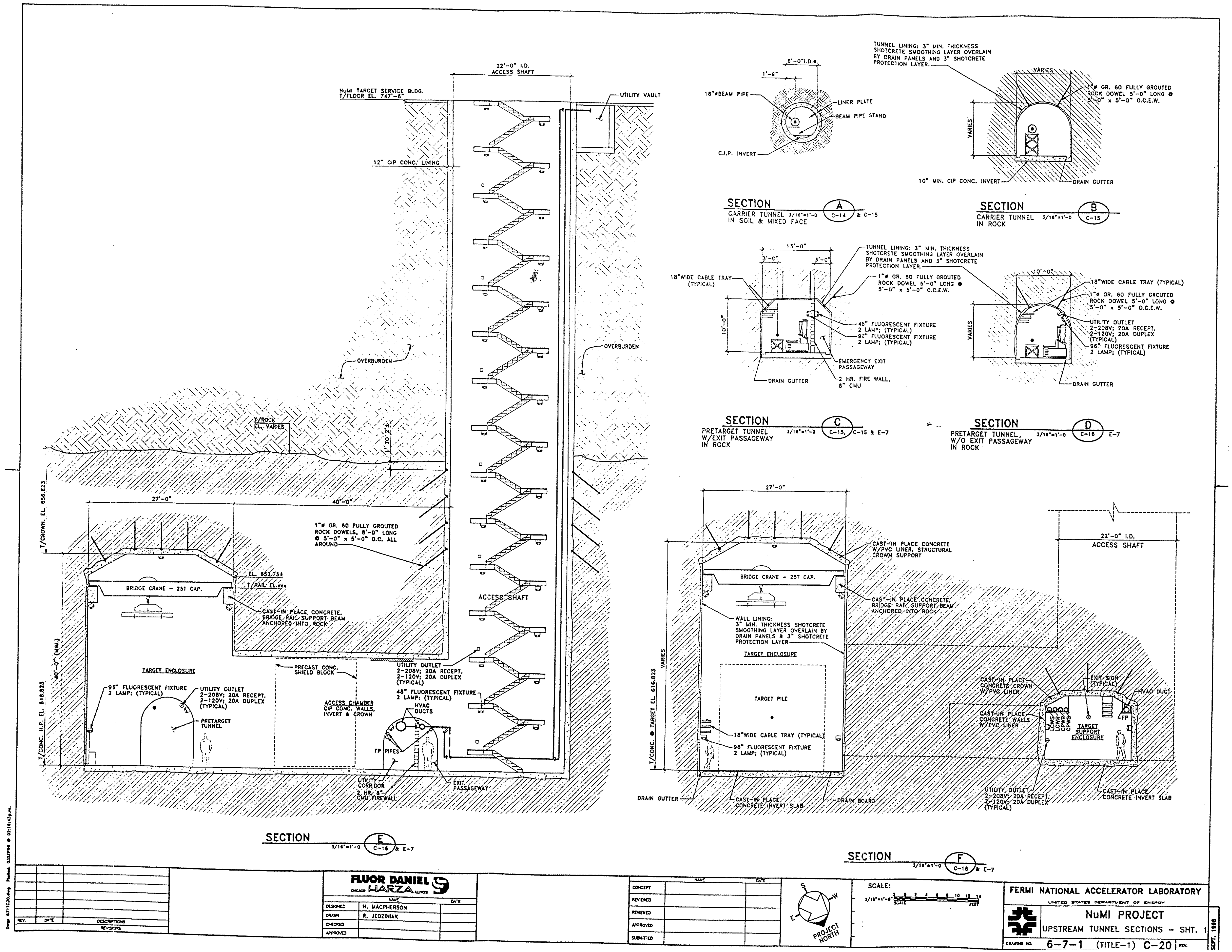

22'-0" I.D. ACCESS SHAFT
NuMI TARGET SERVICE BLDG. T/FLOOR EL. 747'-6"
UTILITY VAULT
12" CIP CONC. LINING
OVERBURDEN
T/ROCK EL. VARIES
1"ø GR. 60 FULLY GROUTED ROCK DOWELS, 8'-0" LONG @ 5'-0" x 5'-0" O.C. ALL AROUND
BRIDGE CRANE - 25T CAP.
CAST-IN PLACE CONCRETE, BRIDGE RAIL SUPPORT BEAM ANCHORED INTO ROCK
ACCESS SHAFT
TARGET ENCLOSURE
PRECAST CONC. SHIELD BLOCK
ACCESS CHAMBER CIP CONC. WALLS, INVERT & CROWN
UTILITY OUTLET 2-208V; 20A RECEPT. 2-120V; 20A DUPLEX (TYPICAL)
48" FLUORESCENT FIXTURE 2 LAMP; (TYPICAL)
HVAC DUCTS
FP PIPES
PRETARGET TUNNEL
UTILITY CORRIDOR
2 HR. 8" CMU FIREWALL
EXIT PASSAGEWAY
SECTION E 3/16"=1'-0 C-16 & E-7
TUNNEL LINING: 3" MIN. THICKNESS SHOTCRETE SMOOTHING LAYER OVERLAIN BY DRAIN PANELS AND 3" SHOTCRETE PROTECTION LAYER.
18"øBEAM PIPE
LINER PLATE
BEAM PIPE STAND
C.I.P. INVERT
10" MIN. CIP CONC. INVERT
DRAIN GUTTER
SECTION A CARRIER TUNNEL IN SOIL & MIXED FACE 3/16"=1'-0 C-14 & C-15
SECTION B CARRIER TUNNEL IN ROCK 3/16"=1'-0 C-15
18"WIDE CABLE TRAY (TYPICAL)
96" FLUORESCENT FIXTURE 2 LAMP; (TYPICAL)
EMERGENCY EXIT PASSAGEWAY
2 HR. FIRE WALL, 8" CMU
SECTION C PRETARGET TUNNEL W/EXIT PASSAGEWAY IN ROCK 3/16"=1'-0 C-15, C-15 & E-7
SECTION D PRETARGET TUNNEL, W/O EXIT PASSAGEWAY IN ROCK 3/16"=1'-0 C-16 E-7
CAST-IN PLACE CONCRETE W/PVC LINER, STRUCTURAL CROWN SUPPORT
WALL LINING: 3" MIN. THICKNESS SHOTCRETE SMOOTHING LAYER OVERLAIN BY DRAIN PANELS & 3" SHOTCRETE PROTECTION LAYER
TARGET PILE
TARGET SUPPORT ENCLOSURE
EXIT SIGN (TYPICAL)
HVAC DUCT
CAST-IN PLACE CONCRETE INVERT SLAB
DRAIN BOARD
SECTION F 3/16"=1'-0 C-16 & E-7
FLUOR DANIEL HARZA
DESIGNED H. MACPHERSON
DRAWN R. JEDZINIAK
CHECKED
APPROVED
CONCEPT
REVIEWED
APPROVED
SUBMITTED
PROJECT NORTH
SCALE:
FERMI NATIONAL ACCELERATOR LABORATORY
UNITED STATES DEPARTMENT OF ENERGY
NuMI PROJECT
UPSTREAM TUNNEL SECTIONS - SHT. 1
DRAWING NO. 6-7-1 (TITLE-1) C-20
SEPT. 1998

Figure 5-8

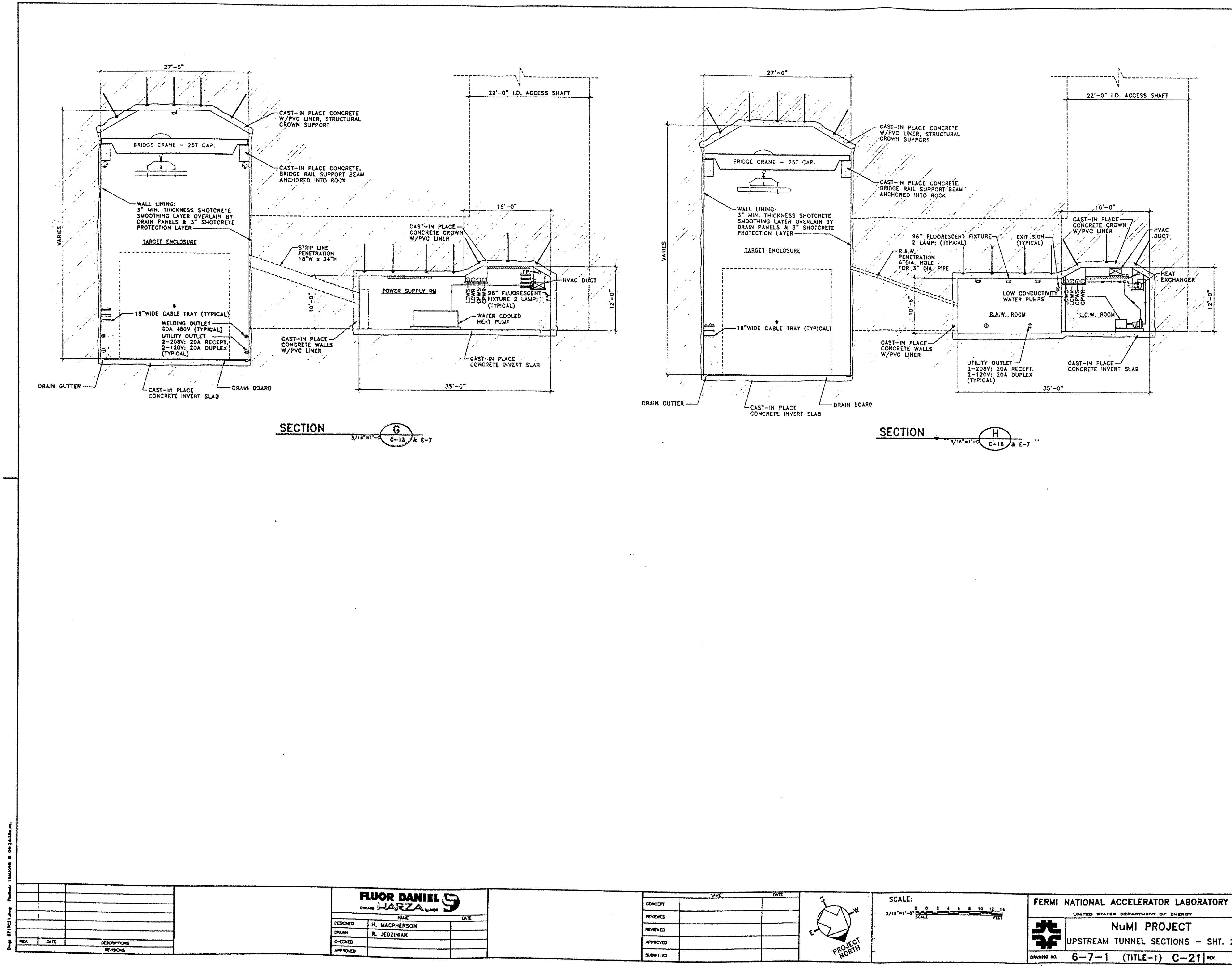
27'-0"
22'-0" I.D. ACCESS SHAFT
CAST-IN PLACE CONCRETE W/PVC LINER, STRUCTURAL CROWN SUPPORT
BRIDGE CRANE - 25T CAP.
CAST-IN PLACE CONCRETE, BRIDGE RAIL SUPPORT BEAM ANCHORED INTO ROCK
WALL LINING: 3" MIN. THICKNESS SHOTCRETE SMOOTHING LAYER OVERLAIN BY DRAIN PANELS & 3" SHOTCRETE PROTECTION LAYER
VARIES
TARGET ENCLOSURE
16'-0"
CAST-IN PLACE CONCRETE CROWN W/PVC LINER
STRIP LINE PENETRATION 18"W x 24"H
POWER SUPPLY RM
HVAC DUCT
96" FLUORESCENT FIXTURE 2 LAMP; (TYPICAL)
WATER COOLED HEAT PUMP
10'-0"
12'-0"
18"WIDE CABLE TRAY (TYPICAL)
WELDING OUTLET 60A 480V (TYPICAL)
UTILITY OUTLET 2-208V; 20A RECEPT. 2-120V; 20A DUPLEX (TYPICAL)
CAST-IN PLACE CONCRETE WALLS W/PVC LINER
CAST-IN PLACE CONCRETE INVERT SLAB
35'-0"
DRAIN GUTTER
DRAIN BOARD
SECTION G C-18 & E-7
96" FLUORESCENT FIXTURE 2 LAMP; (TYPICAL)
EXIT SIGN (TYPICAL)
HVAC DUCT
R.A.W. PENETRATION 6"DIA. HOLE FOR 3" DIA. PIPE
HEAT EXCHANGER
LOW CONDUCTIVITY WATER PUMPS
R.A.W. ROOM
L.C.W. ROOM
10'-6"
UTILITY OUTLET 2-208V; 20A RECEPT. 2-120V; 20A DUPLEX (TYPICAL)
SECTION H C-18 & E-7
REV. DATE DESCRIPTIONS REVISIONS
FLUOR DANIEL HARZA
DESIGNED H. MACPHERSON
DRAWN R. JEDZINIAK
CHECKED
APPROVED
CONCEPT
REVIEWED
APPROVED
SUBMITTED
PROJECT NORTH
SCALE: 3/16"=1'-0"
FERMI NATIONAL ACCELERATOR LABORATORY
UNITED STATES DEPARTMENT OF ENERGY
NuMI PROJECT
UPSTREAM TUNNEL SECTIONS - SHT. 2
DRAWING NO. 6-7-1 (TITLE-1) C-21
SEPT. 1998

Figure 5-9

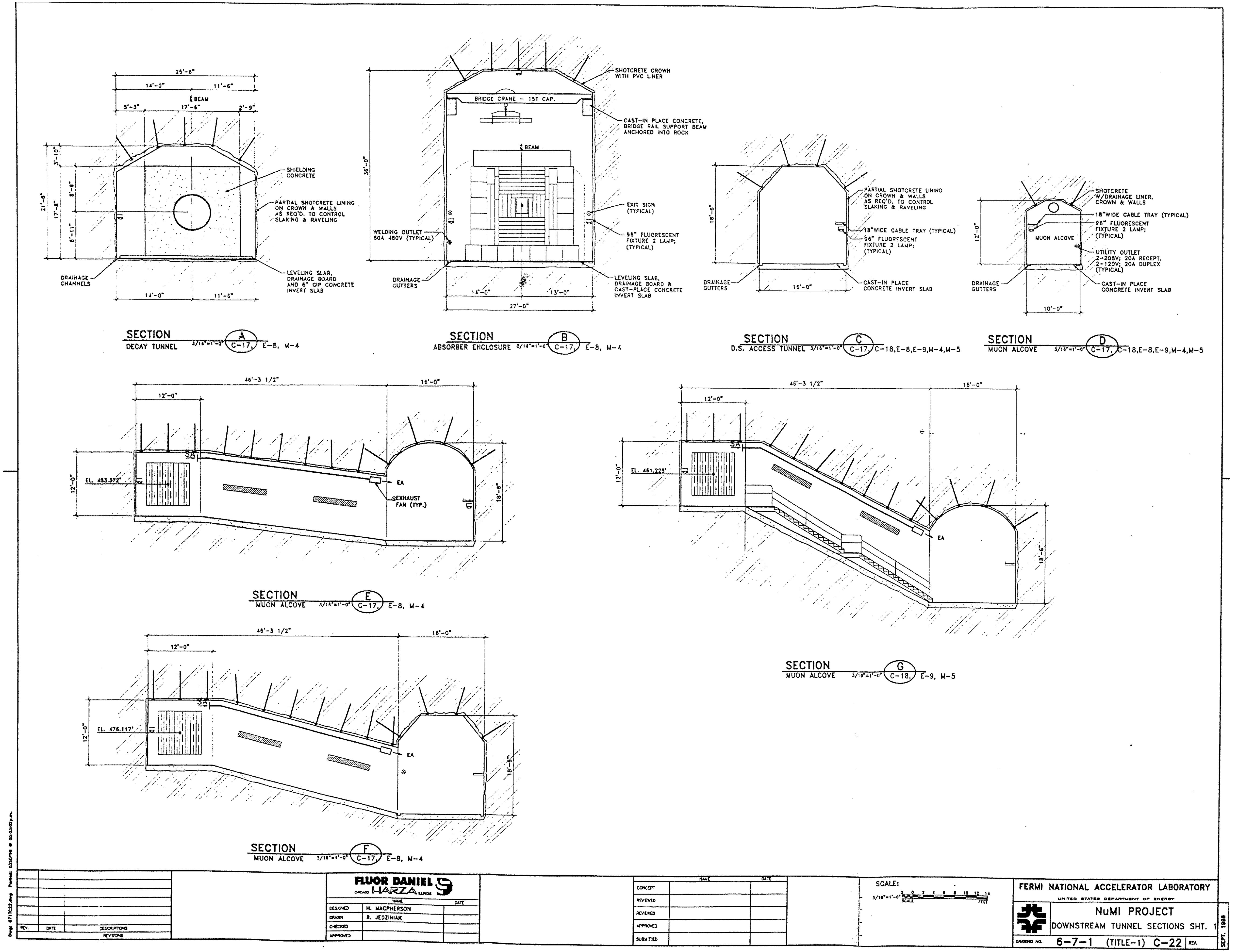

SECTION A
DECAY TUNNEL 3/16"=1'-0" C-17, E-8, M-4
25'-6"
14'-0"
11'-6"
℄ BEAM
5'-3"
17'-6"
2'-9"
3'-10"
8'-9"
21'-6"
17'-8"
8'-11"
SHIELDING CONCRETE
PARTIAL SHOTCRETE LINING ON CROWN & WALLS AS REQ'D. TO CONTROL SLAKING & RAVELING
DRAINAGE CHANNELS
LEVELING SLAB, DRAINAGE BOARD AND 6" CIP CONCRETE INVERT SLAB
SECTION B
ABSORBER ENCLOSURE 3/16"=1'-0" C-17, E-8, M-4
SHOTCRETE CROWN WITH PVC LINER
BRIDGE CRANE - 15T CAP.
CAST-IN PLACE CONCRETE, BRIDGE RAIL SUPPORT BEAM ANCHORED INTO ROCK
℄ BEAM
36'-0"
EXIT SIGN (TYPICAL)
WELDING OUTLET 60A 480V (TYPICAL)
98" FLUORESCENT FIXTURE 2 LAMP; (TYPICAL)
DRAINAGE GUTTERS
LEVELING SLAB, DRAINAGE BOARD & CAST-PLACE CONCRETE INVERT SLAB
14'-0"
13'-0"
27'-0"
SECTION C
D.S. ACCESS TUNNEL 3/16"=1'-0" C-17, C-18, E-8, E-9, M-4, M-5
18'-6"
PARTIAL SHOTCRETE LINING ON CROWN & WALLS AS REQ'D. TO CONTROL SLAKING & RAVELING
18"WIDE CABLE TRAY (TYPICAL)
96" FLUORESCENT FIXTURE 2 LAMP; (TYPICAL)
DRAINAGE GUTTERS
16'-0"
CAST-IN PLACE CONCRETE INVERT SLAB
SECTION D
MUON ALCOVE 3/16"=1'-0" C-17, C-18, E-8, E-9, M-4, M-5
SHOTCRETE W/DRAINAGE LINER, CROWN & WALLS
18"WIDE CABLE TRAY (TYPICAL)
96" FLUORESCENT FIXTURE 2 LAMP; (TYPICAL)
MUON ALCOVE
12'-0"
UTILITY OUTLET 2-208V; 20A RECEPT. 2-120V; 20A DUPLEX (TYPICAL)
DRAINAGE GUTTERS
10'-0"
CAST-IN PLACE CONCRETE INVERT SLAB
SECTION E
MUON ALCOVE 3/16"=1'-0" C-17, E-8, M-4
46'-3 1/2"
16'-0"
12'-0"
SA
EL. 483.372'
EA
EXHAUST FAN (TYP.)
18'-6"
SECTION F
MUON ALCOVE 3/16"=1'-0" C-17, E-8, M-4
46'-3 1/2"
16'-0"
12'-0"
SA
EL. 476.117'
EA
18'-6"
SECTION G
MUON ALCOVE 3/16"=1'-0" C-18, E-9, M-5
46'-3 1/2"
16'-0"
12'-0"
SA
EL. 461.225'
EA
18'-6"
REV.
DATE
DESCRIPTIONS
REVISIONS
FLUOR DANIEL
CHICAGO HARZA ILLINOIS
NAME
DATE
DESIGNED H. MACPHERSON
DRAWN R. JEDZINIAK
CHECKED
APPROVED
CONCEPT
REVIEWED
REVIEWED
APPROVED
SUBMITTED
SCALE:
3/16"=1'-0"
2 0 2 4 6 8 10 12 14
SCALE
FEET
FERMI NATIONAL ACCELERATOR LABORATORY
UNITED STATES DEPARTMENT OF ENERGY
NuMI PROJECT
DOWNSTREAM TUNNEL SECTIONS SHT. 1
DRAWING NO. 6-7-1 (TITLE-1) C-22
REV.
SEPT. 1998

Figure 5-10

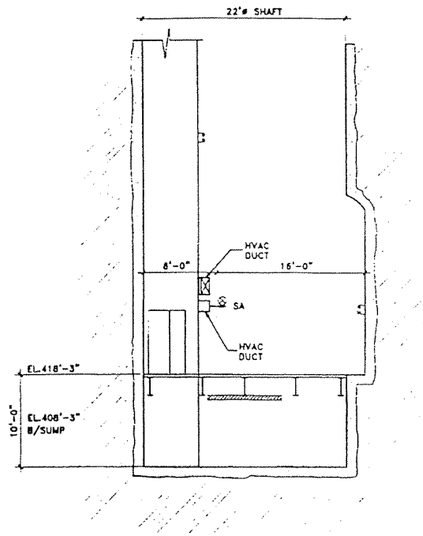

SECTION
D.S. ACCESS SHAFT 3/16"=1'-0" H C-18, E-9

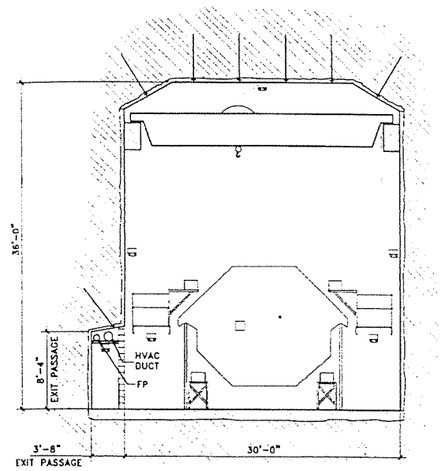

SECTION
MINOS ENCLOSURE 3/16"=1'-0" J C-19, E-10

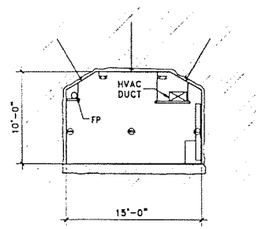

SECTION
COUNTING ROOM 3/16"=1'-0" K C-19, E-10

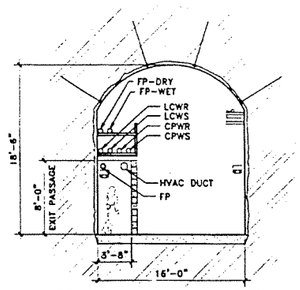

SECTION
D.S. ACCESS TUNNEL W/EXIT PASSAGE 3/16"=1'-0" L C-18, C-19, E-9, E-10

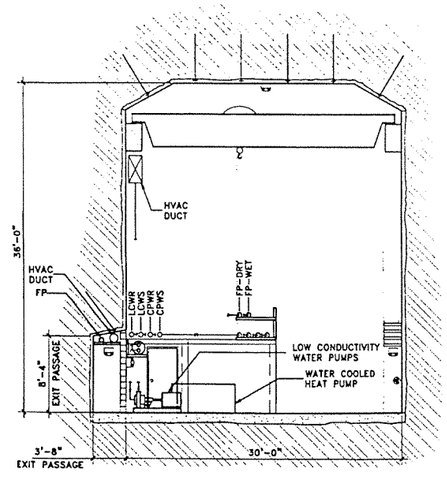

SECTION
MINOS ENCLOSURE 3/16"=1'-0" M C-19, E-10

REV.	DATE	DESCRIPTIONS
		REVISIONS

FLUOR DANIEL
CHICAGO HARZA ILLINOIS

	NAME	DATE
DESIGNED	H. MACPHERSON	
DRAWN	R. JEDZINIAK	
CHECKED		
APPROVED		

	NAME	DATE
CONCEPT		
REVIEWED		
REVIEWED		
APPROVED		
SUBMITTED		

SCALE: 3/16"=1'-0" 0 2 4 6 8 10 12 14 SCALE FEET

FERMI NATIONAL ACCELERATOR LABORATORY
UNITED STATES DEPARTMENT OF ENERGY

NuMI PROJECT
DOWNSTREAM TUNNEL SECTIONS SHT. 2

DRAWING NO. 6-7-1 (TITLE-1) C-23 REV.

SEPT. 1998

Dwgs 871TC23.dwg PltMod: 03SEP98 @ 09:00:41p.m.

6.0 Cost and Schedule

Table of Contents

6.0 COST AND SCHEDULE 1

6.1 INTRODUCTION 2

6.2 COST ESTIMATES 2

6.3 SCHEDULE AND FUNDING CONSIDERATIONS 4

6.4 FOOT NOTES FOR THE COST TABLE IN THE NUMI TDR: 5

Table of Tables

Table 6-1 Cost breakdown for NuMI WBS 1.0. ..... *6*

Table 6-2 Schedule for NuMI WBS 1.0. ..... *7*

6.1 Introduction

The NuMI Cost and Schedule Plan (C&S) includes the entire scope of work within the TEC (Total Estimated Cost) as shown on the DOE Schedule 44. Specifically, it includes the Technical Components (WBS 1.1), the Facility Construction (WBS 1.2), and the Project Management (WBS 1.3). The Technical Components are further broken down into eight level three systems: Extraction and Primary Beam, Neutrino Beam Devices, Power Supply Systems, Hadron Decay and Absorber, Neutrino Beam Monitoring, Alignment, Utility Systems, and lastly, Installation and Integration. The Facility Construction includes the Title I and Title II Engineering Design Efforts, the Title III EDIA, and the construction of the facility. Facility construction is further broken into the follow areas: Site Preparation, Underground Facilities (Carrier Tunnel, Pre-Target Tunnel, Upstream Access Shaft, Target Hall, Decay Tunnel, Beam Absorber Cavern, Downstream Access Tunnel, and MINOS Cavern), Service Buildings, and Government Furnished Equipment. Project Management is not broken down.

A single Microsoft Project (MS Project 98) file has been used to collect all cost and schedule information. This file includes all of the Salary, Wages and Fringes (SWF) costs and all of the Material and Services (M&S) costs. Two excerpts from the MS Project Schedule are included: 1) the level 4 cost summary and 2) the schedule summary. The cost summary provides a single page overview of the costs associated with each level 4 system. The schedule summary provides a single page overview of the summary tasks for the level 4 systems.

6.2 Cost Estimates

Salary, Wages and Fringes (SWF) costs will be accrued by the Technical Components and by Facilities Engineering Section (FES) EDIA on the Facility Construction. The Technical Components SWF represents the Fermilab labor costs for engineering and fabrication efforts necessary for designing and building the components within the scope of the Technical Components. The Technical Components SWF costs have been

calculated by estimating the level of effort required for each task and applying the appropriate labor rates based on the 1998 Beams Division average rates for exempt and non-exempt labor types. Likewise, the FES EDIA labor costs have been calculated by estimating the level of effort required for each phase and applying the FES charge-back rate.

Material and Services (M&S) costs have been estimated for items within the Technical Components and for the Facility. Each M&S cost has four tasks associated with it: 1). Preparation of a Purchase Req. (this task requires labor and accrues SWF costs). 2). Submission of a Purchase Order (this task incurs an obligation against the project). 3). Delivery of the Material or Execution of the Service (this task incurs a cost against the project). 4). Inspection of the Material or Work Performed (this task requires labor and accrues a SWF cost). By explicitly scheduling each of these steps, SWF costs associated with M&S expenditures are accurately included in the total cost, and both obligation and cost profiles can be generated. Since it is essential to schedule the work so that obligations do not exceed the funding profile, the ability to generate both the obligation and the cost profiles is very important and warrants the significant additional entries to the project schedule file.

A bottoms-up application of contingency has been performed by assigning the appropriate contingency to each lowest level item in the cost and schedule plan. The percentage contingencies shown on the summary tasks are the calculated, weighted sums of the contingencies for the items under that summary.

Escalation for each lowest level item has been calculated based on the January 1998 update of the DOE Anticipated Economic Escalation Rates and uses the index for Energy Research. Each years index has been corrected to a FY 98 base year (the January 1998 update is in FY '97 base). The indexes used are FY '98, 1.0; FY '99, 1.0235; FY '00, 1.0512; FY '01, 1.0778; FY'02, 1.1075. Escalation is based on the task start date.

Indirect Costs for each lowest level item have been calculated based on the latest guidance from the laboratory budget office. M&S indirect costs include G&A and MSA and equal 18.78775%. SWF costs include G&A and CSS and equal 43.0975%. Indirect Costs have been escalated to the fiscal year in which the costs are planned to accrue.

The sum of the base cost, contingency, escalation, and indirect costs for the TEC is just less than the $76.2M.

6.3 Schedule and Funding Considerations

This cost summary does not include the planned obligation profile or the planned cost profile. Those profiles are shown in the Project Summary Document and demonstrate that the project obligation profile can be made to match the funding profile. The NuMI Costs and Schedule Plan is a resource loaded, funding profile matched schedule. Resources have been identified and assigned for each task and an estimated limit on the maximum number of available resources for each labor type has been made. From the sum of the required resources and the sum of the estimated available resources, task durations have been calculated. The start of some tasks has been intentionally delayed to match the funding and obligation profiles. These tasks could be advanced and float increased (schedule risk reduced) if the funding profile allowed. A more front loaded funding profile would allow larger contracts to be let for the Facility Construction and would allow the facility construction to advance at a faster rate. This would reduce the indirect charges and likely reduce the overall base costs if one assumes that mobilization and start-up costs would not be duplicated as they are for multiple, smaller contracts. But more importantly, this would allow more time for the installation and pre-commissioning of the technical components and the MINOS near detector. These are labor intensive efforts. Although they fit within the scheduled project completion date, the schedule is very tight.

6.4 Foot Notes for the Cost Table in the NuMI TDR:

SWF Cost, '98$	is the labor cost in 1998 dollars.
M&S Cost, '98$	is the material and services cost in 1998 dollars.
Base Cost, '98$	is the sum of the SWF and M&S costs and is in 1998 dollars.
% Cont.	is the contingency on the summary task calculated using a weighted sum of the individually assigned percent contingency for each lowest level task.
Contingency, '98$	is the base cost times the % contingency, in 1998 dollars
Indirect, TY$	is the indirect costs (including G&A, MSA and CSS) in then-year dollars.
Escalation, TY$	is the escalation which is the product of the base cost times the applicable DOE anticipated economic escalation rate index (corrected to a FY 98 base year).
Full Cost, TY$	is the sum of the Base Cost + Contingency + Indirect + Escalation

Table 6-1 Cost breakdown for NuMI WBS 1.0.

Level 4 w/o 0 costs

ID	WBS	Task Name	SWF Cost, '98$	M&S Cost, '98$	Base Cost, '98$	% Cont.	Contingency, '98$	Indirect, TY$	Escalation, TY$	Full Cost, TY$	Start	Finish
8	1.0	WBS 1.0 (TEC)	$9,115,748	$44,702,967	$53,818,715	23.9	12862931.43	6560863.79	2954997.55	$76,197,508	3/17/97	10/3/02
25	1.1	WBS 1.1 Technical Components (Beamline, Focusing, Absorber)	$4,252,778	$6,889,318	$11,142,096	32.04	3570147.79	3334411.88	777521.73	$18,824,178	4/6/98	10/3/02
26	1.1.1	Extraction and Primary Beam (WBS 1.1.1)	$675,182	$792,094	$1,467,276	32.39	475212.2	469704.36	103396.93	$2,515,590	5/7/98	9/30/02
47	1.1.1.1	Extraction and Primary Conceptual Design Phase	$73,964	$0	$73,964	43.1	31881.6	32313.75	1014.26	$139,174	5/8/98	11/2/01
62	1.1.1.2	Extraction and Primary Beam Design Phase (Title 1 and Title 2)	$186,078	$0	$186,078	64.8	120586	85315.94	11882.29	$403,862	10/1/98	3/14/02
90	1.1.1.3	Extraction and Primary Beam Construction Phase	$415,140	$792,094	$1,207,234	26.73	322744.6	352074.67	90500.38	$1,972,554	12/7/98	9/27/02
284	1.1.2	Neutrino Beam Devices (WBS 1.1.2)	$1,169,782	$3,139,726	$4,309,508	37.83	1630157.74	1155581.45	258141.03	$7,353,389	4/6/98	10/3/02
345	1.1.2.1	Neutrino Beam Conceptual Design Phase	$72,980	$50,000	$122,980	54.42	66920	40846.43	0	$230,746	4/6/98	9/23/99
357	1.1.2.2	Neutrino Beam Devices Design Phase (Title 1 and Title 2)	$764,716	$348,330	$1,113,047	38.84	432315.36	407563.06	34859.42	$1,987,785	4/6/98	7/10/01
557	1.1.2.3	Neutrino Beam Devices Construction Phase	$332,086	$2,741,396	$3,073,482	36.8	1130922.38	707171.96	223281.6	$5,134,857	4/6/98	10/3/02
815	1.1.3	Power Supply System (WBS 1.1.3)	$523,737	$841,204	$1,364,941	28.2	384963.53	411718.6	100746.86	$2,262,370	4/6/98	9/30/02
862	1.1.3.2	Power Supply System Design Phase (Title 1 and Title 2)	$207,523	$46,208	$253,731	34.02	86313.04	103465.96	13954.31	$457,464	7/28/98	9/23/02
998	1.1.3.3	Power Supply System Construction Phase	$316,214	$794,996	$1,111,210	26.88	298650.49	308252.64	86792.55	$1,804,906	4/6/98	9/30/02
1190	1.1.4	Hadron Decay and Absorber (WBS 1.1.4)	$178,343	$434,275	$612,618	38.55	236175.48	169193.83	46282.39	$1,064,270	4/6/98	7/2/02
1208	1.1.4.1	Hadron Decay and Absorber Conceptual Design Phase	$88,948	$0	$88,948	14.99	13335.6	38557.08	516.78	$141,358	4/6/98	3/13/00
1222	1.1.4.2	Hadron Decay and Absorber Design Phase (Title 1 and Title 2)	$35,084	$0	$35,084	60.45	21206.72	16302.12	2742.14	$75,335	11/1/99	1/4/02
1248	1.1.4.3	Hadron Decay and Absorber Construction Phase	$54,311	$434,275	$488,586	41.27	201633.16	114334.63	43023.47	$847,578	12/7/98	7/2/02
1338	1.1.5	Neutrino Beam Monitoring (WBS 1.1.5)	$313,264	$111,800	$425,064	20.85	88615.42	164516.28	24522.73	$702,718	4/6/98	8/20/02
1350	1.1.5.1	Neutrino Beam Monitoring Conceptual Design Phase	$109,224	$0	$109,224	18	19660.32	47620.94	1271.82	$177,777	4/6/98	11/29/99
1355	1.1.5.2	Neutrino Beam Monitoring Design Phase (Title 1 and Title 2)	$60,548	$0	$60,548	24.51	14841.28	27430.72	3100.06	$105,920	2/1/00	8/16/00
1388	1.1.5.3	Neutrino Beam Monitoring Construction Phase	$143,492	$111,800	$255,292	21.2	54113.82	89464.62	20150.85	$419,021	4/6/98	8/20/02
1499	1.1.6	Alignment Systems (WBS 1.1.6)	$320,225	$76,230	$396,455	17.72	70256.43	159122.71	17240.9	$643,075	4/6/98	9/12/02
1501	1.1.6.1	Alignment Systems Conceptual Design Phase	$72,160	$0	$72,160	18.18	13120	31099.16	0	$116,379	6/1/98	5/16/02
1504	1.1.6.2	Alignment Design Phase (Title 1 and Title 2)	$59,040	$9,012	$68,052	15.95	10855.6	28609.82	3415.3	$110,933	4/6/98	8/1/02
1520	1.1.6.3	Alignment Construction Phase	$189,025	$67,218	$256,243	18.06	46280.83	99413.73	13825.6	$415,763	7/17/98	9/12/02
1607	1.1.7	Water, Vacuum and Gas Systems (WBS 1.1.7)	$296,788	$477,388	$774,176	23.46	181647.35	235877.18	64617.07	$1,256,318	4/6/98	9/3/02
1626	1.1.7.1	Water, Vacuum and Gas Systems Conceptual Design Phase	$17,328	$0	$17,328	23.17	4014.4	7543.63	175.64	$29,062	4/6/98	6/14/00
1637	1.1.7.2	Water, Vacuum and Gas System Design Phase (Title 1 and Title 2)	$38,868	$0	$38,868	30	11660.4	17467.47	1662.12	$69,658	6/1/99	6/15/01
1674	1.1.7.3	Water, Vacuum, and Gas System Construction Phase	$240,592	$477,388	$717,980	23.12	165972.55	210866.08	62779.31	$1,157,598	12/16/99	9/3/02
1808	1.1.8	Installation and Integration (WBS 1.1.8)	$775,457	$1,016,601	$1,792,058	28.07	503119.65	568697.48	162573.63	$3,026,449	4/6/98	9/30/02
1841	1.1.8.1	Installation and Intergration Conceptual Design Phase	$15,088	$0	$15,088	0	0	6502.55	0	$21,591	4/6/98	6/8/98
1843	1.1.8.2	Installation and Integration Design Phase (Title 1 and Title 2)	$217,628	$66,500	$284,128	35.8	101726.2	113683.42	21196.55	$520,734	5/26/98	5/27/02
1890	1.1.8.3	Installation and Integration Construction Phase	$542,741	$950,101	$1,492,842	26.89	401393.45	448511.5	141377.28	$2,484,124	11/2/98	9/30/02
2085	1.2	WBS 1.2 Facility (Civil Construction: Tunnels, Shafts and Service Buildings)	$2,996,650	$37,813,649	$40,810,299	20.94	8546255.64	2375697.38	2069772.92	$53,802,025	4/6/98	3/15/02
2097	1.2.2	Facility Construction Title I Design Phase	$379,620	$1,137,037	$1,516,657	5	75832.85	257545.48	0	$1,850,035	6/1/98	10/23/98
2105	1.2.3	Facility Construction Title II Design Phase	$420,660	$1,596,880	$2,017,540	20	403508	281700.66	47412.19	$2,750,161	10/23/98	5/21/99
2111	1.2.4	Facility Construction Phase	$2,196,370	$35,079,732	$37,276,102	21.64	8066914.79	1836451.24	2022360.73	$49,201,828	11/30/98	3/15/02
2147	1.2.4.2	Title III Inspection and Oversight Efforts	$2,196,370	$1,703,807	$3,900,177	19.69	768035.32	1143831.46	171264.26	$5,983,308	3/1/99	3/15/02
2158	1.2.4.3	Execute Site Preparation and Utilities (Site Work)	$0	$802,332	$802,332	18	144419.76	96146.31	18854.8	$1,061,753	3/29/99	6/4/99
2160	1.2.4.4	Execute Underground Sub-Contract	$0	$23,597,321	$23,597,321	24.5	5781343.64	96146.31	1171438.39	$30,646,249	7/5/99	4/16/01
2166	1.2.4.6	Execute Target Service Building Sub-Contract	$0	$2,720,106	$2,720,106	13.6	369934.42	101247.18	211624.25	$3,402,912	4/5/01	2/5/02
2172	1.2.4.5	Execute MINOS Service Building Sub-Contract	$0	$4,348,986	$4,348,986	13.2	574066.15	101247.18	338351.11	$5,362,651	11/15/00	10/30/01
2179	1.2.4.7	Fermilab Procurements of GFE: Cranes, Decay Pipe,and Shielding, Gove	$0	$1,907,180	$1,907,180	22.5	429115.5	297832.79	110827.92	$2,744,956	2/3/00	5/25/01
2183	1.3	WBS 1.3 Project Management	$1,866,320	$0	$1,866,320	40	746528	850754.52	107702.9	$3,571,305	4/6/98	9/30/02

Page 1

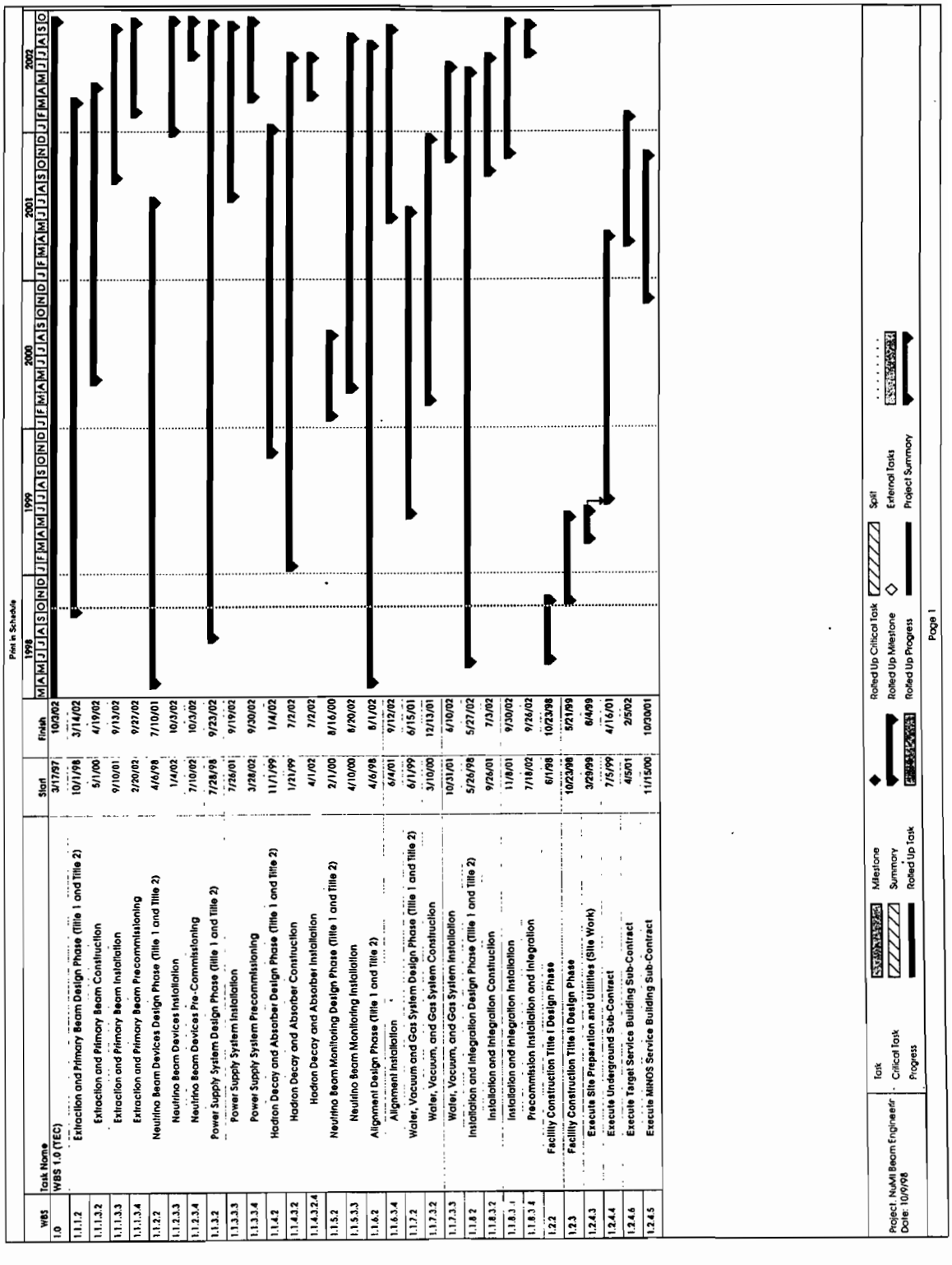

WBS	Task Name	Start	Finish
1.0	WBS 1.0 (TEC)	3/17/97	10/3/02
1.1.1.2	Extraction and Primary Beam Design Phase (Title 1 and Title 2)	10/1/98	3/14/02
1.1.1.3.2	Extraction and Primary Beam Construction	5/1/00	4/19/02
1.1.1.3.3	Extraction and Primary Beam Installation	9/10/01	9/13/02
1.1.1.3.4	Extraction and Primary Beam Precommissioning	2/20/02	9/27/02
1.1.2.2	Neutrino Beam Devices Design Phase (Title 1 and Title 2)	4/6/98	7/10/01
1.1.2.3.3	Neutrino Beam Devices Installation	1/4/02	10/3/02
1.1.2.3.4	Neutrino Beam Devices Pre-Commissioning	7/10/02	10/3/02
1.1.3.2	Power Supply System Design Phase (Title 1 and Title 2)	7/28/98	9/23/02
1.1.3.3.3	Power Supply System Installation	7/26/01	9/19/02
1.1.3.3.4	Power Supply System Precommissioning	3/28/02	9/30/02
1.1.4.2	Hadron Decay and Absorber Design Phase (Title 1 and Title 2)	11/1/99	1/4/02
1.1.4.3.2	Hadron Decay and Absorber Construction	1/21/99	7/2/02
1.1.4.3.2.4	Hadron Decay and Absorber Installation	4/1/02	7/2/02
1.1.5.2	Neutrino Beam Monitoring Design Phase (Title 1 and Title 2)	2/1/00	8/16/00
1.1.5.3.3	Neutrino Beam Monitoring Installation	4/10/00	8/20/02
1.1.6.2	Alignment Design Phase (Title 1 and Title 2)	4/6/98	8/1/02
1.1.6.3.4	Alignment Installation	6/4/01	9/12/02
1.1.7.2	Water, Vacuum and Gas System Design Phase (Title 1 and Title 2)	6/1/99	6/15/01
1.1.7.3.2	Water, Vacuum, and Gas System Construction	3/10/00	12/13/01
1.1.7.3.3	Water, Vacuum, and Gas System Installation	10/31/01	6/10/02
1.1.8.2	Installation and Integration Design Phase (Title 1 and Title 2)	5/26/98	5/27/02
1.1.8.3.2	Installation and Integration Construction	9/26/01	7/3/02
1.1.8.3.3	Installation and Integration Installation	11/8/01	9/30/02
1.1.8.3.4	Precommission Installation and Integration	7/18/02	9/26/02
1.2.2	Facility Construction Title I Design Phase	8/1/98	10/23/98
1.2.3	Facility Construction Title II Design Phase	10/23/98	5/21/99
1.2.4.3	Execute Site Preparation and Utilities (Site Work)	3/29/99	8/4/99
1.2.4.4	Execute Underground Sub-Contract	7/5/99	4/16/01
1.2.4.6	Execute Target Service Building Sub-Contract	4/5/01	2/5/02
1.2.4.5	Execute MINOS Service Building Sub-Contract	11/15/00	10/30/01

Table 6-2 Schedule for NuMI WBS 1.0.

This Page Intentionally Left Blank

7.0 Project Management Summary

Table of Contents

7.0 PROJECT MANAGEMENT SUMMARY 7-1

7.1 PROJECT MANAGEMENT PHILOSOPHY 7-2

7.2 ROLES AND RESPONSIBILITIES IN THE NUMI FACILITY SUBPROJECT 7-3

7.2.1 Fermilab Beams Division 7-3

7.2.2 Level 2 Managers 7-3

7.2.3 Level 3 Managers 7-4

7.3 PROJECT CONTROLS 7-4

7.3.1 Baseline Development 7-4

7.3.2 Performance Measurement 7-5

7.3.3 Configuration Management 7-5

7.3.4 Reporting 7-5

7.4 QUALITY ASSURANCE 7-5

Table of Figures

Figure 7-1 Work Breakdown Structure of the NuMI Project to Level 2. ____ 7-7

Figure 7-2 Work breakdown structure of the NuMI Facility Subproject to Level 3. This work is included in the TEC for the NuMI Project. ____ 7-8

7.1 Project Management Philosophy

The multi-faceted nature of the NuMI Project, which includes the construction of a beamline, experimental facilities off-site and experimental detectors, dictates a project management philosophy that is flexible enough to meet the demands of these different subprojects. The project management philosophy also reflects the project's budget structure, for which the Total Estimated Cost (TEC) includes the civil construction and technical components of the NuMI beamline, but not the MINOS experiment or work at Soudan. Work covered by the TEC will be accomplished mainly by Fermilab personnel and subcontractors, with a relatively small amount of the work performed by other research institutions. Much of the research work on the MINOS Subproject will be accomplished by the various institutions of the MINOS collaboration. Work at the Soudan Underground Laboratory will be performed under an agreement with the University of Minnesota. Hence, the project management structure is somewhat different for each Level 1 branch of the NuMI Project (see Figure 7-1). The NuMI project management systems are fully described in the NuMI Project Execution Plan (PEP), which describes the Department of Energy project management systems, and the NuMI Project Management Plan (PMP), which describes Fermilab's project management systems. A detailed description of the cost and schedule is given in the NuMI Cost and Schedule Plan. The WBS of the NuMI Project is shown to Level 2 in Figure 7-1.

The NuMI Facility Subproject encompasses the neutrino beamline and all construction, both underground and on the surface, at the Fermilab site. The Fermilab Beams Division and its subcontractors bear the main responsibility for carrying out this part of the NuMI Project. Where outside institutions are collaborating with Fermilab in the NuMI Facility Subproject, their work and responsibilities are set forth in Memoranda of Understanding (MOU). An example is the MOU between Fermilab and IHEP, where work on the NuMI target is being conducted.

7.2 Roles and Responsibilities in the NuMI Facility Subproject

7.2.1 Fermilab Beams Division

The Fermilab Beams Division (BD) has created the NuMI Beam Development Group and is responsible for line management of the Fermilab personnel directly assigned to the NuMI Project. The NuMI Project Manager is an Associate Director of the Beams Division and reports to the Beams Division Head in this capacity. As a member of the NuMI Project Management Group, the Division Head appoints the NuMI Facility Safety Review Committee, which is charged with the responsibility of assuring that the NuMI line organization develops the NuMI Facility in accordance with applicable ES&H regulations and practices.[1]

7.2.2 Level 2 Managers

There are two Level 2 Managers on the NuMI Facility Subproject. These are for the Technical Components (WBS 1.1) and the conventional construction (WBS 1.2). WBS item 1.3, Project Management, is primarily a budgetary division and is overseen by the NuMI Project Manager.

Level 2 Subproject managers are appointed by the NuMI Project Manager and are responsible for design, fabrication, integration, installation and testing of all components which comprise their Level 2 WBS element. They generate and maintain the cost-estimate, schedule, and resource requirements for their Subprojects. They also manage work performed by outside contractors. The Level 2 managers will provide information on cost, schedule and performance to the NuMI Project Manager and update their resource-loaded schedules monthly.

---

[1] NuMI Preliminary Safety Assessment Document, October 1998

7.2.3 Level 3 Managers

Level 3 subproject managers are appointed by the NuMI Project Manager and are responsible for the design, procurement, fabrication, installation and commissioning of their Level 3 subsystem. Level 3 managers document the scope and baseline of the Level 3 subsystem by maintaining the relevant portion of the NuMI Technical Design Report and the NuMI/MINOS Cost and Schedule Plan. Level 3 managers advise the NuMI Project Manager on the negotiation of Memoranda of Understanding with outside institutions working on their Level 3 subsystem. Figure 7-2 shows the Level 3 WBS elements and Level 3 Managers, where appropriate, for the part of the project covered by the TEC (WBS 1.0). WBS 1.2 is directed by the Level 2 Manager (or performed by a subcontractor) and therefore does not indicate Level 3 managers.

7.3 Project Controls

The major elements of the project controls system are baseline development, monitoring project performance and configuration management.

7.3.1 Baseline Development

Baseline development includes the actions necessary to define the scope of work, cost and schedule for the project. The scope of the NuMI Facility Subproject is defined in this Technical Design Report. This document kept current by scheduled periodic updates provided by the Level 3 Project Managers. Additional updates may be provided if a Level 3 subproject undergoes a major change between scheduled revisions.

Each Level 3 element of the NuMI Facility Subproject will have a formal cost estimate and schedule, which is documented in the NuMI/MINOS Cost and Schedule Plan (CSP). The CSP is kept current through monthly project management reports provided by the Level 3 Project Managers.

7.3.2 Performance Measurement

The principal functions of performance measurement are to identify, analyze and initiate corrective actions for any significant deviations from the baseline as early as possible. A monthly earned value analysis will be performed to assess the labor and fiscal resources expended and the work completed. This will ensure that shortfalls that could lead to cost or schedule variances are identified.

7.3.3 Configuration Management

Configuration Management refers to the process of having the NuMI Project Management Group (PMG) consider changes to technical, cost and schedule baselines and approve them as appropriate. Changes are accomplished through the submission of an Engineering Change Request to the NuMI PMG and its subsequent approval by that body. Where time constraints dictate, changes may be effected through a Field Change Order subject to the approval of the NuMI Project Manager.

7.3.4 Reporting

Level 3 Project Managers provide monthly reports on the status of their subprojects. Fermilab in turn provides monthly project reports to the DOE through the DOE Project Manager. The basic information in these reports will include:

- A summary of work progress including milestones achieved
- A summary of relevant ES&H information
- An up-to-date project schedule
- An up-to-date summary of funds appropriated and obligated
- Any significant changes in cost, schedule or technical scope
- Any variances from cost and schedule goals.

7.4 Quality Assurance

Quality Assurance for NuMI is implemented in conformance with the Fermilab Quality Assurance Plan (FQAP). Quality Assurance is an integral part of the design,

procurement, fabrication, construction and installation of all aspects of the NuMI Project. A Specific Quality Implementation Plan for NuMI will be developed as stipulated by the FQAP.

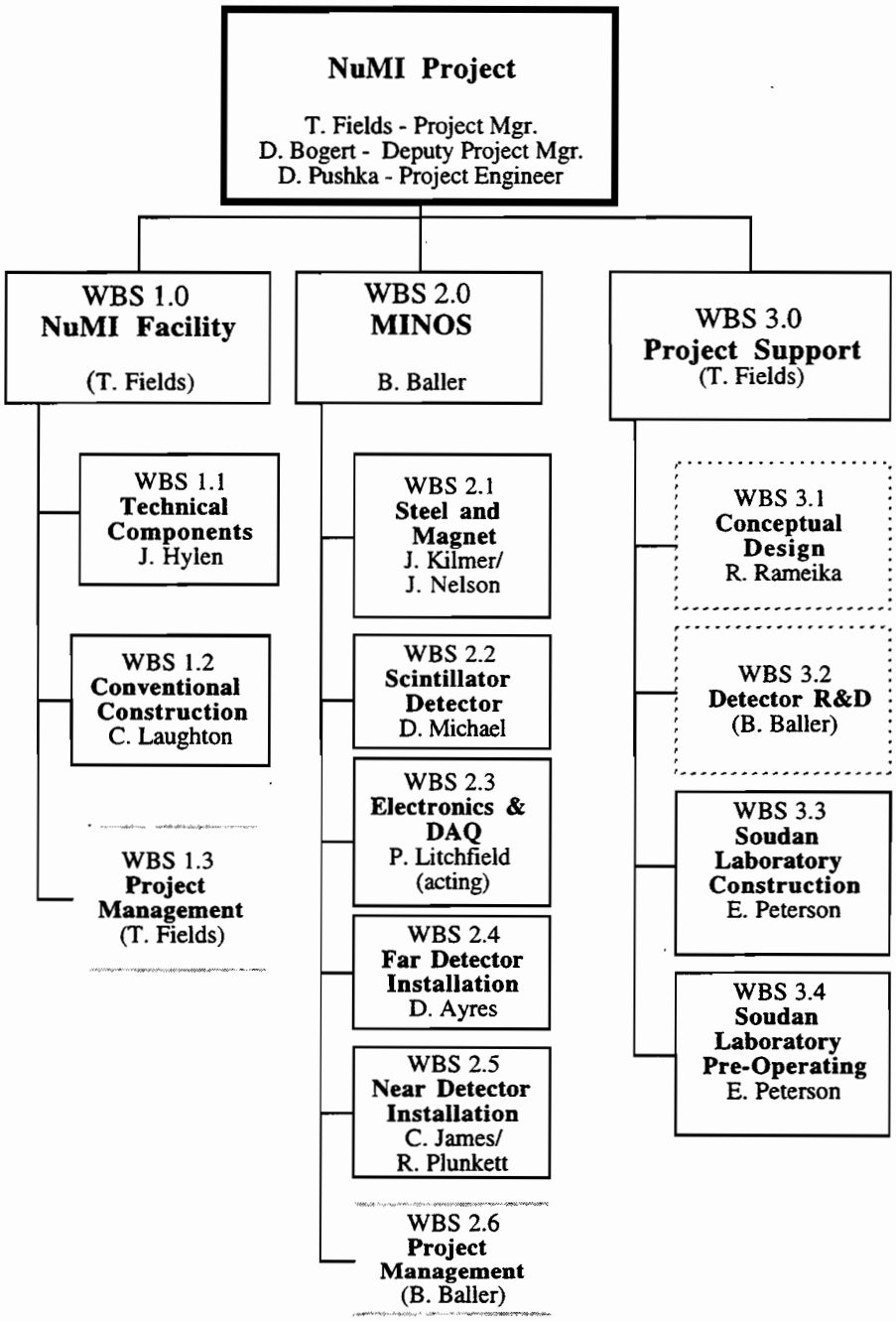

Figure 7-1 Work Breakdown Structure of the NuMI Project to Level 2.

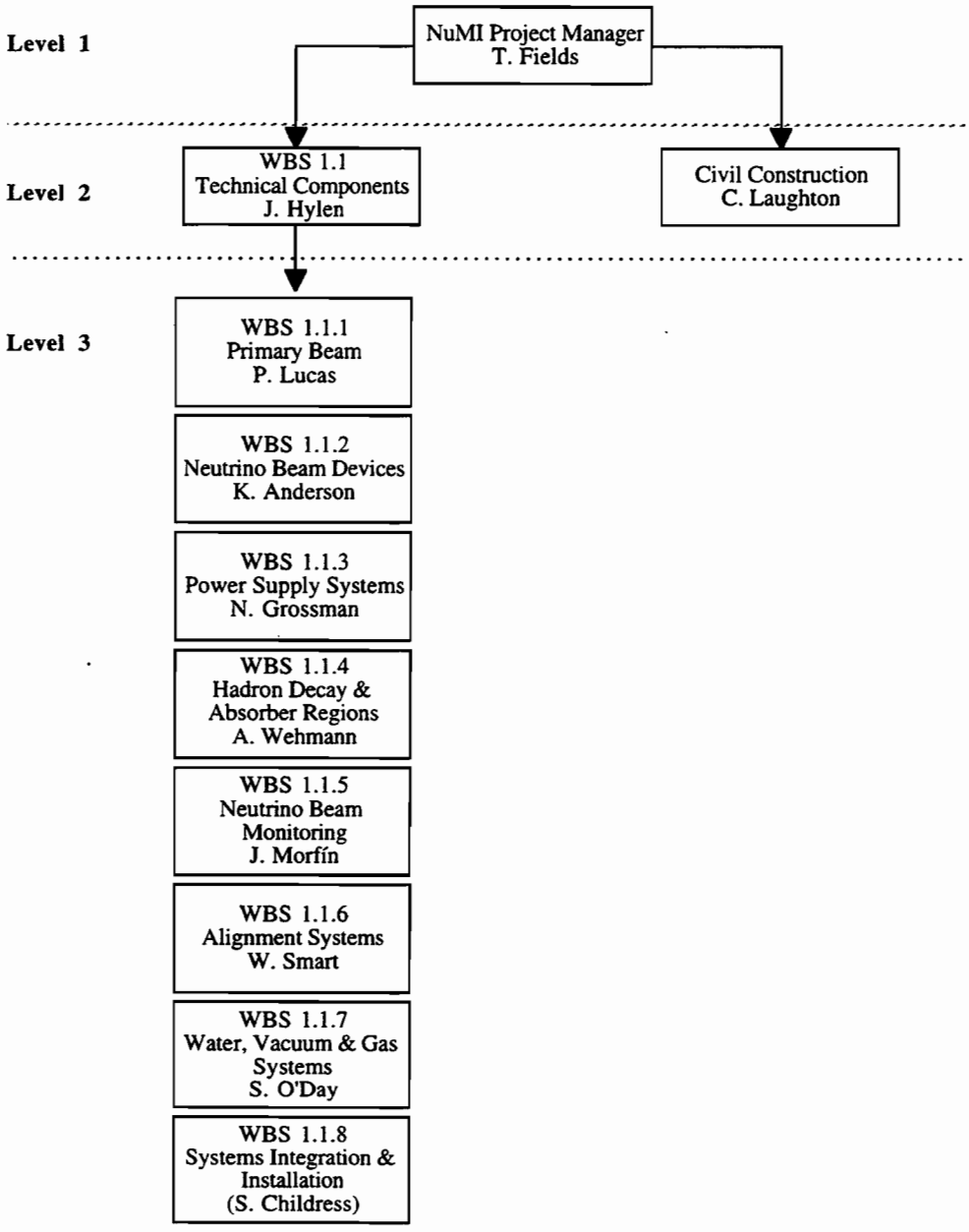

Figure 7-2 Work breakdown structure of the NuMI Facility Subproject to Level 3. This work is included in the TEC for the NuMI Project.

A Beam Sheet

Program ces (A Construction Engineering Survey format) (11/26/91) Mon Aug 31 10:32:12 1998
Site coordinates for beamline: horn2_ces
NOTES: Coordinates are given for the entrance of the device in DUSAF coordinate system.
.Site +x-axis (EAST); site +y-axis (NORTH); Site z-axis (ELEVATION) .
Positive bearing is ccw wrt site EAST.
Pitch is the vertical angle about the x-y plane.

line	location	typ_ code	distance [ft]	x [ft]	y [ft]	z [ft]	brng [deg]	pitch [deg]	yaw [deg]
0000	S1_BML	marker	-156.34483	101468.341	97163.814	715.724	148.76849	0.000	0.000
0001	Q606	3Q84-2	-156.34483	101468.341	97163.814	715.724	148.76849	0.000	0.000
0002	Q607	3Q84-2	-103.12368	101422.833	97191.409	715.724	148.76849	0.000	0.000
0003	Q607	3Q84-2	-99.62369	101419.840	97193.224	715.724	148.76849	0.000	0.000
0004	C_608	MIHC	-59.26711	101385.332	97214.148	715.724	148.76849	0.000	0.000
0005	L6081	LAM_1	-56.88634	101383.296	97215.383	715.724	148.76849	0.000	77.395
0006	Q608	3Q84-2	-46.40256	101374.332	97220.819	715.724	148.76849	0.000	0.000
0007	Q608	3Q84-2	-42.90257	101371.339	97222.633	715.724	148.76849	0.000	0.000
0008	L6082	LAM_1	-37.53762	101366.751	97225.415	715.724	148.76849	0.000	84.385
0009	L6083	LAM_1	-26.33974	101357.176	97231.221	715.724	148.76849	0.000	87.880
0010	V100	CMG_1	-14.75532	101347.271	97237.228	715.724	148.76849	0.000	85.874
0011	HQ101	3Q120-2	0.49938	101334.268	97245.203	716.540	148.69573	1.631	0.000
0012	HQ101	3Q120-2	5.49937	101329.998	97247.800	716.683	148.69573	1.631	0.000
0013	HP101R	SYBPM_S	10.99935	101325.300	97250.656	716.839	148.69573	1.631	0.000
0014	VP101R	SYBPM_S	12.03843	101324.413	97251.196	716.869	148.69573	1.631	0.000
0015	HV1011	EPB	25.12912	101313.233	97257.995	717.242	149.00426	1.631	0.000
0016	HV1012	EPB	36.29583	101303.661	97263.738	717.560	149.62163	1.631	0.000
0017	HV1013	EPB	47.46250	101294.028	97269.377	717.878	150.23841	1.609	-3.939
0018	HV1014	EPB	58.62921	101284.335	97274.912	718.191	150.85434	1.566	-3.939
0019	HV1015	EPB	69.79589	101274.583	97280.343	718.496	151.33248	1.287	-56.482
0020	HV1016	EPB	80.96260	101264.786	97285.696	718.741	151.67281	0.772	-56.482
0021	HV1017	EPB	92.12928	101254.956	97290.991	718.887	152.01315	0.257	-56.482
0022	HQ102	3Q120-2	110.47586	101238.743	97299.579	718.932	152.18332	0.000	0.000
0023	HQ102	3Q120-2	115.47585	101234.321	97301.912	718.932	152.18332	0.000	0.000
0024	HQ103	3Q120-2	126.47583	101224.592	97307.045	718.932	152.18332	0.000	0.000
0025	HQ103	3Q120-2	131.47582	101220.170	97309.378	718.932	152.18332	0.000	0.000
0026	HP103R	SYBPM_S	136.97581	101215.306	97311.945	718.932	152.18332	0.000	0.000
0027	VP103R	SYBPM_S	138.01485	101214.387	97312.430	718.932	152.18332	0.000	0.000
0028	PM103	SYSWIC	139.35599	101213.200	97313.055	718.932	152.18332	0.000	0.000
0029	HC103	MIHC	141.26022	101211.516	97313.944	718.932	152.18332	0.000	0.000
0030	HC103	MIHC	142.27245	101210.621	97314.416	718.932	152.18332	0.000	0.000
0031	VC103	MIVC	143.28469	101209.726	97314.889	718.932	152.18332	0.000	0.000
0032	HP104R	SYBPM_S	293.41903	101076.940	97384.949	718.932	152.18332	0.000	0.000
0033	VP104R	SYBPM_S	294.45807	101076.021	97385.434	718.932	152.18332	0.000	0.000
0034	PM104	SYSWIC	295.79921	101074.835	97386.059	718.932	152.18332	0.000	0.000
0035	HQ104	3Q120-2	297.91876	101072.961	97387.048	718.932	152.18332	0.000	0.000
0036	HQ104	3Q120-2	302.91875	101068.538	97389.382	718.932	152.18332	0.000	0.000
0037	HQ105	3Q120-2	321.26123	101052.316	97397.941	718.932	152.18332	0.000	0.000
0038	HQ105	3Q120-2	326.26122	101047.893	97400.274	718.932	152.18332	0.000	0.000
0039	V1050	B2	332.17788	101042.660	97403.035	718.932	152.18332	-0.733	-90.000
0040	V1051	B2	353.26176	101024.015	97412.873	718.634	152.18332	-2.298	-90.000
0041	V1052	B2	374.34564	101005.384	97422.703	717.773	152.18332	-3.831	-90.000
0042	V1053	B2	395.42952	100986.780	97432.519	716.348	152.18332	-5.364	-90.000
0043	V1054	B2	416.51341	100968.216	97442.314	714.361	152.18332	-6.897	-90.000
0044	HQ106	3Q120-2	437.68062	100949.633	97452.118	711.803	152.18332	-7.663	0.000
0045	HQ106	3Q120-2	442.68061	100945.250	97454.431	711.136	152.18332	-7.663	0.000
0046	HC106	MIHC	448.46528	100940.179	97457.106	710.364	152.18332	-7.663	0.000
0047	HC106	MIHC	449.47751	100939.292	97457.574	710.229	152.18332	-7.663	0.000
0048	VC106	MIVC	450.48975	100938.405	97458.042	710.094	152.18332	-7.663	0.000
0049	HQ107	3Q120-2	453.60602	100935.673	97459.484	709.679	152.18332	-7.663	0.000
0050	HQ107	3Q120-2	458.60601	100931.291	97461.796	709.012	152.18332	-7.663	0.000
0051	HP107R	SYBPM_S	464.10599	100926.470	97464.340	708.279	152.18332	-7.663	0.000
0052	VP107R	SYBPM_S	465.14503	100925.559	97464.820	708.140	152.18332	-7.663	0.000
0053	PM107	SYSWIC	466.48617	100924.383	97465.440	707.961	152.18332	-7.663	0.000
0054	STUB_E	MIHC	480.63286	100911.983	97471.983	706.074	152.18332	-7.663	0.000
0055	PRE_E	MIHC	922.50337	100524.665	97676.339	647.145	152.18332	-7.663	0.000
0056	HP108R	SYBPM_S	934.90755	100513.792	97682.076	645.491	152.18332	-7.663	0.000

0057	VP108R	SYBPM_S	935.94659	100512.881	97682.556	645.352	152.18332	-7.663	0.000
0058	PM108	SYSWIC	937.28776	100511.706	97683.176	645.173	152.18332	-7.663	0.000
0059	HQ108	3Q120-2	939.40727	100509.848	97684.157	644.891	152.18332	-7.663	0.000
0060	HQ108	3Q120-2	944.40726	100505.465	97686.469	644.224	152.18332	-7.663	0.000
0061	HC108	MIHC	950.19193	100500.395	97689.144	643.452	152.18332	-7.663	0.000
0062	HC108	MIHC	951.20417	100499.507	97689.612	643.317	152.18332	-7.663	0.000
0063	VC108	MIVC	952.21640	100498.620	97690.081	643.182	152.18332	-7.663	0.000
0064	HQ109	3Q120-2	959.37679	100492.344	97693.392	642.227	152.18332	-7.663	0.000
0065	HQ109	3Q120-2	964.37678	100487.961	97695.705	641.561	152.18332	-7.663	0.000
0066	V1090	EPB-R	982.26979	100472.277	97703.980	639.174	152.18332	-7.354	-90.000
0067	V1091	EPB-R	993.43650	100462.481	97709.148	637.751	152.18332	-6.736	-90.000
0068	V1092	EPB-R	1004.60321	100452.673	97714.323	636.447	152.18332	-6.118	-90.000
0069	V1093	EPB-R	1015.76988	100442.852	97719.505	635.263	152.18332	-5.500	-90.000
0070	V1094	EPB-R	1026.93656	100433.021	97724.692	634.199	152.18332	-4.881	-90.000
0071	V1095	EPB-R	1038.10327	100423.180	97729.884	633.255	152.18332	-4.263	-90.000
0072	V1096	EPB-R	1049.26995	100413.330	97735.081	632.432	152.18332	-3.645	-90.000
0073	HQ110	3Q120-2	1067.08166	100397.607	97743.377	631.341	152.18332	-3.336	0.000
0074	HQ110	3Q120-2	1072.08165	100393.192	97745.706	631.050	152.18332	-3.336	0.000
0075	HC110	MIHC	1078.00496	100387.962	97748.466	630.705	152.18332	-3.336	0.000
0076	HC110	MIHC	1079.01723	100387.068	97748.937	630.647	152.18332	-3.336	0.000
0077	VC110	MIVC	1080.02947	100386.174	97749.409	630.588	152.18332	-3.336	0.000
0078	HP110R	SYBPM_S	1080.98078	100385.334	97749.852	630.532	152.18332	-3.336	0.000
0079	VP110R	SYBPM_S	1082.01985	100384.417	97750.336	630.472	152.18332	-3.336	0.000
0080	PM110	SYSWIC	1083.36099	100383.233	97750.961	630.394	152.18332	-3.336	0.000
0081	BAFLE1	BAFFLE	1084.98054	100381.803	97751.715	630.299	152.18332	-3.336	0.000
0082	HPTAR	SYBPM_S	1127.66418	100344.116	97771.600	627.816	152.18332	-3.336	0.000
0083	VPTAR	SYBPM_S	1128.70322	100343.198	97772.084	627.755	152.18332	-3.336	0.000
0084	PMTAR	SYSWIC	1130.04436	100342.014	97772.709	627.677	152.18332	-3.336	0.000
0085	BAFL2U	BAFFLE	1131.66391	100340.584	97773.463	627.583	152.18332	-3.336	0.000
0086	BAFL2D	BAFFLE	1134.94474	100337.687	97774.992	627.392	152.18332	-3.336	0.000
0087	HALTA	TAR-2	1146.09958	100327.838	97780.188	626.743	152.18332	-3.336	0.000
0088	HALTA	TAR-2	1147.67438	100326.448	97780.922	626.651	152.18332	-3.336	0.000
0089	IHHRN1	HORN	1149.38041	100324.941	97781.717	626.552	152.18332	-3.336	0.000
0090	IHHRN2	HORN	1218.27791	100264.109	97813.813	622.542	152.18332	-3.336	0.000
0091	DECAY	DECAY	1307.48377	100185.345	97855.370	617.351	152.18332	-3.336	0.000
0092	DENCU	DU_ENU	3522.04627	98230.009	98887.039	488.477	152.18332	-3.336	0.000
0093	DUMP	DUMP	3528.60794	98224.216	98890.096	488.095	152.18332	-3.336	0.000
0094	DENCD	DU_END	3552.62364	98203.011	98901.284	486.698	152.18332	-3.336	0.000
0095	MUOND	MUON	3576.97575	98181.510	98912.629	485.281	152.18332	-3.336	0.000
0096	MUOND	MUON	3609.83979	98152.493	98927.939	483.368	152.18332	-3.336	0.000
0097	MUOND	MUON	3734.88085	98042.088	98986.190	476.091	152.18332	-3.336	0.000
0098	MUOND	MUON	3909.21794	97888.158	99067.406	465.946	152.18332	-3.336	0.000
0099	TUNNEL	TUNNEL	4397.40653	97457.115	99294.832	437.536	152.18332	-3.336	0.000
0100	M_ENCU	EX_ENU	4472.99378	97390.376	99330.045	433.138	152.18332	-3.336	0.000
0101	MIN_ND	EXP	4558.63744	97314.757	99369.943	428.154	152.18332	-3.336	0.000
0102	M_ENCD	EX_END	4613.22460	97266.560	99395.372	424.977	152.18332	-3.336	0.000
0103	ROCK	ROCK	4623.24154	97257.715	99400.039	424.394	152.18332	-3.336	0.000

B Glossary

A&E	Architecture and Engineering contractor
ACNET	Computer network of software controls for Fermilab's accelerators
ALARA	As Low As Reasonably Achievable; this is the radiological protection philosophy adopted by DOE and Fermilab
CASIM	Cascade Simulation; a Monte Carlo computer program for simulation of radiation production
CATV	Cable television; used for monitoring beamline and accelerator status
CDR	Conceptual Design Report
CORS	Continuously Observed Reference Station for the National Geodetic Survey
CPU	Central Processing Unit; "cpu time" refers to the amount of machine time a computer spends running a program.
CSP	Cost and Schedule Plan
DAC	Derived Air Concentration; this concentration of a radionuclide in air will deliver the annual limit of dose equivalent to a person who works full time in that environment.
DAQ	Data Acquisition
EDIA	Engineering, Design, Installation & Administration
FESHM	Fermilab Environment, Safety & Health Manual
FIRUS	Facility Incident Reporting & Utility System, Fermilab's integrated system for fire, critical equipment and security alarms
FNAL	Fermi National Accelerator Laboratory (Fermilab)
FQAP	Fermilab Quality Assurance Plan
FRCM	Fermilab Radiological Control Manual, part of the FESHM
GeV	Giga electron Volt (10^9 eV), a unit of energy

GPS	Global Positioning System
HVAC	Heating, Ventilation & Air Conditioning
ICW	Industrial Cooling Water; used in non-radioactive environments
IEPA	Illinois Environmental Protection Agency
IHEP	State Research Center of Russia, Institute for High Energy Physics
LAMPF	Los Alamos Meson Physics Facility
LCW	Low Conductivity Water; used for cooling magnets
MARS	A Monte Carlo computer program for simulation of radiation production
Mb	millibarn; 10^{-27} cm^2
MI60	Main Injector Service Building MI60
MI62	Main Injector Service Building MI62
MINOS	Main Injector Neutrino Oscillation Search, Fermilab Experiment E875
Monte Carlo	A type of computer program which simulates a large number of similar events using random numbers to obtain a distribution of possible outcomes.
MOU	Memorandum of Understanding
MUX	Multiplex
NBB	Narrow Band Beam; a neutrino beam having a narrow range of energies
NESHAPS	National Environmental Standards for Hazardous Air Pollutants, as established in 40 CFR Part61
NGS	National Geodetic Survey
NuMI	Neutrinos at the Main Injector; project to build a neutrino beam
PEP	Project Execution Plan; describes DOE management systems
PH2he	High energy neutrino beam produced with 2 parabolic horns
PH2le	Low energy neutrino beam produced with 2 parabolic horns

PH2me	Medium energy neutrino beam produced with 2 parabolic horns
PLC	Programmable Logic Controller
PMG	Project Management Group; consists of NuMI/MINOS personnel responsible for project management and change control.
PMP	Project Management Plan; describes Fermilab management systems
PSAD	Preliminary Safety Assessment Document
RAW	RadioActive Water; water used for cooling beamline components in high radiation environments
Star Density	The number of nuclear interactions (stars) per unit volume as calculated by a Monte Carlo program for radiation simulations
TARP	Chicago Tunnel and Reservoir Plan
TDR	Technical Design Report
VE	Value Engineering
WBB	Wide Band Beam; a neutrino beam having a broad range of energies
WBS	Work Breakdown Structure